Functional significance of islet amyloid polypeptide anti-fibrillation compounds as a novel treatment for type 2 diabetes management

Raliat Oyekemi Abioye

Thesis submitted to the University of Ottawa
in partial Fulfillment of the requirements for the
Doctorate in Philosophy degree in Chemistry

Department of Chemistry and Biomolecular Sciences
Faculty of Science
University of Ottawa

GENERAL DECLARATION

This thesis resulted in the publication of one review article, one perspective article, and two original research articles in international peer reviewed journals, along with two original research manuscripts submitted for consideration for publication. The motivation for this project was the objective to understand the "functional significance of islet amyloid polypeptide anti-fibrillation compounds as a novel treatment for type 2 diabetes management".

The research candidate was responsible for project conceptualization, formal analysis, investigation, methodology, validation, visualization, writing original article, and reviewing and editing the original article. This research was conducted at the University of Ottawa under the supervision of Professor Chibuike C. Udenigwe. The inclusion of co-authors in the manuscripts of various chapters indicates minor internal collaborations, which fit within the main subject framework of this study.

I hereby declare that the data and materials contained in this thesis have not previously been published by another author or approved for the award of a diploma or degree by any institution, except where appropriate acknowledgement has been made. Since no animal or human was used in this study, no research ethics approval was required for its conduct or inclusion.

Signed by: …….. Date: ……..

Raliat Oyekemi Abioye

(PhD Candidate)

The peer-reviewed scientific articles published or submitted by the candidate and utilized in the formulation of this thesis, are listed in the table below:

Thesis Chapter	Title of Publication	Co-authors	Type of Publication	Status of Publication	Candidate Contribution
1	Potential of peptides and phytochemicals in attenuating different phases of islet amyloid polypeptide fibrillation for type 2 diabetes management	C.C. Udenigwe	Review article	Food Science and Human Wellness, 10(3), 259-269, (2021)	Conceptualization, writing, and review and editing [90%]
1	Structural basis and functional significance of food-derived inhibitors of islet amyloid polypeptide fibrillation towards antidiabetic effects	C.C. Udenigwe	Perspective article	Current Opinions in Food Science, 56, 101146, (2024)	Conceptualization, writing, and review and editing [90%]
2	Inhibition of islet amyloid polypeptide fibrillation by structurally diverse phenolic compounds and fibril disaggregation potential of rutin and quercetin	O.D. Okagu; C.C. Udenigwe	Research article	Journal of Agricultural and Food Chemistry, 70(1), 392-402, (2021)	Conceptualization, methodology, validation, formal analysis, investigation, writing, review and editing, and visualization [80%]
3	Disaggregation of islet amyloid polypeptide fibrils as a potential anti-fibrillation mechanism of	O.D. Okagu; C.C. Udenigwe	Research article	International Journal of Molecular Science, 23(4), 1972, (2022)	Conceptualization, methodology, validation, formal analysis, investigation, writing, review and editing, and

	tetrapeptide TNGQ				visualization [80%]
4	Cross-domain binding of anti-fibrillation peptide TNGQ to islet amyloid polypeptide provides cytoprotective effects in giant unilamellar vesicles and pancreatic β-cells	M.S. Yiridoe; C. Wang; T.J. Avis; T.A.E. Ahmed; R. Hammami; C.C. Udenigwe	Research article	Food & Function, submitted	Conceptualization, methodology, validation, formal analysis, investigation, writing, review and editing, and visualization [65%]
5	Peptide-polyphenol interaction: Influence of anti-fibrillation inhibitors TNGQ-rutin combination on β-cell cytoprotective effects against IAPP-induced cell death, insulin secretion, and oxidative stress	O.H. Adetula; J. Diem Hum; C.C. Udenigwe	Research article	Biochemical and Biophysical Research Communications, submitted	Conceptualization, methodology, validation, formal analysis, investigation, writing, review and editing, and visualization [80%]

The candidate presented the following research, included in this thesis, at scientific conferences listed below:

	Title of Presentation	Conference	Candidate's Contribution
1	Anti-fibrillation activity of peptides and polyphenols and their physiological implications on β-cell functionality	Canadian Lipids and Proteins Conference, 2024	Conceptualization, methodology, validation, formal analysis, investigation, writing, review and editing, and visualization [75%]
2	Cross-domain binding of anti-fibrillation peptide TNGQ to islet amyloid polypeptide provides cytoprotective effects in giant unilamellar vesicles and pancreatic β-cells	Canadian Lipids and Proteins Conference, 2024	Conceptualization, methodology, validation, formal analysis, investigation, writing, review and editing, and visualization [70%]
3	Functional significance of food-derived peptides in inhibiting islet amyloid polypeptide (IAPP) fibrillation in Type 2 diabetes management	Canadian Black Scientists Network BE-STEMM, 2024	Conceptualization, methodology, validation, formal analysis, investigation, writing, review and editing, and visualization [85%]
4	Functional significance of food-derived peptides in inhibiting islet amyloid polypeptide (IAPP) fibrillation in type 2 diabetes management	American Oil Chemists' Society Annual Meeting & Expo, 2024	Conceptualization, methodology, validation, formal analysis, investigation, writing, review and editing, and visualization [85%]
5	Quantitative structure-activity relationship modelling of penta- and hexapeptide inhibitors of islet amyloid polypeptide fibrillation	3rd International Symposium on Bioactive Peptides, 2023	Conceptualization, methodology, validation, formal analysis, investigation, writing, review and editing, and visualization [80%]
6	Quantitative structure-activity relationship modelling of penta- and hexapeptide inhibitors of islet amyloid polypeptide fibrillation	Fall 2023 American Chemical Society, 2023	Conceptualization, methodology, validation, formal analysis, investigation, writing, review and editing, and visualization [80%]
7	Disaggregation of islet amyloid polypeptide fibrils as a potential anti-fibrillation mechanism of tetrapeptide TNGQ	American Oil Chemists' Society Annual Meeting & Expo, 2022	Conceptualization, methodology, validation, formal analysis, investigation, writing, review and editing, and visualization [80%]
8	Phase-specific inhibition of islet amyloid polypeptide fibrillation by tetrapeptides	13th International Conference and Exhibition on Nutraceuticals and Functional Foods, 2021	Conceptualization, methodology, validation, formal analysis, investigation, writing, review and editing, and visualization [90%]

9	Investigating the structure-function relationship of natural polyphenols in inhibiting islet amyloid polypeptide fibril formation	Fall 2021 American Chemical Society, 2021	Conceptualization, methodology, validation, formal analysis, investigation, writing, review and editing, and visualization [90%]
10	Inhibition of islet amyloid polypeptide fibril formation by natural polyphenols	112th Annual Meeting & Expo of the American Oil Chemists' Society, 2021	Conceptualization, methodology, validation, formal analysis, investigation, writing, review and editing, and visualization [90%]

Signed by: ……. Date: …….

Prof. Chibuike C. Udenigwe

(Primary Supervisor)

Signed by: ……. Date: …….

Prof. Paul Mayer

(Co-supervisor)

ACKNOWLEDGEMENTS

In the name of Allah, the Most Gracious, the Most Merciful.

They say it takes a village to raise a child, but in bringing this thesis to life, it felt like I had the support of an entire country. Starting with my mother, my Queen, my number one cheerleader, Modupe Olanrewaju Abioye and my dearest father, Dr. Oyekanmi Abioye. I dedicate this thesis to you, my beloved parents, whose love, support, and sacrifices have made me who I am today. You have always been my pillars of strength, providing me with the foundation and encouragement I needed to pursue my dreams. Your unwavering belief in my abilities, even when I doubted myself, has been a constant source of motivation.

Mom and Dad, you have worked tirelessly to ensure that I had every opportunity to succeed, often putting my needs before your own. Your guidance, wisdom, and unconditional love have given me the courage to face challenges and the confidence to strive for excellence. I am forever thankful for the values you instilled in me — like never giving up, staying true to myself, and the importance of hard work. Thank you for answering my late-night calls when I was doubting my decision to pursue a PhD and for praying with me. Thank you for staying up with me on DuDu (Google Duo) during my late-night stints in the lab. This thesis is a testament to your enduring support, faith in my potential, and endless prayers. I could not have reached this milestone without you, and I dedicate this work to you with all my love and gratitude. Thank you for being my greatest champions and for always reminding me that I can accomplish anything I set my mind to. This achievement is as much yours as it is mine.

To the one person that always understands me before I understand myself, my older brother, Hakeem Bamidele Abioye. Thank you for offering your encouragement and lending a listening ear whenever I needed it. Thank you for always being there for me to listen to my emails before I send them. Thank you for being my biggest defender. Thank you for never giving up on me, for always knowing when to drag me away from work and take some time for myself, even if I'm fighting you all the way through. Thank you for the bike rides, roller skating attempts, swimming lessons, and random adventures along the way. Your pride in me and your ability to always lift me up when I needed it most, is one of the main driving forces behind my successes. This thesis is a reflection of the bond we share, and I dedicate it to you with immense love and appreciation.

To my GamGam Muinat Morenike Yusuf, I dedicate this thesis to you. Kí Ọlọ́run Olódùmarè máa fi àlàáfíà, ìgbà áyé pípẹ́, inú dídùn, àti àṣeyọrí pọ̀ sí yín. Mo gbàdúrà pé kí Ọlọ́run Olódùmarè bùkún mí pẹ̀lú agbára láti tójú yín gẹ́gẹ́ bí ẹ ṣe tójú ìyá mi. I love you so much.

To my thesis supervisor and mentor, Professor Chibuike Udenigwe I struck gold having you as a supervisor. Your passion for mentorship, research, and empowerment is admirable and having been on the receiving end, I only hope to inspire others in the same way. I often reflect back to the very beginning, when I was first interviewing for the lab, I felt truly welcomed. Even though you didn't know me yet, the confidence with which you introduced me to your colleagues, toured me through the building and your lab, and took the time to take me out for coffee was unparalleled. From the very start, it was clear that this was the right place for me, and talking to your current students only confirmed it—they had nothing but praise for you.

Throughout this journey, your unwavering support and guidance have meant the world to me. You consistently pushed me to reach my full potential, encouraging me to push myself and aim higher. As such, your mentorship has helped me achieve milestones I never imagined possible. Working in your lab, I have also gained the skills and confidence that will equip me for the future. Thank you for your understanding and patience, especially during the times when I needed it most. Your mentorship has not only shaped my academic work but has also played a significant role in my personal growth. This thesis is a testament to your dedication and excellence as a mentor, and I am incredibly thankful for the opportunity to have worked under your supervision.

To my mentors who have been with me from the very beginning in my undergraduate days, Dr. Saphida Migabo and Jean Bowen. I often reflect on the tearful days in your office shortly after graduation, fretting over my next steps. Seeing how far I have come since then is a testament to trusting the process and showing up every day. Thank you for continuing to be my champions, and for your invaluable mentorship. My journey could not be complete without you. I can only hope that I have made you both proud.

To Dr. Ayman ElSayed, the literal glue that keeps the lab together. Thank you for your words of wisdom, incredible support, and expertise. Your dedication to keeping the lab running smoothly and your willingness to assist with any tasks have made a huge difference in my research. I truly appreciate your patience, professionalism, and constant help, and I am deeply grateful.

To Dr. Tamer Ahmed, thank you for imparting your invaluable knowledge of cell culture work on me. Thank you for your patience throughout the training process, your words of encouragement, and your support.

To the people who, my journey through graduate studies would be incomplete without their mention, starting with the past and present Udenigwe lab family, honorable mentions to my mentors/colleagues Dr. Ruth T. Boachie, Dr. Ogadimma D. Okagu, and Dr. Xiaohong Sun, for situating me and getting me settled when I first started in the lab. To Martha, Judith, and Seyi for keeping the lab bubbly and exciting – there was never a dull moment with you guys both in and outside of the lab. Thank you for the laughs, epic lab parties, impromptu dance parties, and enjoyment endeavors.

To Joy, thank you for bamboozling me into this blessing of a friendship. We quite literally are, bonded for life.

To my childhood bestie, Chelsea C., I love and appreciate you so much. Thank you for always being understanding, and patient with me. Thank you for your wisdom and perspectives. Thank you for being you.

To my heaven-sent sisters, Zviko G. and Alice O., my story in Ottawa could never be complete or as fulfilling as it was with you both in my life. I thought our first hang out was just a means to end my burnout. Never, in a million years would I have imagined the beautiful sisterhood and bond I would been blessed to build with you both. To my dearest soul sisters, thank you for the countless moments of laughter, understanding, and encouragement. Your companionship has been a source of joy and strength, helping me to stay balanced and motivated. I appreciate your never-ending encouragements, support, uplifting words, TikTok dance challenges, and ‘For-the-plot’ experiences that got me through some of the most grueling periods. Geography could never keep us apart.

Shout out to the kitchen and our unofficial office space. Some of the best s’mores were created there.

I wish to thank the University of Ottawa and NSERC for their financial support through the duration of my graduate studies having awarded me the University Admission Scholarships and Vanier Canada Graduate Scholarship.

To everyone that I haven't mentioned in this section, although your names may not appear individually, your impact on my life and this work is profound. You supported me in ways both big and small throughout this journey. Whether through a kind word, a listening ear, or just being there when I needed a break, you have all contributed to this achievement. This work is a reflection of the collective strength and love that surrounds me. I am deeply grateful for each and every one of you, and I dedicate this thesis to all of you with heartfelt thanks.

And to anyone reading this looking for inspiration or is unsure about what direction life is taking them and where to go next, all it takes is putting one footstep in front of the other. Progression looks different depending on the day, but giving ourselves grace and self-compassion is always the way to go. If I can do it, so can you.

ABSTRACT

Amyloidogenic proteins and peptides have been implicated in many diseases including Alzheimer's, Parkinson's, Huntington's, and even prion disease. Islet amyloid polypeptide (IAPP) is one amyloidogenic peptide that has been implicated in the prognosis of type 2 diabetes (T2D). IAPP is a hormonal peptide which functions primarily in postprandial glucose regulation. However, fibrillation renders it nonfunctional and induces β-cell dysfunction via mechanisms including oxidative stress and membrane rupture, resulting in toxicity and apoptosis. Hence, the identification of anti-fibrillation compounds is a common approach to mitigating fibrillation and fibrillation-induced β-cell toxicity. In comparison to other more popular antidiabetic targets, however, IAPP fibrillation is largely understudied as a potential treatment of T2D. Furthermore, natural compounds such as polyphenols, peptides, and polysaccharides, are not commonly considered as antidiabetic agents. Thus, this thesis seeks to expand the known anti-fibrillation compounds, with a special emphasis on structure-activity relationships. This will enhance the understanding of important anti-fibrillation features, and pave way to the rational design or identification of novel IAPP fibrillation inhibitors.

This research employed techniques to screen for potential fibrillation inhibitors using thioflavin T fluorescence kinetics. The effects of the biomolecular interactions between the identified inhibitors and IAPP on fibrillation and secondary structure were monitored using dynamic light scattering, and circular dichroism techniques. Morphological characterization of IAPP fibrils were carried out using transmission electron microscopy and fluorescence microscopy. The theoretical binding interactions between the anti-fibrillation compounds and IAPP were determined via *in silico* molecular docking, using monomeric and pentameric IAPP and binding models. The manifestation of the observed anti-fibrillation activity on membrane leakage and cytotoxicity was assessed using calcein-encapsulated giant unilamellar vesicles (GUVs) and rat insulinoma β-cells (RIN-m) respectively. Finally, the effect of IAPP fibrillation inhibition on β-cell functionality was evaluated by monitoring oxidative stress and glucose-stimulated insulin secretion.

From this study, IAPP anti-fibrillation polyphenols caffeic acid, gallic acid, rutin, and quercetin, and peptides MANT, YMSV, and TNGQ were discovered. These compounds demonstrated significant reductions in IAPP fibrillation, average particle sizes, stabilized IAPP secondary structure, and altered the fibrillar morphology of IAPP. Docking interactions studies identified

unique binding sites of each anti-fibrillation peptide to IAPP. Subsequent investigations into how domain-specific binding of peptides MANT, YMSV, and TNGQ translates to membrane-protective effects uncovered the role of cross-domain interactions by TNGQ in preventing IAPP fibrillation-induced membrane leakage and β-cell toxicity. Peptide-polyphenol interactions between rutin and MANT, YMSV, or TNGQ revealed a non-additive effect on anti-fibrillation activity. Nevertheless, rutin-TNGQ combinations demonstrated enhanced fibrillar disaggregation activity and decreased prevalence of membrane-bound toxic oligomeric species which translated to an enhanced ability to minimize β-cell oxidative stress; an effect that was not observed in the presence of rutin or TNGQ alone. Despite this, no significant effect was observed on glucose-stimulated insulin secretion. Obtained results highlighted the importance of multifunctional anti-fibrillation compounds that retain individual activity and shed a positive light on the benefits of non-additive inhibitor systems.

Taken together, this work demonstrated novel perspectives in fibrillation inhibitor design, the role of IAPP cross-domain interactions in mitigating fibrillation induced β-cell dysfunction, and the importance of structure on observed anti-fibrillation activity.

PUBLICATION DETAILS

This is to acknowledge that the following review article, perspective article, and original research articles published in or submitted to international peer reviewed journals and presented in scientific conferences were used in formulating this thesis.

Original Research Articles

Abioye, R. O.; Okagu, O. D.; Udenigwe, C. C. Inhibition of Islet Amyloid Polypeptide Fibrillation by Structurally Diverse Phenolic Compounds and Fibril Disaggregation Potential of Rutin and Quercetin. *Journal of Agricultural and Food Chemistry*, **2022**, *70(1)*, 392-402.

Abioye R. O.; Okagu O. D.; Udenigwe C. C. Disaggregation of islet amyloid polypeptide fibrils as a potential anti-fibrillation mechanism of tetrapeptide TNGQ. *International Journal of Molecular Science*, **2022**, *23*(*4*), 1972.

Abioye R. O.; Yiridoe M. S.; Wang C.; Avis T. J.; Ahmed T. A. E.; Hammami R.; Udenigwe C. C. Cross-domain binding of anti-fibrillation peptide TNGQ to islet amyloid polypeptide provides cytoprotective effects in giant unilamellar vesicles and pancreatic β-cells. *Food & Function,* **2024**, (Submitted).

Abioye R. O.; Adetula O. H.; Diem Hum J.; Udenigwe C. C. Peptide-polyphenol interaction: Influence of anti-fibrillation TNGQ-rutin combination on β-cell cytoprotective effects against IAPP-induced cell death, insulin secretion, and oxidative stress. *Biochemical and Biophysical Research Communications,* **2024**, (Submitted).

Review Articles

Abioye, R. O.; Udenigwe, C. C. Potential of Peptides and Phytochemicals in Attenuating Different Phases of Islet Amyloid Polypeptide Fibrillation for Type 2 Diabetes Management. *Food Sciences and Human Wellness*, **2021**, *10(3)*, 259-269.

Abioye R. O.; Udenigwe C. C. (2024). Structural basis and functional significance of food-derived inhibitors of islet amyloid polypeptide fibrillation towards antidiabetic effects. *Current Opinions in Food Science*, **2024**, *56*(*2024*), 101146.

Dedicated to my family and friends for their unwavering love, support, and prayers.

"Verily, with hardship comes ease;
Surely with [that] hardship ease, [is guaranteed];
So once you have fulfilled [your duty], strive in devotion;
And to your Lord direct [your] longing."
~ Quran; 94:5-8

TABLE OF CONTENTS

ABBREVIATIONS

ADME	Absorption, distribution, metabolism, and excretion
AGE	Advanced glycation end products
Ala	Alanine
ALS	Autophagy-lysosomal system
ANOVA	One-way analysis of variance
Arg	Arginine
Asn	Asparagine
Aβ	β- amyloid
BLAST	Basic local alignment search tool
CA	Caffeic acid
CCPG1	Cell cycle progression 1
CD	Circular dichroism
CLogP	Logarithm of compound partition coefficient between n-octanol and water
CYP3A4	Cytochrome P450 3A4
Cys	Cysteine
DLS	Dynamic light scattering
DNA	Deoxyribonucleic acid
DOPC	1,2-dioleoyl-sn-glycero-3-phosphocholine
DPP-IV	Dipeptidyl peptidase

EGCG	Epigallocatechin gallate
EOSL	Estimated solubility
ER	Endoplasmic reticulum
F_f	Final ThT fluorescence
F_i	Initial ThT fluorescence
F_{max}	Maximum fluorescence intensity
FTIR	Fourier-transform infrared
GA	Gallic acid
GIA	Gastrointestinal absorption
Gly	Glycine
GUV	Giant unilamellar vesicle
HBA	Hydrogen bond acceptors
HBD	Hydrogen bond donors
HFIP	1,1,1,3,3,3-Hexafluoro-2-propanol
hIAPP	Human islet amyloid polypeptide
His	Histidine
HS	Highly soluble
IAPP	Islet amyloid polypeptide
IC_{50}	Half maximal inhibitory concentration
Ile	Isoleucine

INS-1	Rat insulinoma cells
ITC	Isothermal calorimetry
K	Kinetic elongation constant
Leu	Leucine
Lys	Lysine
MW	Molecular weight
NIT-1	Mouse insulinoma cells
PDI	Polydispersity index
Phe	Phenylalanine
Pro	Proline
Q	Quercetin
QGlcA	Glucuronide-substituted derivative
R	Rutin
rIAPP	Rat islet amyloid polypeptide
RIN-m	Rat insulinoma cells
RIN-m5F	Rat insulinoma cells
ROS	Reactive oxygen species
ROTB	Rotatable bonds
Ser	Serine
τ	Reciprocal of the kinetic elongation constant

$t_{1/2}$	Time taken to reach half elongation phase
t_{obs}	Fluorescence intensity observed at time
T2D	Type 2 diabetes
TEM	Transmission electron microscopy
Thr	Threonine
ThT	Thioflavin T
TPSA	Topological polar surface area
TS1	Tanshinone I
TS2	Tanshinone IIA
Tyr	Tyrosine
UPS	Ubitquitin proteasome system
Val	Valine
ZnT8	$Zinc^{2+}$ transporter

LIST OF SCHEMES

Scheme 1.1.1. (A) IAPP is a 37-residue basic hormonal polypeptide consisting of a Cys2–Cys7 disulfide bond and three domains/regions: the N-terminal membrane binding domain (Lys1–Ser19), the amyloidogenic region (Ser20–Ser29), and the C-terminal self-association region (Thr30–Tyr37). **(B)** Model of fibrillar IAPP, adapted with permission from Marek et al. 2012.[1] On the left, the top-down view of the IAPP fibrillar axis (indicated by "**·**"). A layer consists of two molecules of IAPP, which interact through a dry "steric zipper" interface. The basic residues (Lys1 and Arg11) are solvent-exposed while His18 points inside the core, shown on the right. Basic groups are shown in space-filling representation, and their heavy atoms are determined using Adaptive Poisson-Boltzmann Solver (according to their electrostatic potential) and the represented charges are color-coded from red to blue (−20 to 20 kbT/ec units). **(C)** IAPP fibrillation kinetics plot. Blue curve represents the classical fibrillation kinetics of monomeric IAPP while the red curve represents the fibrillation kinetics of seeded fibrillation. Schematic outlines the classical fibril formation process separated into the three phases: lag, exponential, and stationary.

Scheme 1.1.2. Role of intracellular and extracellular IAPP fibrillation in the induction of apoptosis in β-cells; ROS, reactive oxygen species.

Scheme 1.1.3. IAPP fibrillation is initiated by the unfolding or misfolding of monomeric IAPP, exposing the self-association and amyloidogenic regions. Subsequent association of unfolded IAPP monomers results in the formation of dimers. Rapid elongation at both ends of IAPP dimers forms soluble oligomers, protofibrils, and finally, mature insoluble fibrils. IAPP-induced cytotoxicity is primarily caused by the fibrillar intermediates or mature fibrils via three main mechanisms: mitochondrial dysfunction, ROS production, and cell membrane disruption

Scheme 1.2.1. (A) ThT fluorescence assay used for the identification of anti-fibrillation compounds. **(B)** The effect of the fibrillation inhibitors can be characterized via secondary structure determination using Fourier-transform infrared (FTIR) or circular dichroism (CD). The extent of inhibitor binding can be characterized using isothermal calorimetry (ITC). The resulting fibrillar species can be assessed using dynamic light scattering (DLS) and visualized using various spectroscopic methods such as transmission electron microscopy (TEM). **(C)** *In vitro* cell culture studies using rat insulinoma β-cells can be used to evaluate the effects of anti-fibrillation compounds on β-cell morphology using immunofluorescence microscopy (IMF) and functionality

(oxidative stress and glucose-stimulated insulin secretion). **(D)** *In vivo* transgenic mouse or rat models can be used to understand the role of IAPP fibrillation inhibition on blood glucose regulation or on pancreatic β-cell morphology.

LIST OF FIGURES

environment and hydrophilicity/hydrophobicity of the binding site with colors ranging from dodger blue for the most hydrophilic to white (zero) to orange red for the most hydrophobic.

Figure S2.1. Thioflavin-T fluorescence-monitored kinetics of IAPP fibrillation process in the absence (control) and presence of the 11 phenolic compounds at IAPP:phenolic molar ratios of **(A)** 1:0.5 and **(B)** 1:2. **(C)** Summary of the IAPP fibrillation kinetic parameters, $t_{\frac{1}{2}}$ (time at half transition in hours), K (elongation constant), lag time (in hours), and F_{max} (maximum relative fluorescence intensity reached) for the IAPP:phenolic molar ratios 1:0.5 and 1:2.

Figure S2.2. Summary of estimated secondary structure contents (in percentage) of IAPP samples upon initial addition of phenolic inhibitor (0 h) and after 48 h. GA, gallic acid; CA, caffeic acid; R, rutin; Q, quercetin.

Figure S2.3. Particle radius (r.nm) size distribution for IAPP in the absence (control) and presence of gallic acid (GA), caffeic acid (CA), rutin (R), and quercetin (Q) at **(A)** 0 h and **(B)** after 48 h incubation. Each curve represents the average of triplicate measurements.

Figure 3.1. (A) Thioflavin-T fluorescence kinetics of IAPP fibrillation in the absence (control) and presence of tetrapeptides MANT, TNGQ, and YMSV. **(B)** Average particle size diameter (nm) and **(C)** polydispersity index of IAPP in the absence (control) and presence of MANT, TNGQ, and YMSV in the late stationary phase of fibrillation. ThT fluorescence microscopy of IAPP in the **(D)** absence (control), and presence of peptides **(E)** MANT, **(F)** TNGQ, and **(G)** YMSV. Scale bars represent 50 μm.

Figure 3.2. Circular dichroism spectra of IAPP in the absence (control) and presence of MANT, TNGQ, and YMSV at (**A)** the initial time point (0 h) and **(B)** late stationary phase (48 h) of fibrillation. Docking scheme showing intermolecular interactions between **(C)** MANT, **(D)** YSMV, or **(E)** TNGQ and monomeric IAPP at the various hydrophobic and hydrophilic regions **(F–H)**, respectively. Kyte–Doolittle scale was used to evaluate hydrophobicity with colors ranging from dodger blue (the most hydrophilic) to white 0.0 to orange-red (the most hydrophobic).

Figure 3.3. Transmission electron microscopy images of **(A)** IAPP control, and IAPP in the presence of **(B)** MANT, **(C)** TNGQ, and **(D)** YMSV, after 48 h incubation. IAPP fibril **(E)** length and **(F)** diameter quantified using ImageJ software (n = 24); ns = not significant ($p \geq 0.05$), * =

significant ($0.01 > p > 0.05$), and ** = very significant ($0.01 > p > 0.001$). Scale bars represent 0.5 μm.

Figure 3.4. Transmission electron microscopy images of pre-formed IAPP fibrils in the absence (control) and presence of TNGQ at 48 h and additional 1, 22.5, and 47.5 h post-incubation. Scale bars represent 0.5 μm. Arrows indicate presence of fibrils amongst amorphous aggregates.

Figure 4.1. (A) Fluorescence kinetics of calcein released from GUV over time when exposed to IAPP in the absence and presence of tetrapeptides YMSV, MANT, and TNGQ. Triton X-100 represents the positive control while 'Control represents GUV alone. **(B)** Calcein release relative to intact GUVs and in the presence of tetrapeptides YMSV, MANT, and TNGQ at 0, 2, 3.5, and 12 h. Bars with different letters denote significantly different mean values ($\alpha = 0.05$).

Figure 4.2. (A) Average particle diameter (nm) and **(B)** PDI of GUVs in the presence of IAPP alone (IAPP control) and IAPP in the presence of tetrapeptides YMSV, MANT, and TNGQ at the initial (0 h) and final (12 h) time points. Bars with different letters denote significantly different mean values ($\alpha = 0.05$).

Figure 4.3. Fluorescence microscopy images of GUVs treated with IAPP alone (IAPP control) and IAPP in the presence of tetrapeptides YMSV, MANT, and TNGQ at the initial timepoint (0 h) and after 2, 3.5, and 12 h of incubation.

Figure 4.4. (A) The viability of RIN-m cells in the presence of 5 μM IAPP alone or in the presence of equimolar concentrations of YMSV, MANT, or TNGQ after 24 h. Bars with different letters denote significantly different mean values ($p < 0.05$). **(B)** Brightfield images of RIN-m cells treated with complete culture medium (live cell control), 70% (v/v) ethanol (dead cell control), and IAPP in the absence and presence of tetrapeptide inhibitors (YMSV, MANT, and TNGQ). Scale bar represents 500 μm.

Figure 4.5. 3D and 2D interactions of **(A-B)** TNGQ, **(C-D)** YMSV, and **(E-F)** MANT with the hIAPP pentamer (PDB: 6VW2). Residues circled in pink participate in electrostatic interactions, indicated as polar residues, and residues circled in green participate in van der Waals interactions, indicated as "greasy" interactions. The green dotted lines indicate interactions facilitated by side chains, and the blue dotted lines indicate interactions facilitated by the backbone. The arrow at the end of the dotted lines indicates the direction of the proton acceptance or donation.

Figure 5.1. (A) Preparation (1), detection (2), and quantification (3) of IAPP fibrillation using ThT fluorescent probe. **(B)** ThT fluorescence intensity and **(C)** percent inhibition of IAPP fibrillation in the absence and presence of single inhibitors (rutin, YMSV, MANT, and TNGQ) and inhibitor combinations (YMSV+rutin, MANT+rutin, and TNGQ+rutin). **(D)** Average particle diameter, **(E)** polydispersity index, and **(F)** size distribution of IAPP species upon the addition of peptide/rutin mixtures (0 h) and after incubation (48 h). Bars with different letters indicate significantly different mean values ($p < 0.05$). R = rutin.

Figure 5.2. TEM images of **(A)** IAPP, **(B)** IAPP+TNGQ, **(C)** IAPP+rutin, and **(D)** IAPP+TNGQ+rutin after 48 h incubation. Scale bars represent 0.5 μm.

Figure 5.3. Cell viability of rat insulinoma (RIN-m) cells in the presence of 5 μM IAPP control and IAPP with rutin or peptide/rutin mixtures (YMSV+rutin, MANT+rutin, and TNGQ+rutin) after 24 h. Bars with different letters indicate significantly different mean values ($p < 0.05$). R = rutin.

Figure 5.4. Fluorescence microscopy images of rat insulinoma (RIN-m) cells post-treatment with 5 μM IAPP in the absence or presence of 5 μM TNGQ, rutin, or a mixture of TNGQ/rutin for 24 h. Green, oligomeric and fibrillar IAPP; red, RIN-m cellular membrane; and blue, RIN-m nuclei. Scale bars represent 50 μm. White squares indicate the region expanded for inset.

Figure 5.5. (A) Time-dependent oxidative response and **(B)** rate of ROS production in RIN-m cells following 6 h treatments with 5 μM IAPP in the absence and presence of TNGQ, rutin, and TNGQ/rutin mixture. **(C)** Mechanism of glucose-stimulated insulin secretion in β-cells, and the effect of IAPP oligomerization on insulin secretion. **(D)** Glucose-stimulated insulin secretion in RIN-m cells in the presence of basal and high glucose concentrations, following 24 h treatments with IAPP and the inhibitors. Bars with different letters indicate significantly different mean values ($p < 0.05$). R = rutin.

LIST OF TABLES

CHAPTER ONE

INTRODUCTION

SECTION 1.1

Islet amyloid polypeptide, fibril formation, and Type 2 diabetes

Excerpt from

Potential of peptides and phytochemicals in attenuating different phases of islet amyloid polypeptide fibrillation for type 2 diabetes management

Raliat O. Abioye and Chibuike C. Udenigwe

in *Food Science and Human Wellness*, **2021**, *10(3)*, 259-269.

https://doi.org/10.1016/j.fshw.2021.02.017

and

Structural basis and functional significance of food-derived inhibitors of islet amyloid polypeptide fibrillation towards antidiabetic effects

Raliat O. Abioye and Chibuike C. Udenigwe

Current Opinions in Food Science, **2024**, *56(2024)*, 101146.

https://doi.org/10.1016/j.cofs.2024.101146

DECLARATION FOR THESIS SECTION 1.1

Potential of peptides and phytochemicals in attenuating different phases of islet amyloid polypeptide fibrillation for type 2 diabetes management

This is to declare that there is no conflict of interest associated with this work and the contribution of the candidate is stated below:

Candidate's contribution	Conceptualization, writing, and review and editing	90%

The following co-authors attest to the candidate's participation in a group publication as a component of their thesis and was active in the creation of this publication. The co-author's permission is as follows:

Name	Signature	Date
Chibuike C. Udenigwe		

DECLARATION FOR THESIS SECTION 1.1

Structural basis and functional significance of food-derived inhibitors of islet amyloid polypeptide fibrillation towards antidiabetic effects

This is to declare that there is no conflict of interest associated with this work and the contribution of the candidate is stated below:

Candidate's contribution	Conceptualization, writing, and review and editing	90%

The following co-authors attest to the candidate's participation in a group publication as a component of their thesis and was active in the creation of this publication. The co-author's permission is as follows:

Name	Signature	Date
Chibuike C. Udenigwe		

1.1.1. INTRODUCTION

Amyloidogenic peptides and proteins have an increased tendency to self-interact and form insoluble fibrils or plaques, which can be extremely harmful.[2] These protein fibrils or plaques are precursors to many diseases such as Parkinson's, Alzheimer's, prion conditions, and type 2 diabetes (T2D), etc.[2,3] The amyloid formation process is similar for these peptides and proteins, consisting of nucleation in the lag phase, followed by oligomerization of the amyloidogenic proteins and exponential fibrillar growth in the elongation phase.[2] Finally, formation of fibrils consisting largely of stable, insoluble, multi-stranded β-sheets indicate transition into the stationary phase of fibril formation.[2]

Islet amyloid polypeptide (IAPP), or amylin, is a hormonal peptide co-produced and co-secreted with insulin by pancreatic β-cells.[4] IAPP primarily functions as a neuroendocrine peptide in postprandial blood glucose regulation.[4] This occurs via the suppression of gastric emptying, glucagon secretion regulation, and modulation of food intake.[4] The role of IAPP in satiety regulation suggests potential binding sites of IAPP within the brain.[4] Despite significant regulatory roles, IAPP has been identified as a key factor in the development of T2D. In excess amounts, monomeric and oligomeric IAPP can form extremely stable IAPP fibrils.[4,5] IAPP aggregates, which form amyloid fibrils, contribute to cytotoxicity of the pancreatic β-cells, resulting in loss of function and subsequent reduction in insulin production. These amyloid fibrils have been linked to T2D onset due to their cytotoxic effects on β-cells, causing cell failure and apoptosis.[4,5]

IAPP also has a potential role in exacerbating the deleterious effects of insulin resistance and stress experienced by β-cells in T2D development. This is because insulin resistance results in the upregulation of insulin production, equally enhancing IAPP co-secretion.[4] Overproduction of IAPP precursors can overwhelm the Golgi apparatus and endoplasmic reticulum, resulting in the secretion of immature or misfolded IAPP.[6] An increase in extracellular IAPP equally increases the likelihood of secreted IAPP to aggregate, resulting in fibrillar IAPP-mediated β-cell cytotoxicity. As a result, surviving β-cells overcompensate for this reduction of insulin production, further contributing to the loss of function because of increased stress and IAPP fibrillation-induced cytotoxicity, thus leading to insulin resistance, and a negative feedback loop, eventually resulting in β-cell failure.[7]

Endogenously, IAPP monomers function in a variety of roles; however, aggregation renders them non-functional. Thus, inhibition of IAPP fibril formation while retaining their endogenous function in glucose metabolism is an emerging approach for the discovery of new antidiabetic compounds.[8] Further, there is need for the identification of natural, food-derived inhibitors as an alternative to synthetic equivalents. The use of naturally occurring compounds, including peptides and phytochemicals, has been explored as a way to mitigate or inhibit IAPP fibril formation.

This section discusses the origin, structural profile, function, regulation, and disease involvement of IAPP in T2D development. Recent advances on inhibitors of IAPP fibril formation, and new insights on the future development and application of food-derived inhibitors towards T2D management is also explored. It also highlights some mechanisms that are proposed to be involved in IAPP fibrillation, the basis for the subsequent section, which discusses various anti-fibrillation compounds and their structural components implicated in their activity.

1.1.2. THE STRUCTURE AND ROLE OF ISLET AMYLOID POLYPEPTIDE IN TYPE 2 DIABETES

1.1.2.1. Structural information

Islet amyloid polypeptide (IAPP), also known as amylin, is a 37-residue basic polypeptide (**Scheme 1.1.1A**).[1,9–11] As a result of the amidated C-terminus, this polypeptide lacks any negatively charged groups. In addition, the presence of four positively charged groups (N-terminus, Lys1, Arg11, and His18) contributes to the cationic nature of IAPP, with net charge ranging from +2 to +4 depending on the pH.[1] The structure of IAPP includes a rigid disulfide bridge between Cys2 and Cys7, embedded within the membrane-binding domain spanning from residues 1–19 of the N-terminus (**Scheme 1.1.1A**).[9,10] Residues 8–19 form the highly dynamic random coil structure that interchanges with an α-helical conformation in aqueous solution, while the central 20–29 residues govern the amyloidogenic region, which plays an instrumental role in fibril formation (**Scheme 1.1.1A**).[10,11] Lastly, the C-terminal region is involved in peptide self-association (**Scheme 1.1.1A**).[10]

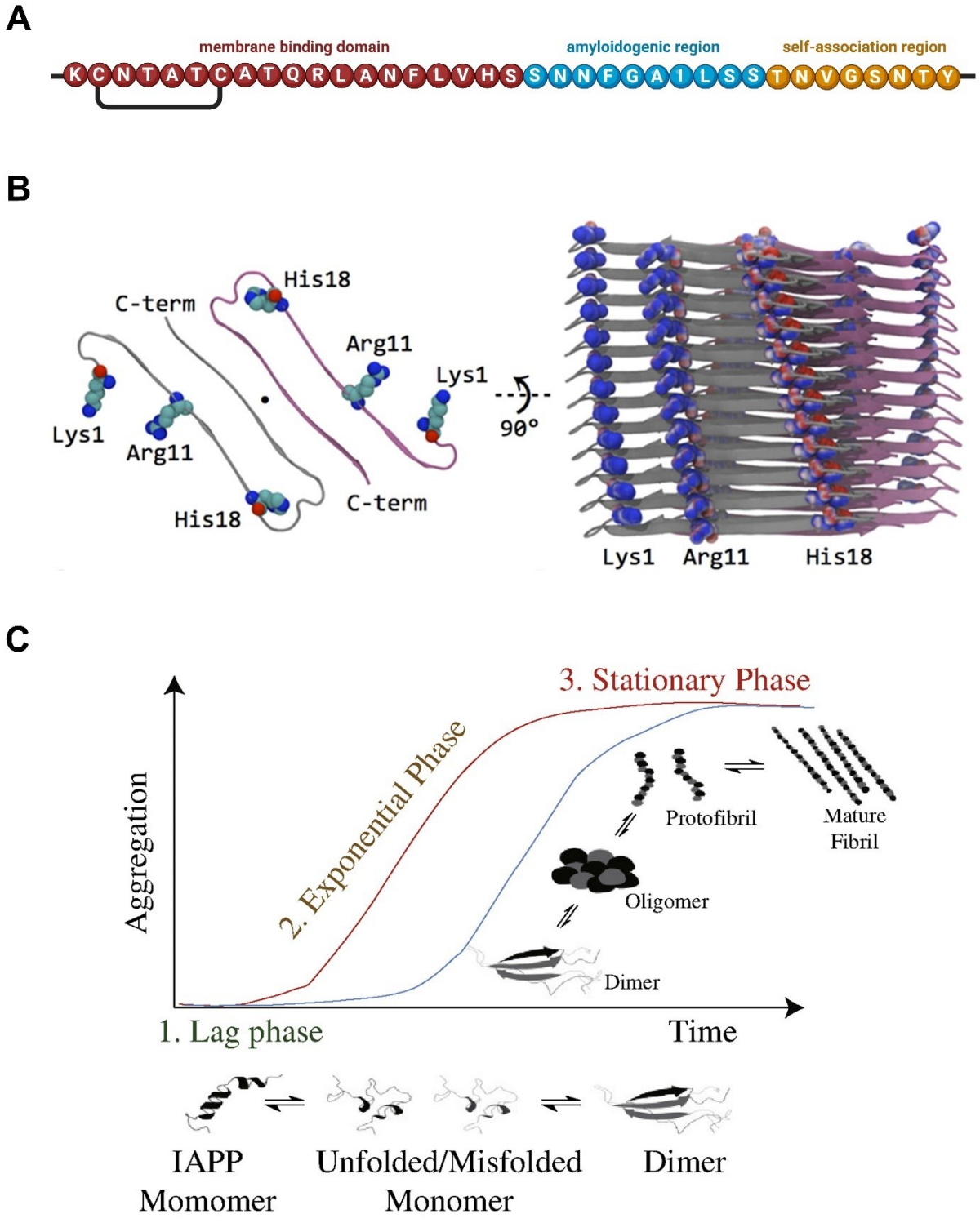

Scheme 1.1.1. (A) IAPP is a 37-residue basic hormonal polypeptide consisting of a Cys2–Cys7 disulfide bond and three domains/regions: the N-terminal membrane binding domain (Lys1–Ser19), the amyloidogenic region (Ser20–Ser29), and the C-terminal self-association region

(Thr30–Tyr37). **(B)** Model of fibrillar IAPP, adapted with permission from Marek et al. 2012.[1] On the left, the top-down view of the IAPP fibrillar axis (indicated by "·"). A layer consists of two molecules of IAPP, which interact through a dry "steric zipper" interface. The basic residues (Lys1 and Arg11) are solvent-exposed while His18 points inside the core, shown on the right. Basic groups are shown in space-filling representation, and their heavy atoms are determined using Adaptive Poisson-Boltzmann Solver (according to their electrostatic potential) and the represented charges are color-coded from red to blue (−20 to 20 kbT/ec units). **(C)** IAPP fibrillation kinetics plot. Blue curve represents the classical fibrillation kinetics of monomeric IAPP while the red curve represents the fibrillation kinetics of seeded fibrillation. Schematic outlines the classical fibril formation process separated into the three phases: lag, exponential, and stationary.

The aggregation of monomeric IAPP, forming protofibrils and subsequent mature fibrils, is a spontaneous and favorable reaction *in vivo*. This transformation consists of a change from the intrinsically disordered IAPP monomer to the highly ordered β-sheets, forming amyloids of varying sizes.[1,10] Each monomer adopts a U-shaped confirmation with residues 18–27 embedded within the turn region between the two β-strands of a monomer (**Scheme 1.1.1B**).[1,12] Initial protofibrils are composed of two C2-symmetric stacks of monomeric IAPP that lack interchain hydrogen bonding or any other charge-charge interactions across the axis between the protofibrils (**Scheme 1.1.1B**). Rather, these chains form a dry steric zipper, held together by hydrophobic interactions.[13] However, hydrogen bonding occurs within monomers of a single stack running parallel to the fibrillary axis.[1]

1.1.2.2. Endogenous roles

IAPP is a small, neuroendocrine hormonal peptide that is co-packaged, co-localized and co-secreted with insulin at an IAPP:insulin ratio of 1:100 by the pancreatic β-cells in the Islets of Langerhans.[9,10,14–16] It is stored in secretory granules along with insulin and released to facilitate glucose and cholesterol metabolism in events of elevated blood glucose levels by inhibiting glucagon secretion.[15,17] IAPP plays several regulatory roles for maintaining post-prandial glucose levels by suppressing gastric emptying, and modulating food intake and glucagon secretion.[9,18] Subsequent suppression of glucagon activity decreases hepatocytic glucose production and excretion, whereas suppression of gastric emptying delays glucose absorption by the small

intestine.[6] Its effects in centrally stimulating satiety suggests the presence of potential IAPP binding sites within the brain cells.[18]

1.1.2.3. IAPP turnover

Under normal circumstances, IAPP routinely undergoes proteolytic degradation via the ubiquitin proteasome system (UPS) where the 26S proteasome complex plays a pivotal role in IAPP turnover.[19] UPS recognizes and degrades damaged and dysfunctional proteins as well as fully functional proteins that are no longer needed.[20] Routine turnover of IAPP helps to prevent intracellular accumulation and cytotoxicity to pancreatic β-cells. During type 2 diabetes (T2D), however, there is a marked decrease in proteasome activity where the polyubiquitinylated proteins become more abundant, indicating functional impairment of the proteolytic complex.[19]

Autophagy-lysosomal system (ALS) is the second most abundant degradation system regulating IAPP turnover.[20] While UPS degrades proteins exclusively, the dynamic membrane recognition system of ALS allows for the degradation of a broader range of macromolecules, in addition to proteins and their aggregates, such as lipids and DNA.[20] With respect to IAPP degradation, the dynamic membrane recognition allows for the identification of IAPP macromolecules in need of degradation. Upon identification of IAPP, uptake via autophagy is induced, followed by intercellular transport to specialized lysosomes called autophagosomes.[20] Autophagosome accumulation occurs because of rapid encapsulation of fibrils by the aforementioned autophagosomes in event of overwhelmingly high levels of fibril formation. In order for degradation to occur, lysosomes must fuse with autophagosomes to form autophagolysosomes. These newly formed specialized lysosomes are able to degrade ubiquitinylated fibrils through a process known as aggrephagy.[6] However, under stress conditions, such as rapid fibril formation, the rate of autophagosome maturation is overburdened. This negatively impacts the rate of amylin degradation in the process and further increases the stress experienced by the pancreatic β-cells.[6,20]

1.1.2.4. Role in T2D development

Type 2 diabetes (T2D), a metabolic disease characterized by the inability to regulate postprandial blood glucose levels, is rapidly becoming a major global health concern. In 2021, it was estimated that 529 million people were living with diabetes, with more than 90% having

T2D.[21] This is projected to more than double, with 1.31 billion people estimated to be living with diabetes by 2050, hence the importance for imminent disease intervention.[21] Before the onset of T2D, the abnormalities in insulin production and secretion by β cells occur in an effort to regulate increased blood glucose levels and combat insulin resistance of skeletal muscle, fat, and liver tissues.[7] Consequently, β cells significantly upregulate the production of insulin to restore sensitivity and enhance glucose uptake, leading to β-cell stress.[7] This stress results in β-cell failure and death, and further exacerbates blood glucose dysregulation and hyperglycemia.[22] Hence, several biomolecules, biochemical pathways, and cellular processes involved in glucose metabolism and insulin resistance have been targeted for their role in T2D toward the development of novel treatment options. In the early stages of T2D, the production of IAPP is noticeably higher than normal, likely a result of the overexertion of β cells to increase circulating insulin levels in compensation for the hyperglycemic state.[23]

Overwhelming evidence points to IAPP cytotoxicity in T2D development, making it an attractive target for T2D mitigation. While IAPP fibrillation is not considered to be the primary cause of T2D, it is still found to be a contributing factor responsible for the decreased level of insulin production by pancreatic β-cells.[9] In events of uncontrolled regulation and subsequent β-cell stress, improper processing of IAPP results in the formation of intracellular and extracellular amyloid deposits.[11,12] IAPP amyloid deposits have been observed in over 90%–95% of T2D patients, and its presence has been linked to membrane damage of β-cells, causing cytotoxicity.[9,15,16,24–26] IAPP amyloid deposits have extremely cytotoxic effects on β cells, and the degree of IAPP fibrillation has been directly correlated with a loss in β-cell mass and function, resulting in a marked decrease in insulin production.[9,11,22] This subsequent loss of β-cell mass and function serves as the initiator of chronic insulin resistance.[11,27] Pancreatic β-cell function has also been shown to be spatially correlated with amylin protein deposition where β-cell mass is strongly reduced in islets containing IAPP deposits while nearby islets lacking amylin remain unaffected.[25,28]

In T2D pathogenesis, IAPP plasma levels decrease significantly, thus explaining the rapidly occurring gastric emptying in advanced disease stages. Moreover, the reduction of β-cell mass as a result of prolonged stress points to the downregulated IAPP production.[23]

Considering the instrumental role of IAPP in blood glucose regulation and the deleterious effects of IAPP aggregates on β-cell viability and insulin response, IAPP has become an important target for T2D management and treatment.

1.1.3. IAPP fibril formation

1.1.3.1. Mechanisms of formation

IAPP fibril formation follows the classical aggregation process consisting of a lag/nucleation, elongation/growth, and stationary phases (**Scheme 1.1.1C**). However, prior to fibril formation, misfolding or unfolding must occur, making the nucleation phase the rate determining step in IAPP fibril formation.[11,29] IAPP is intrinsically transient in its native α-helical state, making unfolding or misfolding highly favorable. The rate-determining nature of this stage presents in the association of two IAPP monomers. At physiological pH, IAPP maintains a positive charge due to the charged N-terminus and basic residues Lys1, Arg11.[1] Of the residues, only Lys1 and Arg11 remain exposed to solvent while His18 is oriented towards the core.[1,10] Due to the orientation of IAPP monomers, nucleation includes the association of two cationic residues needing to overcome repulsive forces, thus explaining the rate determining nature of the nucleation phase.[1,30] Formation of dimers from IAPP monomers indicates the beginning of the nucleation phase while subsequent aggregation into oligomers mark the transition into the elongation phase. Following dimerization, rapid elongation of dimers into short-lived fibrillar intermediates such as soluble oligomers and protofibrils occurs in the elongation or growth phase. Protofibrils are intermediate molecules that form immediately afterwards, leading to mature fibril formation and the stationary phase where fibrils are in equilibrium with monomers.[11,29] As shown in **Scheme 1.1.1C**, the reaction curve of IAPP fibril assembly has been described by many as a sigmoidal curve, similar to that of an allosteric enzyme kinetics plot.

The N-terminus of IAPP is not overly instrumental in fibrillation, possibly due to the Cys2–Cys7 disulfide bond, which introduces rigidity and restricts β-sheet formation (**Scheme 1.1.1A**).[31] Nonetheless, the N-terminus disrupts synthetic lipid vesicles in the absence of fibers, owing to the membrane-binding capabilities of this domain.[32] The amyloidogenic region contains a number of hydrophobic and aromatic residues (**Scheme 1.1.1A**).[33,34] The fibrillation propensity of IAPP is largely driven by this region; thus, it has become the most targeted region in search for anti-

fibrillation agents. Interestingly, the first point of contact for IAPP self-association occurs at the C-terminus (**Scheme 1.1.1A**), yet it is not as strongly targeted for inhibition compared with the amyloidogenic region.[9]

Fragments of mature fibrils are often used as "seeds" or templates to form additional fibrils. This alternative template pathway to fibril formation is more favorable and less energy demanding compared to nucleation initiated by the aggregation of two monomers. Consequently, the process results in a much shorter lag phase followed by a rapid elongation phase, and finally the expected stationary phase observed with the template pathway (**Scheme 1.1.1C**).[11,30] This favorability is explained by the initial nucleation and elongation phases in normal fibril formation. Dimerization and oligomerization of IAPP monomers are unfavorable steps in fibrillation that result in the formation of highly unstable fibril intermediates, which may dissociate to form shorter fibrillar fragments in order to achieve a more stable arrangement. The fragment in turn serves as a template for binding additional monomers, forgoing the nucleation phase almost completely and increasing the elongation phase in the process.[30]

IAPP-advanced glycation end products (AGE) conjugates (AGE-IAPP) can also play the role of "seeds" for new fibril formation, resulting in a dramatically reduced nucleation phase, and in causing more lethal cytotoxicity compared to native IAPP.[11,35] AGE-IAPP can also be used to seed fibrillation with as low a ratio as 10% total AGE-IAPP present.[11] This non-enzymatic conversion to AGE-IAPP renders the modified polypeptide resistant to proteolytic degradation, thus promoting its accumulation *in vivo*.[11] AGE-IAPP plays a role in activating fibril formation compared to native IAPP, even at low pH where aggregation is largely unfavorable. It is hypothesized that the AGE modification drastically changes the aggregation rate by promoting conformational change from the intrinsically disordered random coil of IAPP to the highly ordered β-sheet structure of fibrils.[11,36] This conversion significantly reduces the high-energy threshold governed by the nucleation step, thus allowing rapid transition to the formation of high-molecular weight cytotoxic IAPP oligomers.[36] Other non-enzymatic self-modifications such as deamidation is known to encourage IAPP aggregation in a similar mechanism as glycation.[37,38]

1.1.3.2. Cytotoxicity

Cytotoxicity associated with IAPP occurs primarily because of the formation of pores within the pancreatic β-cell membrane, which reduces membrane integrity and permeability,

leading to disrupted ionic homeostasis and signal transduction and triggering cell death (**Scheme 1.1.2**).[10] This hypothesis is plausible given the presence of the 19-residue membrane-binding domain of human IAPP (hIAPP), which modulates fibril formation and incites membrane leakage upon aggregation.[39] While this is the widely accepted mechanism, there is no consensus on the species causing the membrane permeating pores. Some studies point to oligomeric species and other pre-fibrillary soluble intermediates whereas others suggest the mature fibrils as the mediators.[10,11,29,39,40]

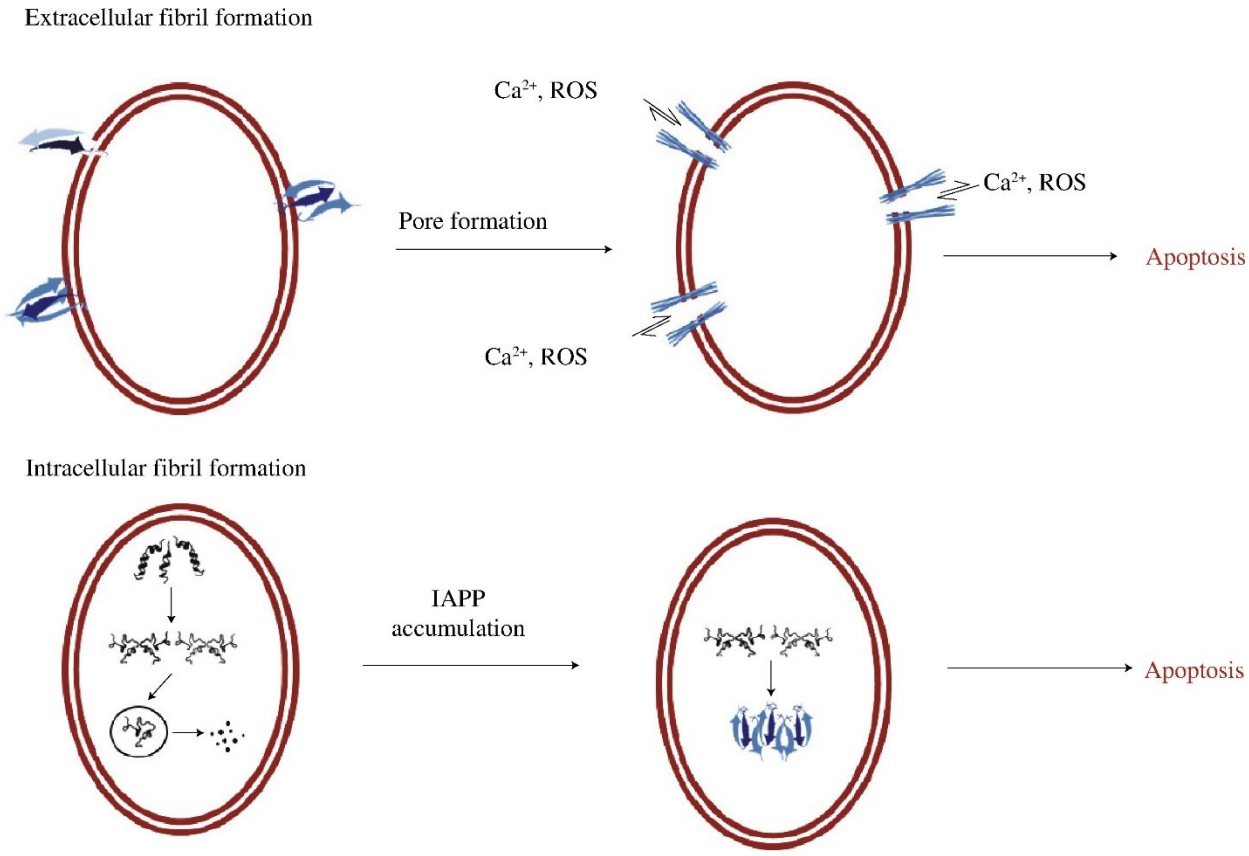

Scheme 1.1.2. Role of intracellular and extracellular IAPP fibrillation in the induction of apoptosis in β-cells; ROS, reactive oxygen species.

Oligomeric species play a principal role in cytotoxicity and disease development.[41] Related amyloidogenic peptides previously implicated in diseases, such as the *β*-amyloids, and pre-fibrillary assemblies, particularly soluble oligomers, have significant cytotoxic effects *in vivo*.[29] Oligomerization causes the initial membrane leakage through pore formation or aspecific leakage of ions, causing aspecific leakage, which may contribute to cytotoxicity.[39] Challenges in

elucidating the true cytotoxic abilities of these oligomeric species are mainly due to the extremely short-lived nature of oligomeric aggregates and, as such, structural characteristics and other cues have yet to be identified (**Scheme 1.1.3**).[10,11,29,30]

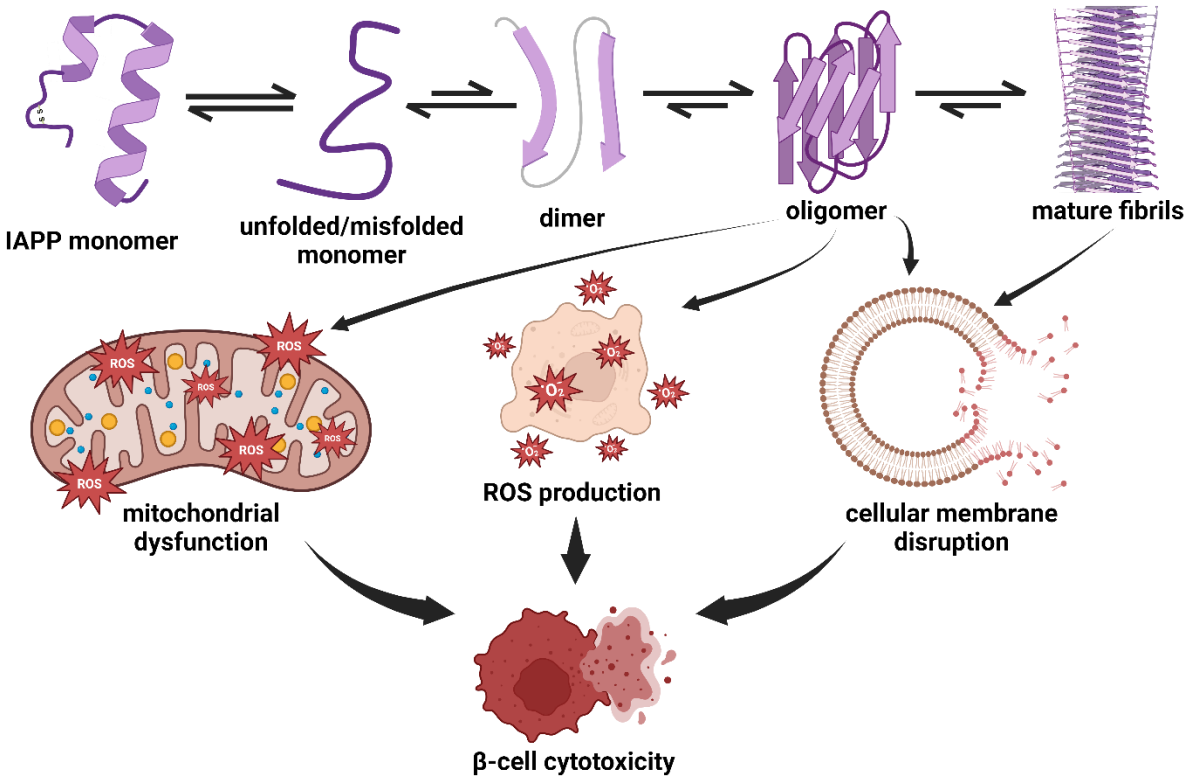

Scheme 1.1.3. IAPP fibrillation is initiated by the unfolding or misfolding of monomeric IAPP (PDB code: 2L86), exposing the self-association and amyloidogenic regions. Subsequent association of unfolded IAPP monomers results in the formation of dimers. Rapid elongation at both ends of IAPP dimers forms soluble oligomers, protofibrils, and finally, mature insoluble fibrils. IAPP-induced cytotoxicity is primarily caused by the fibrillar intermediates or mature fibrils via three main mechanisms: mitochondrial dysfunction, ROS production, and cell membrane disruption.

In contrast, insoluble amyloid fibrils play an indirect role in β-cell cytotoxicity.[6,35] Alone, these insoluble fibrils are relatively inert and not cytotoxic, but their negative effect may be facilitated through the formation of fibrils (**Scheme 1.1.3**).[6] Monomeric IAPP interacts with the lipid membrane of the β-cell through the membrane-binding domain.[42] This insertion leaves the

amyloidogenic region of IAPP free to aggregate. Cytotoxicity comes with the growth of the fibrils to form larger pores, which eventually disrupts the membrane altogether and an imbalance in water and ion homeostasis, also triggering apoptosis.[6] In addition, another indirect model suggests that cytotoxicity is also triggered by a number of changes in the cellular environment because of fibril formation.[33] These changes include an increase in the formation of reactive oxygen and nitrogen species, abnormalities in cellular redox systems, loss of protein function post-aggregation, and hyper-phosphorylation of proteins that accumulate in aggregative protein deposits.[33] Specific contributors to aggregation-induced cytotoxicity including the roles of monomeric, oligomeric, and protofibrillar species in inducing β-cell death have been reviewed elsewhere.[43]

Furthermore, intracellular overproduction of IAPP followed by delays or errors in processing may result in the accumulation of IAPP due to the overwhelmed IAPP turnover mechanisms, thus causing fibril formation intracellularly.[7] Subsequent pores formed within the cell membrane by extracellular IAPP fibrils can function as calcium-permeable ion channels, resulting in the increased influx of calcium ions into the cell.[7] Thus, the prolonged increase in intracellular calcium concentrations results in cell damage and apoptosis. Further exacerbation of this process may occur with the release of intracellular pre-fibrillar intermediates into the extracellular environment followed by subsequent formation of IAPP fibrils, where cytotoxicity can be induced in surrounding β cells by interaction between the oligomeric species and mature fibrils with the cell membrane (**Scheme 1.1.3**).[10,26]

1.1.3.3. Role of microenvironment in fibril formation

The local environment of IAPP also influences the switch from stable monomeric IAPP to fibrils. Factors such as salt concentration, ionic strength and glucose concentration play a major role in fibril formation.[24]

Salt concentration and ionic strength have a complex effect on amyloidogenesis. These conditions are hypothesized to play a major role in establishing favorable conditions for IAPP amyloid formation.[1] In general, amyloidogenesis increases significantly with increasing ionic strength; however, the interplay between ionic strength and fibril formation is more complex than a simple linear correlation because pH, ion species, and concentration also affect the behavior of IAPP.[1] At high salt concentration, the effect of ion strength in IAPP fibrillation is directed by the Hofmeister effect, which associates protein solubility to the concentration of salt in solution.[44]

Thus, IAPP fibrillation will be more favorable in conditions of high salt concentration, which explains the increased rate of fibril formation as a result.[1,45] Furthermore, a higher salt concentration in the presence of anions yields an increased dependence on anion binding between salt and polypeptide, which favors fibril formation.[1] More research on the effects of salt alone on fibril formation would provide independent insights on the interplay between the two, as well as potential targets for IAPP fibrillation inhibition. Similar to the effect of monovalent anionic composition on fibrillation, IAPP aggregation accelerates in the presence of anionic lipids such as phosphatidylglycerol and phosphatidylserine.[10]

Zinc ions play an indirect role in fibril formation through the modulation of insulin concentration. Insulin, along with IAPP, is stored in granular forms within pancreatic β-cells where the intracellular environment consists of a high Zn^{2+} concentration and ionic strength.[1,24] The Zn^{2+} transporter in pancreatic β-cells, ZnT8, is responsible for transporting zinc against its concentration gradient into the β-cells, thus indirectly modulating IAPP aggregation through insulin binding.[24] Insulin monomers and dimers preferentially bind IAPP monomers, whereas insulin oligomers are insoluble and do not bind IAPP. Instead, zinc ions bind and stabilize insulin hexamers, retaining their crystal forms within the β-cell granules. As a result, zinc ions modulate insulin granulation, thus altering the concentration of insulin monomers and dimers in the process, and impacting the formation of insulin-IAPP complexes and IAPP aggregation.[24,46] The binding of insulin monomers and dimers to IAPP occurs at the amyloidogenic region of IAPP, thus preventing IAPP self-assembly and inhibiting aggregation in the process.[24] Zinc ions also bind to the monomeric IAPP at His18, destabilizing the α-helical region and favoring the β-hairpin conformation instead.[47] While the β-hairpin is an intermediate structure in the formation of the amyloidogenic β-sheet, Zn^{2+} blocks the process by stabilizing the much lesser amyloidogenic hairpin conformation.[46,47] A decrease in extracellular Zn^{2+} concentration allows for an increase in oligomerization of insulin and, as a result, the concentration of monomeric and dimeric IAPP increases. Since both insulin conformations bind competitively to IAPP monomers, an increase in insulin-IAPP complexes is observed with increased Zn^{2+} concentration, thus blocking the amyloidogenic region of IAPP and decreasing the propensity of IAPP aggregation.[24] Insulin-IAPP complex formation provides another route for IAPP shuttling in environments of excess peptide as well.

A number of other changes in the micro-environment can affect IAPP aggregation, either encouraging or discouraging fibrillation. Additional factors that play a role in fibril formation of IAPP include the presence of other metal ions such as Cu^{2+}.[48,49]

1.1.3.4. Role of IAPP sequence in fibril formation

Like humans, IAPP analogues are present in many different mammalian species, including baboon, cat, dog, rat, mouse, and cow.[6] However, unlike hIAPP, some analogues do not exhibit fibril formation and, more importantly, these mammals do not develop hyperglycemia or T2D.[24] Rat IAPP (rIAPP) analogues have been extensively studied to understand the importance of the 6-residue difference in the sequence that seem to eliminate the amyloidogenic propensity.[6,14,28] A high sequence conservation exists in rats and human's IAPP, except for the amyloidogenic region, half of which consist of proline substitutions. Amyloidogenesis studies suggest the importance of Pro25 of rIAPP in fibril formation.[14,50] This is likely because proline plays the role of a β-breaker, preventing the formation of β-sheet at the C-terminal and disrupting the U-shape topology seen in fibril formation, thus reducing the ability of IAPP to form aggregates.[14,51,52] The Pro25 residue introduces a kink in the middle of the peptide fragment of the mature fibrils, resulting in the loss of β-sheet topology in favor of aggregated coils.[14]

Although the driving forces in IAPP self-assembly are not completely elucidated, many hypotheses have been proposed. Originally, it was thought that aromatic residues, specifically phenylalanine, played a fundamental role in facilitating the π-π interactions that encourage aggregation.[53] Mutational studies revealed that phenylalanine, and other aromatic residues alone, were not absolutely required for the formation of fibrils. This led to the rationale that hydrophobic interactions, amongst other intermolecular forces, were the driving force behind fibril formation, while aromacity simply provided structural stabilization.[54,55] While no consensus exists on what plays the decisive factor on fibril formation, Profit et al. suggested that both π-π and hydrophobic interactions play roles in fibril formation and when either is disrupted, disaggregation is expected to occur.[56]

SECTION 1.2

Mechanisms of inhibition of islet amyloid polypeptide fibril formation

Excerpt from

Potential of peptides and phytochemicals in attenuating different phases of islet amyloid polypeptide fibrillation for type 2 diabetes management

Raliat O. Abioye and Chibuike C. Udenigwe
Food Science and Human Wellness, **2020**, *10(3)*, 259-269.

https://doi.org/10.1016/j.fshw.2021.02.017

and

Structural basis and functional significance of food-derived inhibitors of islet amyloid polypeptide fibrillation towards antidiabetic effects

Raliat O. Abioye and Chibuike C. Udenigwe
Current Opinions in Food Science, **2024**, *56(2024)*, 101146.

https://doi.org/10.1016/j.cofs.2024.101146

1.2.1 FOOD-DERIVED ISLET AMYLOID POLYPEPTIDE FIBRILLATION INHIBITORS

Several approaches are taken in type 2 diabetes (T2D) management to increase insulin effectiveness through incretin-based approaches to increase insulin circulation (e.g., glucagon-like peptide-1 (GLP-1), glucose-dependent insulinotropic polypeptide (GIP), and dipeptidyl peptidase IV (DPP-IV)), the reduction of hepatic glucose production, release and reabsorption (e.g. sodium−glucose co-transporter 2), and enzyme inhibition (e.g., α-amylase and α-glucosidase). These approaches are geared toward treating the downstream effects of β-cell malfunction rather than minimizing the initial source of stress contributing to the loss of β-cell mass. Nutraceuticals are increasingly gaining interest as natural agents for reverting or slowing the progression of T2D, given their affordability, safety, and translatability for routine use compared with pharmaceutical-based therapies. Furthermore, many antidiabetic food-derived compounds were discovered from the context of the inhibition of glucose-metabolizing enzymes, such as α-amylase, and α-glucosidase, while their effects in mitigating IAPP fibrillation were not considered. Of the few food-derived compounds identified for anti-IAPP fibrillation activity, structural diversity is quite apparent, as is the mechanism in which IAPP fibrillation is inhibited. This highlights the role of physicochemical properties on mechanism and extent of anti-fibrillation activity. In some cases, fibrillation inhibition occurs at the intermediate stages of fibril formation, whereas in others, activity is observed through the disaggregation of mature fibrils into monomers and other less toxic fibrillar intermediates. In some instances, the inhibitors exhibit anti-fibrillation activity by both mechanisms.

IAPP fibrillation inhibitors are commonly identified *in vitro* via thioflavin T (ThT) fluorescence assays, where the fluorescent dye (ThT) binds to the β-sheet–rich regions of IAPP during fibrillation to produce fluorescence.[57] The intensity of the fluorescence is directly proportional to the extent to which IAPP fibrillation is enhanced or diminished in the presence of inhibitors (**Scheme 1.2.1A**). Because of the high throughput nature of this assay, large screening assays for potential IAPP fibrillation inhibitors can be performed rapidly, and the extent of inhibition can be easily quantified.[57] Additional characterization techniques such as circular dichroism (CD) and Fourier-transform infrared spectroscopy (FTIR) are used to elucidate the predominant secondary structures present, while techniques such as fluorescence spectroscopy,

dynamic light scattering, molecular docking, molecular dynamics simulation, and isothermal calorimetry (ITC) are commonly used to assess binding interactions, globular structure, and species diversity of IAPP fibrillar intermediates in solution (**Scheme 1.2.1B**). *In vitro* cell viability studies can be used to validate ThT fluorescence results and report on the extent at which the identified inhibitors can provide cellular protective effects, revert IAPP fibrillation-induced damages, and maintain cellular homeostasis (**Scheme 1.2.1C**). The *ex vivo* model system generally consists of the isolation of pancreatic islets from diabetic animal models and treatment with hIAPP in the absence and presence of inhibitor compounds. In this case, anti-fibrillation activity is evaluated via the glucose-stimulated insulin secretion assay to evaluate the effect on β-cell restoration.[58] Finally, *in vivo* animal models are used to observe the effects of anti-fibrillation compounds on glucose tolerance, presence of intracellular and extracellular IAPP fibrils, and insulin sensitivity (**Scheme 1.2.1D**).[59]

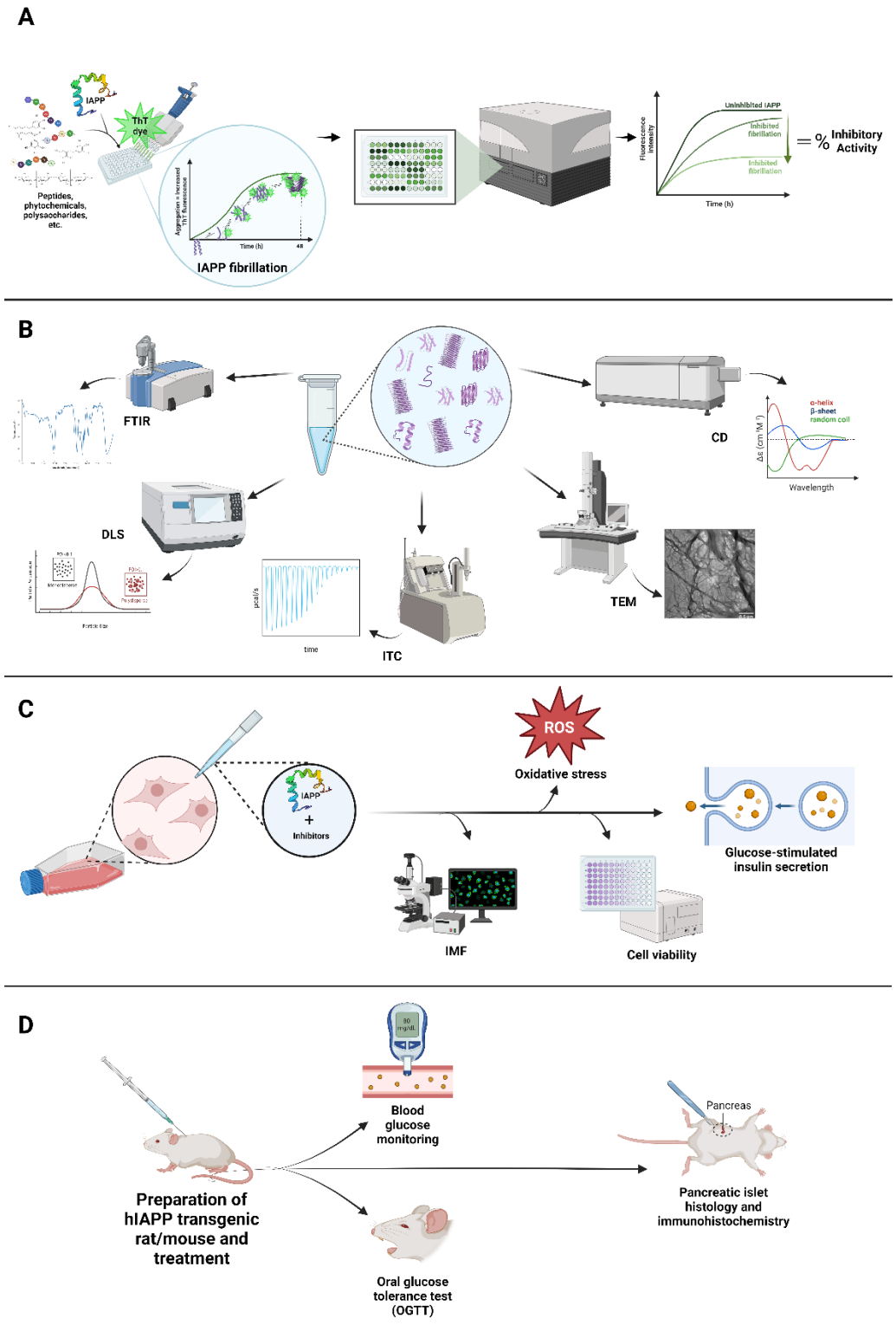

Scheme 1.2.1. (A) ThT fluorescence assay used for the identification of anti-fibrillation compounds. **(B)** The effect of the inhibitors on IAPP fibrillation can be characterized via secondary structure determination using Fourier-transform infrared (FTIR) or circular dichroism (CD). The

extent of inhibitor binding can be characterized using isothermal calorimetry (ITC). The resulting fibrillar species can be assessed using dynamic light scattering (DLS) and visualized using various spectroscopic methods such as transmission electron microscopy (TEM). **(C)** *In vitro* cell culture studies using rat insulinoma β-cells can be used to evaluate the effects of anti-fibrillation compounds on β-cell morphology using immunofluorescence microscopy (IMF) and functionality (oxidative stress and glucose-stimulated insulin secretion). **(D)** *In vivo* transgenic mouse or rat models can be used to understand the role of IAPP fibrillation inhibition on blood glucose regulation or on pancreatic β-cell morphology.

1.2.2 MECHANISMS OF INHIBITION OF IAPP FIBRIL FORMATION

Aromatic and π-π interactions have been hypothesized to play an instrumental role in IAPP fibrillation.[53–56] As a result, potential agents that can compete with the major interactions governing fibril formation have been extensively studied. Preventing these interactions can lead to the inhibition of fibril formation and mitigation of the deleterious effects of IAPP aggregation on pancreatic β-cells. Consequently, inhibitors of IAPP fibrillation can be used in preventing and managing T2D.

1.2.2.1 Peptides

Peptides have been attracting increasing interest as natural inhibitors of IAPP fibrillation, toward the management, prevention, or treatment of T2D. This group of inhibitors are produced specifically to target IAPP or can also be cross-reactive peptides that are repurposed for fibrillation inhibition. Nonetheless, the peptides interact with some conformation of IAPP and induce local changes, promoting the monomeric and other less harmful IAPP conformations in the process.

The use of hairpin peptides provides a novel approach to peptide-based fibrillation inhibition which, until then, had been explored using hIAPP-derived peptide truncations with additional modifications.[17,60] Through these studies, tyrosine and tryptophan-rich peptides were observed to be more effective at fibrillation inhibition, likely as a result of the aromatic moieties allowing for the formation of π-π interactions with the aromatic residues of hIAPP.[17] In this approach, the cyclized *β*-hairpin, cyclo-WW2, mimics the secondary structure that commonly occurs in early stages of aggregation in the fibrillation pathway, subsequently competing with the self-association propensity of IAPP. Aryl-rings of the *β*-hairpin allows for its more favorable

binding to the hydrophobic hot spots of IAPP compared to the self-association with other IAPP monomers, thus inhibiting subsequent aggregation.[60] The added stability of the inhibitor by way of cyclization further increases its potent inhibitory effects down to substoichiometric levels of inhibitor concentration.[17] Cyclo-WW2 appears to be a general fibrillation inhibitor as favorable inhibition was also observed with other amyloidogenic peptides, such as α-synuclein.[17] The study by Sivanesam et al. provided a crucial perspective on maximizing inhibitor stability and its potential role in potency, which is an important factor that should always be addressed when considering feasibility.[17]

The pentapeptide inhibitor FLPNF was originally designed to mimic the RLANF sequence of the membrane-binding domain of hIAPP, where residue substitutions were made in order to increase hydrophobicity of the peptide. The alanine residue of RLANF was substituted with a proline to prevent the pentapeptide from forming β-strands and subsequent self-assembly.[61] Based on a BLAST search, peptide FLPNF is present in several plant-based food proteins, such as soy, pigeon pea, cowpea and rice proteins. Anchoring of this peptide with monomeric hIAPP was facilitated via π-π and cation-π interactions of phenylalanine and proline, as well as hydrogen bonding afforded by the asparagine and phenylalanine residues. While it has some inhibitory effects, its potency was not enough to completely block IAPP fibrillation.[61] Based on ThT fluorescence, a novel pentapeptide, FLPNF, reduced IAPP fibrillation by 15% after 24 hours compared with control, with microscopy showing a reduced number and density of IAPP fibrils. The mechanism of action of FLPNF was likely through the binding and stabilization of monomeric IAPP, thus temporarily arresting IAPP in the lag phase for as long as possible.[61] The favorable interaction of FLPNF with IAPP was hypothesized to prevent IAPP self-association. FLPNF favorably binds (−6.4 kcal/mol) the N-terminus and amyloidogenic regions of IAPP where it interacts with Leu12, Phe15, and Ala25 via hydrophobic interactions, Lys1 and Arg11 via cation–π interactions, and Phe15 via π–π stacking interactions.[42] Furthermore, the peptide inhibitor also made contact with Asn31 of IAPP C-terminus via H-bonding. This highlights the importance of aromaticity and amphipathicity, in addition to hydrophobicity, in enhancing IAPP binding by peptide-based inhibitors. FLPNF successfully increased the viability of INS-1 rat cells in a dose-dependent manner. The peptide also demonstrated cellular protective effects against rat insulinoma (INS-1) cells by increasing cell viability by ∼20% in the presence of IAPP.[42] This effect was likely due to FLPNF associating with monomeric IAPP, thus preventing the formation of toxic oligomers

and other pre-fibrillar species. Radical scavenging studies should be considered to elucidate potential antioxidative activities of the peptide as an inhibitory mechanism.

A different approach with synthetic peptides by Xuan et al. resulted in the creation of the peptide, LA12, designed to specifically bind the amyloidogenic core of IAPP.[62] This peptide binds both residues 11–16 and 19–28 of the membrane-binding domain and α-helical region of IAPP (**Scheme 1.1.1**). LA12 functions by inserting into the key amyloidogenic sites, destabilizing parallel β-sheets and initiating disaggregation of existing fibrils. In addition, LA12 associated with monomeric IAPP at the same loci, preventing further self-aggregation by stabilizing the random coil region.[62] Consequently, a 78% reduction of fibrils was reported after 7-day incubation of IAPP fibrils with LA12 at a molar concentration ratio range of 30:1 to 50:1, LA12:amylin.[62] Based on these findings, a comprehensive mining of the food proteome stands to provide a structurally diverse array of natural peptide motifs with the potential to bind IAPP and inhibit its fibrillation.

Understanding the intrinsic interactions governing IAPP fibrillation is crucial when considering peptide-based inhibitors. Notably, identifying key interactions highlights hotspots and noncovalent interactions to be disrupted to achieve maximal inhibition. For instance, three highly conserved aromatic residues, Phe15, Phe23, and Tyr37, are proposed to enhance self-association and subsequent aggregation of IAPP via hydrophobic and π–π interactions.[63] However, the Phe23Leu substitution was less toxic and inhibited IAPP fibrillation the most out of several aromatic mutations.[63] Conversely, mutations at Phe15, Tyr37, or both residues had no effect or drastically enhanced fibrillation activity and cytotoxicity. This indicates the central role of Phe23 in IAPP fibrillation, likely because of its participation in the formation of a transient β-hairpin intermediate during fibrillation.[63] This highlights the importance in the amyloidogenic region as a domain target for potential fibrillation inhibitors. **Table 1.2.1** summarizes recent examples of food-derived peptide and polysaccharide IAPP fibrillation inhibitors, their bioactivity, and IAPP binding interaction sites.

1.2.2.2 Polysaccharides

There is limited information on polysaccharide inhibitors of IAPP fibrillation. A recent study reported that OHSS2, a green algae-derived sulfated galactoarabinan, dose-dependently inhibited IAPP fibrillation by up to 30% at 200 μg/mL.[64] The polysaccharide also increased cell viability in the presence of hIAPP by 44%. This suggests that the molecule also inhibited the

formation of toxic IAPP aggregates. hIAPP enhances reactive oxygen species (ROS) production in cells, likely contributing to oxidative stress–related comorbidities observed in late stages of T2D. However, OHSS2 diminished the IAPP fibrillation-induced intracellular ROS production and oxidative stress in mouse insulinoma (NIT-1) cells. The hIAPP fibrillation-induced inhibition of mitochondrial complexes I, II, and III activity was also restored by OHSS2 before and after treatment, indicating its protective and recovery effects on mitochondrial activity and ATP production levels.[64] The multitargeted effects of OHSS2 in decreasing IAPP fibrillation and intracellular ROS production, increasing cellular viability, and restoring mitochondrial function demonstrate the strong potential of food-derived polysaccharides as anti-fibrillation agents.

Table 1.2.1. Food-derived peptide and polysaccharide inhibitors of IAPP fibrillation and fibrillation-induced cytotoxicity.

Compound Type	Sequence/name	Source	Activity	Binding sites/interactions/residues	Ref.
Peptide	cyclo-WW2	n.d.	Fibrillation inhibition, increased cell viability	n.d.	[17]
Peptide	FLPNF	n.d.	Fibrillation inhibition	Hydrophobic interactions with Lys1, Arg11, and Phe15 of the N-terminus and hydrogen bonding with Asn31 of the C- terminus	[61]
Peptide	LA12	n.d.	Fibrillation inhibition, increased cell viability	π-electrostatic interactions with Arg11, π-hydrophobic interactions with Leu12, Leu16, and π-π stacking interactions with Phe15 of the membrane binding domain and alkyl-hydrophobic interactions with Ile26 and Leu27 of the amyloidogenic region	[62]
Polysaccharide, Sulfated galactoarabinan	OHSS2	*Cladophora oligoclada*	Fibrillation inhibition, increased cell viability, ROS production and oxidative stress inhibition, increased mitochondrial function	n.d.	[64]
Abbreviations: n.d., not determined.					

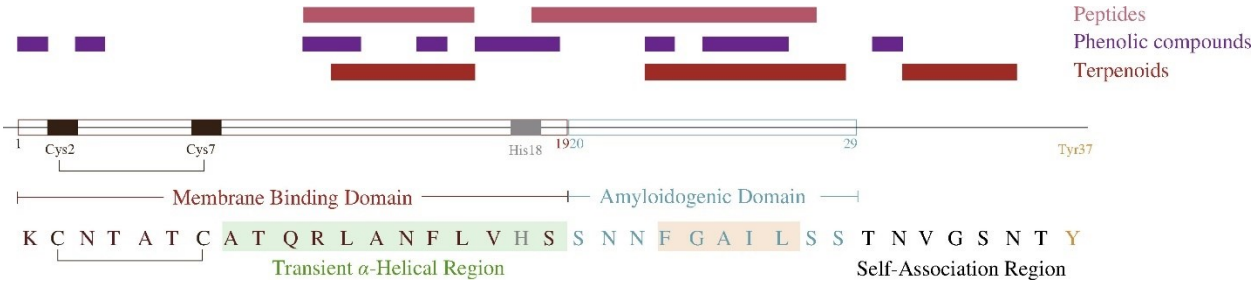

Figure 1.2.1. Domain outline of IAPP as well as inhibitor binding regions grouped by compound class. Bottom: amino acid sequence of IAPP showing the transient-helical region and amyloidogenic FGAIL region.

1.2.2.3 Phenolic compounds

Polyphenolic compounds contain aromatic rings that competitively interact with the aromatic residues of IAPP, disrupting π-π interactions and impacting IAPP self-assembly.[50] As a result, aromatic interactions are considered to be very important to the amyloidogenic process as they are used to stabilize the anti-parallel β-sheet structure.[33] Many natural and food-derived compounds containing multiple aromatic rings possess disaggregative properties that can disrupt the π-π interactions and break down of IAPP fibrils. **Table 1.2.2** outlines all polyphenolic compounds and extract with anti-fibrillation activity, along with their pharmacophores discussed in this section.

Epigallocatechin gallate (EGCG) is a well-studied polyphenol that has been repurposed as a broad inhibitor for amyloidogenic proteins and is especially functional for disaggregating IAPP fibrils.[33,65] Due to its disaggregative properties, EGCG is also able to protect rat insulinoma (INS-1) β-cells from IAPP-induced cytotoxicity. EGCG potency assays revealed that a working ratio of 2:1 to 5:1 (IAPP:EGCG) yields significant effects on lowering IAPP aggregation.[65] A multitude of interactions facilitate the binding of EGCG to hIAPP monomers, including the π-π, van der Waals, alkyl-alkyl, π-alkyl, conventional hydrogen bonds, and carbon-hydrogen bond interactions. The preferential binding site of EGCG is between the coil and helix of hIAPP, specifically at Arg11, Leu12, Ser19, Ala25, Ile26, Leu27, and Tyr37 residues (**Figure 1.2.1**).[66] Due to the strong affinity of EGCG to IAPP monomers, it is likely to successfully inhibit the formation of IAPP dimers, thus preventing aggregation at the earlier steps of self-aggregation.[66,67]

Genistein (4,5,7-trihydroxyisoflavone), a phytoestrogen from soybeans, plays a dual role in the inhibition of fibril formation of both hIAPP and Aβ.[68] Genistein exclusively binds IAPP monomers to prevent fibril formation and, upon seeding, its inhibitory abilities are effectively minimized.[68] Interaction of genistein with monomeric IAPP is facilitated through π-π interactions afforded by the two phenolic rings of this natural isoflavone compound (**Table 1.2.1**). In addition, genistein binds preferentially to the *β*-turn and N-terminal region of IAPP.[67,68] Molecular interaction simulations revealed that genistein binds to Lys1, Asn3, Arg11, Phe15, Val17, His18, Phe23, Ala25, Asn31, and Tyr37 residues of IAPP (**Figure 1.2.1**).[66] While genistein is a potent inhibitor of fibril formation at the early stages of self-assembly, it is rendered ineffective once nucleation has occurred.[68] Despite the inability of genistein to disaggregate formed fibrils, the polyphenol is still able to mitigate the cytotoxic effects of IAPP fibrils. This is accomplished through genistein-induced remodeling of IAPP fibrils into unstructured aggregates, thus reducing the cytotoxic effects on rat insulinoma (RIN-m5F) cells.[68] More research should be done to identify if other isoflavone compounds have more potent and multifaceted inhibitory mechanisms in fibril formation beyond IAPP self-aggregation inhibition.

Lycopus lucidus, from the family Lamiaceae, is commonly consumed for its role in traditional medicine, and also as food. Many compounds such as flavonoids and phenolic acids have been isolated from the rhizome and studied for their health applications.[69] Schizoteniun A, lycopic acid A, and lycopic acid B are polyphenols with catechol moieties isolated from *Lycopus lucidus* and suggested to exhibit anti-aggregative properties on hIAPP.[69] The three compounds showed extremely strong inhibitory effects on IAPP fibrillation with IC_{50} values of 0.58, < 0.01, and 0.023 μmol/L, respectively. The presence of multiple catechol moieties within their structures supports the suggestion that π-π interactions between the phenolic compounds and monomeric IAPP are more favorable than hIAPP self-association, thus resulting in potent inhibition of the lag phase.[69] Moreover, reduction of cytotoxicity was suggested given the antioxidative activities afforded by the phenolic compounds, which act as reactive oxygen species (ROS) scavengers. However, the true protective abilities of these compounds against IAPP fibril toxicity still need to be verified using cell cultures.

Rosmarinic acid, isolated from the plant *Isodon japonicus*, has been studied for its anti-aggregative properties against hIAPP fibrillation.[70] The aerial part of the plant are used as

functional food and in traditional Chinese and Japanese medicine. Rosmarinic acid and its derivative, caffeic acid, were observed to possess inhibitory abilities on IAPP fibrillation, with IC_{50} values of 3.1 and 57.6 μmol/L, respectively. As previously mentioned, polyphenols are known for their ability to inhibit aggregation *via* the disruption of the π-π interactions between the aromatic residues of monomeric IAPP. Hence, the stronger inhibitor potency observed for rosmarinic acid in the lag phase may be a result of its additional catechol moieties compared to caffeic acid. The increased aromaticity suggests the presence of a stronger affinity of rosmarinic acid for hIAPP, facilitated by an increased hydrophobic and π-π interactions. In terms of protective abilities, the compounds also acted as antioxidants, with rosmarinic acid exhibiting stronger effects than caffeic acid, thus minimizing the presence and subsequent damages and cytotoxicity caused by ROS, which become more prevalent during IAPP fibrillation.[70]

Dihydrocaffeic acid isolated from the Lycii Cortex, a dried root bark of *Lycium chinense*, commonly used as a Chinese medicinal herb, has also been reported to exhibit dose-dependent anti-aggregative properties towards IAPP.[71] The inhibition occurred through the disruption of the π-π interactions between the amyloidogenic regions of IAPP, possibly during the lag phase where the interactions most frequently occur. The IC_{50} value reported for dihydrocaffeic acid was 9.3 μmol/L, which is higher than those reported for compounds with multiple aromatic moieties, suggesting a correlation between the number of phenolic moieties present within a structure and its potency in IAPP fibrillation inhibition.[71] Interestingly, caffeic acid, a structural analogue to dihydrocaffeic acid exhibited a significantly higher IC_{50} value compared to dihydrocaffeic acid. This suggests that other moieties apart from the aromatic ring may be playing important roles in inhibitor potency. In the case of caffeic acid, the presence of α, β unsaturation seems to reduce the potency of the inhibitor, compared to dihydrocaffeic acid, possibly by introducing structural flexibility that potentially influence the stability of the IAPP-phenolic complex and thus reducing binding favorability. As a result, a decreased ability for an inhibitor to form a stable complex with IAPP would potentially diminish its sustained inhibitory role in mitigating fibrillation.

Flavonoids isolated from the halophyte *Tamarix gallica* L. have also been extensively studied for its numerous biochemical and pharmacological functions.[72] Hmidene et al. studied the effects of some of the flavonoids on mitigating IAPP fibril formation, and also the effect of flavonoids containing glucuronide moieties to provide insight on the seemingly absolute

requirement of aromatic compounds in a potent inhibitor.[72] From the studies, the strongest inhibitory activities were observed for quercetin and its glucuronide-substituted derivative (QGlcA), with IC_{50} values of 1.8 and 1.7 μmol/L, respectively. Notably, antioxidative activities used to mitigate the effects of ROS and reactive nitrogen species caused by the formation of oligomeric species should be taken into consideration when evaluating inhibitor suitability and potency. QGlcA showed a much higher antioxidant activity than quercetin.[72] While the sugar substitution itself may have enhanced the activity, it is also possible that the increased interaction with IAPP was due to the significant increase in hydroxyl groups present on the sugar moiety, or the solubility and accessibility of QGlcA compared to quercetin. As a result, the glucyronide derivative has the potential to provide a stronger protective effect on cells against damage caused by IAPP fibrillation. It is also possible that inhibition of IAPP fibril formation occurred earlier at the lag phase where the inhibitors are able to bind more favorably with monomeric IAPP, thus decreasing the favorability for self-assembly and mitigating fibril formation.[67,68]

Extracted from *Salvia miltiorrhiza* Bge or red sage, for use as functional food and medicine, the tanshinone class of compounds has been explored for their pharmacological uses in treatment of a myriad of diseases.[73] Notably, tanshinone I (TS1) and tanshinone IIA (TS2) were reported to inhibit IAPP fibrillation, disaggregate preformed fibrils, and mitigate IAPP fibrillation-induced cytotoxicity in cultured rat insulinoma cells.[73] Incubation of the tanshinone derivatives with IAPP resulted in a dose-dependent reduction in the exponential/growth phase but no effect on the lag phase, indicating that binding of the compounds does not favor the monomeric conformation.[73] While TS1 and TS2 bind to hydrophobic and aromatic residues of IAPP, the preferred binding sites are located on opposing ends of IAPP.[73] TS1 binds the N-terminal β-strand on the interior face, towards the U-bent cavity, interacting with Leu12, Ala13, Asn14, Phe23, Gly24, Ala25, and Ile26, whereas TS2 binds the exterior face of the N-terminal β-sheet at Ala13, Asn14, Phe15, and Leu16 (**Figure 1.2.1**). TS2 also exhibits favorable binding to the C-terminal β-sheet residues of Leu27, Ser28, Ser29, Val32, Gly33, Ser34, and Asn35 (**Figure 1.2.1**). The mechanisms of inhibition of TS1 and TS2 are similar in that they both prevent self-association of IAPP monomers by binding to the β-strands of IAPP sites, thus blocking elongation as well as subsequent transformation to pleated β-sheet structure, a common hallmark of IAPP fibrillation.[73] In addition to the contribution of hydrophobic interactions, charge-transfer complex interactions

mainly in the form of parallel (TS1) and T-shaped (TS2) π-π interactions were observed between the terpenoids and the aromatic residues of IAPP.[73]

Kukoamines A and B, also isolated from Lycii Cortex, are polyamine spermidine alkaloids that exhibited dose-dependent inhibitory abilities against IAPP fibrillation.[71] Potency was also likely due to the aromatic rings, which enhance binding of the alkaloids to monomeric IAPP, thus leading to a more favorable interaction than self-association with another IAPP monomer. The IC_{50} values for kukoamine A and B were 8.7 and 3.3 μmol/L, respectively.[71] Despite their effectiveness in inhibiting IAPP fibrillation, there is a dearth of information on the aggregation phases targeted by the alkaloids. However, it is reasonable to hypothesize that the compounds inhibited aggregation at the lag phase where association with monomeric IAPP is more favorable but may not be as potent in disaggregation of preformed fibrils. As both alkaloids contain the same number of catechols, the distance between the catechol moieties and the alkylamine substitution needs to be investigated to understand the interaction with IAPP hydrophobic pocket and in making the IAPP binding more favorable. Notably, the alkylamine chain might enhance binding of kukoamine B with IAPP instead of introducing stearic hindrance, especially through additional hydrogen bonding with the amine group, thus further stabilizing its interaction with IAPP and increasing its potency.

1.2.2.3.1 Structural requirements for phenolic compounds

1.2.2.3.1.1 Aromatic substitutions and stereochemistry

The degree of substitution and structural configuration of some compounds significantly affect their anti-IAPP fibrillation activity. For example, flavonolignan diastereoisomers silybin A and silybin B are *trans*-diasteroisomers with different configurations at stereocenters C-7″ and C-8″ (7″R, 8″R in silybin A and 7″S, 8″S in silybin B).[74] Silibinin, derived from milk thistle extract, comprising of equal parts of the two flanonolignan isomers, exhibited antifibrillatory effects, with silybin B having relatively more activity (60% fibrillation inhibition at 1:0.8, IAPP:ligand) and cellular protective effects than silybin A (50% fibrillation inhibition). Molecular dynamics simulation revealed more interactions of ring E in silybin B with hIAPP compared with silybin A due to the different chirality of the stereocenter at C-7″.[74] The methoxy and hydroxyl groups at C-3″ and C-7 of both diasteroisomers interact significantly with hIAPP, in addition to the hydroxyl group at C-9″ of silybin B as an additional contact with Thr4 and His18 of the N-terminus, Gly24-

Ile26 and Ser28–Ser29 of the amyloidogenic region, and Ser34-Tyr37 of the C-terminus of hIAPP.[74] Thus, the stereochemistry of silybin B allows for more contacts with IAPP, which translated to increased anti-fibrillation activity.

Biflavones polyphenolic compounds have equally highlighted the importance of structural configuration. For example, amentoflavone and bilobetin are structurally identical except for a C8 substitution of the hydroxyl group in amentoflavone with a methoxy group in bilobetin. Consequently, amentoflavone exhibited stronger anti-fibrillation and disaggregation activity with the hydroxyl group strongly binding the Phe23 of IAPP, a part of the amyloidogenic region that contributes to fibrillation.[75] In contrast, bilobetin showed minimal and weaker contacts with Phe23, hence its inability to effectively disaggregate preformed IAPP fibrils. Furthermore, both biflavones exhibited increased cell-protective effects, although amentoflavone showed a stronger effect with 82.8% cell viability compared with bilobetin with 78.1% and the untreated IAPP control with 39.5%.[75] Triterpenoid isomers, maslinic acid and momoridicin I, showed similar activity. In this case, maslinic acid exhibited more potency than momoridicin I, likely because of its carboxyl group, preventing stronger self-interactions of IAPP from occurring. Furthermore, strong inhibition and disaggregating effects have been suggested to be driven by H-bonding and disruption of hydrophobic interactions, electronic interactions, and salt-bridge formation between IAPP monomers.[76] Notwithstanding their structural differences, momoridicin I and maslinic acid inhibited IAPP fibrillation effectively, providing cellular protective effects and minimizing IAPP-induced cytotoxicity.[76]

1.2.2.3.1.2 Vicinal hydroxyl aromatic substitutions

Vicinal hydroxyl groups of polyphenols, such as luteolin, fisetin, and mangiferin, are necessary to stabilize monomeric IAPP, resulting in prolonged lag phase and inhibition of IAPP fibrillation.[77] Lag-phase elongating activity was also observed for baicalein and its aglycone, baicalin, but in this case, the aglycone exhibited stronger anti-fibrillation activity.[77] Likewise, vicinal hydroxyl group containing polyphenolic compounds, including *trans*-scirpusin B, *cis*-scirpusin B, *trans*-scirpusin A, *trans*-piceatannol, and *cis*-piceatannol, derived from passion fruit seed, exhibited strong anti-IAPP fibrillation activity with IC_{50} values of 3–4.4 μM, while *trans*-tetramethylpiceatannol, which has vicinal methoxyl substitutions on the phenyl group, had lower anti-fibrillation activity with an IC_{50} of >100 μM.[78]

1.2.2.3.1.3 Catechol moieties

Catechol moieties are important for anti-fibrillation activity and, along with redox-related quinones and anthraquinones, are known as a broad class of strong amyloid inhibitors.[79] Such effect is observed with L-clovamide and derivatives where at least one catechol moiety is required for inhibitory activity and the potency increases with increasing number of the group.[80] L-clovamide resulted in the loosening and disaggregation of preformed fibrils, and direct inhibition of IAPP fibrillation. Furthermore, for A-type procyanidins and their derivatives, the presence and number of catechol moieties correlated with anti-fibrillation activity.[81] It is possible that the quinone form inhibited aggregation by covalent bonding (Michael addition or Schiff base formation) with the nucleophilic amino acid residues of the amyloid. The changes in aggregation inhibition in relation to the number of catechol moieties are suggested to be due to this mechanism.[80] Similar anti-fibrillation and disaggregation activities were observed for some procyanidins, such as A-type procyanidins and their derivatives.[80,81] *Washingtonia filifera* seed extracts also inhibited IAPP fibrillation and some catechol-containing compounds within the extract demonstrated favorable binding energies with IAPP, that is, catechin (−6.9 kcal/mol), protocatechuic acid (−4.9 kcal/mol), *p*-hydroxybenzoic acid (−4.5 kcal/mol), and B-type procyanidin dimer (−7.8 kcal/mol).[82] This highlights the potential of plant-based foods rich in catechol-containing compounds in developing novel anti-fibrillation nutraceuticals.

1.2.2.3.2 Polyphenols in pancreatic β-cell protection

Polyphenols have been largely identified to possess dose-dependent protective effects on pancreatic β-cells, especially in minimizing oxidative stress.[83,84] EGCG, cinnamon and red wine polyphenols were previously reported to exert hypoglycemic effects through the modulation of oxidative stress.[83,84] While the mechanisms of these polyphenols in relation to β-cell protection have been studied primarily in the context of their antioxidative abilities, further investigations linking the role of polyphenols in mitigating antioxidative stress and IAPP fibrillation should be considered. This is important given that the phenolic compounds have demonstrated IAPP binding activities *in vitro* and beneficial roles in glucose metabolism, suggesting a potential link between the two properties.[85] Furthermore, IAPP fibril formation induces cellular oxidative stress, which suggests a potential antioxidative mechanism of phenolic compounds in inhibiting IAPP fibrillation and β-cell toxicity.[86]

Table 1.2.2. Structure of natural IAPP fibrillation inhibiting compounds from different sources. Natural phenolic inhibitors of IAPP fibrillation, IAPP-induced oxidation, and fibrillation-based cellular toxicity.

Compound (food sources)	Class	Structure	Activity	Binding sites/interactions/residues	Pharmacophore	Ref.
Epigallocatechin gallate (green tea)	Catechin	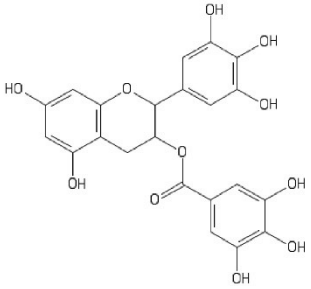	Fibrillation inhibition, disaggregation of preformed fibrils, increased cell viability	Binding facilitated with π-π, Van der Waals, alkyl, π-alkyl, H-bonding, and carbon-hydrogen bond interactions. Interacts specifically with Arg11, Leu12, and Ser19 of the membrane binding domain, Ala25, Ile26, and Leu27 of the amyloidogenic region, and Tyr37 residue in the C-terminal domain	Catechol	[33,65–67]
Genistein (Soybean)	Isoflavone	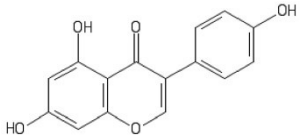	Fibrillation inhibition, increased cell viability	Preferentially binds the membrane-binding domain via π-π interactions with Lys1, Asn3, Arg11, Phe15, Val17, and His18. Also interacts with Phe23 and Ala25 of the amyloidogenic region, and Asn31 and Tyr37 of the C-terminal domain.	Chromen-4-one	[68]

Schizoteniun A (*Lycopus lucidus)*	Alkaloid	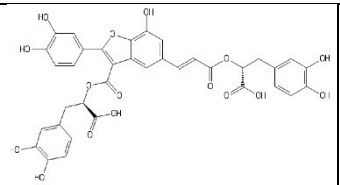	Fibrillation inhibition	Binding facilitated by π-π interactions	Catechol	[69]
Lycopic acid A (*Lycopus lucidus)*	Sesquiterpene	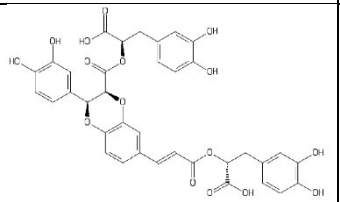	Fibrillation inhibition	Binding facilitated by π-π interactions	Catechol	[69]
Lycopic acid B (*Lycopus lucidus)*	Sesquiterpene	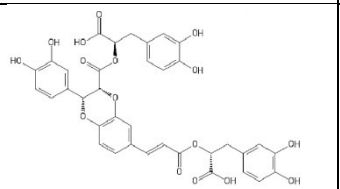	Fibrillation inhibition	Binding facilitated by π-π interactions	Catechol	[69]
Rosmarinic acid (*Isodon japonicus)*	Polyphenolic acid	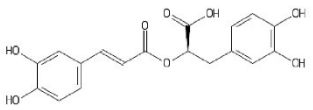	Fibrillation inhibition	n.d.	Catechol	[70]
Caffeic acid (*Isodon japonicus)*	Phenolic acid	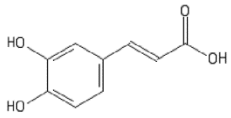	Fibrillation inhibition	n.d.	Catechol	[70]
Dihydrocaffeic acid (*Lycium chinense,* Lycii Cortex)	Phenolic acid	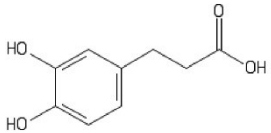	Fibrillation inhibition	n.d.	Catechol, fully saturated hydroxypropyl side chain	[71]

Quercetin (*Isodon japonicus*)	Flavonoid	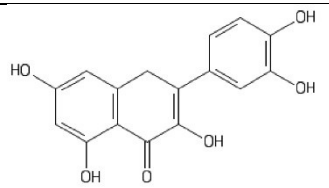	Fibrillation inhibition	n.d.	Catechol	[72]
Quercetin glucuronide-substituted derivative, QGlcA (*Isodon japonicus*)	Flavonoid glycoside	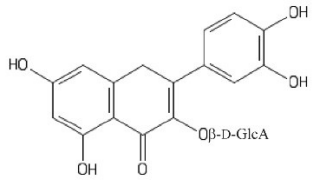	Fibrillation inhibition	n.d.	Catechol, bulk (glucyronide moiety)	[72]
Tanshinone I, TS1 (*Salvia miltiorrhiza* Bge)	Diterpenoid	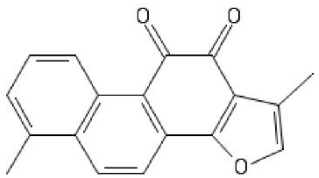	Fibrillation inhibition, disaggregation of preformed fibrils, increased cell viability	Binds the N-terminal β-strand on the interior face, interacting with Leu12, Ala13, and Asn14 of the membrane-binding domain, and Phe23, Gly24, Ala25, and Ile26 of the amyloidogenic region. Binding facilitated by hydrophobic, π-π, and charge-transfer complex interactions.	Bulk (phenanthrene backbone)	[73]
Tanshinone IIA, TS2 (*Salvia miltiorrhiza* Bge)	Diterpenoid	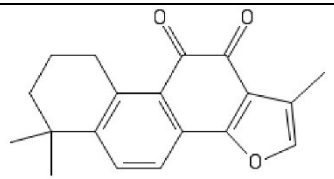	Fibrillation inhibition, disaggregation of preformed fibrils, increased cell viability	Binding facilitated by hydrophobic, π-π, and charge-transfer complex interactions. Binds the exterior face of the N-terminal *β*-sheet at Ala13, Asn14,	Bulk (phenanthrene backbone)	[73]

				Phe15, and Leu16, the amyloidogenic region with Leu27, Ser28, and Ser29, and in the C-terminal domain with Val32, Gly33, Ser34, and Asn35.		
Kukoamine A (*Lycium chinense,* Lycii Cortex)	Alkaloids	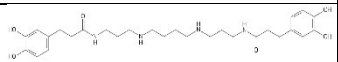	Fibrillation inhibition	n.d.	Catechol	[71]
Kukoamine B (*Lycium chinense,* Lycii Cortex)	Alkaloids	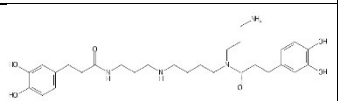	Fibrillation inhibition	n.d.	Catechol, bulk (alkylamine chain)	[71]
Silybin-A (milk thistle extract)	Flavonolignan	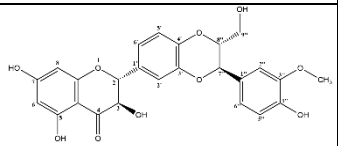	Fibrillation inhibition, increased cell viability	Primary contacts with Arg11 and surrounding residues (Ala8-Thr9 and Gln10, Leu12) in the N-terminus	Methoxy and hydroxyl groups in positions C-3′ and C-7	[25]
Silybin-B (milk thistle extract)	Flavonolignan	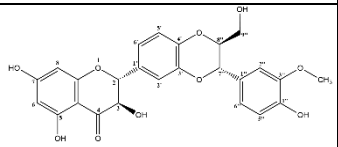	Fibrillation inhibition, increased cell viability	Same contacts as silybin-A as well as secondary interaction hotspots with Phe23 and surrounding residues (S20- Asn22 and Ile26-Leu27) within the amyloidogenic core of IAPP	Methoxy group in position C-3″ and the hydroxyl groups in positions C-7 and 9″	[25]

Amentoflavone (*Selaginella tamariscina*, *Selaginella rupestris*, and *Ginko biloba*)	Biflavone	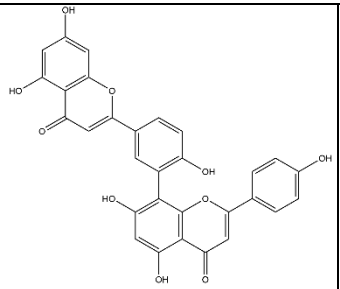	Fibrillation inhibition, disaggregation of preformed fibrils, decreased peptide oligomerization, increased cell protective effects	H-bonding of the compound with Asn22, Gly24, Ile26, Ser28 of the amyloidogenic region, hydrophobic interactions with Ala25, Ile26, Phe23, and Leu27, some π–π interactions with aromatic residues	Hydroxyl substitution on C8	[26]
Bilobetin (*Ginko biloba*)	Biflavone	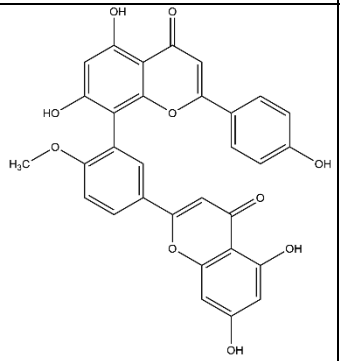	Fibrillation inhibition, decreased peptide oligomerization, increased cell protective effects	H-bonding of the compound with Asn22, Ser28, Ala25, and Ile26 of the amyloidogenic region, hydrophobic interactions with Ala25, Ile26, Phe23, and Leu27, some π–π interactions with aromatic residues	Methyloxyl substitution on C8	[26]
Maslinic acid (olive, loquat leaves, red dates, eucalyptus, crape myrtle, sage, plantain, *Prunella vulgaris*, spiny leaf dong)	Triterpenoid	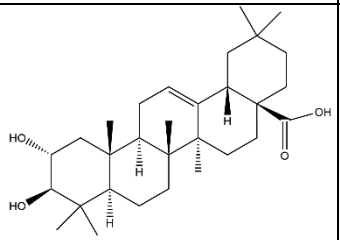	Fibrillation inhibition, disaggregation of preformed fibrils, increased cell viability and cell protective effects, reduction in hIAPP	H-bonding with oxygen atoms (O1 and O2) acting as donors to Asn21 and Asn22 residues in the amyloidogenic region, hydrophobic interactions with Val32, possible electronic interactions and salt-bridge formation	Carboxyl group, bulk	[27]

			oligomer formation			
Momordicin I (*Momordica charantia* L. *J. Kimia*)	Triterpenoid	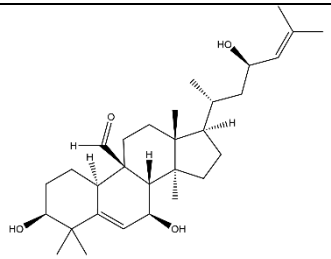	Fibrillation inhibition, disaggregation of preformed fibrils, increased cell viability and cell protective effects, reduction in hIAPP oligomer formation	H-bonding with the oxygen atoms (O1 and O4) acting as donors to Asn14 and Asn21 residues while O2 acted as a H-bond acceptor from Asn14 in the amyloidogenic region, hydrophobic interactions with Ala25, possible electronic interactions and salt-bridge formation	Bulk	[27]
Baicalin and baicalein (Scutellaria baicalensis Georgi)	Extract – flavonoids	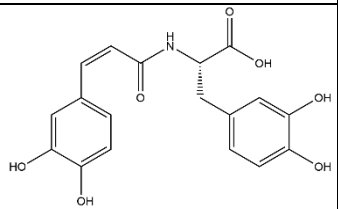	Fibrillation inhibition at nucleation phase via monomeric IAPP stabilization, increased cell viability	n.d.	Vicinal hydroxyl groups on the phenyl ring	[28]

L-Clovamide (cocoa bean-derived)	Polyphenol	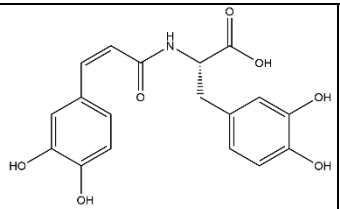	Fibrillation inhibition, disaggregation of preformed fibrils	IC_{50} of 6.2 μM on hIAPP aggregation and 5.1 μM on preformed hIAPP fibril disaggregation; Michael addition or Schiff base reaction with nucleophilic amino acid residues to form complexes that inhibit fibrillation or disaggregate preformed fibrils	Catechol	[36]
Procyanidins, A-type procyanidins, and derivatives (fruits, cereals, beans, and nuts)	Polyphenol	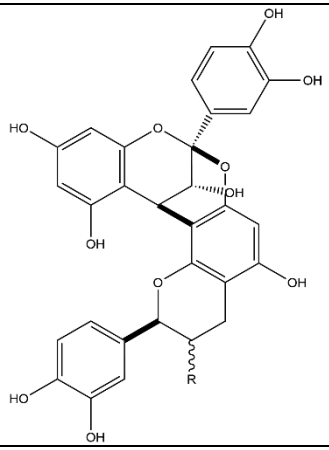	Fibrillation inhibition, disaggregation of preformed fibrils	n.d.	Catechol, bulk	[37]
Abbreviations: n.d., not determined						

1.2.3 CONCLUSIONS AND FUTURE DIRECTIONS

The shift to identifying natural or food-derived compounds as a treatment for T2D via the inhibition of IAPP fibril formation has several benefits, especially considering the relative safety of these compounds compared to synthetic drugs. However, there are potential drawbacks. Polyphenolic compounds, for example, are generally not very soluble, posing difficulties in choosing their delivery vehicles. In addition, they may have low bioavailability, thus higher concentrations would be ingested in order to observe beneficial effects. For the most part, these issues have not been specifically studied for IAPP-induced toxicity and will need to be taken into consideration when elucidating the practicality of using natural compounds for controlling the prevalence of IAPP fibrils. Future investigations should also be considered in identifying the governing mechanisms behind IAPP cytotoxicity as it can allow for deliberate targeted treatments. Understanding the governing interactions controlling fibril assembly, particularly in elucidating the importance of hydrophobic and π-π stacking in fibril formation, would be beneficial in identifying the modes of inhibition. Furthermore, a majority of the proposed natural and food-derived inhibitors need to be evaluated *in vivo* to validate their appropriateness as candidates for controlling IAPP fibril formation and T2D treatment. In addition to aromatic moieties that are thought to play an important role in the disruption of π-π interactions between monomeric IAPP, the contribution of other structural factors in inhibitor potency should be investigated through rational design and structure-function relationship studies. Lastly, there is a disproportionate focus of research on the inhibition of IAPP fibrils and little focus on preventative measures. Particularly, there is a need to understand the mechanisms that trigger IAPP misfolding and dimerization with other misfolded IAPP monomers, and the role of the natural and food-derived compounds at these early stages. A combination of the preventative and treatment approaches with natural and food-derived compounds promises to provide a powerful, safer and effective approach for controlling IAPP fibril formation towards the prevention, management and treatment of T2D.

SECTION 1.3

Potential approaches for mitigating islet amyloid polypeptide fibrillation by nutraceuticals

Excerpt from

Structural basis and functional significance of food-derived inhibitors of islet amyloid polypeptide fibrillation towards antidiabetic effects

Raliat O. Abioye and Chibuike C. Udenigwe
Current Opinions in Food Science, **2024**, *56(2024)*, 101146.

https://doi.org/10.1016/j.cofs.2024.101146

1.3.1. POTENTIAL APPROACHES FOR MITIGATING ISLET AMYLOID POLYPEPTIDE FIBRILLATION BY NUTRACEUTICALS

IAPP is largely understudied as a target for T2D management using nutraceuticals, considering its instrumental role in disease progression through uncontrolled expression, processing, and turnover, resulting in significant deleterious effects on pancreatic β cells.[6] Here, we offer some suggestions on promising approaches that should be explored for mitigating IAPP fibrillation using food-derived compounds, beyond the classic direct binding, for IAPP regulation.

1.3.1.1. Role of IAPP anti-fibrillation compounds and antioxidative activity

To evaluate anti-fibrillation activity, ThT fluorescence kinetic assay is commonly used followed by binding interaction studies, such as fluorescence spectroscopy, circular dichroism, molecular docking, and molecular dynamics simulations. Considering that T2D is a multifaceted disease and oxidative stress plays a significant role in its progression, IAPP interactions and fibrillation mitigation are only half the story. Thus, future studies are needed to understand the β-cell protective effects of fibrillation inhibitors in the presence of IAPP. This is crucial because *in vitro* bioactivity does not guarantee physiological effects or improved prognosis. As such, anti-fibrillation ThT assays should be followed up with biomolecular interaction studies, assessment of effect on oxidative stress triggered by IAPP fibrillation intermediates, mitochondrial function and recovery (related to oxidative stress), effect on membrane integrity, activation of inflammasomes, promotion of apoptosis via procaspase 3 cleavage, β-cell viability, and ROS generation in the presence of these compounds. These assessments would provide more comprehensive evidence to support the antidiabetic effects of nutraceutical compounds via reduced IAPP fibrillation.

1.3.1.2. Potential mechanism of multitarget antidiabetic compounds

A myriad of food-derived compounds have been extensively studied for their antidiabetic properties, for example, through the inhibition of classic targets such as α-amylase, α-glucosidase, and DPP-IV.[87,88] Some of these compounds have also shown glucose-regulating effects *in vivo*. However, IAPP has not been considered as the main antidiabetic target. Thus, future research should focus on the anti-IAPP fibrillation potential of previously identified antidiabetic nutraceutical compounds toward a multitargeted approach to glucose regulation and T2D prevention and management.

1.3.1.3. Role of food-derived compounds in autophagy and the unfolded protein response in IAPP regulation and T2D pathogenesis

Cell cycle progression 1 (CCPG1) was identified as an endoplasmic reticulum (ER) autophagy receptor protein that mediates IAPP degradation in mammalian cells.[89] Therefore, CCPG1 and the unfolded protein response (via the ER-associated degradation) could be transcriptionally regulated by nutraceutical compounds to control IAPP degradation. Furthermore, polyphenols from various food sources have been shown to induce autophagy *in vitro* in human cells and *in vivo* in mouse models, which may be connected to IAPP degradation.[90] The anti-fibrillation peptide, FLPNF, also demonstrated autophagy-stimulating activity, increasing the autophagy flux, thereby promoting hIAPP oligomer degradation.[91] Thus, enhancing IAPP autophagic degradation by nutraceutical compounds is a promising area for future studies.

1.3.1.4. Biostability and bioavailability of antidiabetic compounds

The use of food as a source of antidiabetic compounds offers many benefits when considering safety and affordability for use in T2D disease management. However, it also poses challenges in biostability and bioaccessibility. It is possible that the extent of anti-fibrillation activity, cellular protective effects, and β-cell regulation observed *in vitro* may not directly correspond with physiological effect after human consumption. This is because considerations for off-target effects, exposure to digestive enzymes, and inefficient uptake can significantly decrease the physiological concentration of the food-derived compounds to levels where their bioactivity is diminished or lost. For example, rutin demonstrated potent anti-fibrillation activity, provided by the bulky glycosidic moiety that blocks subsequent fibrillar elongation upon rutin–IAPP complexation.[92] However, rutin is poorly absorbed in the small intestine of humans and is more readily metabolized into its aglycone derivative, quercetin. As a result, the potency of the inhibitory activity is also diminished in the quercetin derivative relative to rutin.[92] Thus, drug delivery methods and other avenues to increase biostability and bioavailability should be considered.

1.3.2. CONCLUSION

IAPP fibrillation plays an instrumental role in T2D, making it an attractive target in mitigating disease development. Despite emerging research, IAPP is still largely underexplored as a physiological target of T2D compared with glucose-metabolizing enzymes, such as α-

glucosidase, α-amylase, and DPP-IV. Nonetheless, several food-derived polyphenols, peptides, and carbohydrates possess anti-IAPP fibrillation activity. The structure, conformation, and composition of the compounds strongly dictate the extent of IAPP binding and anti-fibrillation effect. Furthermore, other targets beyond the amyloidogenic region of IAPP, including the self-associating C-terminus and the membrane binding N-terminus, are equally important for inhibitor binding to reduce fibrillation. Future research should focus on expanding the inhibitor characterization beyond the classic anti-fibrillation activity to consider their effect on IAPP-mediated ROS production and oxidative stress, as well as cell membrane integrity and mitochondrial recovery. Given the wide range of food compounds with antidiabetic activity, future studies should elucidate if their glucose-regulating function is mediated via reduced IAPP fibrillation. Additionally, the use of food-derived compounds in regulating unfolded, misfolded, or aggregated IAPP turnover is highly recommended for future research. Finally, consideration should be given to the biostability and bioavailability of anti-fibrillation compounds to ensure translatability in T2D disease treatment.

SECTION 1.4. RESEARCH GAPS AND PROJECT NOVELTY

A multitude of anti-fibrillation compounds have been identified from various sources and, to some extent, their mechanisms of inhibition have also been assessed. Furthermore, systematic mutational studies have proposed the amyloidogenic region as the main region of fibrillation and hence, the expected target of anti-fibrillation compounds[93–95] To date, an increasing amount of research has gone into the identification of natural polyphenolic compounds, from diverse sources with varying extents of inhibitory activities against IAPP fibrillation.[67,96] While considerable efforts have gone into understanding the potential anti-fibrillation mechanisms of these phenolic compounds by considering potential binding sites to IAPP, the consideration for the role of inhibitor structure on activity is not always considered.[97] As a result, the relationship between structure and function of anti-fibrillation compounds and understanding general physicochemical properties that contribute positively to activity, is still unclear. Hence, additional research into understanding the governing interactions controlling anti-fibrillation activity, especially when it comes to interfering with π-π stacking and hydrophobic interactions, needs further considerations. Gaining a better understanding of these concepts will allow for a more systematic approach to the identification or production of novel anti-fibrillation compounds for T2D prevention and treatment.

The first part of this thesis addresses these research gaps through the screening of diverse polyphenolic compounds for their anti-fibrillation activity. Subsequent analyses in understanding the role of structure on activity by selecting structurally unique polyphenols, gallic acid, caffeic acid, rutin, and quercetin, allowed for the identification of structural features, and more targeted mechanism for anti-fibrillation activity. This provides valuable insights into the ideal phenolic inhibitors and intermolecular interactions supporting their effects on IAPP fibrillation. Apart from impaired bioavailability, the challenge with polyphenols is their enhanced susceptibility to degradation by metabolic enzymes in the gastrointestinal phase. Given the metabolic nature of this disease, this is an important consideration for anti-fibrillating compounds. As such, the effect of digestion on anti-fibrillation activity was explored using rutin and the aglycone derivative, quercetin, as a model.

Natural anti-fibrillating peptides from food sources are scarce. To date, only a few unmodified peptides have been reported to have anti-fibrillation activities against IAPP.[61,98]

Equally, their structural requirements for anti-fibrillation peptides are equally understudied. This underscores the need for the identification of anti-fibrillating natural peptides. An understanding of their structure-function relationships will also provide important insights into structural motifs that can enhance anti-fibrillation activity. The second part of this thesis seeks to fill this gap by identifying anti-fibrillation peptides from screening random peptides, and then selecting inhibitors to understand how binding interactions with IAPP influences activity and fibrillating kinetics.

IAPP fibrillation significantly impacts the health and functionality of β-cells, which is crucial in the context of T2D, multifaceted disease.[6,99,100] Therefore, translating anti-fibrillation effect of compounds in cellular environments provides an understanding of their cytoprotective effects, and their role in mitigating IAPP fibrillation-induced cytotoxicity. It also highlights the importance of the membrane-binding domain in β-cell toxicity; however, this region is largely overlooked when considering anti-fibrillation activity. Hence, for the third part of this thesis, the selected peptides were studied for their effects in maintaining cellular membrane integrity and inhibiting IAPP fibrillation-induced β-cell toxicity. These activities are related to the differential binding behaviors of each peptide to provide novel perspective on the role of IAPP domains in IAPP fibrillation and associated cytotoxicity.

Additionally, multi-functional inhibitors or dual inhibitor systems to effectively prevent IAPP fibrillation, and their downstream deleterious effects have not been considered for these applications. This is especially important, considering the multifactorial aspects of T2D prognosis. Given that the large extent of IAPP fibrillation-induced cytotoxicity is due to the downstream implications of membrane interactions and impacts on membrane integrity, it is highly relevant to understanding how inhibitor binding can mitigate these effects. The final part of this thesis addresses dual inhibitor systems and the role of anti-fibrillation compounds on cellular protective effects. Furthermore, the physiological implications of anti-fibrillation activity on pancreatic β-cell functionality were considered.

SECTION 1.5. RESEARCH QUESTIONS

Based on research gaps highlighted in **section 1.3**, the following research questions helped shape the main idea of this study:

1. What are the structural requirements of anti-fibrillation polyphenols in preventing IAPP fibrillation?
2. How does the biostability (metabolism) of polyphenols affect anti-fibrillation activity?
3. What are the structural requirements of peptides and are π-π interactions really the driving force behind anti-fibrillation activity?
4. The amyloidogenic region of IAPP is commonly targeted for anti-fibrillation compounds. Is the ability for compounds to bind this region the main determinant of the potency of an inhibitor?
5. How does region-specific binding of anti-fibrillation compounds influence cellular protective effects against IAPP fibrillation-induced membrane damage and cytotoxicity?
6. What are the effects of dual inhibitor systems on anti-fibrillation activity, and how do peptide-polyphenol interactions play a role?
7. What are the physiological implications of anti-fibrillation activity on β-cell functionality?
8. In considering dual inhibition to enhance anti-fibrillation activity, beyond anti-fibrillation activity what are other important considerations surrounding IAPP fibrillation-induced toxicity?

SECTION 1.6. AIM OF STUDY

The aim of this thesis is to understand the structural basis and activity of food-derived anti-fibrillation compounds, and their effects on mitigating IAPP fibrillation-induced β-cell dysfunction and toxicity.

SECTION 1.7. SIGNIFICANCE OF STUDY

This study provided a comprehensive review of the existing natural phytochemicals with anti-fibrillation properties and proposes some structural features of polyphenols, peptides, and polysaccharide that contribute to enhancing activity. This thesis follows up on the hypotheses outlined in the review, in studying the effect of structurally diverse polyphenols on anti-fibrillation to uncover the effect of biostability on inhibiting IAPP fibrillation by using rutin and quercetin as a model. The second aspect of this thesis sought to expand the list of known anti-fibrillation peptides by screening random peptides for bioactivity. The binding interactions between the peptides and IAPP were elucidated and used to understand their role in activity. Furthermore, the

third aspect of this thesis explored the effect of peptide-IAPP regional binding in maintaining β-cell membrane integrity and fibrillation-induced toxicity. This study highlighted the role of regional binding on activity and provided novel perspectives on the importance of the membrane-binding and C-terminal self-association domain on IAPP fibrillation and associated β-cell toxicity. The final study, to our knowledge, is the first time a dual inhibition system is applied towards IAPP fibrillation. This research provides important perspectives on the potential of multifunctional compounds and their role in reverting the deleterious effects associated with IAPP fibrillation on β-cell viability and functionality. Overall findings from these studies expands existing knowledge about anti-fibrillation compounds, particularly considering structure-activity relationships, IAPP binding interactions, and the resulting effect on mitigating IAPP fibrillation-induced cytotoxicity.

SECTION 1.8. THESIS LAYOUT

The chapters of this thesis addressed the various research objectives comprehensively as follows:

Chapter two addressed the first objective by screening various polyphenols for potential anti-fibrillation activity, and then selecting structurally different compounds to understand the role of structure on activity. Furthermore, the effect of biostability on activity was considered by using rutin and its metabolite, quercetin, as a model.

Chapter three addressed the second objective of expanding the amount of known peptide fibrillation inhibitors by screening a peptide library for anti-fibrillation activity. Binding interaction studies highlighted the effect of regional IAPP binding on activity.

Chapter four followed up on the previous study by elucidating the effects of regional IAPP binding on maintaining membrane integrity and IAPP fibrillation-induced β-cell toxicity.

Chapter five addressed the final goal by considering the effect of dual inhibition systems and peptide-polyphenol interactions on anti-fibrillation activity. These activities were also applied to pancreatic β-cells to understand their effect in maintaining cell viability and functionality in the presence of IAPP and provides insights into the importance of multifunctional compounds in IAPP fibrillation inhibition.

The conclusion is given in **Chapter six**, along with a summary of the major discoveries from this study, and suggestions for further investigation.

CHAPTER TWO

IDENTIFICATION OF ISLET AMYLOID POLYPEPTIDE ANTI-FIBRILLATION POLYPHENOLS: THE ROLE OF STRUCTURE AND BIOSTABILITY ON FUNCTION

Inhibition of islet amyloid polypeptide fibrillation by structurally diverse phenolic compounds and fibril disaggregation potential of rutin and quercetin

Raliat O. Abioye and Chibuike C. Udenigwe
Journal of Agricultural and Food Chemistry, **2022**, *70(1)*, 392-402.

https://doi.org/10.1021/acs.jafc.1c06918

DECLARATION FOR THESIS CHAPTER TWO

Inhibition of islet amyloid polypeptide fibrillation by structurally diverse phenolic compounds and fibril disaggregation potential of rutin and quercetin

This is to declare that there is no conflict of interest associated with this work and the contribution of the candidate is stated below:

Candidate's contribution	Conceptualization, methodology, validation, formal analysis, investigation, writing, review and editing, and visualization	80%

The following co-authors attest to the candidate's participation in a group publication as a component of their thesis and was active in the creation of this publication. The co-author's permission is as follows:

Name	Signature	Date
Ogadimma D. Okagu		
Chibuike C. Udenigwe		

2.0. Abstract

The influence of 12 food-derived phenolic compounds on islet amyloid polypeptide (IAPP) fibrillation was investigated. Results from thioflavin T assay demonstrated that gallic acid, caffeic acid, and rutin and its aglycone, quercetin, inhibited IAPP fibrillation at 1:0.5, 1:1, and 1:2 IAPP-phenolic molar ratios. Circular dichroism and dynamic light scattering at the 1:1 IAPP-phenolic ratio confirmed the inhibition of fibril formation. Rutin and quercetin increased the lag time by 90 and 6%, and the relative α-helix content by 63 and 48%, respectively. Gallic acid decreased the elongation rate by 30%, whereas caffeic acid decreased the maximum fluorescence intensity by 65%. Furthermore, fluorescence microscopy and transmission electron microscopy (TEM) showed IAPP fibril morphologies indicative of fibrillation reduction by the compounds. Molecular docking and TEM showed that rutin and quercetin disaggregated preformed IAPP fibrils potentially through fibrillar–monomeric equilibrium shifts. These findings demonstrate important structural features of phenolic compounds for disaggregating IAPP fibrils or inhibiting their formation.

Keywords: islet amyloid polypeptide; fibril formation; phenolic compounds; aggregation; disaggregation; structure−activity relationship

2.1. Introduction

Islet amyloid polypeptide (IAPP), or amylin, is a hormonal, 37-residue polypeptide that functions primarily in postprandial glucose metabolism.[4,101] Co-produced and co-packaged along with insulin by the β-cells of the pancreatic Islets of Langerhans, IAPP plays an instrumental role in regulating blood glucose levels.[102] Aggregation of IAPP has been implicated in the further exacerbation of type-2 diabetes. In fact, IAPP fibrillation occurs in 90–95% of patients with T2D.[6,7,103] Consequently, IAPP fibrillation has been identified to play an instrumental role in the loss of β-cell mass, resulting in the worsening of T2DM prognosis.[104] Despite its common prevalence in patients with T2DM, medication for treating IAPP fibrillation currently does not exist. Furthermore, antidiabetic drugs that target β-cells for the upregulation of insulin production inadvertently result in IAPP production, thus increasing the likelihood for subsequent IAPP fibrillation.

IAPP mature insoluble fibrils are highly cytotoxic to pancreatic β-cells due to their ability to permeate the membrane of β-cells, thus reducing membrane integrity through mechanical stress,

increasing the presence of reactive oxidative species, disrupting ion homeostasis and signal transduction, and directly activating enzymes involved in cell death, among other deleterious effects.[4,6,100,105,106] Alternatively, cytotoxicity could be a result of the formation of transient soluble preamyloid oligomeric species, which are able to disrupt and permeabilize cell membranes through the formation of pores.[86] This is particularly the case with many intrinsically disordered proteins in membrane models. Notably, anchoring of the peptide monomers to the membrane, via the membrane-binding domain in the case of IAPP, allows for subsequent dimerization and rapid formation of oligomeric β-sheet species.[9,107,108] Membrane disruption via prefibrillar species is electrostatically driven whereby the prefibrillar species embed within one side of the bilayer, effectively disrupting lipid packing while enhancing the dysregulated flow of water, ions, and small molecules across the bilayer.[107] This causes an imbalance in Ca^{2+} influx and triggers apoptotic pathways.[4,107] Regardless of how inert fibrillar IAPP is sometimes portrayed, secondary nucleation caused by the fragmentation of mature fibrils can still give rise to oligomeric species in the presence of membrane lipids.[107–109] Therefore, it is imperative to discover IAPP-targeting inhibitors that discourage fibrillation for the prevention, management, and treatment of T2D.

Given the central role of IAPP in T2D, natural inhibitors of IAPP fibrillation, such as phenolic compounds, terpenoids, alkaloids, and peptides, have been reported.[4,8,110,111] It is likely that IAPP fibrillation inhibition contributes as an antidiabetic mechanism of these compounds, especially the food-derived phenolic compounds. For instance, rutin, a flavonol glycoside, has been noted for its drug-like antidiabetic effects in mice and as one of the most active flavonoids in improving glucose tolerance and reducing fasting blood glucose and serum lipid levels.[112] Gallic acid has also been reported to increase glucose tolerance and regenerate pancreatic islet β-cells in mice models of T2D.[113] While the exact anti-diabetic mechanism of gallic acid has not been fully elucidated, it is believed to play an important role in normalizing biochemical parameters related to T2D, such as increasing plasma insulin, C-peptide, and glucose tolerance levels.[114] Last, caffeic acid has demonstrated antidiabetic effects through its protective effects on β-cells via gene regulation.[115]

Despite the structural diversity of natural polyphenolic inhibitors of IAPP fibrillation, their structure–function relationship is still not clear. Understanding these concepts will allow for the identification of more targeted mechanisms of natural inhibitors for T2DM prevention and

treatment. Therefore, the objectives of this study were to investigate (i) structurally diverse food-derived phenolic compounds for the inhibition of IAPP fibrillation and (ii) the structure–function aspects of selected phenolic inhibitors to understand the criteria that govern inhibition mechanisms of fibrillation. The study provides valuable insights into the ideal phenolic inhibitors and intermolecular interactions supporting their effects on IAPP fibrillation.

2.2. Materials and Methods

2.2.1. Chemicals and Reagents

Human IAPP [amylin (1–37), human, >95% pure] containing an amidated C-terminus and Cys2-Cys7 disulfide bond was purchased from AnaSpec (Fremont, CA). 1,1,1,3,3,3-Hexafluoro-2-propanol (HFIP), ThT, phenolic compounds (gallic acid, naringenin, sinapinic acid, 4-hydroxybenzoic acid, gentisic acid, caffeic acid, chlorogenic acid, ferulic acid, p-coumaric acid, syringic acid, rutin, and quercetin), Tris base, sodium phosphate monobasic, and sodium phosphate dibasic were purchased from MilliporeSigma (Oakville, ON). UranylLess counterstain was purchased from Electron Microscopy Sciences (Hatfield, PA).

2.2.2. IAPP Preparation

To ensure disaggregation of potential fibrils prior to analysis, 1 mg of IAPP was dissolved in 10 mL of HFIP on ice for 30 min and then stored in 1 mL aliquots of 0.1 mg/mL per tube. Aliquots were sonicated in an ice water bath for 30 min and subsequently centrifuged at 14,000×g for 30 min. Samples were frozen overnight at −80 °C and lyophilized the following day. The resulting pellets were stored at −80 °C until use. Pellets were redissolved by first adding 12.5% (v/v) HFIP, and then brought to 1 mL with buffer. For circular dichroism (CD) analysis, 100 mM phosphate buffer (pH 7.4) was used as the diluent, and for all other analyses, 1 M Tris buffer (pH 7.4) was used.

2.2.3. ThT Fluorescence Screening Assay

The 12 phenolic compounds were screened for inhibitory activities at three different IAPP:phenolic ratios, 1:0.5, 1:1, and 1:2. Initially, 10 mM stock solutions of the phenolic compounds were predissolved with 7.3% dimethyl sulfoxide (v/v) in 1 M Tris buffer (pH 7.4). Assays were then performed in triplicate using black 96-well microplates with clear bottoms, and each 200 μL assay mixture contained 5 μM IAPP, phenolic compound (2.5, 5, or 10 μM), and 10

μM ThT in 1 M Tris buffer (pH 7.4). Plates were sealed with Parafilm prior to fluorescence measurements to minimize evaporation. Fluorescence intensity was measured at λ_{ex} 430 nm and λ_{em} 480 nm using the Spark multimode microplate reader (Tecan, Stockholm, Sweden) in kinetic mode, where a bottom measurement was taken every 15 min for 50 h at 37 °C. Results were presented as means, and kinetic parameters were calculated using the nonlinear regression Boltzmann sigmoid function from GraphPad Prism version 9.1.2 for Windows (GraphPad Software, La Jolla, CA), as shown in eq 2.1:

$$F_{obs} = \frac{(F_i + F_f)}{1+\exp\left(\frac{t_{\frac{1}{2}} - t_{obs}}{\tau}\right)} \qquad 2.1$$

F_{obs} is the log fluorescence intensity observed at time t_{obs}, F_i and F_f are the initial and final ThT fluorescence, respectively, $t_{\frac{1}{2}}$ is the time taken to reach half the elongation phase, and τ is the reciprocal of the kinetic elongation constant, K, an apparent rate constant that describes the growth of fibrils during the elongation phase. Furthermore, the lag time (h) of IAPP fibrillation for each sample was calculated using eq 2.2

$$lag\ time = t_{\frac{1}{2}} - 2\tau \qquad 2.2$$

2.2.4. CD Spectroscopy

Changes in the IAPP secondary structure in the absence and presence of caffeic acid, gallic acid, rutin, and quercetin were evaluated using the Jasco J-715 CD spectrophotometer (Jasco Corp., Tokyo, Japan). Measurements were performed at an IAPP:phenolic molar ratio of 1:1 and a final individual IAPP and phenolic concentration of 20 μM, in 100 mM phosphate buffer (pH 7.4). Each sample was measured at two time points, initial (0 h) and final (48 h), using a quartz cuvette with a path length of 1 mm at room temperature in nitrogen gas. Three scans were recorded and averaged at a wavelength range of 185–260 nm at a scanning speed of 100 nm/s. Samples were incubated at 37 °C between the initial and final measurements. Baseline subtraction of the spectral output was performed using a phosphate buffer blank and then converted into mean residue ellipticity (deg cm2 dmol–1) using a mean residue weight of 105.49 Da and an IAPP concentration of 0.078 mg/mL. All data processing was performed using CDToolX. Plotting and smoothing of the resulting data were done with GraphPad Prism version 9.1.2 for Windows

(GraphPad Software, La Jolla, CA). The calculations for secondary structure contents in each sample were performed using the CD fitting software, BeStSel.[116]

2.2.5. Fluorescence Microscopy

The progression of IAPP fibrillation in the absence and presence of phenolic inhibitors caffeic acid, gallic acid, rutin, and quercetin at a ratio of 1:1 was observed throughout the process. Four time points, 0, 10.5, 24, and 48 h, representing the lag, mid-exponential, early stationary, and late stationary phases, respectively, were investigated. An initial sample of 5 μM IAPP incubated with 5 μM of the respective phenolic inhibitor and the control were incubated at 37 °C. At each time point, 30 μL of the sample was mixed with 10 μM ThT and then incubated in the dark for 2 min at 25 °C. Thereafter, samples were visualized using the Axio Imager 2 fluorescence microscope equipped with an Axiocam 506 camera (Carl Zeiss, Germany) using the FITC channel with λ_{ex} 495 nm and λ_{em} 519 nm. Images were processed using the Zen 2.3 pro software (Carl Zeiss, Germany).

2.2.6. Dynamic Light Scattering

Dynamic light scattering was performed using a Nano-ZS Zetasizer (Malvern Instruments Ltd., Malvern, UK) to determine the average particle size and polydispersity of the IAPP-phenolic samples. Samples consisted of IAPP:phenolic ratios of 1:1 with 5 μM of each component added to 1 M Tris buffer (pH 7.4) and incubated at 37 °C. Measurements were taken in triplicate at the initial (0 h) and final (48 h) time points.

2.2.7. Transmission Electron Microscopy

To characterize the types of fibrils formed in the presence of phenolic inhibitors caffeic acid, gallic acid, rutin, and quercetin, transmission electron microscopy (TEM) was performed at an IAPP:phenolic ratio of 1:1. In each sample, 5 μM IAPP and 5 μM phenolic compound were added to the 1 M Tris buffer (pH 7.4) to a final volume of 100 μL and the mixture was incubated at 37 °C for 48 h. From each sample, 10 μL of the aliquot was placed on a 300-mesh Formvar–carbon-coated copper grid on Parafilm for 2 min and the excess sample was blotted with Kimwipes. Thereafter, grids were stained with UranyLess for 1 min in the dark and excess was removed. Samples were imaged using a transmission electron microscope (JEM-1400Flash

Electron Microscope, JEOL, Tokyo, Japan) with an accelerating voltage of 120 kV. Fibril length and diameter measurements were performed using the ImageJ software (NIH, Bethesda, MD).[117]

2.2.8. Fibril Disaggregation Analysis

To observe the effects of rutin and quercetin on preformed fibrils, IAPP was incubated at 37 °C for 48 h and then imaged by TEM. Afterward, an equimolar ratio of IAPP and rutin or quercetin was added. At 1, 22.5, and 47.5 h after the addition of phenolic compounds, sample aliquots were placed on the grids and TEM imaging was performed as outlined previously. Samples were incubated at 37 °C throughout the experiments.

2.2.9. Molecular Docking Analysis

Molecular docking was carried out with UCSF chimera software version 1.15 interfaced with Autodock vina package version 1.2.2 using a monomeric IAPP model retrieved from the RCSB Protein Data Bank (PDB code 2L86).[118,119] Prior to docking, structural optimization was performed to minimize internal clashes, solvents excluded, and Gasteiger charges and polar hydrogen atoms were added while ignoring nonstandard amino acid residues. Blind docking was performed by selecting the entire region of the monomeric IAPP at a grid box dimension, center: 2.778310, 0.858269, and −0.399841 and size: 27.7853, 28.3178, and 12.8696. The docking score of the best pose was selected, residues within 3 Å were highlighted, and intermodel hydrogen bonds were determined by relaxing the constraints by 0.4 Å and 20°.

2.2.10. Statistical Analysis

Experiments were conducted in triplicate, and results were expressed as mean ± standard deviation. Statistical analysis was performed using the one-way analysis of variance (ANOVA) using GraphPad Prism version 9.1.2 for Windows (GraphPad Software, La Jolla, CA). Significant difference between mean values was defined at $p < 0.05$ using Dunnett's multiple comparison test.

2.3. Results and Discussion

2.3.1. Molar Ratio and Structural Dependence of Phenolic Compounds on the IAPP Fibrillation Inhibitory Activity

ThT fluorescence analysis was used to select polyphenols that inhibited IAPP fibrillation and characterize the mechanism of inhibition through the kinetic fibrillation parameters. As shown

in **Figure 2.1**, it is evident that the phenolic structure and molar ratio affected the inhibition mechanism and potency. For example, naringenin showed molar ratio-dependent inhibition of IAPP fibrillation where at a lower molar ratio (1:0.5), naringenin inhibited IAPP fibrillation, while at higher molar ratios (1:1 and 1:2), fibrillation was promoted based on ThT fluorescence (**Figure 2.1** and **Figure S2.1**). It is possible that the flavone structure of naringenin (**Figure 2.2**) encourages π–π stacking or hydrophobic interactions with IAPP, which have been postulated as driving forces in promoting IAPP oligomerization and subsequent fibrillation.[4,120,121] Such interactions may also facilitate the seeding of IAPP fibrils and encourage bypassing of the nucleation step during fibrillation. This phenomenon could explain the significant shortening of the lag phase as observed with the addition of naringenin to IAPP at 1:1 and 1:2 M ratios (**Figure 2.1**, **Table 2.1**, and **Figure S2.1C**).[30] Similar results were reported for epigallocatechin gallate where the promotion of $A\beta_{42}$ aggregation was observed at increasing molar ratios, equally characterized by a decrease in lag time.[122] Naringenin was previously reported as potentially antidiabetic as its intake was associated with significantly lower T2D risk in humans, and it also inhibited IAPP fibrillation *in vitro*.[72,123] Conversely, molar ratio-dependent increase in inhibitor potency was observed when IAPP was incubated with sinapinic acid, with minimal deviation in IAPP fibrillation, compared to the control at the lowest inhibitor molar ratio (**Figure S2.1A**). The inhibitory effects at a higher molar ratio, indicated by a lower F_{max} compared to the IAPP control, suggests that the phenolic compound also influenced the later phase of fibrillation (**Figure 2.1**, **Table 2.1**, and **Figure S2.1B**).

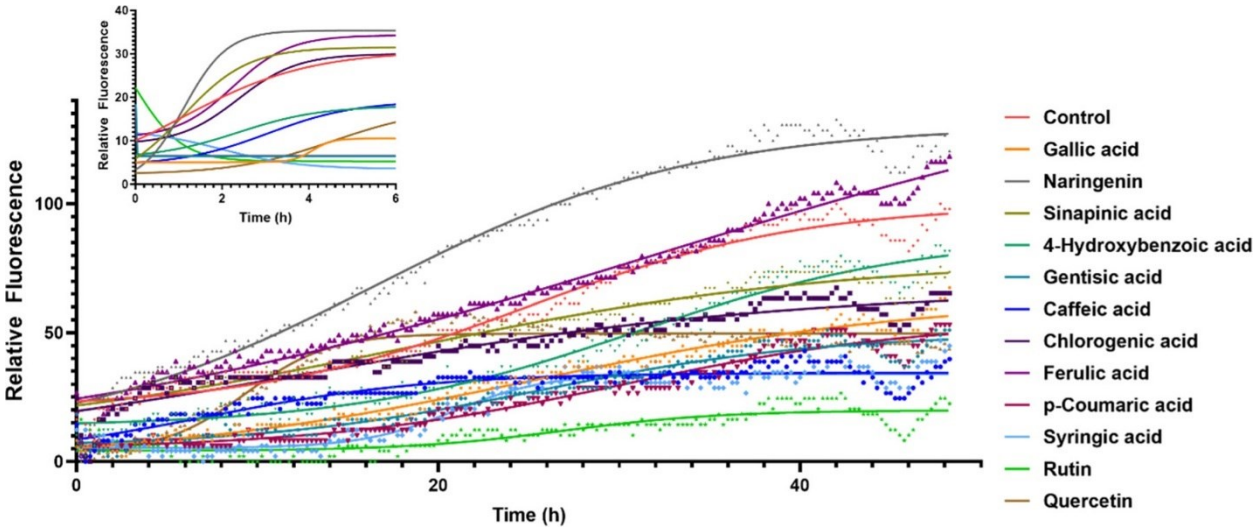

Figure 2.1. ThT fluorescence-monitored kinetics of the IAPP fibrillation process in the absence (control) and presence of the 12 phenolic compounds at IAPP:phenolic molar ratios of 1:1. The inset shows the kinetics during the first 6 h of fibrillation.

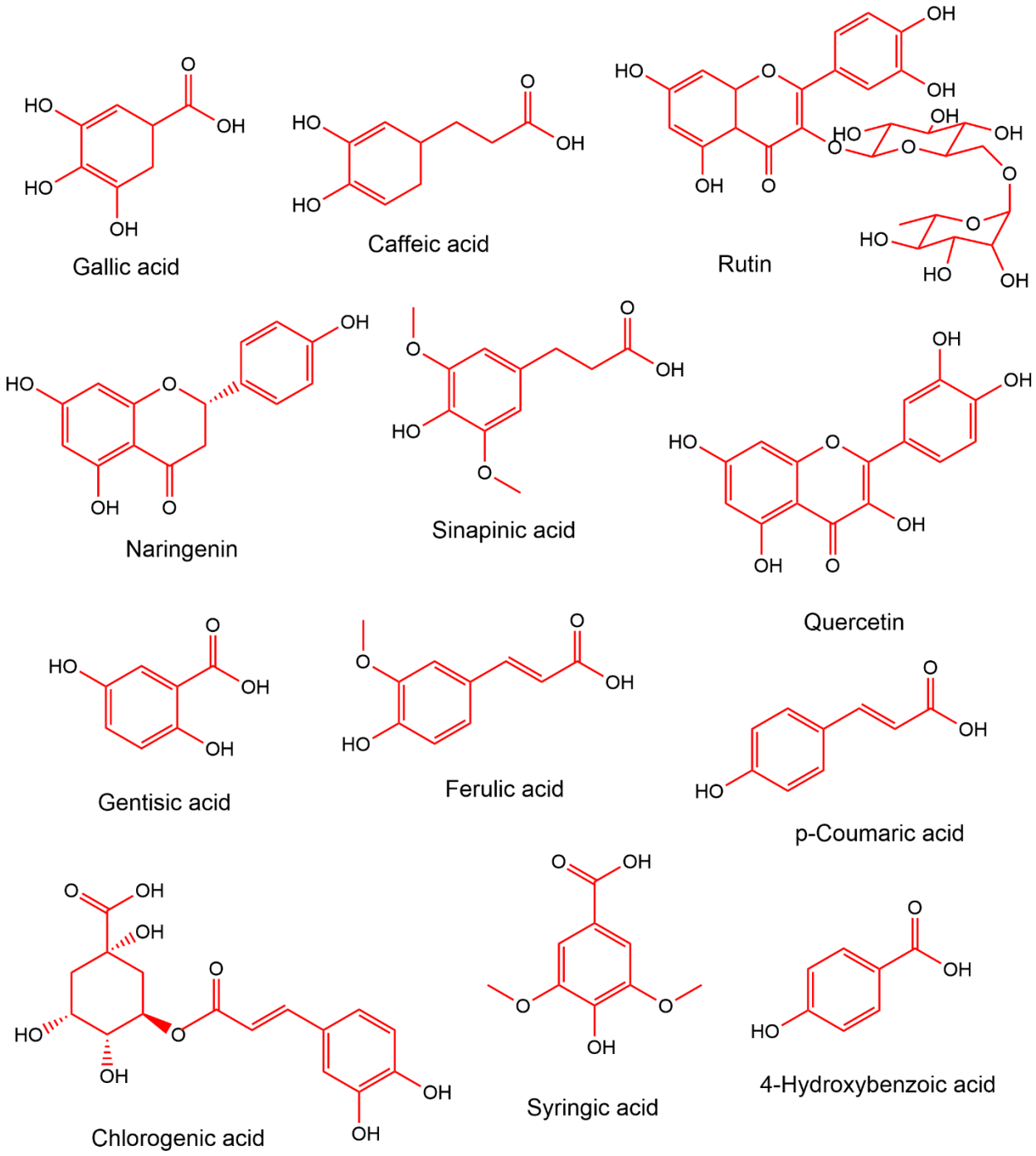

Figure 2.2. Chemical structures of all polyphenolic compounds evaluated for inhibitory activities using ThT fluorescence kinetics.

Table 2.1. Parameters for thioflavin-t fluorescence-monitored kinetics of IAPP fibrillation at a 1:1 IAPP:phenolic molar ratio

	$t_{\frac{1}{2}}$	τ	K	Lag time (h)	F_{max}
control	24.95	7.66	0.13	3.00	99.76
gallic acid	25.31	10.81	0.09	2.16	63.27
naringenin	16.57	8.75	0.11	1.66	130.3
sinapinic acid	17.91	12.11	0.08	1.31	78.43
4-hydroxybenzoic acid	30.98	7.92	0.13	3.66	87.53
gentisic acid	25.58	7.78	0.13	3.03	49.63
caffeic acid	7.09	6.34	0.16	0.80	34.46
chlorogenic acid	12.23	13.80	0.07	0.74	66.97
ferulic acid	31.84	18.55	0.05	1.61	159.8
p-coumaric acid	30.02	8.42	0.12	3.33	54.70
syringic acid	20.87	2.57	0.39	7.35	33.98
rutin	26.95	4.38	0.23	5.69	19.83
quercetin	9.38	2.31	0.43	3.19	49.67
Abbreviations: $t_{\frac{1}{2}}$, time at half transition in hours; K, elongation constant; and F_{max}, maximum relative fluorescence intensity reached.					

Of all phenolic compounds investigated, ferulic acid did not inhibit IAPP fibrillation, independent of the molar ratio. Rather, it had an enhancing effect, indicated by higher F_{max}, except at the highest molar ratio, as well as reduced $t_{\frac{1}{2}}$ and lag phase, while the elongation constant increased compared to the IAPP control (**Figure 2.1**, **Table 2.1**, and **Figure S2.1**). This indicates that the addition of ferulic acid may have expedited the nucleation step that initiates IAPP aggregation. Moreover, the shortened lag phase and $t_{\frac{1}{2}}$ indicate that ferulic acid influenced the elongation phase since this phase occurred earlier and faster compared to the IAPP control. Although a higher F_{max} indicates the presence of fibrillar species compared to the IAPP control, it may also indicate the aggregation of the IAPP–phenolic complexes. However, this effect disappeared at higher molar ratios of ferulic acid where it inhibited IAPP fibrillation. Previously, ferulic acid was reported to inhibit IAPP fibrillation by 27.7% at 40 μM, which is similar to our findings.[124] However, our study provides more insights into the potentially phase-specific inhibitory effects of ferulic acid on IAPP fibrillation.

Based on ThT fluorescence kinetics, there are notable patterns between the structural features of the phenolic compounds and fibrillation inhibitory activities. For example, phenolic

compounds with catechol moieties, such as chlorogenic acid, caffeic acid, rutin, and quercetin (**Figure 2.2**), were more active inhibitors of IAPP fibrillation compared to other compounds, such as sinapinic acid. It is possible that the hydroxyl groups of the catechol form hydrogen bonds with IAPP, thus stabilizing IAPP monomers and preventing their subsequent conversion into β-sheets for fibrillation. The presence of catechol moieties in active compounds against fibrillation has been previously attributed to increased inhibitor potency.[72] Consequently, rutin, which contains a catechol and equally has the highest number of hydroxyl groups, resulted in the longest lag phase at 18.2 h, almost double the lag phase of the IAPP control (**Figure 2.1**, **Figure 2.2**, **Table 2.1**, and **Figure S2.1**). This suggests that the interactions between the inhibitor and IAPP can arrest IAPP in its monomeric form and thus prevent or delay its subsequent aggregation through this mechanism.

Furthermore, gallic acid, 4-hydroxybenzoic acid, caffeic acid, chlorogenic acid, and rutin consistently discouraged IAPP fibrillation, independent of their molar ratio. This is the first report of inhibition of IAPP fibrillation by 4-hydroxybenzoic acid. Caffeic acid and chlorogenic acid have been previously reported to dose-dependently inhibit IAPP fibrillation.[4,125,126] Gallic acid was shown to possess anti-fibrillar activity against β-amyloid, and rutin has also been demonstrated to disaggregate oligomers and suppress misfolding *in silico* and effects of misfolded IAPP in transgenic mice.[67,127,128] Due to differences in structural backbones and substituents (**Figure 2.2**), gallic acid (hydroxybenzoic acid), caffeic acid (hydroxycinnamic acid), rutin (flavonol glycoside), and quercetin (flavonoid) were selected from the active phenolic compounds for further biomolecular studies to elucidate structure–function relationships and phase-specific inhibition mechanisms. Gallic acid appears to inhibit the exponential phase of IAPP fibrillation indicated by the increased $t_{\frac{1}{2}}$ value and reduced elongation rate, K. Considering the shortened lag phase, gallic acid possibly encouraged IAPP seeding but slowed down fibril growth in the elongation phase. Conversely, caffeic acid appears to discourage late-phase fibrillation based on the characteristic three-fold reduction in F_{max} compared to the IAPP control (**Figure S2.1**). Visually, caffeic acid induced a faster rate of fibrillar growth initially resulting in undetectable lag phase and near-absent $t_{\frac{1}{2}}$. However, an early plateau was attained compared to the IAPP control (**Figure 2.1**). Gallic acid and caffeic acid were both reported to prevent the conversion of $A\beta_{42}$ protofibrils into mature fibrils, suggesting that the observed inhibitory effects in the exponential and stationary

phases of IAPP fibrillation are likely through similar fibrillation inhibition mechanisms.[129] Rutin strongly inhibited the lag phase of IAPP fibrillation, resulting in almost doubling of the lag phase compared to the IAPP control (**Figure 2.1** and **Table 2.1**). This effect is supported by molecular dynamics and binding interaction simulation studies, which suggested that rutin binds and disaggregates IAPP pentamers, thus preventing the formation of oligomers and subsequent fibrillation.[67] Finally, quercetin showed slight inhibitory effects against IAPP fibrillation at 1:0.5 and 1:1 M ratios, while at the highest molar ratio, it appeared to induce fibrillation, characterized by the shortening of the lag time by almost half (**Figure 2.1**, **Table 2.1**, and **Figure S2.1**).

2.3.2 Effect of Phenolic Inhibitors on the IAPP Secondary Structure during IAPP Fibrillation

To evaluate the effect of the selected inhibitors on the IAPP structure in the late stationary phase, CD spectroscopy was carried out before and after the 48 h incubation period. The IAPP:phenolic ratio of 1:1 was used to achieve IAPP fibrillation inhibition and avoid potential self-aggregation of the inhibitor that may occur at higher molar ratios. Consistent with the ThT fluorescence kinetic results, the structurally different phenolic compounds exhibited varying modes of IAPP fibrillation inhibition as shown by the differing secondary structures present before and after fibrillation (**Figure 2.3**). A shift from a negative peak at 222 nm in control IAPP to a double negative peak at 227 and 208 nm in IAPP with rutin indicates a shift toward higher total α-helical content (**Figure 2.3**). This confirms the ThT fluorescence data that rutin suppressed the lag phase of IAPP fibrillation. Furthermore, rutin appears to have disaggregative properties because of the increased α-helical structures and decreased β-sheet contents after 48 h incubation (**Figure S2.2**). This observation confirms the previously proposed inhibition mechanism of rutin based on molecular docking studies.[67] This secondary structural pattern demonstrates that rutin may have reverted the preformed fibrillar structures into the monomeric α-helical confirmation while also stabilizing the IAPP monomer structure, indicated by the higher proportion of regular α-helices compared to the distorted counterparts (**Figure 2.3** and **Figure S2.2**).

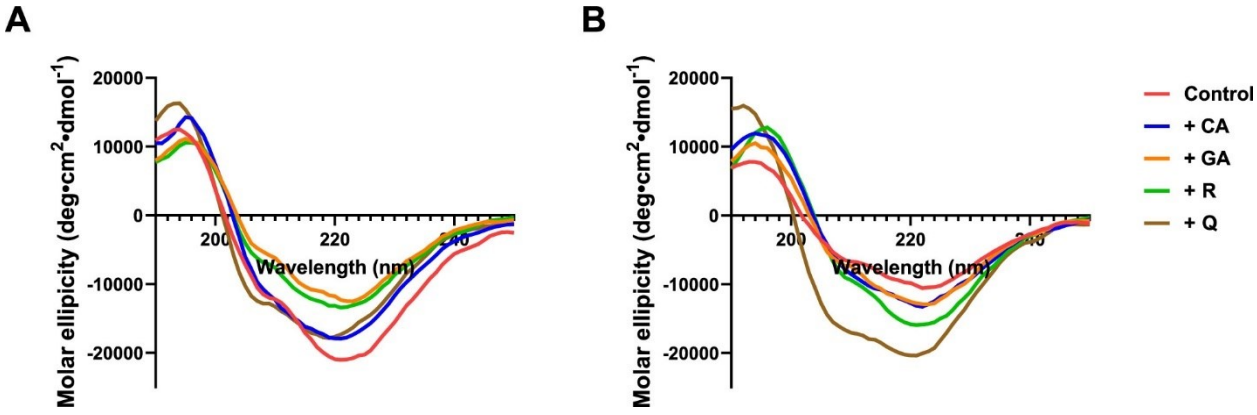

Figure 2.3. CD spectra of IAPP in the absence (control) and presence of the phenolic inhibitors at the **(A)** starting point (0 h) and **(B)** after 48 h of incubation. GA, gallic acid; CA, caffeic acid; R, rutin; and Q, quercetin.

Furthermore, quercetin showed a similar pattern in the relative secondary structure compared to rutin. After 48 h incubation, the α-helical content appears to increase more than other treatments with the double negative peaks at approximately 225 nm with a shoulder at approximately 210 nm (**Figure 2.3** and **Figure S2.2**). Equally, the increase in the relative α-helical content in the late stationary phase suggests disaggregatory effects of quercetin. The relative secondary structure of quercetin compared to that of rutin at the initial and final timepoints follows the same trends indicated by an increase in the α-helical content, unchanged β-sheet content, and decrease in turns and "others".

In the presence of caffeic acid, the CD spectra indicates that the inhibition of IAPP fibrillation was more prominent at the stationary phase rather than during fibril elongation, which corroborates the fibrillation kinetic results. The strong negative peak originally observed at 220 nm was significantly reduced after 48 h, which indicates a reduction in the β-sheet contents. Moreover, a decrease in the α-helical content from 21.2 to 14.6% indicates that the disaggregated fibrils likely remained as random coils (**Figure S2.2**). Although gallic acid was observed to inhibit IAPP fibrillation based on ThT fluorescence kinetics, the CD spectra indicates that the extent of its inhibitory activity is lesser compared to the effects of caffeic acid and rutin. The strong negative peak observed at 220 nm retained about the same intensity from time 0 to 48 h (**Figure 2.3**). Similarly, the relative secondary structure contents were consistent across the two time points (**Figure S2.2**). This suggests that gallic acid inhibited the progression of IAPP fibrillation, but

disaggregation or inhibition of IAPP nucleation likely did not occur since the total α-helical content was relatively the same before and after fibrillation.

Both rutin and caffeic acid were identified to possess potential disaggregative properties, in addition to inhibitory activities. Caffeic acid and rutin are relatively bulkier than gallic acid, caffeic acid with the α,β-unsaturated monocarboxylic acid group and rutin with the rutinose (disaccharide) moiety attached to the bulky 3-hydroxyflavone backbone (**Figure 2.2**). This suggests the potential link between the molecular size of inhibitors and disaggregative properties.

2.3.3. Effect of Phenolic Inhibitors on the Fluorescence Morphology of IAPP Fibrils

Visualization of fibrillation progression was done via ThT fluorescence microscopy at four time points 0, 10.5, 24, and 48 h, which represent the lag, mid-exponential, early stationary, and late stationary phases, respectively (**Figure 2.4**). Gallic acid lowered the duration of the exponential phase because of the consistently shortened and smaller fibrillar species present in early and late stationary phases of the treated sample compared to those of the IAPP control (**Figure 2.4**). It is possible that caffeic acid initially enhanced IAPP fibrillation, leading to late exponential/early stationary phases where larger aggregates are observed compared to the IAPP control. However, in the later stages of fibrillation, starting from the early stationary phase, the relative sizes of the aggregates were consistent and later reduced in the late stationary phase (**Figure 2.4**). This observation supports the conclusions from ThT fluorescence kinetics and CD spectra that caffeic acid influenced fibrillation within the later phases, with the potential disaggregation mechanism. Fluorescence images also confirmed that rutin stalled the lag phase where minimal fluorescence is observed in the first 24 h of incubation, indicating the suppression of IAPP fibrillation. Even in the late stationary phase where the resulting IAPP fibrillar structures are present, the fibril morphology was altered by rutin compared to the IAPP control, suggesting the presence of disordered IAPP species or nonmature fibrils (e.g., protofibrils) late into the fibrillation process (**Figure 2.4**). ThT fluorescence microscopy of IAPP with quercetin shows a different fibrillation pattern (**Figure 2.4**). In the presence of quercetin, fibril growth slowed down after 10.5 h wherein fibril sizes appeared to remain constant but increased in amount by 48 h. This differs from the fluorescence image for the control, which shows the occurrence of fully formed mature fibrils by 48 h (**Figure 2.4**).

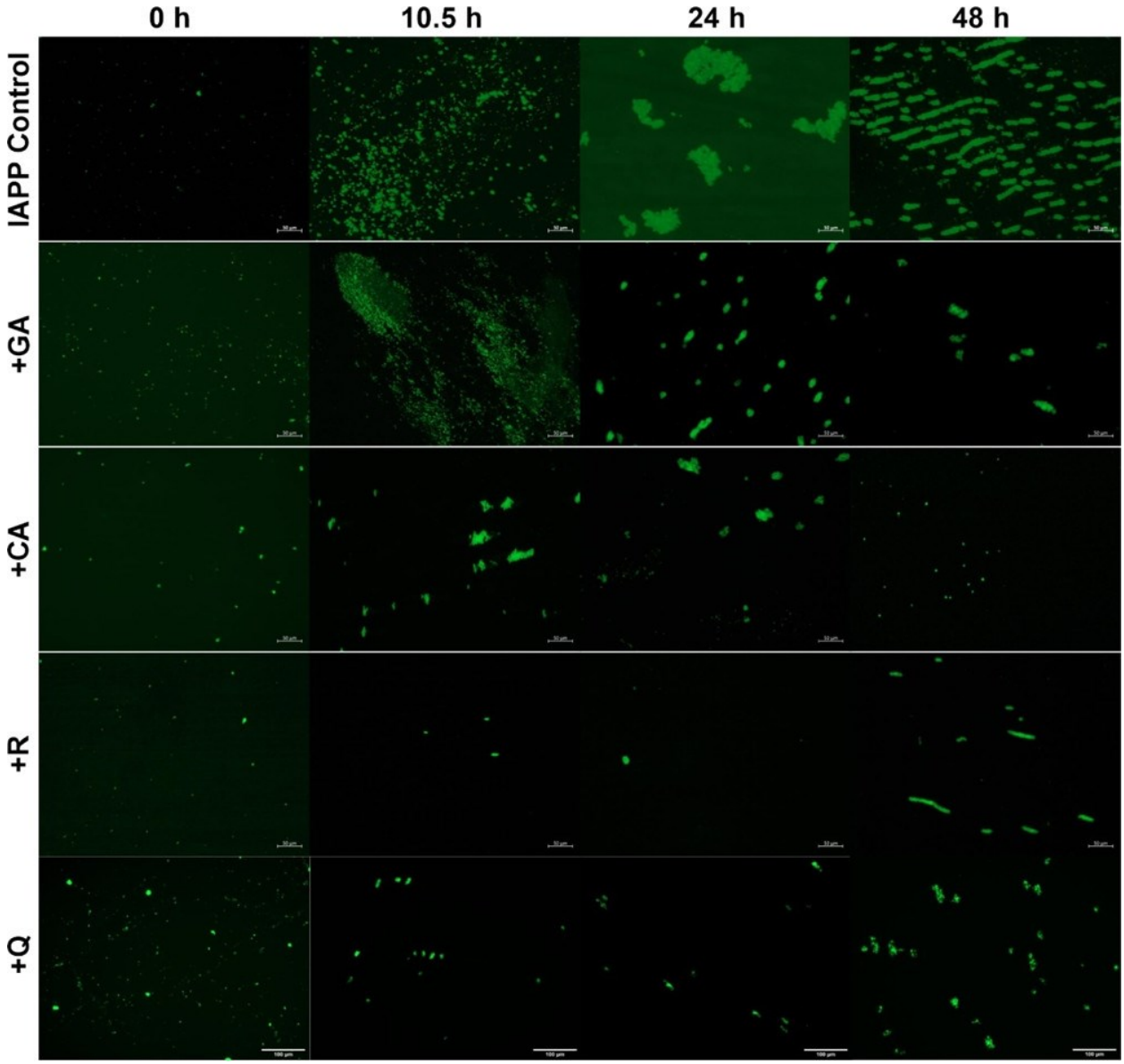

Figure 2.4. Time-course ThT fluorescence microscopy of IAPP in the absence (control) or presence of the phenolic compounds at an IAPP:phenolic ratio of 1:1. GA, gallic acid; CA, caffeic acid; R, rutin; and Q, quercetin. Scale bars represent 50 μm.

2.3.4. Effect of Phenolic Inhibitors on the Progression of IAPP Fibrillation

Dynamic light scattering was performed to monitor the changes in size distribution and polydispersity index (PDI) of the IAPP species before and after fibrillation in the presence of the phenolic inhibitors. The average apparent hydrodynamic radii of IAPP fibrils at the end of the stationary phase was reported to get as large as 1100 nm.[26] As expected, a significant increase in

average particle size was observed upon the addition of the phenolic inhibitors (**Figure 2.5A**). Although comparable to the size range indicative of fibrillation, this immediate size increase could be due to the complexes formed by interactions between the phenolic compounds and IAPP monomers. This is illustrated by the shift toward an increase in particle radius distribution peaks of phenolic inhibited samples above 1000 nm compared with the control (**Figure S2.3**). A further increase in average particle size was observed post 48 h incubation. No significant difference in particle size was observed between the gallic acid, caffeic acid, and rutin-inhibited samples, and IAPP control. This reflects the inevitable fibrillation of IAPP, presence of IAPP-phenolic complexes, or disordered and nonfibrillar IAPP species in the samples. Additionally, no significant difference was observed in the average PDI between the IAPP control and inhibited samples (**Figure 2.5B**). After the 48-h incubation, an increase in PDI was observed, indicating an increase in the heterogeneity of species produced during IAPP fibrillation. An increase in PDI is also characteristic of the progression of IAPP fibrillation from the lag phase to the exponential phase, accompanied by the formation of new particles that indicate protofibrils.[26] Additionally, it could also indicate the fragmentation of larger fibrillary aggregates into smaller species, thus forming seeds to produce additional fibrils in the process. On the other hand, a significant increase in average particle radius compared to the control was observed with quercetin-inhibited samples (**Figure 2.5A**). This trend continued after 48 h of incubation with a 3.58-fold increase in particle radius in the presence of quercetin (**Figure 2.5A**). This is countered with a decrease in average PDI from 0.9 (which is significantly higher than the control) to 0.33 after 48 h (**Figure 2.5B**). The concomitant increase in average particle radius and decrease in PDI suggest the presence of large aggregates at the end of the 48-h incubation period. This is supported by a single peak observed at 10, 800 nm, indicating the uniformity of species present (**Figure S2.3B**).

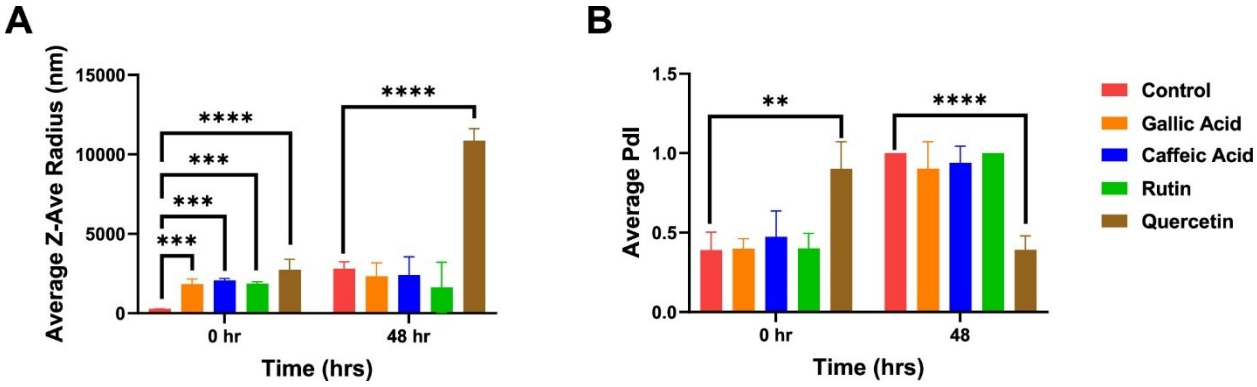

Figure 2.5. Average particle size (Z-Ave) radius (A) and PDI (B) of species present in IAPP samples before (0 h) and after (48 h) incubation in the absence and presence of the phenolic compounds. *= significant ($0.01 < p < 0.05$) and **= very significant ($0.001 < p < 0.01$).

2.3.5. Effect of Phenolic Inhibitors on IAPP Fibril Morphology

TEM analysis was used to better characterize the types of fibrils formed and effect of the phenolic inhibitors on IAPP fibril morphology. The TEM image of the IAPP control revealed the formation of dense fibrils in addition to the presence of compact aggregates (arrows) (**Figure 2.6A**). The presence of gallic acid resulted in a slight change in IAPP fibril morphology and, notably, the formation of loosely packed aggregates indicated by the arrow (**Figure 2.6B**). Conversely, caffeic acid acted in the late stationary phase as a disaggregant. Extensive networks of IAPP fibrils were observed with samples incubated with caffeic acid (**Figure 2.6C**); however, the fibrils were noticeably thinner and less dense than those formed in the IAPP control (**Figure 2.6A**). Moreover, the formation of large amorphous aggregates (indicated by arrows) was observed throughout the TEM grids (**Figure 2.6C**). The increase in the particle diameter could be due to the formation of the large granular aggregates in addition to the extensive fibrillary networks (**Figure 2.6C,G**). Of the three phenolic inhibitors, rutin was observed to significantly decrease the IAPP fibril length compared to the control (**Figure 2.6D,F**). This supports all the previous data and confirms that rutin functions as a strong early-acting inhibitor toward reducing the lag phase by binding the IAPP monomer to prevent unfolding and subsequent self-association. This effect would delay the nucleation step of IAPP fibrillation. Loosely packed aggregates were also present in the IAPP sample treated with rutin instead of the fibrillar network, indicating potent inhibition of IAPP fibrillation possibly because of disaggregation. Molecular docking studies showed that rutin preferentially binds two regions of IAPP, Leu12–Ala13–Asn14 and Asn31–Val32–Gly33–Ser34–Asn35 within IAPP pentameters, thus loosening the chain A and chain B of hIAPP.[67] (37) This effect would result in the disaggregation of the toxic IAPP oligomers. Despite the strong inhibitory effect of rutin, fibrillation still occurred (indicated by arrows), albeit to a significantly lesser extent compared to the IAPP control, and the resulting fibrils were also much shorter and less dense (**Figure 2.6D**). IAPP treated with quercetin resulted in a significant decrease in fibril length after 48 h (**Figure 2.6F**) and a slight decrease in fibril diameter, although not significant (**Figure 2.6G**). Inhibitory effects of quercetin on IAPP fibrillation have been

reported, but the potential mechanism of inhibition has yet to be elucidated.[72] Quercetin was reported to be a lag-phase inhibitor of bovine insulin fibrillation.[67] The hydrophobicity of quercetin was suggested to enhance its binding to proteins to form soluble or insoluble complexes, thus facilitating fibrillation inhibition and disaggregatory effects.[67] It is possible that a similar mechanism of inhibition was present against IAPP fibrillation, characterized by the increased lag phase, thus causing truncated fibrils at 48 h (**Figure 2.6E**).

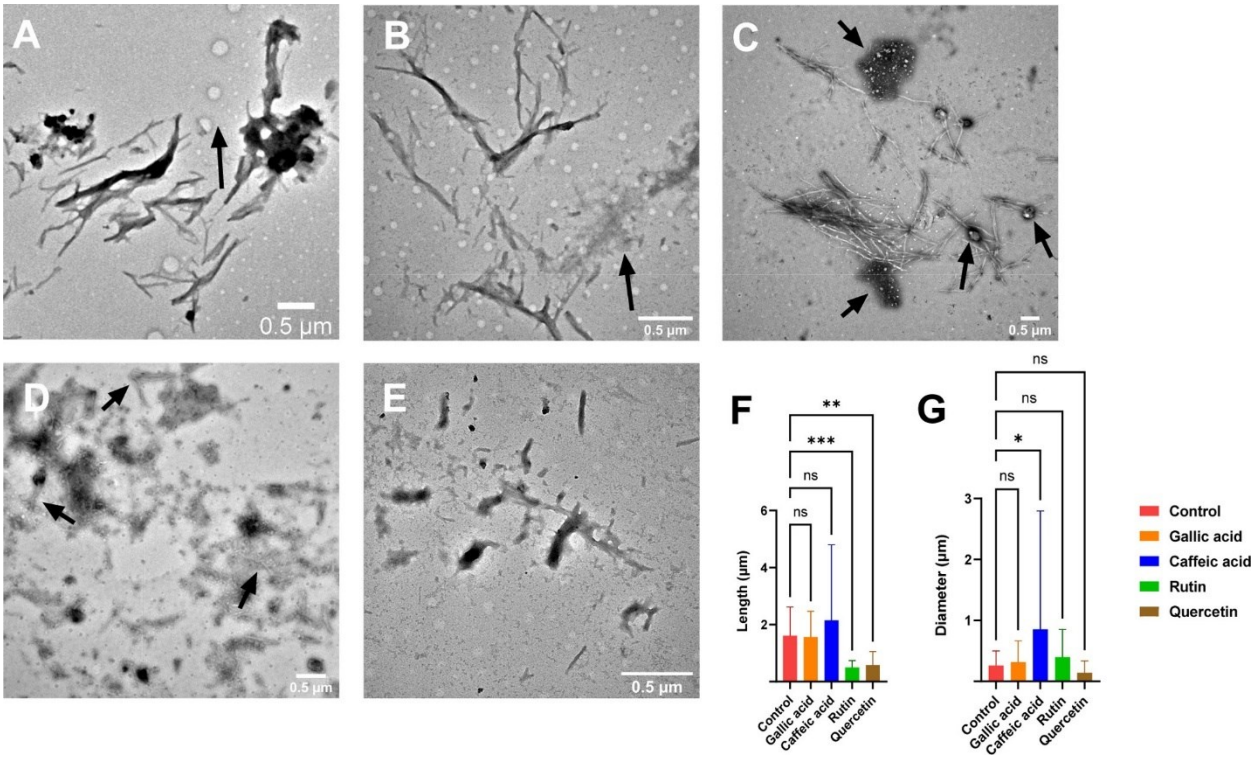

Figure 2.6. TEM images of **(A)** IAPP control, **(B)** IAPP with gallic acid, **(C)** IAPP with caffeic acid, **(D)** IAPP with rutin, and **(E)** IAPP with quercetin after 48 h incubation. Scale bars represent 0.5 µm. Fibrils and aggregate **(F)** lengths and **(G)** diameters were quantified using ImageJ. Error bars indicate standard deviation, $n = 42$; ns = not significant ($p \geq 0.05$), *= significant ($0.01 < p < 0.05$) and **= very significant ($0.001 < p < 0.01$).

2.3.6. Disaggregatory Effects of Rutin and Quercetin on Preformed IAPP Fibrils

To observe the potential disaggregatory effects, rutin and quercetin were added to preformed IAPP fibrils and TEM images were taken at various time intervals. Rutin showed disaggregatory effects on preformed IAPP fibrils as immediate as 1 h after addition where fragments at the edges of the fibrillar networks are observed (indicated by arrows in **Figure 2.7**).

After 22.5 h, loosely packed aggregates are observed around the fragmented fibrils (arrows in **Figure 2.7**). Finally, after 47.5 h of incubation, mixed species of both smaller, spherical structures (arrows), and shorter fibrils are present. The images are a significant contrast to the extensive fibrillar network of the IAPP control (**Figure 2.7**). Therefore, in addition to being an early phase inhibitor, rutin demonstrates the disaggregatory effects on preformed IAPP fibrils. On the other hand, incubation of quercetin with preformed fibrils resulted in the formation of amorphous aggregates as early as 1 h after incubation (**Figure 2.7**). Interestingly, a similar effect of quercetin on preformed bovine insulin fibrils was reported where it resulted in amorphous aggregates of a similar shape.[67]

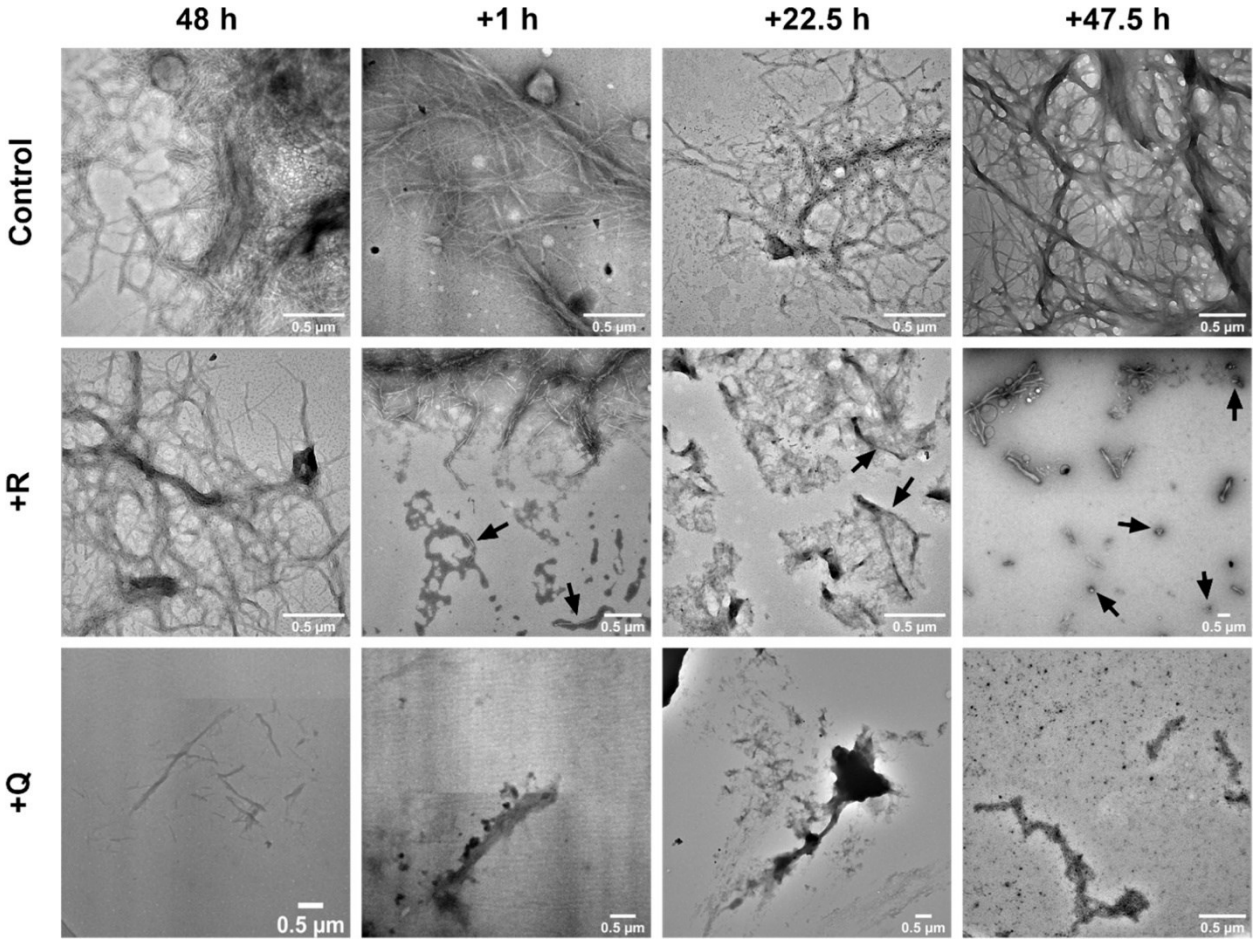

Figure 2.7. Disaggregation of preformed fibrils imaged using TEM. **(A)** IAPP control, **(B)** IAPP with rutin (+R), and **(C)** IAPP with quercetin (+Q). Scale bars represent 0.5 µm.

2.3.7. Peptide/Polyphenol Complexation with Monomeric IAPP

The IAPP monomer is suggested to undergo strong intermolecular interaction with rutin (estimated molecular docking binding energy, −8.3 kcal/mol) involving one hydrogen bonding each with the phenolic and sugar moieties of rutin and Asn3 and Arg11 of IAPP. The phenolic moiety is suggested to bind in the amphipathic pocket involving Asn14, Phe15, Asn21, Asn22, Ala25, Asn31, and Val32, while the sugar group forms electrostatic interaction in the hydrophilic region with Asn3, Arg11, Leu12, and Asn31 of IAPP (**Figure 2.8A-B**). In contrast, quercetin is suggested to undergo moderate binding with IAPP with a binding energy of −6.8 kcal/mol. The binding is predicted to occur in the hydrophilic pocket and is facilitated by a network of four hydrogen bonding involving Arg11 and Asn21 of the IAPP monomer (**Figure 2.8C-D**). Strong rutin-IAPP monomer binding could be responsible for its fibril disaggregation effect due to the distortion of the equilibrium favoring aggregation. The moderate quercetin-IAPP binding might not be strong enough to distort the equilibrium, but it may have promoted IAPP conformational change that led to the formation of the amorphous aggregates.

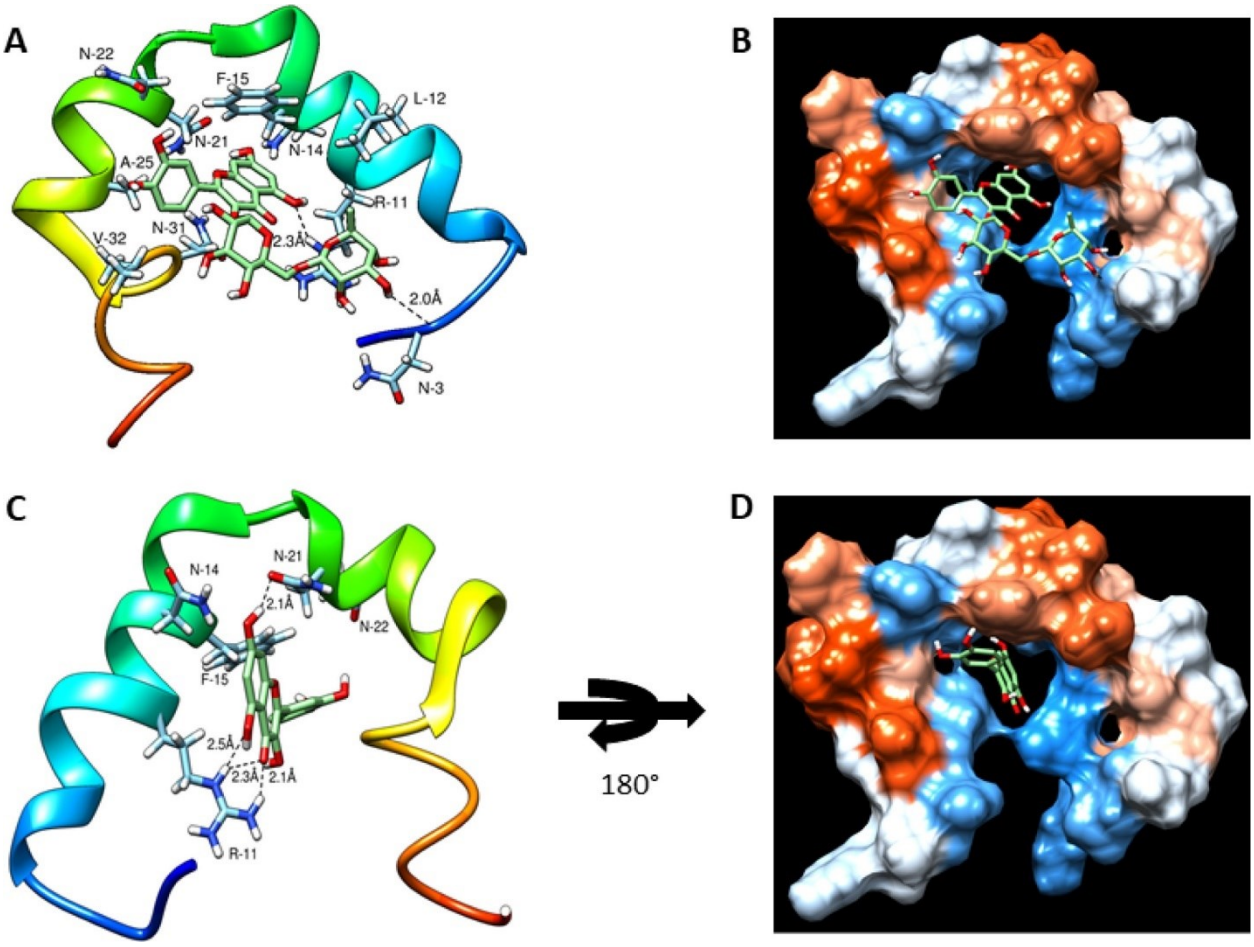

Figure 2.8. Docking scheme showing potential intermolecular interactions of monomeric IAPP (PDB code: 2L86) with **(A)** rutin and **(C)** quercetin and the hydrophobic/hydrophilic pockets of **(B)** rutin and **(D)** quercetin. The Kyte-Doolittle scale is represented in **(B and D)** showing charge environment and hydrophilicity/hydrophobicity of the binding site with colors ranging from dodger blue for the most hydrophilic to white (zero) to orange red for the most hydrophobic.

Docking studies suggests how both rutin and quercetin might interact with monomeric IAPP resulting in the formation of peptide–polyphenol complexes. Mature fibrils exist in a thermodynamic equilibrium with free monomeric IAPP present in solution.[130] Thus, any delineation from relative quantities of each species at equilibrium can result in a shift to reestablish a new equilibrium.[130] Understanding the mechanism behind the equilibrium formed between mature fibrils and monomeric IAPP species can explain the mechanism behind the fibril disaggregation effects of rutin and quercetin. Highly favorable complexation between rutin or quercetin with monomeric IAPP would decrease the amount of monomeric IAPP, thus shifting the

equilibrium toward the production of more monomeric IAPP to re-establish the initial thermodynamic equilibrium. This process would require the disaggregation of preformed IAPP fibrils to allow for the liberation of monomeric species.

As expected, the poor biostability and bioavailability of phenolic compounds can attenuate their physiological effects. As such, biomolecular-based nanodelivery systems are used as vehicles for these polyphenols.[131–133] Additionally, food matrix effects, digestion, microbial activity in the colon, and food-processing treatments can affect the stability and bioactivity of phenolic compounds.[134–136] Given that rutin is a glycoside, consisting of a flavonol and a disaccharide rutinose (**Figure 2.2**), it was important to evaluate the aglycone, quercetin, for IAPP fibrillation inhibitory activity. While rutin is widely recognized as a potent bioactive compound, it has poor bioavailability and a slow absorption rate in rats.[137] This minimizes the probability of intact rutin being absorbed and subsequently reaching the pancreas to inhibit IAPP fibrillation. Quercetin is a major metabolite of rutin and has a higher absorption rate within the small intestine of rats compared to rutin.[137] In our study, the relative inhibitory activity and mechanism of quercetin and rutin are comparable. Slight differences in average particle radius and morphology of the disaggregated IAPP fragments could be attributed to the rutinose residue in rutin. Considering its higher bioavailability, quercetin has a higher chance of interacting with IAPP and inhibiting its fibrillation in pancreatic β-cells compared to rutin.

2.4. Conclusion

In conclusion, this study demonstrated the effect of the structure and molar ratio of 12 phenolic compounds on IAPP fibrillation inhibition. Using four structurally different phenolic compounds, gallic acid, caffeic acid, rutin, and quercetin, biomolecular analysis provided further mechanistic insights into the structure-dependent inhibition of IAPP fibrillation. Notably, rutin and quercetin, gallic acid, and caffeic acid were found to alter the lag, exponential, and stationary phases of IAPP fibrillation. Rutin and quercetin exerted inhibitory effects early in the lag phase of IAPP fibrillation, likely by interacting with and stabilizing monomeric IAPP. This could reduce the likelihood of unfolding and subsequent nucleation of IAPP, resulting in the extended lag time, increased α-helical content, and lower F_{max}. Conversely, gallic acid inhibited the exponential phase likely by binding to IAPP protofibrils, thus decreasing the rate of elongation and F_{max}. Last, caffeic acid strongly inhibited IAPP fibrillation of the early stationary phase, also causing a

significant decrease in F_{max}. Furthermore, rutin and quercetin disaggregated preformed IAPP fibrils through the potential formation of phenolic/IAPP monomer complexes, suggesting the ability of the inhibitor to shift the thermodynamic equilibrium of mature fibrils toward the reformation of monomeric IAPP. Future studies are needed to elucidate the possible contributions of phenolic metabolites produced in the colon toward the inhibition of IAPP fibrillation. Taken together, this study demonstrated the inhibition of IAPP fibrillation and disaggregation of preformed fibrils by the phenolic compounds, thus highlighting the need to elucidate the interactions governing IAPP fibrillation as a potential mechanism of food-derived antidiabetic compounds.

2.5. Acknowledgements

This work was supported by the Natural Sciences and Engineering Research Council of Canada (NSERC) through the Discovery Grant Program, reference number RGPIN-2018-06839, and the University of Ottawa through the University Research Chairs Program.

Notes

The authors declare no competing financial interest.

2.6. Supplementary Information

Phase-specific Inhibition of Islet Amyloid Polypeptide Fibrillation by Structurally Diverse Food-derived Phenolic Compounds

Raliat O. Abioye, Ogadimma D. Okagu, Chibuike C. Udenigwe

Journal of Agricultural Food Chemistry **2022**, *70(1)*, 392-402.
https://doi.org/10.1021/acs.jafc.1c06918.

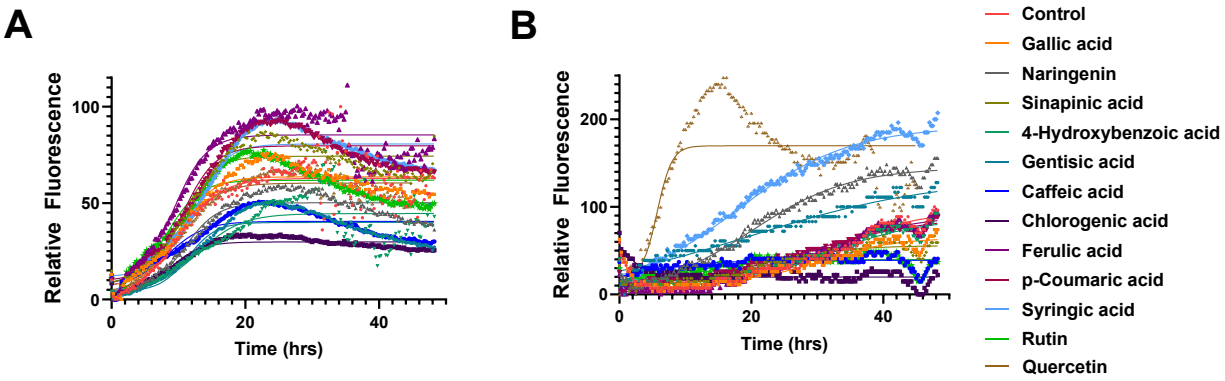

C

		1:0.5						1:2				
		$t_{1/2}$	τ	K	Lag time	F_{max}		$t_{1/2}$	τ	K	Lag time	F_{max}
Control		9.78	3.17	0.32	2.46	62.85		33.21	5.98	0.17	5.22	94.94
Gallic acid		10.01	2.52	0.4	3.17	63.6		30.9	5.45	0.18	5.3	64.67
Naringenin		10.94	2.45	0.41	3.64	50.15		20	7.48	0.13	2.41	145
Sinapinic acid		10.35	2.37	0.42	3.52	74.28		21.82	5.78	0.17	3.43	55.84
4-Hydroxybenzoic acid		12.83	3.31	0.3	3.27	44.57		31.86	7.18	0.14	4.16	87.12
Gentisic acid		11.42	2.09	0.48	4.51	39.97		19.92	14.34	0.07	1.25	134
Caffeic acid		8.38	2.76	0.36	2.31	40.5		0	5.83	0.17	n/a	39.02
Chlorogenic acid		8.74	2.33	0.43	2.89	29.84		0	2.02	0.5	n/a	19.8
Ferulic acid		9.22	2.49	0.4	2.9	85.34		29.68	7.3	0.14	3.79	90.85
p-Coumaric acid		10.63	2.46	0.41	3.51	79.68		28.35	9.66	0.1	2.73	90.83
Syringic acid		12	2.46	0.41	4.06	80.63		17.77	8.6	0.12	1.83	192.1
Rutin		8.35	2.42	0.41	2.63	61.82		12.08	4.07	0.25	2.48	39.65
Quercetin		9.95	2.83	0.35	2.81	60.38		5.72	1.13	0.88	3.3	169.8

Figure S2.1. Thioflavin-T fluorescence-monitored kinetics of IAPP fibrillation process in the absence (control) and presence of the 11 phenolic compounds at IAPP:phenolic molar ratios of **(A)** 1:0.5 and **(B)** 1:2. **(C)** Summary of the IAPP fibrillation kinetic parameters, $t_{\frac{1}{2}}$ (time at half transition in hours), K (elongation constant), lag time (in hours), and F_{max} (maximum relative fluorescence intensity reached) for the IAPP:phenolic molar ratios 1:0.5 and 1:2.

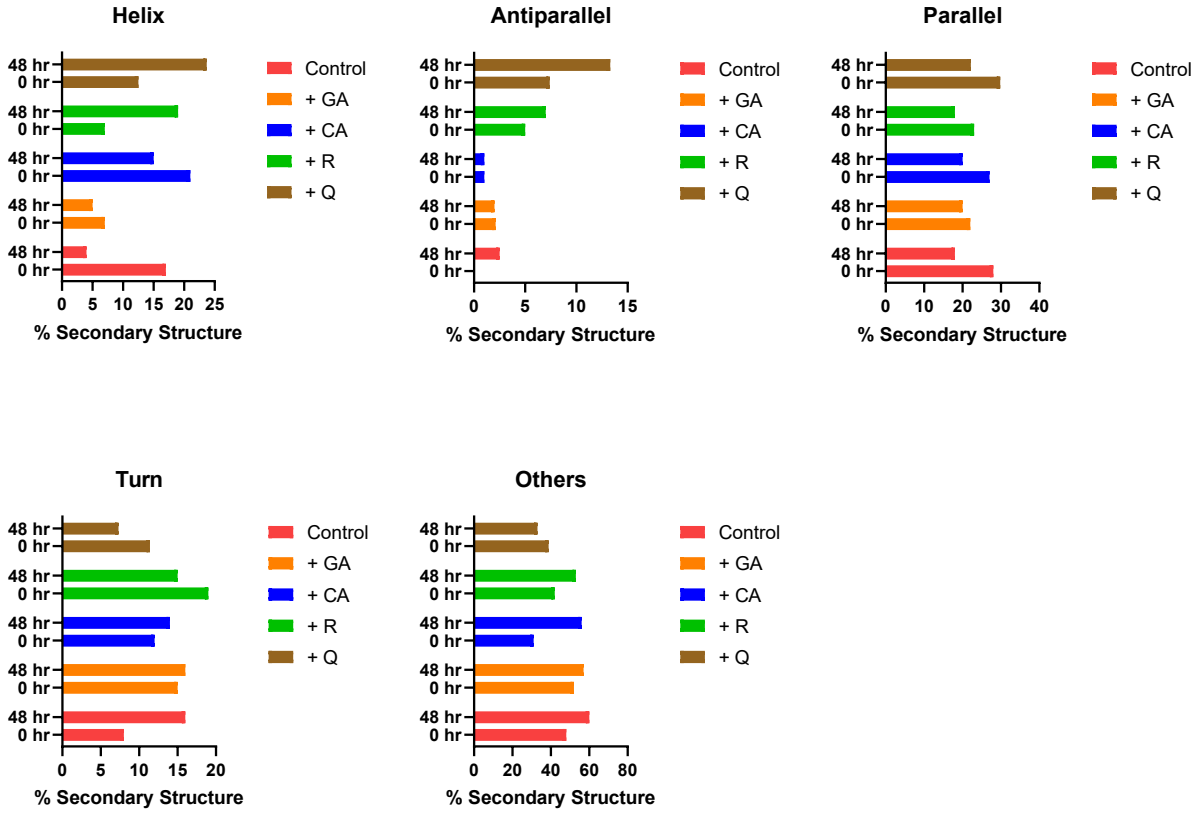

Figure S2.2. Summary of estimated secondary structure contents (in percentage) of IAPP samples upon initial addition of phenolic inhibitor (0 h) and after 48 h. GA, gallic acid; CA, caffeic acid; R, rutin; Q, quercetin.

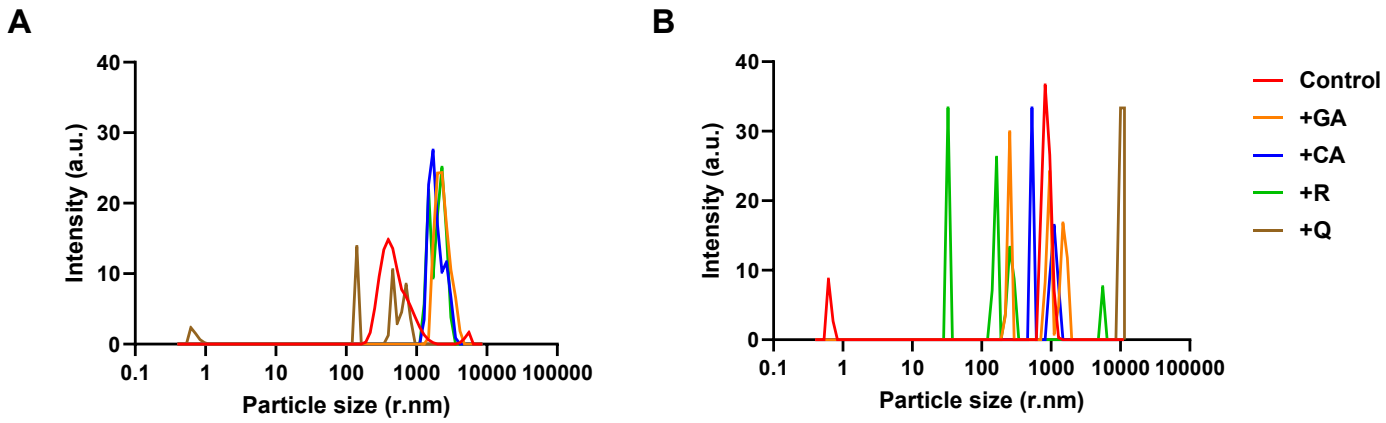

Figure S2.3. Particle radius (nm) size distribution for IAPP in the absence (control) and presence of gallic acid (GA), caffeic acid (CA), rutin (R), and quercetin (Q) at **(A)** 0 h and **(B)** after 48 h incubation. Each curve represents the average of triplicate measurements.

CHAPTER THREE

IDENTIFICATION OF ISLET AMYLOID POLYPEPTIDE ANTI-FIBRILLATION PEPTIDES: THE ROLE OF PHYSICOCHEMICAL PROPERTIES AND BINDING INTERACTIONS ON FUNCTION

Disaggregation of islet amyloid polypeptide fibrils as a potential anti-fibrillation mechanism of tetrapeptide TNGQ

Raliat O. Abioye, Ogadimma D. Okagu, and Chibuike C. Udenigwe
International Journal of Molecular Sciences, **2022**, *23(4)*, 1972.

https://doi.org/10.3390/ijms23041972

DECLARATION FOR THESIS CHAPTER THREE

Disaggregation of islet amyloid polypeptide fibrils as a potential anti-fibrillation mechanism of tetrapeptide TNGQ

This is to declare that there is no conflict of interest associated with this work and the contribution of the candidate is stated below:

Candidate's contribution	Conceptualization, methodology, validation, formal analysis, investigation, writing, review and editing, and visualization	80%

The following co-authors attest to the candidate's participation in a group publication as a component of their thesis and was active in the creation of this publication. The co-author's permission is as follows:

Name	Signature	Date
Ogadimma D. Okagu		
Chibuike C. Udenigwe		

3.0. Abstract

Islet amyloid polypeptide (IAPP) fibrillation has been commonly associated with the exacerbation of type 2 diabetes prognosis. Consequently, inhibition of IAPP fibrillation to minimize β-cell cytotoxicity is an important approach towards β-cell preservation and type 2 diabetes management. In this study, we identified three tetrapeptides, TNGQ, MANT, and YMSV, that inhibited IAPP fibrillation. Using ThT fluorescence assay, circular dichroism (CD) spectroscopy, dynamic light scattering (DLS), and molecular docking, we evaluated the potential anti-fibrillation mechanism of the tetrapeptides. ThT fluorescence kinetics and microscopy as well as transmission electron microscopy showed that TNGQ was the most effective inhibitor based on the absence of normal IAPP fibrillar morphology. CD spectroscopy showed that TNGQ maintained the α-helical conformation of monomeric IAPP, while DLS confirmed the presence of varying fibrillation species. Molecular docking showed that TNGQ and MANT interact with monomeric IAPP mainly by hydrogen bonding and electrostatic interaction, with TNGQ binding at IAPP surface compared to YMSV, which had the highest docking score, but interact mainly through hydrophobic interaction in IAPP core. The highly polar TNGQ was the most active and appeared to inhibit IAPP fibrillation by disaggregation of preformed IAPP fibrils. These findings indicate the potential of TNGQ in the development of peptide-based anti-fibrillation and antidiabetic nutraceuticals.

Keywords: islet amyloid polypeptide; aggregation; disaggregation; fibril formation; bioactive peptides; biomolecular interaction; antidiabetic agents; nutraceuticals

3.1. Introduction

Islet amyloid polypeptide (IAPP), or amylin, is a highly amyloidogenic, 37-residue polypeptide that has been strongly linked to the exacerbation of type 2 diabetes (T2D) prognosis.[4,138] Mature IAPP fibrils induces β-cell cytotoxicity due to their permeation through the cell membrane, resulting in intracellular ion imbalance, formation of reactive oxidative species, membrane disruption, and other deleterious effects.[4,86] Co-packaged and co-secreted along with insulin from pancreatic β-cells, IAPP plays many roles in regulating glucose metabolism.[4,6,102,139] As a result, disease treatments that target the upregulation of insulin secretion may inadvertently encourage IAPP fibrillation due to the increased production and secretion of IAPP, resulting in the additional loss of β-cell mass due to IAPP fibril-induced cytotoxicity.[7]

The mechanism governing IAPP fibrillation-induced β-cell toxicity is not well understood, and many hypotheses point to varying species as the source of cytotoxicity.[4,100] The fibril-induced toxicity hypothesis proposes β-cell cytotoxicity due to mechanical stress imparted on cell membranes by the insoluble IAPP mature fibrils.[100] This results in membrane disruption, causing imbalance in water and ion hemostasis, triggering apoptosis and cell death.[4,6,100] In fact, IAPP mature fibrils, in the absence of oligomeric species, caused notable β-cell cytotoxicity.[140,141] Alternatively, soluble oligomeric species could also cause membrane disruption through the formation of pores, leading to a dysregulated flow of ions and membrane disruption, thus triggering apoptotic pathways.[32] In this hypothesis, insoluble fibrils are regarded as relatively inert and incapable of exerting cytotoxic effects on β-cells. Recently, it has been highlighted that reduced proteolytic turnover of IAPP as a result of impaired proteasome and autophagy machinery could also facilitate the accumulation of toxic hIAPP species and encourage β-cell death.[101] As such, stabilization of monomeric IAPP is the most effective approach for inhibiting IAPP fibrillation. This approach discourages self-association of IAPP, thus preventing fibrillation and oligomeric or fibrillar-induced cytotoxicity, while also retaining the intrinsic function of IAPP. Some natural compounds, such as polyphenols, alkaloids, and peptides, have demonstrated promising anti-fibrillation activities.[33,142] This property may be a contributing mechanism of the antidiabetic properties of some of the compounds. Therefore, IAPP fibrillation provides an important target for the development of new antidiabetic nutraceutical compounds.

Bioactive peptides are promising candidates for use as inhibitors of IAPP fibrillation. In fact, many food-derived peptides have demonstrated physiological antidiabetic properties, but their bioactivity mechanisms have yet to be linked to IAPP fibrillation.[143,144] Furthermore, peptides are more easily modifiable to enhance their biostability, bioavailability, functionality, and bioactivity. To date, only a few unmodified linear peptides, such as pentapeptide FLPNF, have been reported as inhibitors of IAPP fibrillation.[4] There is equally a dearth of information regarding the important structural requirements of peptides for increasing inhibitor potency. This underscores the need for library screening and rational design for the identification of natural peptide inhibitors of IAPP fibrillation. Therefore, the objective of this study was to evaluate the effect and mechanism of three tetrapeptides as inhibitors of IAPP fibrillation. The findings provide important insight into a new structural motif for an effective inhibitor that can disaggregate IAPP fibrils, and platform for the discovery of peptide-based antidiabetic nutraceuticals.

3.2. Materials and Methods

3.2.1. Materials

Human IAPP (amylin (1–37), human, >95% pure) modified with an amidated C-terminus and Cys2-Cys7 disulfide bond was purchased from AnaSpec (Fremont, CA, USA). 1,1,1,3,3,3-Hexafluoro-2-propanol (HFIP), ThT, Tris base, sodium phosphate monobasic, and sodium phosphate dibasic were purchased from MilliporeSigma (Oakville, ON, Canada). Tetrapeptides MANT (98.7% purity), YMSV (95.5% purity), and TNGQ (95.7% purity) were synthesized by GenScript (Piscataway, NJ, USA). UranyLess counterstain was purchased from Electron Microscopy Sciences (Hatfield, PA, USA).

3.2.2. IAPP Preparation

For inhibition experiments, 1 mg IAPP was dissolved in 10 mL HFIP on ice for 10 min and then separated into 1 mL aliquots with a final concentration of 0.1 mg/mL per tube. Samples were sonicated in an ice bath for 30 min and centrifuged at 14,000× *g* for 30 min to disaggregate preformed fibrils. Each tube was frozen overnight at −80 °C and lyophilized the following day. Peptide films were stored at −80 °C until use. The films were reconstituted with 12.5% (*v/v*) HFIP in 1 M Tris buffer (pH 7.4) immediately prior to experimentation. For circular dichroism analysis, 100 mM phosphate buffer (pH 7.4) was used as the diluent instead.

3.2.3. ThT Fluorescence Assay

To observe fibrillation kinetics, ThT fluorescence assays was performed in triplicate. In black 96-well microplates with clear bottoms, 5 μM IAPP was mixed with 5 μM tetrapeptide and 10 μM ThT in 1 M Tris buffer (pH 7.4). Plates were sealed with Parafilm to minimize evaporation and fibrillation was monitored via fluorescence kinetic measurements. Fluorescence intensity was measured at λ_{ex} = 430 nm and λ_{em} = 480 nm using the Spark multimode microplate reader (Tecan, Stockholm, Sweden). Under the kinetic mode, bottom measurements were taken every 15 min for 49 h at 37 °C. Results were presented as means and kinetic parameters and were calculated using the non-linear regression Boltzmann sigmoidal function from GraphPad Prism version 9.2.0 for Windows (GraphPad Software, La Jolla, CA, USA) using the equation:

$$F_{obs} = \frac{(F_i + F_f)}{1+\exp\left(\frac{t_{\frac{1}{2}} - t_{obs}}{\tau}\right)} \quad 3.1$$

F_{obs} is the log fluorescence intensity observed at time t_{obs}, F_i, and F_f are the initial and final ThT fluorescence, respectively, $t_{\frac{1}{2}}$ is the time taken to reach half the elongation phase, and τ is reciprocal of the kinetic elongation constant, K, an apparent rate constant that describes the growth of fibrils during the elongation phase. Additionally, the lag time, in hours, of IAPP fibrillation was calculated using the equation:

$$lag\ time = t_{\frac{1}{2}} - 2\tau \quad 3.2$$

3.2.4. Circular Dichroism (CD) Spectroscopy

The secondary structure of IAPP was analyzed using the Jasco J-715 Circular Dichroism spectrophotometer (Jasco Corp., Tokyo, Japan). Each sample consisted of 20 µM IAPP and 20 µM tetrapeptide in 10 mM phosphate buffer (pH 7.4). Two time points, initial (0 h) and final (48 h), were measured using a quartz cuvette with a path length of 1 mm at room temperature in nitrogen gas. Samples were incubated at 37 °C in between the time point measurements. Three scans were recorded and averaged at a wavelength range of 200–250 nm at a scanning speed of 100 nm/sec. Baseline subtraction was done using a phosphate buffer blank and results were converted to mean residue ellipticity (deg × cm^2 × $dmol^{-1}$) using a mean residue weight of 105.49 Da and IAPP concentration of 0.078 mg/mL. All data processing was performed using CDToolX.[145] Plotting and smoothing of resulting data was achieved with GraphPad Prism version 9.2.0 for Windows (GraphPad Software, La Jolla, CA, USA). Calculation of the secondary structure contents was performed using the CD fitting software, BeStSel .[116]

3.2.5. Molecular Docking of IAPP-Tetrapeptide Interaction for Determination of Substantive Binding Site and Relative Binding Affinity

Molecular docking was performed by uploading the NMR structure of IAPP (PDB code: 2L86) retrieved from RCBS protein data bank and the amino acid sequence of the tetrapeptides to HPEPDOCK web server. MODPEP program was used for conformational refinement of the peptides.[146] Chimera UCSF software version 1.15 equipped with Autodock Vina package version

1.1.2 was used for preparation and structural optimization of the crystal structure of IAPP prior to docking.[118,119] This involves eliminating solvents, adding Gastejger charges and polar hydrogen, ignoring non-standard amino acid residues, and energy minimization to reduce internal clashes. Docking results of the top model were analyzed and visualized with Chimera for intermolecular interactions within 3 Å.

3.2.6. Fluorescence Microscopy

An initial sample consisting of IAPP and tetrapeptide at a ratio of 1:1, with 5 μM of each component, was added to 1 M Tris buffer (pH 7.4) and incubated at 37 °C for 48 h. Thereafter, each sample was stained with 10 μM ThT and kept in the dark for 2 min at room temperature. The samples were then mounted on microscope slides and secured with a coverslip prior to imaging. The Axio Imager 2 fluorescence microscope equipped with an Axiocam 506 camera (Carl Zeiss, Germany) was used to image the samples, using the fluorescein isothiocyanate channel with λ_{ex} = 495 nm and λ_{em} = 519 nm. Images were subsequently processed using the Zen 2.3 pro software (Carl Zeiss, Germany). Aggregate length and diameter measurements were done using the ImageJ software (NIH, Bethesda, MD, USA).[117]

3.2.7. Dynamic Light Scattering (DLS)

The average particle size and polydispersity index of uninhibited IAPP and IAPP incubated with the tetrapeptides were determined using the Nano-ZS Zetasizer (Malvern Instruments Ltd., Malvern, UK). Samples, consisting of IAPP:tetrapeptide ratio of 1:1 with 5 μM of each component in 1 M Tris buffer (pH 7.4), were incubated at 37 °C for 48 h. Particle size and polydispersity index measurements were subsequently taken in triplicate.

3.2.8. Transmission Electron Microscopy (TEM)

TEM was used to observe the effect of the peptides on IAPP fibril morphology. Samples, consisting of 5 μM IAPP and 5 μM tetrapeptide in 1 M Tris buffer (pH 7.4), were incubated at 37 °C for 48 h. Thereafter, 10 μL of the mixture was placed on Parafilm and a 300-mesh Formvar-carbon-coated copper grid was placed on top of the droplet for 2 min. Excess sample was blotted with a Kimwipe. The grids were then counterstained with UranyLess for 1 min in the dark and dried. Grids loaded with sample were imaged using the JEM-1400Flash Electron Microscope (JEOL, Tokyo, Japan) at an accelerating voltage of 120 kV. Fibril length and diameter were

measured using the ImageJ software (NIH, Bethesda, MD, USA).[117] For fibril disaggregation analysis, TNGQ at a 1:1 ratio was added to pre-formed fibrils grown for 48 h at 37 °C. Sample aliquots were taken for TEM imaging at 1, 22.5, and 47.5 h after the addition of TNGQ to the preformed fibrils.

3.2.9. In Silico ADME/Tox and Physicochemical Properties of the Peptides

Physicochemical properties of the tetrapeptides (molecular weight, hydrophobicity, net charge at pH 7, Boman index, instability index, and aliphatic index) were calculated using the Peptides package in R. Gastrointestinal proteolytic stability was predicted using ExPASy PeptideCutter. Drug-likeness and pharmacokinetics of the peptides were evaluated using SwissADME (**http://www.swissadme.ch/index**, date accessed; 6 August 2021), which predicts the ADME (absorption, distribution, metabolism, and excretion) properties based on Lipinski's rule-of-five.[147] For this analysis, SMILES strings of the peptides were retrieved from BIOPEP-UWM. Lastly, potential toxicity of the peptides was predicted using ToxinPred; a threshold of 0.0 (automated) was applied.[148]

3.2.10. Statistical Analysis

Experiments were performed in triplicate and statistical analysis was performed using one-way analysis of variance with GraphPad Prism version 9.2.0 for Windows (GraphPad Software, La Jolla, CA, USA). Significant difference between the mean values was defined at $p < 0.05$ using the Dunnett's multiple comparison test.

3.3. Results

3.3.1. Thioflavin T Fluorescence Kinetics

Several random linear peptides from our library were screened for their anti-IAPP fibrillation activity. Thereafter, based on ThT fluorescence kinetic parameters, tetrapeptides TNGQ, YMSV, and MANT were selected for subsequent analyses. ThT is a dye that strongly fluoresces upon binding to β-sheet rich regions within peptide aggregates. Thus, the stronger the fluorescence intensity, the higher the amount of β-sheets present. Based on ThT fluorescence kinetics, the three tetrapeptides alone did not form fibrils (data not shown), but their presence decreased the maximum fluorescence intensity (F_{max}) of IAPP. Notably, TNGQ showed the highest inhibitory activity in reducing ThT fluorescence, with 32% lower F_{max} compared to the

IAPP control at the end of IAPP fibrillation (**Figure 3.1A**, **Table 3.1**). In terms of physicochemical properties, TNGQ also had the lowest instability, aliphatic, and hydrophobicity indices, as well as the highest Boman index compared to MANT and YMSV (**Table 3.1**).

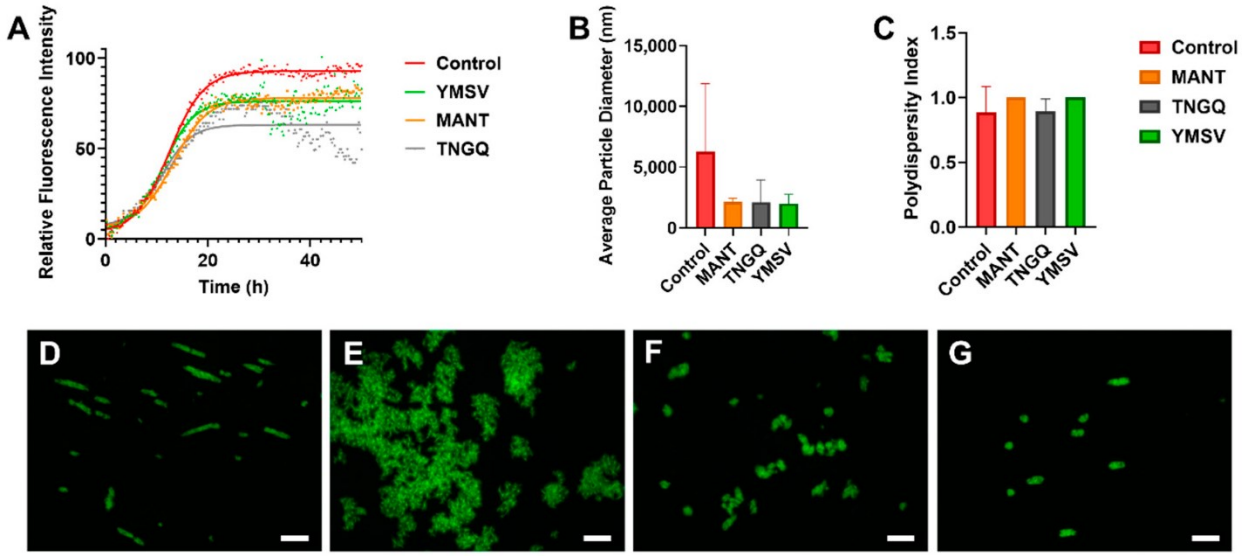

Figure 3.1. (**A**) Thioflavin-T fluorescence kinetics of IAPP fibrillation in the absence (control) and presence of tetrapeptides MANT, TNGQ, and YMSV. (**B**) Average particle size diameter (nm) and (**C**) polydispersity index of IAPP in the absence (control) and presence of MANT, TNGQ, and YMSV in the late stationary phase of fibrillation. ThT fluorescence microscopy of IAPP in the (**D**) absence (control), and presence of peptides (**E**) MANT, (**F**) TNGQ, and (**G**) YMSV. Scale bars represent 50 μm.

Table 3.1. Physicochemical properties and fibrillation kinetic parameters derived from ThT fluorescence assay of IAPP fibrillation in the absence (control) and presence of tetrapeptides MANT, TNGQ, and YMSV.

	Physicochemical Properties						Fibrillation Parameters				
	MW (Da)	Hydrophobicity	Net Charge	Boman Index	Instability Index	Aliphatic Index	F_{max}	$t_{\frac{1}{2}}$ (h)	τ	K	Lag time (h)
Control	n/a	n/a	n/a	n/a	n/a	n/a	92.89	12.45	3.33	0.30	5.79
MANT	435.50	-0.13	-0.002	1.26	17.13	25	77.89	13.13	3.41	0.29	6.31
TNGQ	418.40	-2.03	-0.002	3.45	-67.65	0	63.11	11.00	2.89	0.35	5.22
YMSV	498.59	1.00	-0.003	-0.71	227.2	72.5	76.15	11.30	2.95	0.34	5.39

Abbreviations: MW, molecular weight; F_{max}, maximum fluorescence intensity reached; $t_{\frac{1}{2}}$, time taken to reach half elongation phase in hours; K, elongation constant; and n/a, not applicable. Boman index estimates peptide–protein interaction based on solubility properties of amino acid side chains. Instability index estimates stability of protein in a test tube (value less than 40 means that the protein is stable). Aliphatic index estimates thermostability of globular proteins based on the relative volume occupied by their aliphatic side chains.

Furthermore, TNGQ and YMSV had more pronounced effects in reducing the elongation phase of fibrillation, by having the largest elongation constant (**Table 3.1**). Furthermore, TNGQ caused a gradual decrease in fluorescence intensity from 35–49 h of incubation, with the largest decrease of 53.8% at 48.75 h relative to control (**Figure 3.1A**). In comparison, much lesser decreases in fluorescence intensities (14.1% and 8%) were observed for YMSV and MANT, respectively, at the same time point (**Figure 3.1A**). YMSV and MANT also reduced the F_{max}, but to a lesser extent (16% and 18%, respectively) than TNGQ compared to control F_{max} (**Table 3.1**). MANT slightly increased the lag time compared to the other tetrapeptides but did not have an apparent effect on the elongation constant compared to control (**Table 3.1**).

3.3.2. Fluorescence Morphology of IAPP Fibrils

Fluorescence imaging of ThT-stained IAPP samples was used for preliminary assessment of the morphology of IAPP fibrils in the late stationary phase. According to the images, TNGQ and YMSV resulted in the formation of smaller IAPP aggregates compared to IAPP control (**Figure 3.1D,F-G**). The ThT-fluorescent aggregates were particularly lesser in the presence of TNGQ. Conversely, MANT resulted in the formation of larger aggregates compared to IAPP control (**Figure 3.1D-E**).

3.3.3. IAPP Fibrillation Progression

Average particle size and polydispersity index were determined by dynamic light scattering (DLS) to further assess fibrillation. MANT, TNGQ, and YMSV alone had particle size diameters of 409.8, 380.8, and 223.3 nm, respectively compared to the 6279 nm average diameter of IAPP control. At the end of fibrillation, the peptides reduced the average particle size of IAPP by 66.7% compared to the control (**Figure 3.1B**), although the change was not statistically significant ($p > 0.05$). The polydispersity index was high (> 0.7), with no significant difference between the peptide-treated and control IAPP samples at 48 h of incubation (**Figure 3.1C**).

3.3.4. IAPP Secondary Structure during Fibrillation

Circular dichroism was used to evaluate the effect of the tetrapeptides on IAPP secondary structure and the potential mechanism of inhibition. As expected, a strong negative peak at 220 nm with a shoulder at approximately 206 nm was observed in IAPP control at the initial time point

due to α-helical structure of monomeric IAPP (**Figure 3.2A**). This α-helical structure appears to decrease upon peptide addition at time 0 h. The relative binding affinities between IAPP and peptides are calculated with a high accuracy molecular docking program, HPEPDOCK web server, based on SIMPLEX minimization algorithm binding scores and specifically designed for studying the nature and strength of protein-peptide and protein-protein interactions. In HPEPDOCK docking score, the original scoring function is replaced with an iterative knowledge-based scoring function for protein-peptide and protein-protein interactions. The binding affinities are based on the contributions of intermolecular forces, such as electrostatic, hydrophobic, Van der Waals, hydrogen bonding, entropy, and conformational state of the ligand.[146,149] The higher their negative values, the greater the strength of the interaction, the stability of the complex formed, and the potential to trigger physiological response at low concentrations. As revealed by molecular docking, TNGQ interacts with monomeric IAPP potentially through its hydrophilic and charged amino acid residues. Interactions with Asn3, Arg11, Asn35, and Thr30 were suggested to be facilitated via five hydrogen bonding and electrostatic interactions at the hydrophilic region in the surface of IAPP (**Figure 3.2E,H**). This interaction yields an estimated relative docking score of −109.1. MANT, with a, estimated docking score of −107.7, interacts with relatively charged and hydrophilic residues at the protein core–surface interface and potentially undergoes three hydrogen bonding with Arg11, Asn14, and Thr30 (**Figure 3.2C,F**). On the other hand, YMSV (**Figure 3.2D,G**), being the most hydrophobic tetrapeptide, appears to undergo mainly hydrophobic interactions with IAPP and lies completely in the core of IAPP, where it is predicted to interact with hydrophobic residues such as Ala8, Leu12, Phe15, and Ala25 while maintaining H-bonding contacts with Asn21, Asn22, and Asn31. This results in an estimated docking score of −128.4. [146,149]At 48 h, following fibrillation, the relative α-helical content of IAPP control decreased by 14.7% with concomitant increase in the undefined secondary structure content by 14.2% (**Figure 3.2B**).

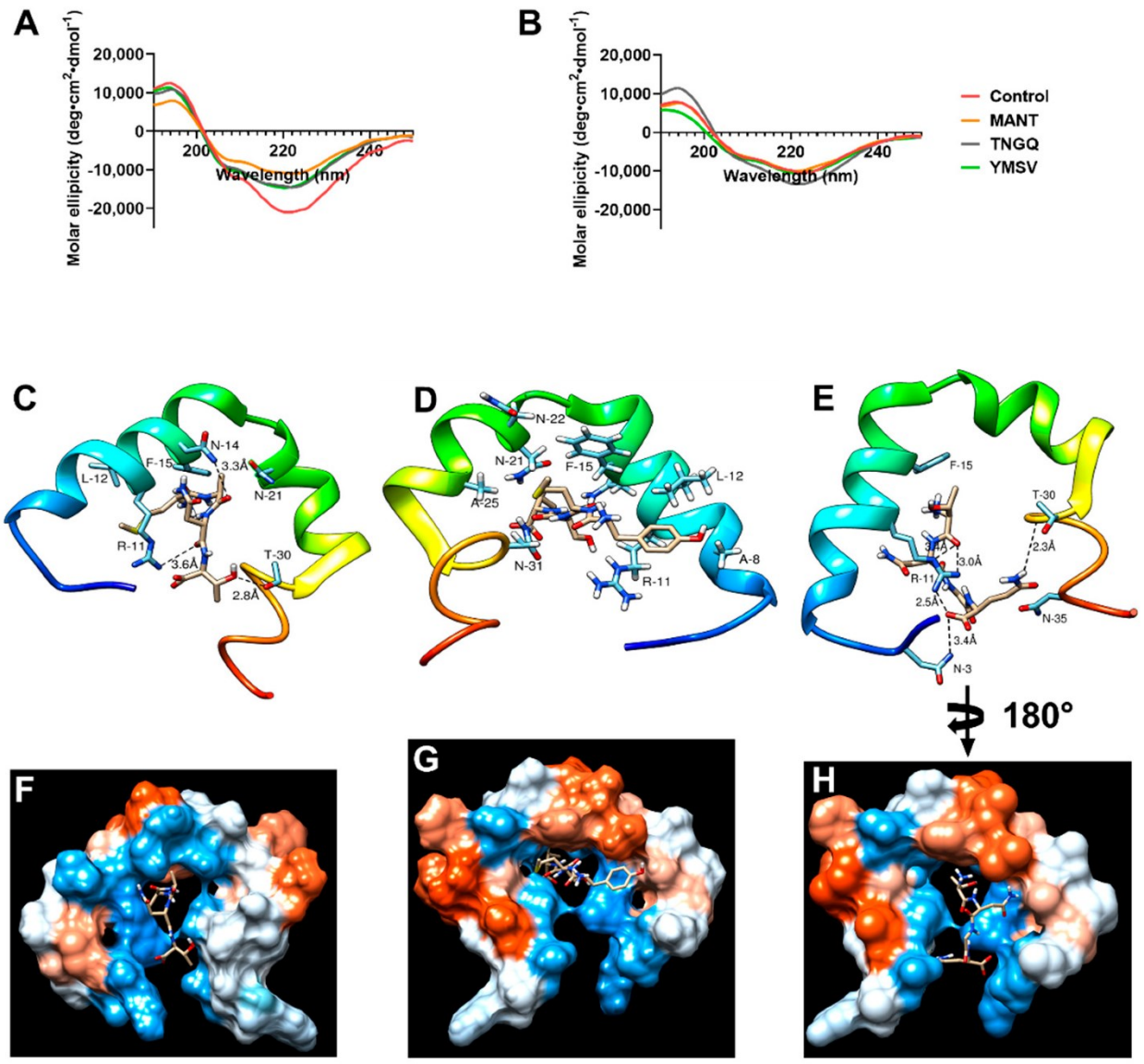

Figure 3.2. Circular dichroism spectra of IAPP in the absence (control) and presence of MANT, TNGQ, and YMSV at (**A**) the initial time point (0 h) and (**B**) late stationary phase (48 h) of fibrillation. Docking scheme showing intermolecular interactions between (**C**) MANT, (**D**) YSMV, or (**E**) TNGQ and monomeric IAPP at the various hydrophobic and hydrophilic regions (**F**–**H**), respectively. Kyte–Doolittle scale was used to evaluate hydrophobicity with colors ranging from dodger blue (the most hydrophilic) to white 0.0 to orange-red (the most hydrophobic).

3.3.5. IAPP Fibril Morphology

To confirm the observed effects of the tetrapeptides on IAPP fibrillation, TEM was employed to evaluate the fibrillar morphology. The tetrapeptides showed different effects on IAPP

fibril morphology. MANT significantly reduced the fibril diameter and density, but not the fibril length, compared to the control (**Figure 3.3A-B**). On the other hand, TNGQ significantly reduced both fibril length and diameter (**Figure 3.3C**), thus confirming its effect as the most potent inhibitor evaluated. Lastly, YMSV significantly increased the fibril length, and not the diameter, resulting in distinctly different fibril morphology compared to IAPP control (**Figure 3.3D**).

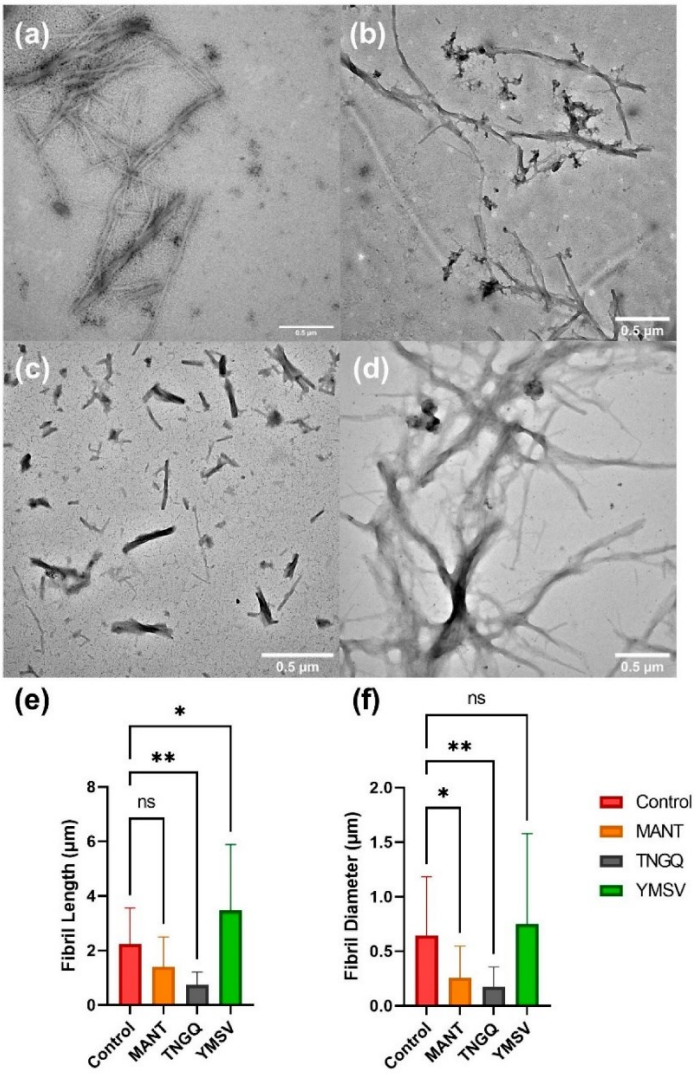

Figure 3.3. Transmission electron microscopy images of (**A**) IAPP control, and IAPP in the presence of (**B**) MANT, (**C**) TNGQ, and (**D**) YMSV, after 48 h incubation. IAPP fibril (**E**) length and (**F**) diameter quantified using ImageJ software (n = 24); ns = not significant ($p \geq 0.05$), * = significant ($0.01 > p > 0.05$), and ** = very significant ($0.01 > p > 0.001$). Scale bars represent 0.5 µm.

3.3.6. Disaggregation of Pre-Formed IAPP Fibrils

To observe the potential disaggregation effect of TNGQ, pre-formed IAPP fibrils were incubated with TNGQ and imaged periodically. As expected, extensive fibrillar networks were observed after 48 h of incubation in both the control and TNGQ-treated IAPP fibrils (**Figure 3.4**). An hour after the addition of TNGQ, amorphous aggregates were observed on the outer perimeter of the fibrils, which was absent in the control fibrils (**Figure 3.4**). At 22.5 h, TNGQ, further reduced the fibrillar networks to form more amorphous aggregates intercalated with fibrils (arrows) (**Figure 3.4**). After 47.5 h post-addition of TNGQ, mature fibrils are observed, albeit less extensive than the control, which had denser and larger fibrillar networks (**Figure 3.4**).

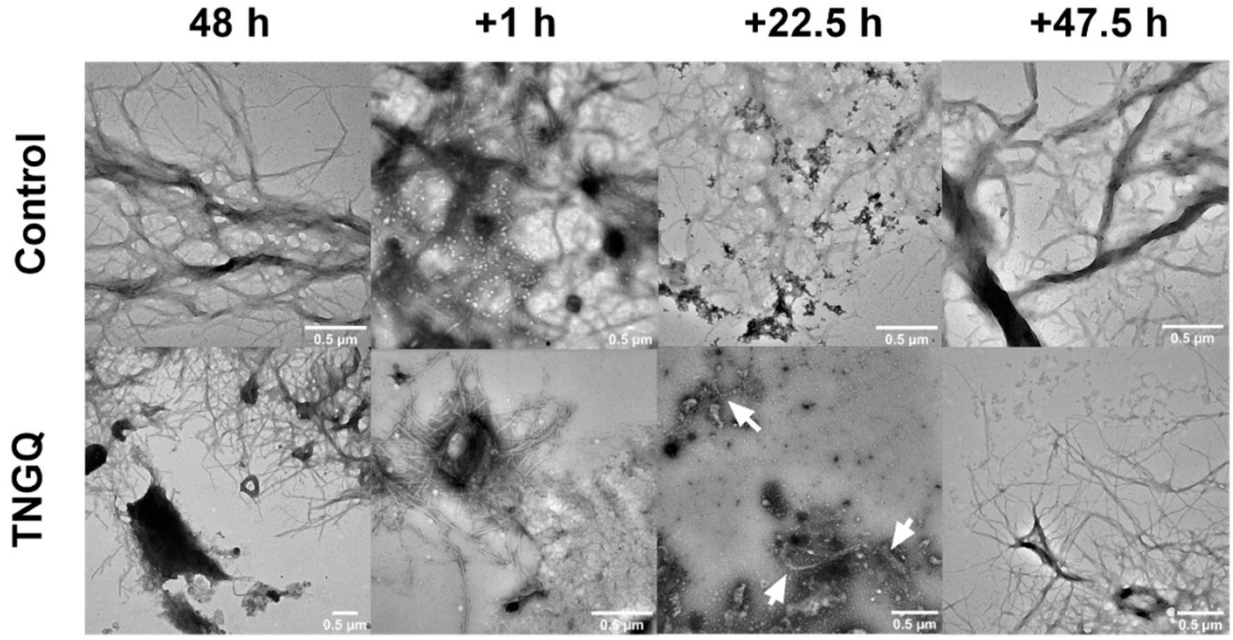

Figure 3.4. Transmission electron microscopy images of pre-formed IAPP fibrils in the absence (control) and presence of TNGQ at 48 h and additional 1, 22.5, and 47.5 h post-incubation. Scale bars represent 0.5 µm. Arrows indicate the presence of fibrils amongst amorphous aggregates.

3.3.7. In Silico Drug-Likeness of the Peptides

In silico ADME/Tox analysis was performed to evaluate the pharmacokinetic and safety properties of the tetrapeptides. All three peptides were predicted to be non-toxic and lack the ability to inhibit cytochrome P450 3A4 (**Table 3.2**). Moreover, the peptides were identified as P-glycoprotein substrates. However, all the peptides were predicted to have low gastrointestinal

absorption. High molecular flexibility indicated by the rotatable bond (ROTB) count greater than 10 and topological polar surface area (TPSA) greater than 140 $Å^2$ indicate low oral bioavailability of the peptides (**Table 3.2**).[150–152] Additionally, the tetrapeptides each had over 12 total hydrogen bond acceptors (HBA) and hydrogen bond donors (HBA), which also indicates potential low oral bioavailability.[152]

Table 3.2. Absorption, distribution, metabolism, excretion, and toxicity (ADME/Tox) profile for tetrapeptides MANT, TNGQ, and YMSV to predict drug-likeness and suitability for human consumption.

Peptide	Physicochemical Properties				Toxicity	Lipophilicity		Drug-Likeness		Pharmacokinetics		
	ROTB (n) < 10	HBA (n) < 10	HBD (n) < 5	ESOL Log S	SVM Score (<0.0)	TPSA (Å^2) < 140	ClogP (o/w) < 5	Bioavailability Score	Lipinski Filter	GIA	P-Gly Substrate	CYP3A4 Inhibitor
MANT	16	8	7	1.83 (HS)	-0.81 Non-toxin	239.24	-2.33	0.17	No	Low	Yes	No
TNGQ	16	9	8	3.32 (HS)	-0.72 Non-toxin	257.03	-3.94	0.17	No	Low	Yes	No
YMSV	17	8	7	0.23 (HS)	-0.89 Non-toxin	216.38	-0.39	0.17	No	Low	Yes	No

Abbreviations: ROTB (*n*), rotatable bonds; HBA (*n*), hydrogen bond acceptors; HBD (*n*), hydrogen bond donors; EOSL, estimated solubility with solubility classes in bracket (HS, highly soluble);[153] Toxicity SVM score (BIOPEP and ToxinPred), support vector machine score;[148] TPSA (Å^2), topological polar surface area; CLogP (o/w) logarithm of compound partition coefficient between n-octanol and water; Bioavailability score, probability of F > 10% in rat;[154] Lipinski filter (based on Lipinski rules of 5, all peptides showed 3 violations); GIA, gastrointestinal absorption; P-gly substrate, permeability-glycoprotein substrate SVM model (SwissADME); and CYP3A4, cytochrome P450 3A4.

3.4. Discussion

Based on IAPP fibrillation inhibitor screening studies of a library of randomly selected peptides, three active tetrapeptides were selected to further investigate their effectiveness and mechanisms of inhibition. TNGQ exhibited the strongest inhibitory effects, primarily influencing the stationary phase of IAPP fibrillation (**Figure 3.1A**, **Table 3.1**). The Boman index (**Table 3.1**) suggests that only TNGQ had high protein binding potential, and yet it had a lower estimated IAPP docking score compared to YMSV. Notably, only TNGQ was suggested to bound outside of the hydrophobic pocket in the amyloidogenic region (**Figure 3.2E,H**). In fact, the predicted TNGQ binding favored interactions with Asn3, Arg11, and Phe15 of the membrane-binding domain, and Thr30 and Asn35 of the self-association/C-terminus region of IAPP. This predicted binding pattern of TNGQ supports the relative secondary structures present. After 48 h of incubation, TNGQ maintained the relative α-helical content of IAPP compared to the control, MANT, and YMSV, which showed marked decreases relative to the initial timepoint (**Figure 3.2A-B**). It is possible that TNGQ binding with monomeric IAPP stabilized the α-helical conformation to alter the thermodynamic equilibrium between IAPP species against fibril formation. The complexation of TNGQ and monomeric IAPP reduces the relative amount of unbound monomeric IAPP, thus halting fibrillation progression and delaying the formation of extensive IAPP fibrillar networks normally found in the stationary phase (**Figure 3.3A, C**). Similarly, amphipathic heptapeptide KPWWPRR-NH_2 was reported to arrest IAPP fibril elongation.[155] The hydrophobic regions of the heptapeptide bound the non-polar regions of IAPP while the hydrophilic regions disrupted elongation by interfering with the formation of H-bonds required for association of monomeric IAPP on the fibril growth end.[155] Consequently, significantly shortened fibrils with smaller diameters were observed in our study (**Figure 3.3C, E-F**). This confirms the strong anti-fibrillation propensity of TNGQ and demonstrates the importance of physicochemical properties of peptides on inhibition mechanism and potency.

The formation of the IAPP-TNGQ complex provides additional insight on the mechanism governing the disaggregation of preformed fibrils (**Figure 3.4**). IAPP fibrils were disaggregated starting from the outer regions of the extensive fibrillar network as soon as 1 h after the addition of TNGQ, indicated by the disordered structures surrounding the fibrils (**Figure 3.4**). The disaggregation effects intensified at 22.5 h of TNGQ treatment where amorphous aggregates are

observed to surround the fibrils (**Figure 3.4**). These aggregates are similar in shape and size to that observed in the initial timepoint of IAPP control (data not shown). This suggests the formation of monomeric or oligomeric species following fibrillar disaggregation by TNGQ. Similar structures have been identified as oligomeric species of α-synuclein.[156] Molecular dynamics simulation predicts the process of nucleation in the presence of lipids to be driven by aromatic interactions within the central part of IAPP, with long-lasting interactions between 14-NFLVH-18 and 25-AILSST-30 driving the formation of β-sheets.[9] Additionally, the prenuclear β-hairpin conformation is an important structural conformation that promotes dimerization, primarily driven by the C-terminal region residues 17-VHSSNNFGAIL-27 and 29-STNVGSTN-35.[157] This provides a mechanistic insight into the IAPP fibril disaggregation effects of TNGQ. As fibrillation is a thermodynamically driven process, species equilibrium will strongly influence fibrillation progression, provided the kinetic barrier is low enough.[130] Formation of the IAPP-TNGQ complex may have shifted the mature fibril/monomeric IAPP equilibrium towards the formation of monomeric IAPP. Visually, this manifested as the disaggregation of preformed fibrils (**Figure 3.4**) wherein monomeric IAPP liberated from the growing ends of the fibrils are used to re-establish equilibrium. This can also explain why the addition of TNGQ inhibited fibrillation even though it did not elongate the lag phase. This finding provides a unique perspective to fibrillation inhibitor design, which hitherto has focused largely on association with the amyloidogenic region.[158–161] Recent investigations on the development of peptide inhibitors have started considering non-amyloidogenic regions, namely the C-terminal self-association region, and N-terminal membrane-binding domain due to their important roles in fibril formation and toxicity.[61,162] Consequently, the ability of TNGQ to bind within the N-terminal membrane-binding domain may reduce the cytotoxic effects commonly observed with fibrillation by preventing membrane association and subsequent pore formation. For instance, pentapeptide FLPNF, which binds within the membrane-binding domain and self-association region of the N- and C-terminus, respectively, was reported to increase the viability of cultured rat insulinoma cells.[61] This illustrates the potential of targeting the non-amyloidogenic regions of IAPP as an alternative mechanism in the development of novel anti-fibrillation agents.

Amino acid composition of peptides can affect the inhibitor potency and mechanism of IAPP fibrillation inhibition. Previous studies have reported that hydrophobic and aromatic interactions are the major forces driving IAPP fibrillation.[56,94] Additionally, some phenolic

compounds were hypothesized to inhibit fibrillation via π-π and hydrophobic interactions within the amyloidogenic core of IAPP.[4,33,94] Thus, we expected that hydrophobicity would correlate with inhibitor potency. However, YMSV was the most hydrophobic of the tetrapeptides tested, and only moderately inhibited fibrillation (**Figure 3.1A**, **Table 3.1**). Incidentally, YMSV also has the lowest protein binding potential of the three tetrapeptides (**Table 3.1**), despite having the highest IAPP docking score. This suggests a wider range of structural requirements for potent inhibitors, beyond hydrophobicity and aromatic content, and that predicted favorable inhibitor binding to IAPP does not guarantee increased activity. Future studies on the effect of peptide sequence and physicochemical properties on inhibition of IAPP fibrillation, for example through the development of scrambled peptide sequences, could be done to further investigate this relationship. MANT, which had the lowest inhibitor strength, slightly inhibited the late stationary phase of IAPP fibrillation due to the lower F_{max} compared to IAPP control (**Figure 3.1A**, **Table 3.1**). However, ThT fluorescence imaging in the late stationary phase revealed that MANT led to the formation of larger aggregates compared to the control (**Figure 3.1D-E**). This may be due to the limitations of ThT fluorescence imaging wherein non-fibrillar species may result in fluorescence. Nonetheless, TEM imaging indicated the formation of fibrillary networks with significantly smaller diameter but similar in length compared to IAPP control (**Figure 3.3F**). This confirms the ThT fluorescence kinetics results, which showed that MANT was not a strong inhibitor of fibrillation compared to TNGQ (**Figure 3.1A**, **Table 3.1**).

Despite the variable inhibitory activities observed with the three tetrapeptides, IAPP fibrillation still occurred in each sample, indicated by the increase in particle size beyond a radius of 1100 nm, which has been reported to be the average size of IAPP fibrils at the end of late stationary phase.[26] Although the IAPP particle size did not differ significantly, IAPP in the presence of MANT, TNGQ, and YMSV reduced the average diameter compared to the control (**Figure 3.1B**). The exceedingly high particle size of uninhibited IAPP suggests the formation of extensive fibrillar networks, which were suppressed in treated samples due to the variable inhibitory activities of the tetrapeptides. Furthermore, the high polydispersity index indicated high heterogeneity of species present within the samples, which is characteristic for IAPP fibrillation (**Figure 3.1C**). The heterogeneity could also be a result of fibril disaggregation resulting in smaller species, or an artifact of active fibrillation inhibition through the formation of IAPP-peptide complexes.[26]

In addition to being the strongest inhibitor, TNGQ also showed promising biostability and pharmacokinetic properties. It was predicted to be more biostable in the gastrointestinal tract than the others, as it lacks the recognition and cleavage sites for pepsin, trypsin, and chymotrypsin. The ADME profile also indicated that the non-toxic tetrapeptide can be rapidly metabolized and removed from cells in the body, thus suggesting its suitability for human consumption. However, TNGQ and the other peptides were predicted to have low oral bioavailability based on their ROTB, HBA, and TPSA.[151,152] This factor must be addressed prior to conducting *in vivo* studies in order to achieve significant IAPP fibrillation inhibitory effects in the pancreas. TNGQ can be found naturally, e.g., in rice oryzain beta chain (f177-180; accession no. P25777 (ORYB_ORYSJ)); thus, future research should include the development of sustainable processing methods, e.g., enzymatic hydrolysis or fermentation, to release the bioactive peptide from its parent proteins.

3.5. Conclusions

This study resulted in the discovery of three tetrapeptides, MANT, TNGQ, and YMSV, that present variable inhibitory effects on IAPP fibrillation. Through biomolecular analysis, potential mechanisms of inhibition and the effect of physicochemical properties of the peptides on activity were proposed. The weak activities of YMSV and MANT demonstrate that strong inhibitor binding to monomeric IAPP does not always translate to potent anti-fibrillation effects. TNGQ, the most active tetrapeptide studied, strongly inhibited IAPP fibrillation wherein it possibly bound IAPP monomers, thus preventing their subsequent attachment to the growing end of the fibril. Furthermore, the disaggregation of pre-formed IAPP fibrils is proposed to be the major anti-fibrillation mechanism of TNGQ. This highlights the importance of the monomer–fibril equilibrium in facilitating anti-fibrillation. The interplay between the physicochemical properties of peptides and anti-fibrillation mechanism and potency, an area that is currently understudied, provides an insight into structure–function relationships of the inhibitors. Lastly, studies to evaluate the antidiabetic and cell protective effects of TNGQ present a promising avenue for future applications.

3.6. Acknowledgements

This research was funded by the Natural Sciences and Engineering Research Council of Canada (NSERC) through the Discovery Grants Program, reference number RGPIN-2018-06839, and the University of Ottawa through the University Research Chairs Program.

Conflicts of Interest

The authors declare no conflict of interest.

CHAPTER FOUR

IMPACT OF DOMAIN-SPECIFIC BINDING OF ANTI-FIBRILLATION PEPTIDES ON MEMBRANE BINDING AND β-CELL PROTECTIVE EFFECTS

Cross-domain binding of anti-fibrillation peptide TNGQ to islet amyloid polypeptide provides cytoprotective effects in giant unilamellar vesicles and pancreatic β-cells

Raliat O. Abioye, Martha S. Yiridoe, Chenyang Wang, Tyler J. Avis, Tamer A. E. Ahmed, Riadh Hammami, and Chibuike C. Udenigwe

Food & Function, **2024**

DECLARATION FOR THESIS CHAPTER FOUR

Cross-domain binding of anti-fibrillation peptide TNGQ to islet amyloid polypeptide provides cytoprotective effects in giant unilamellar vesicles and pancreatic β-cells

This is to declare that there is no conflict of interest associated with this work and the contribution of the candidate is stated below:

Candidate's contribution	Conceptualization, methodology, validation, formal analysis, investigation, writing, review and editing, and visualization	65%

The following co-authors attest to the candidate's participation in a group publication as a component of their thesis and was active in the creation of this publication. The co-author's permission is as follows:

Name	Signature	Date
Martha S. Yiridoe		
Chenyang Wang		
Tyler J. Avis		
Tamer A. E. Ahmed		
Riadh Hammami		
Chibuike C. Udenigwe		

4.0. Abstract

Islet amyloid polypeptide (IAPP) fibrillation induces β-cell dysfunction and toxicity in patients with type 2 diabetes. Cytotoxicity is caused by the ability of IAPP fibrils and fibrillar intermediates to permeate the cellular membrane of pancreatic β-cells, trigger endoplasmic reticular stress, induce reactive oxygen species production, and upregulate apoptosis-related genes. Thus, inhibition of IAPP fibrillation is of great interest for preventing associated cytotoxicity. In this study, the cellular protective effects of three anti-fibrillation tetrapeptides, YMSV, MANT, and TNGQ, against IAPP-induced membrane leakage in giant unilamellar vesicles (GUVs) and toxicity in RIN-m cells were evaluated. The anti-fibrillation activity of TNGQ translated to cytoprotective effect as it resulted in a 69.0 ± 7.9% decrease in calcein release in GUVs and a significant increase in cell viability from 6.4 ± 6.4% with IAPP to 47.5 ± 3.8% with the addition of TNGQ. MANT slightly inhibited IAPP-induced GUV leakage and increased cell viability. In contrast, the protective effect of YMSV against IAPP-induced membrane damage in GUVs was completely diminished in β-cells. Molecular docking of pentameric IAPP showed that Asn21 and Asn22 of IAPP are important for inhibitor binding, which, coupled with the cross-domain binding interactions of TNGQ, explains its stronger anti-fibrillation and cytoprotective effects than MANT and YMSV. These findings provide insights into the functional significance of peptide-IAPP binding interactions in mitigating fibrillation and IAPP-induced cytotoxicity.

Keywords: bioactive peptides; islet amyloid polypeptide; fibrillation; pancreatic β-cells; biomembrane; cytotoxicity; type 2 diabetes

4.1. Introduction

Common protein conformational diseases, such as Parkinson's, Huntington's, Alzheimer's, and prion diseases, and other less common diseases, such as transthyretin amyloidosis, are characterized by naturally endogenous proteins and peptides that are predisposed to the formation of amyloid plaques and disease progression.[163,164] One such peptide is the islet amyloid polypeptide (IAPP) or amylin, which has been implicated in the progression of type 2 diabetes (T2D). IAPP is a 37-residue basic polypeptide that primarily functions in the postprandial metabolism of glucose and lipids, with peripheral roles in gastric emptying and satiety regulation.[6] This hormonal peptide is co-produced, co-packaged, and co-secreted along with insulin at an IAPP:insulin ratio of 1:100, posing a challenge to antidiabetic treatments that upregulate insulin

secretion, as this equally increases the production and secretion of the highly amyloidogenic peptide.[7,102,139]

IAPP fibrillogenesis induces pancreatic β-cell toxicity as a result of toxic fibrillar intermediates such as soluble oligomers, which disrupt cellular membrane integrity via pore formation, or insoluble mature fibrillar end products, which impart mechanical stress on cellular membranes, causing ruptures and inducing apoptosis.[4,100] IAPP fibrillation-induced cytotoxicity is also caused by the formation of reactive oxygen species, induction of inflammatory responses, and inhibition of the autophagy response, among other effects.[6,86] Although not as well studied as popular T2D clinical targets, such as α-glucosidase, dipeptidyl peptidase-IV, and glucose transporters, IAPP fibril formation occurs at a high incidence in T2D, with more than 95% of patients presenting with the accumulation of IAPP fibrillar species in the pancreatic Islets of Langerhans.[6,87,88,165] Thus, it is imperative to identify the inhibitors of IAPP fibrillation. A wide range of fibrillation inhibitors from different classes of natural compounds, including polyphenols, peptides, terpenoids, and carbohydrates, has been reported.[134]

IAPP consists of three main domains: the N-terminal membrane-binding domain, amyloidogenic region, and C-terminus self-association domain.[4] The amyloidogenic region has been identified as the driving force behind fibril formation and its associated cytotoxic effects, thus making it a popular binding region for potential anti-fibrillation agents.[33,93,94] Our previous study alluded to the potential effect of regional binding to IAPP on the anti-fibrillation mechanism and the disaggregative effect of peptides, YMSV, MANT, and TNGQ.[166] However, it is not apparent whether binding interactions and IAPP fibrillation inhibition would translate to reduced IAPP fibrillation-induced cytotoxicity. Thus, to explore their differential binding behaviors and to understand their potential cellular protective effects, the role of these anti-fibrillation tetrapeptides in maintaining cellular membrane integrity and pancreatic β-cell viability was investigated. The findings from this study will provide novel perspectives on the importance of IAPP domains in fibril formation and insight into the important regions that inhibit fibril formation and associated cytotoxic effects.

4.2. Materials and methods

4.2.1. Materials

1,1,1,3,3,3-Hexafluoro-2-propanol (HFIP), ThT, chloroform (≥99.5%), 1,2-dioleoyl-sn-glycero-3-phosphocholine (DOPC, ≥99%), 1,2-dioleoyl-sn-glycero-3 phosphoethanolamine-N-(lissamine rhodamine B sulfonyl) (ammonium salt) (≥99%), ethylenediaminetetraacetic acid (EDTA) (99.4-100.6%) and calcein were purchased from MilliporeSigma (Oakville, ON, Canada). Polyethylene glycol tert-octylphenyl ether (Triton X-100) was purchased from VWR (Mississauga, ON, Canada). Tris(hydroxymethyl)aminomethane (Tris-base; ≥100.1%), sodium chloride (≥99%), sodium hydroxide (≥98%), dimethyl sulfoxide (DMSO), fetal bovine serum (FBS), penicillin-streptomycin, l-glutamine, and 0.25% trypsin-EDTA were purchased from Thermo Fisher Scientific (Nepean, ON, Canada). Human islet amyloid polypeptide (IAPP, amylin (1-37), human; >95%) modified with an amidated C-terminus and a Cys2-Cys7 disulfide bond was purchased from AnaSpec (Fremont, CA, USA). Tetrapeptides MANT (98.7%), YMSV (95.5%), and TNGQ (95.7%) were synthesized by GenScript (Piscataway, NJ, USA). RIN-m rat insulinoma (CRL-2057) cells and RPMI-1640 medium (cat. No. 30-2001) were purchased from ATCC (Manassas, VA, USA). The CyQUANT™ MTT Cell Viability Assay Kit (cat. No. V13154) was purchased from Invitrogen (Waltham, MS, USA).

4.2.2. Preparation of IAPP

To disaggregate any existing fibrils prior to the experiments, 1 mg of IAPP was dissolved in 10 mL HFIP on ice for 30 min and then separated into aliquots of 500 µL with a final concentration of 0.1 mg/mL. Aliquoted tubes were sonicated for 30 min in an ice bath, immediately centrifuged at 4 °C for 30 min at 14,000 × g, and then frozen overnight at -80 °C. The samples were lyophilized the following day, and the resulting peptide films were stored at -80 °C until use. For each experiment, lyophilized peptide films were reconstituted with 12.5% (v/v) HFIP in leakage buffer (10 mM Tris, 150 mM NaCl, and 1 mM EDTA, pH 7.4) and used immediately.

4.2.3. Preparation of giant unilamellar vesicles

Calcein-loaded and empty giant unilamellar vesicles (GUVs) were prepared according to a previously described protocol.[167,168] For imaging purposes, empty GUVs labelled with rhodamine were used, and loaded GUVs containing calcein were used for leakage studies (fluorescence and dynamic light scattering analyses). First, a solution of 1,2-dioleoyl-sn-glycero-3-phosphocholine (7.2 mg/mL) was dissolved in 5 mL of chloroform in a 50 mL centrifuge tube for both types of GUV. In addition, 1 mg of 1,2-dioleoyl-sn-glycero-3 phosphoethanolamine-N-

(lissamine rhodamine B sulfonyl) was added to the imaging GUV tube, and each tube was briefly vortexed, covered with aluminum foil, and placed in a vacuum flask covered with aluminum foil. The mixture was dried under a stream of nitrogen for 4 h and vacuum dried for another 12-48 h. Calcein solution (70 mM, 30 mL, pH 7.5) was prepared with leakage buffer (10 mM Tris, 150 mM NaCl, 1 mM EDTA, pH 7.4), and 10 mL was added to only the calcein-loaded GUV tube, followed by vortex mixing for 1 min. Each tube was sonicated at 30 °C for 2 h and subjected to five freeze/thaw cycles consisting of repeated freezing in liquid nitrogen for 3 min, thawing in 60 °C water for 5 min, and vortexing for 1 min. The GUV formed were stored in aliquots at -80 °C until use.

To prepare GUVs for imaging or leakage analysis, unencapsulated calcein was separated from the calcein-loaded GUVs via size exclusion chromatography (Sephadex G-50, Sigma-Aldrich) using leakage buffer for equilibration and elution. The eluted calcein-loaded GUVs were stored for a maximum of 72 h at 4 °C before the leakage study.

4.2.4. Fluorescence GUV leakage assay

This assay was used to examine the cytotoxicity of IAPP on GUVs by monitoring the amount of calcein leakage caused by membrane rupture in the presence of IAPP and the effectiveness of the tetrapeptide inhibitors in decreasing calcein permeation. In black 96-well microplates, 5 μM IAPP was mixed with 5 μM tetrapeptide and 80 μL of GUV in leakage buffer (10 mM Tris, 150 mM NaCl, and 1 mM EDTA, pH 7.4), and the plate was sealed with Parafilm to minimize evaporation. In kinetic mode, samples were shaken once for 5 s at the beginning, and then the fluorescence intensity of the calcein released from GUVs was measured at λex 485 nm and λem 535 nm using top fluorescence intensity measurements at an interval of 30 min for 12 h at 37 °C using a Spark multimode microplate reader (Tecan, Stockholm, Sweden). The samples evaluated in this study included a positive control, a negative control, an IAPP control, and tetrapeptide samples YMSV, MANT, and TNGQ, all in triplicate. The positive control, which consisted of GUVs mixed with 10% (v/v) Triton X-100 in leakage buffer, provided the maximum calcein leakage, F_M. The negative control, consisting of GUVs in the leakage buffer, provided the baseline fluorescence intensity, F_0, of GUVs in buffer. The effect of tetrapeptides alone on GUVs was also evaluated in the absence of IAPP. The following equation was used to calculate the percentage leakage of calcein for each sample at each time point:

$$\% \, leakage = \left(\frac{F - F_0}{F_M - F_0}\right) \times 100 \quad 4.1$$

The final fluorescence intensity, F, was measured at 12 h.

4.2.5. Dynamic light scattering

The interactions between the loaded GUV, tetrapeptides, and IAPP were explored using two parameters: particle size and polydispersity index (PDI) using a Nano-ZS Zetasizer (Malvern Instrument Ltd., Malvern, UK). Dynamic light scattering was conducted at 0 h and 12 h for each sample and incubated at 37 °C between measurements. Solutions of 5 μM IAPP and 5 μM tetrapeptides, and 400 μL of GUVs in leakage buffer were mixed and analyzed with the Mark-Houwink parameters for size, where the A parameter was 0.428 and K parameter was 7.67e-5 cm2/s, the backscattered angle was 173°, and the refractive index was 1.330. All measurements were performed in triplicate at 37 °C using a disposable polystyrene cuvette after 120 s of equilibration. Positive (10% (v/v) Triton X-100), negative (GUVs in leakage buffer), and tetrapeptide controls were analyzed as described in the previous section.

4.2.6. Fluorescence microscopy imaging

Fluorescence microscopic imaging was conducted with the EVOS M5000 Cell Imaging System (Thermo Fisher Scientific, Nepean, ON) using a Texas Red light cube with λex of 585 nm and λem of 624 nm. Samples were prepared by depositing 5 μL of each sample on microscope slides, secured with a coverslip, and sealed with nail polish to prevent evaporation. High-resolution images of GUV were captured at four time points (0, 2.5, 3, and12 h), with the samples incubated in a 37 °C water bath between imaging. Images were processed using Zen 2.3 pro software (Carl Zeiss, Germany) and ImageJ software (NIH, Bethesda, MD, USA).[117] The samples and controls were consistent with those used for the GUV leakage assay and dynamic light scattering analysis, except that empty GUV were used instead of calcein-loaded GUV.

4.2.7. Thioflavin T kinetics assay

To understand the complex dynamics among IAPP, tetrapeptide inhibitors, and GUVs on subsequent IAPP fibrillation, ThT fluorescence assays were performed. In black 96-well microplates, 5 μM IAPP was mixed with 5 μM tetrapeptide, 10 μM ThT, and 80 μL GUV in leakage buffer (10 mM Tris, 150 mM NaCl, and 1 mM EDTA, pH 7.4). Fluorescence assays were

conducted in the kinetics mode, where the top measurements were taken every 30 min for 12 h at 37 °C. The plates were sealed with paraffin to minimize evaporation. The fluorescence intensity was measured at λ_{ex} 430 nm and λ_{em} 480 nm using a Spark multimode microplate reader (Tecan, Stockholm, Sweden). The results are presented as the mean values of triplicate samples.

4.2.8. Molecular docking

Molecular docking of the human IAPP (hIAPP) pentamer with selected peptides was performed using the LibDock program in the Discovery Studio software. Three-dimensional (3D) structures of the peptides were produced using ChemBio3D Ultra 14.0. The crystal structure of the hIAPP pentamer (PDB ID 6VW2) was downloaded from Protein Data Bank (PDB) (http://www.rcsb.org/pdb). The hIAPP pentamer was composed of two symmetrically related protofilaments. The model was modified by removing one of the symmetrical protofilaments and then optimized using the Prepare Protein module. The binding site was determined from current selection using the Receptor-Ligand Interactions module. After docking, the best pose was selected based on LibDockScore values. The results of molecular docking were visualized using the Molecular Operating Environment (MOE) software.

4.2.9. Cell culture

RIN-m rat insulinoma cells were cultured in sterile RPMI-1640 medium supplemented with 10% (v/v) FBS, 100 U/mL penicillin, 100 μg/mL streptomycin, and 2 mM glutamine and maintained in a humidified incubator at 37 °C with 5% CO_2. At confluency (80-95%), the cells were expanded using 0.25% trypsin-EDTA or used for the experiments. Cells were passaged on a weekly basis, and passages 6–8 were used for all experiments. IAPP and peptide inhibitors were prepared in complete culture medium and then filter-sterilized prior to incubation with RIN-m cells.

4.2.10. Cell viability assays

Cell viability was quantified using a CyQUANT^{TM} MTT Cell Viability assay. Briefly, 1×10^4 cells per well were plated in 100 μL complete culture medium in transparent 96-well plates. After culturing, the cells were grown to 80% confluency. Thereafter, 100 μL of 5 μM IAPP, with or without the addition of 5 μM tetrapeptides (YMSV, MANT, and TNGQ), was added to the cells, and incubated for 24 h at 37 °C with 5% CO_2. Following incubation, the cells were harvested by

replacing the medium with MTT reagent dissolved in complete culture medium and incubated for 3 h to allow for the conversion of yellow tetrazolium salt into purple formazan crystals by mitochondrial reductases in surviving cells. The resulting formazan crystals were dissolved in DMSO and the absorbance at 569 nm was measured using a Spark multimode microplate reader (Tecan, Stockholm, Sweden). Cell viability was expressed as a percentage of MTT reduction and calculated as follows:

$$\%\ cell\ viability = \left(\frac{C-A}{B-A}\right) \times 100 \qquad 4.2$$

C is the absorbance of the cells treated with IAPP with or without tetrapeptide inhibitors, A is the mean absorbance of the dead cell control samples, and B is the mean absorbance of the live cell controls. Ethanol (70%, v/v) was used as the dead cell control, whereas complete culture media was used as the live cell control. All IAPP, peptide, and ethanol solutions were sterile filtered prior to use, and all experiments involving cells were performed in quadruplicates.

4.2.11. Statistical analysis

Results are expressed as the mean values of experimental replicates ± standard deviation. Statistical differences were determined using one-way or two-way analysis of variance with GraphPad Prism version 10.2.3 for Windows (GraphPad Software, La Jolla, CA, USA) or SPSS Statistics version 29.0.2.0 (IBM, Armonk, NY, USA). Significant differences between the mean values were defined at α level = 0.05, using Šídák's multiple comparisons test.

4.3. Results and discussion

4.3.1. Decreased IAPP fibrillation-induced calcein leakage in the presence of anti-fibrillation tetrapeptides

The fluorescence intensity was used to determine the percentage of calcein released through the GUV membranes. As shown in **Figure 4.1A**, IAPP demonstrated membrane disruptive effects on the calcein-loaded GUVs, characterized by a gradual increase in fluorescence intensity within the first 4 h, followed by a slight decrease and plateau (**Figure 4.1A**). This corresponds to a significant time-dependent increase in calcein fluorescence from 8.3% at 0 h to 12.9%, 18.6%, and 17.2% at 2, 3.5, and 12 h, respectively, compared to the intact GUVs control (**Figure 4.1A** and **B**). A rapid increase in the ThT fluorescence kinetics of IAPP indicates rapid

fibrillation and potential secondary nucleation, which are characteristic of the elongation phase of IAPP fibrillation.[169] This highlights the membrane-disruptive effects of soluble fibrillar intermediates, such as dimers and oligomers, which are abundant in the early elongation phase. These intermediates may be responsible for the increased calcein leakage due to pore formation, which compromises the membrane integrity.[170] After 12-h of incubation, all three tetrapeptides decreased GUV calcein leakage, with TNGQ producing the strongest inhibition of IAPP-induced calcein leakage, followed by YMSV and then MANT (**Figure 4.1B**). TNGQ was also the most effective inhibitor for maintaining GUV membrane integrity and preventing leakage ($0.01 > p > 0.05$) at every time point compared to the IAPP control (**Figure 4.1B**). Interestingly, the tetrapeptides exhibited strong inhibitory effects at 2 h. Over time, the initial protective effect of MANT was completely lost, given the continuous increase in fluorescence, which reached that of IAPP at 12 h (**Figure 4.1A**). In contrast, YMSV and TNGQ treatments resulted in a rapid fluorescence plateau over time with IAPP fibrillation, suggesting potential inhibition of IAPP-membrane interactions. Overall, the addition of TNGQ, YMSV, and MANT decreased GUV calcein release by 12.1, 10.4, and 0.2%, respectively (**Figure 4.1B**). Transmission electron microscopy showed breakthrough fibrillation of IAPP in the presence of MANT and YMSV after 48 h, illustrating the limits to the observed anti-fibrillation activity and associated fibrillation-induced membrane leakage.[166]

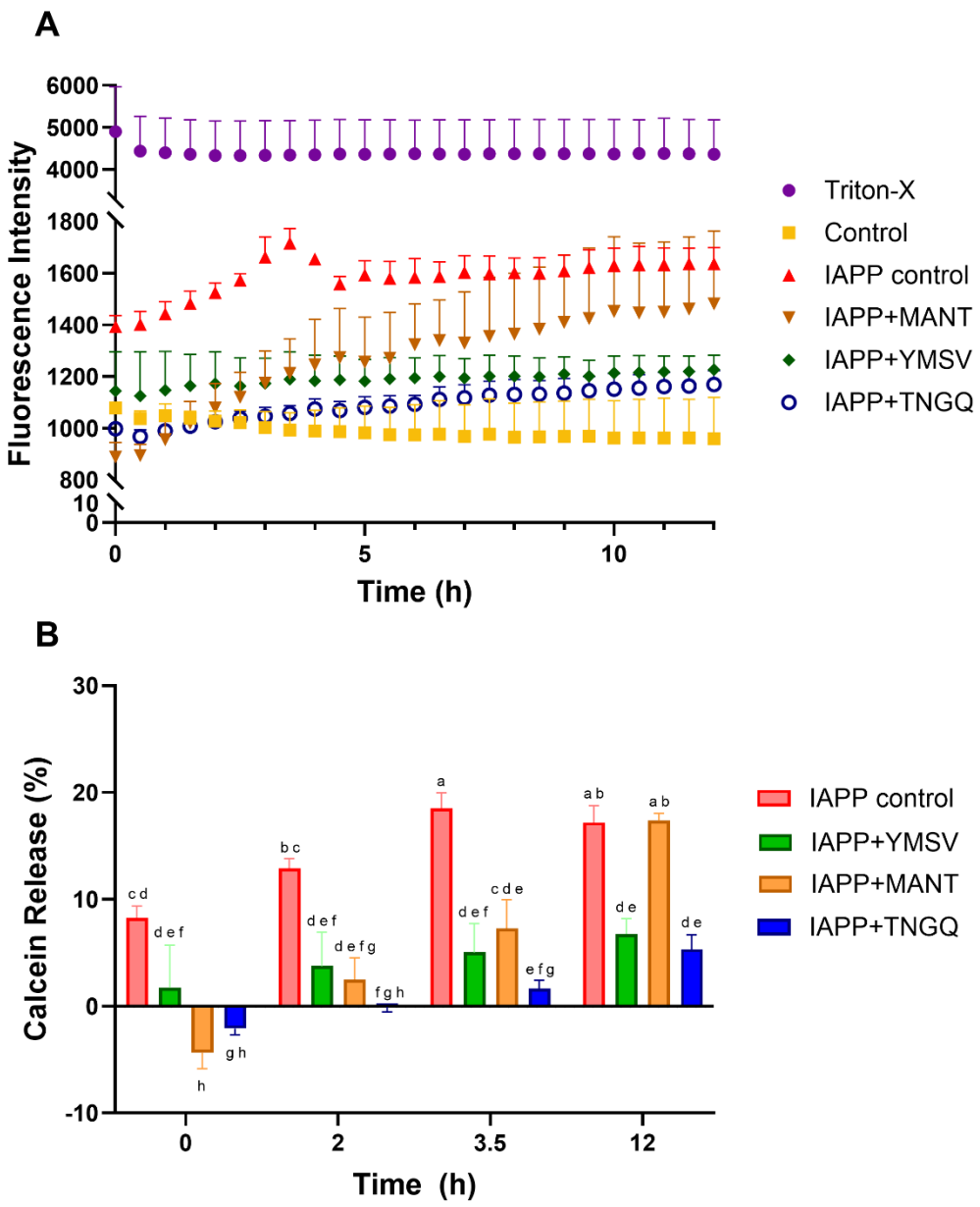

Figure 4.1. (A) Fluorescence kinetics of calcein released from GUV over time when exposed to IAPP in the absence and presence of tetrapeptides YMSV, MANT, and TNGQ. Triton X-100 represents the positive control while 'Control represents GUV alone. **(B)** Calcein release relative to intact GUVs and in the presence of tetrapeptides YMSV, MANT, and TNGQ at 0, 2, 3.5, and 12 h. Bars with different letters denote significantly different mean values ($\alpha = 0.05$).

4.3.2. Anti-fibrillation activity of tetrapeptides also minimized IAPP fibrillation-induced increase in particle size

To elucidate the average particle size and species homogeneity of GUV in the presence of IAPP and IAPP-tetrapeptides, dynamic light scattering was performed at 0 and 12 h after treatment. GUVs in the presence of the strong detergent Triton X-100 (10%, v/v) were used as a positive control to evaluate the average hydrodynamic diameter of the GUVs in the event of complete disruption of the monolayer membranes. This resulted in average particle diameters of 14.8 ± 0.22 and 14.9 ± 0.12 nm at 0 and 12 h, respectively for the detergent-disrupted GUVs (**Figure 4.2A**). The negative control GUVs, in the presence of a leakage buffer, were evaluated for their relative stability over time. As expected, the GUV maintained a consistent size with average particle diameters of 1268 ± 38.7 and 1363 ± 52 nm at 0 h and 12 h, respectively (**Figure 4.2A**). Similarly, the PDI of both controls was very low (< 0.5), indicating their relative stability over time **(Figure 4.2B)**. The addition of IAPP to GUV significantly ($p < 0.0001$) increased the particle diameter to 2139 ± 34 nm at 0 h and more than 3 folds to 7912 ± 127.5 nm after 12 h, relative to the negative control **(Figure 4.2A)**. Similarly, the slight increase in PDI at 0 h relative to the negative control became more pronounced at 12 h, illustrating the large species diversity and heterogeneous environment upon the addition of IAPP **(Figure 4.2B)**. High PDI and average particle diameter (> 6000 nm) are characteristic of IAPP fibrillation.[166] However, the average particle size of GUVs in the presence of IAPP-MANT or IAPP-YMSV was larger than that of IAPP alone at 0 h. This suggests that the presence of lipophilic membranes enhanced the initial fibrillation process beyond the extent attained by IAPP alone or that fibrillation occurred on the GUV surface, which is more plausible given the subsequent increase in calcein leakage **(Figure 4.1A)**. MANT and YMSV reduced the average particle diameter at 12 h compared with GUV treated with IAPP. Similar results were previously observed for both peptides in the presence of IAPP, confirming the inhibition of IAPP fibrillation by tetrapeptides.[166] In contrast, TNGQ reduced the average particle size upon addition of IAPP-GUVs at 0 h and after further incubation for 12 h, relative to IAPP-treated GUVs **(Figure 4.2A)**. Notably, the sample containing TNGQ tended to have a slightly lower PDI **(Figure 4.2B)**, which still indicates a heterogeneous environment, but to a lesser extent than the other inhibited samples **(Figure 4.2B)**.

The addition of IAPP resulted in an increase in the average particle diameters observed in all GUV samples. However, the variation in size both at the initial and final time points when the tetrapeptides were added indicates that fibrillation inhibition occurred to a certain degree, as previously reported.[166] However, there were apparent variations in the particle diameters. For

instance, the IAPP control was reported to have a diameter of 6279 nm, while MANT-, YMSV-, and TNGQ-treated IAPP had sizes of 409.8, 223.3, and 380.8 nm, respectively.[166] Therefore, the presence of GUV might have enhanced the fibrillation propensity of IAPP, thus diminishing the inhibitory activity of tetrapeptides and resulting in larger particles. The role of anionic lipids in IAPP fibrillation has been studied extensively. It is believed that the negatively charged head groups of the lipid membrane interact with the positively charged amino acid residues at the N-terminus of the IAPP.[171] Although it is unclear how this interaction promotes IAPP aggregation, the concentration of free lipids has been reported to correlate positively with the acceleration of IAPP aggregation kinetics.[171] Given the relatively uncharged nature of DOPC GUVs, our findings suggest that other forces, such as hydrophobic interactions, play a role in facilitating IAPP fibril-GUV interactions, thus creating additional layers around the GUVs and increasing the average particle diameter. Furthermore, rodent IAPP (rIAPP), which is more positively charged, has poor membrane insertion capabilities in anionic lipid membranes compared with hIAPP, further illustrating the importance of the hydrophobic core region of IAPP in membrane interactions.[172]

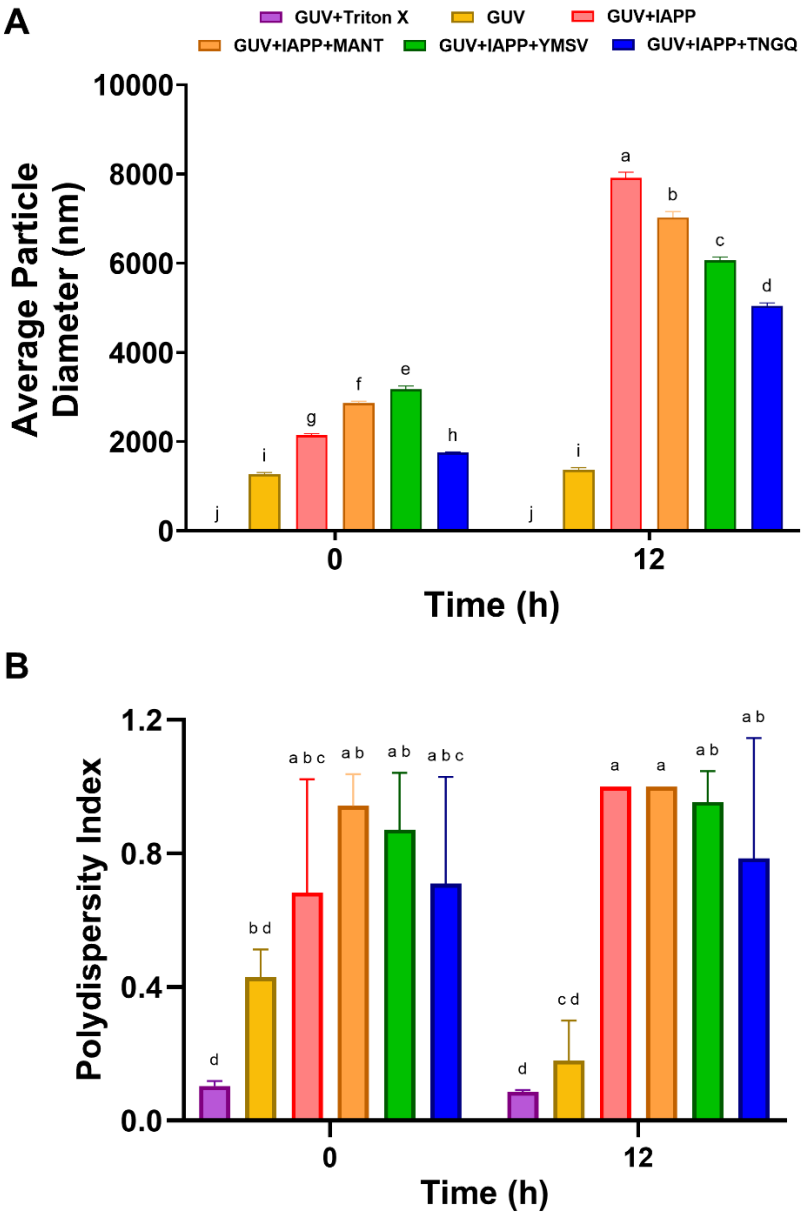

Figure 4.2. (A) Average particle diameter (nm) and **(B)** PDI of GUVs in the presence of IAPP alone (IAPP control) and IAPP in the presence of tetrapeptides YMSV, MANT, and TNGQ at the initial (0 h) and final (12 h) time points. Bars with different letters denote significantly different mean values ($\alpha = 0.05$).

4.3.3. Anti-fibrillation tetrapeptides minimized lipid membrane-induced IAPP fibrillation

Fluorescence images of each sample were obtained at four time points (0, 2, 3.5, and 12 h) to visualize the effects of IAPP and IAPP tetrapeptides on the general morphology and dispersion of rhodamine-labelled GUVs. The Triton X-100 positive control provided the baseline with complete disruption of the GUVs, corroborating the dynamic light scattering results (**Figures 4.2** and **4.3**). Conversely, the GUVs alone showed an even distribution of GUVs at each time point, demonstrating stability in maintaining general morphology and distribution over 12 h (**Figure 4.3**). The addition of IAPP resulted in uniform distribution and consistent GUV morphology after 2 h of incubation. However, an increase in the number of larger, irregularly shaped puncta was observed at 3.5 h, with a further increase in number at 12 h (**Figure 4.3**). The increase in puncta size corroborates the increased average particle diameter (**Figure 4.2A**), whereas the more heterogeneous dispersion of puncta confirms the high degree of polydispersity (**Figure 4.2B**). The increased presence of larger puncta could be a result of the agglomeration of liberated fluorescent-labelled lipids with the hydrophobic regions of IAPP fibrils present in the complex mixture. Comparing the effects of the tetrapeptides in maintaining a similar dispersity to the negative control, MANT gradually lost its GUV content, which was most evident at 12 h, where large puncta were visible (**Figure 4.3**). The few GUVs lacked a spherical shape, suggesting the destruction of the membrane. Of the three tetrapeptides, YMSV appeared to perform best in maintaining the general dispersion and GUV morphology of the negative control within the first 3.5 h (**Figure 4.3**). This was followed by TNGQ, with slightly larger puncta as early as 2 h, which increased in size over time (**Figure 4.3**). This effect did not appear to translate to increased calcein leakage (**Figure 4.1A**). At 12 h, TNGQ resulted in the least number of larger puncta compared to YMSV and MANT, which corroborates their effects on the average particle size of IAPP-GUVs (**Figure 4.2A**).

IAPP disrupts cellular membrane integrity by extracting lipids from the membrane, resulting in the formation of heterogeneous fibrillar structures with phospholipid molecules tangled within the complex matrix of the fibrils.[173] The IAPP-induced lipid membrane "pulling" mechanism has been previously illustrated, whereby the exposure of the hydrophobic regions of the lipid membrane to IAPP enhances the incorporation of lipids into the hydrophobic IAPP fibrils. This process further enhances fibrillation, thus creating a positive feedback loop between lipid-IAPP interactions, IAPP fibrillation, and enhanced lipid liberation because of fibril-induced membrane damage.[172] The presence of covalently attached rhodamine to some of the lipids enabled tracking of aggregation of the fibrils that were entangled with the lipids, hence explaining the

increased presence of larger puncta over time. Thus, with the change in puncta size and distribution relative to the negative and IAPP controls, it can be concluded that the interactions between IAPP and the tetrapeptides play a role in reducing subsequent IAPP fibrillation in GUVs, with TNGQ consistently outperforming the other two tetrapeptides.

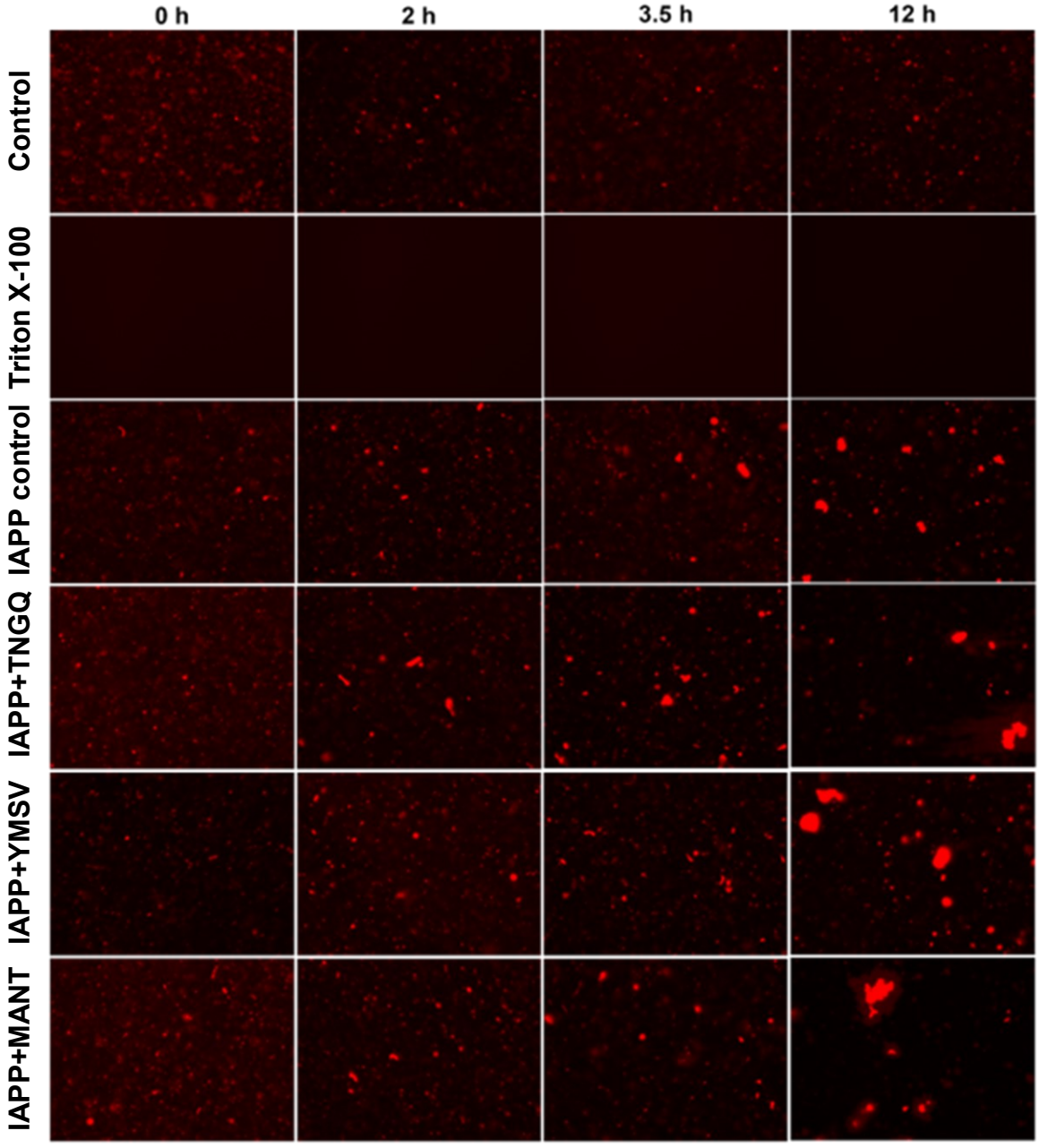

Figure 4.3. Fluorescence microscopy images of GUVs treated with IAPP alone (IAPP control) and IAPP in the presence of tetrapeptides YMSV, MANT, and TNGQ at the initial timepoint (0 h) and after 2, 3.5, and 12 h of incubation.

4.3.4. Increased cytoprotective effects of TNGQ on pancreatic β-cells in the presence of IAPP

The tetrapeptides demonstrated anti-fibrillation activity with variable binding regions, resulting in variable inhibitory mechanisms and associated inhibitor strengths. However, anti-fibrillation does not guarantee a decrease in IAPP-induced cytotoxicity, especially because inhibition results in the production of various fibrillar intermediates, some of which may maintain their cytotoxicity. This highlights the importance of evaluating the effectiveness of anti-fibrillation inhibitors in demonstrating cytoprotective effects during IAPP fibrillation. Thus, cell viability was assessed using the MTT assay to determine whether the anti-fibrillation activities of the tetrapeptides translate to cytoprotective effects against IAPP fibrillation-induced toxicity in pancreatic β-cells. Significant deleterious effects of 5 μM IAPP were observed on RIN-m cells, with its addition reducing cell viability to 6.4 ± 6.4% after 24 h (**Figure 4.4A**). Similarly, the treatment of rat insulinoma (INS-1) cells with 20 μM hIAPP oligomers reduced β-cell viability by 95%.[174] Fibrillation intermediates, such as soluble oligomers and protofibrils, diminish cell viability via the induction of apoptotic markers, such as Fas receptor and caspase-8, reactive oxygen species production, endoplasmic reticulum stress, defects in autophagic response, and the disruption of cellular membranes through pore formation on the membrane surface.[4,174] Interestingly, despite their moderate anti-fibrillation activity and membrane protective effects, YMSV and MANT failed to increase cell viability, relative to IAPP-treated cells (**Figure 4.4A**). TNGQ maintained the strongest effect, increasing cell viability to 47.5 ± 3.8% in the presence of IAPP (**Figure 4.4A**). Fibrillation occurred more rapidly in the presence of GUVs, where the maximum fluorescence intensity was reached within the first two hours (data not shown), compared to in the absence of GUVs, where the maximum fluorescence intensity was achieved after 24 h of incubation.[166] Similar lipid effects on IAPP fibrillation have been reported previously whereby incubation of IAPP with 0.25-1.0 mg/mL phospholipids isolated from whole pancreas of a Type 2 diabetic patient accelerated fibrillation by 10-fold.26 However, anti-fibrillation activity was maintained for TNGQ and MANT over time with the largest fluorescence decrease of 31.9 ±

1.9% and 37.1 ± 2.1%, respectively, was observed at 12 h and to a lesser extent, YMSV with a fluorescence decrease of 17.1 ± 14.5% at 12 h (data not shown). The extent of fibrillation inhibition may explain the observed cytoprotective effects of tetrapeptides against IAPP fibrillation-induced toxicity.

By observing the fibrillation kinetics of IAPP in the presence of membrane-like environments, light microscopy of the RIN-m cells showed morphological changes in the cells upon addition of IAPP, some of which were restored in the presence of the TNGQ inhibitor, corresponding to cell viability (**Figure 4.4B**).

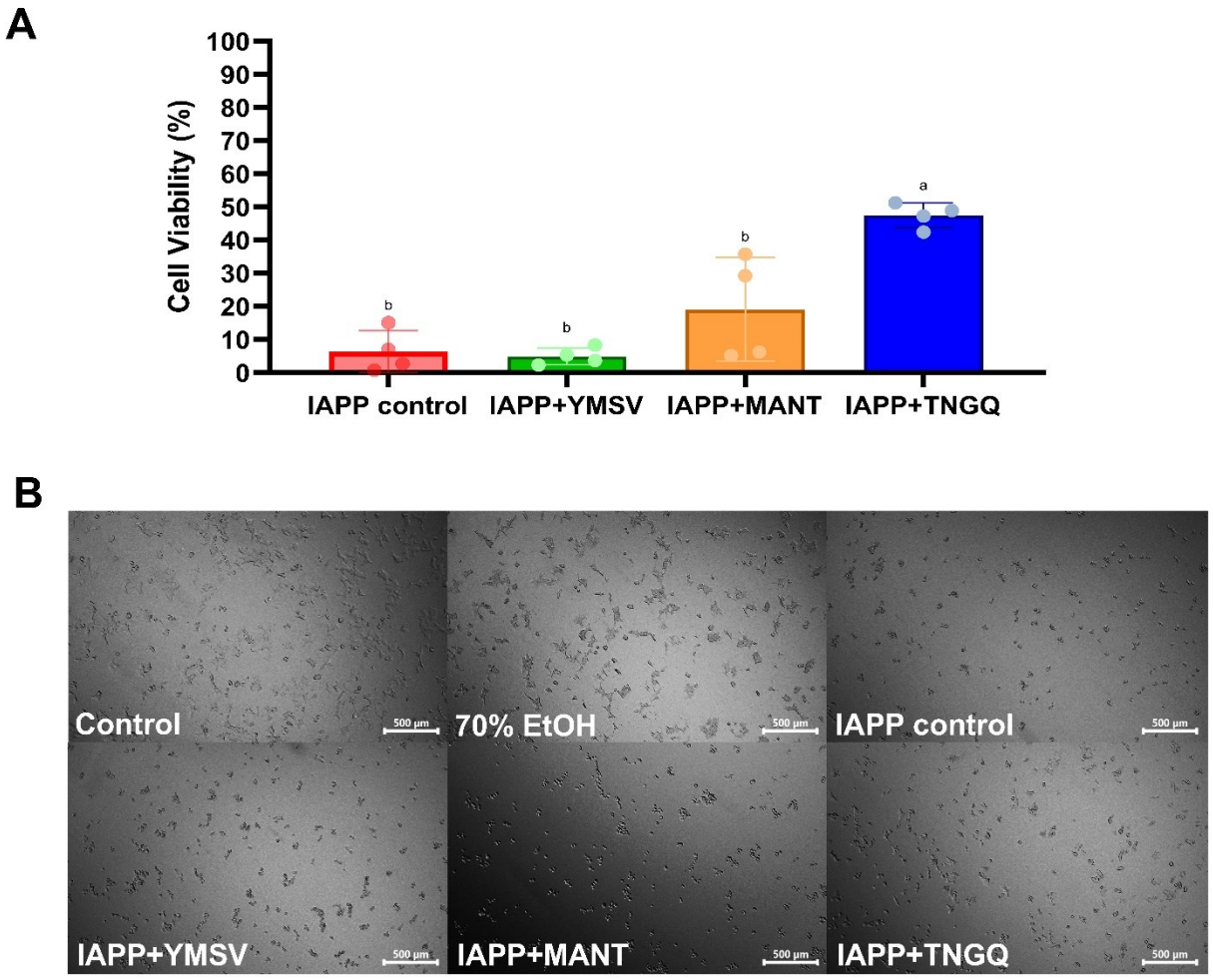

Figure 4.4. (A) The viability of RIN-m cells in the presence of 5 µM IAPP alone or in the presence of equimolar concentrations of YMSV, MANT, or TNGQ after 24 h. Bars with different letters denote significantly different mean values ($p < 0.05$). **(B)** Brightfield images of RIN-m cells treated

with complete culture medium (live cell control), 70% (v/v) ethanol (dead cell control), and IAPP in the absence and presence of tetrapeptide inhibitors (YMSV, MANT, and TNGQ). Scale bar represents 500 μm.

4.3.5. Importance of IAPP cross-domain interactions in anti-fibrillation activity of TNGQ

We have previously reported the docking of tetrapeptides with monomeric IAPP.[166] However, given the complexity of IAPP fibrillation and the likelihood of tetrapeptide inhibitors binding to multiple species, it is imperative to observe oligomer binding to better evaluate the mitigation of IAPP-induced cytotoxicity, especially for TNGQ. IAPP fibrils consist of two symmetrically related protofilaments with ordered residues 14-37.[162] Residues 1-13 are not involved in IAPP fibrillation because the segment cannot form fibrils independently.[54,162] The hIAPP segment corresponding to positions 20-29 was proposed to be the amyloidogenic core region. Subsequent studies have proposed additional residues within the fibril core of hIAPP, including residues 12-17, 13-18, 15-20, and 30-37.[95,175] The interactions between each tetrapeptide and the pentameric IAPP binding site are shown in **Figure 4.5**. The tetrapeptides preferentially bind to pentameric hIAPP at the amyloidogenic core of residue 20-22 and 27-28. TNGQ binds to the IAPP pentamer with four chains, showing the highest docking score of 94.38 (**Table 4.1**). Polar interactions between TNGQ and IAPP were facilitated by the formation of three hydrogen bonds, two of which were backbone donors to Asn22 residues of the A and C chains and a side-chain donor from Thr to Ser20 of the A chain (**Figure 4.5B**). Conversely, YMSV interacted with three chains across the two regions of residue 20-22 and 27-28, forming interactions with Ser20, Asn21, Asn22, Leu27, and Ser28 (**Figure 4.5C**). Furthermore, YMSV had the most favorable binding energy of -5.6529 kcal/mol, maintaining its highly favorable binding, as previously observed with monomeric IAPP.[166] Additionally, YMSV had the least number of polar interactions, with three hydrogen bonding interactions formed between two residues: Ser20 of the B chain and Ser28 of the A chain (**Figure 4.5D**). Similar to TNGQ, MANT also demonstrated interactions with four chains in the core region (**Figure 4.5E**). However, its extent of interaction was comparable to that of YMSV, which spans the entirety of the core amyloidogenic region, forming hydrogen bonding interactions with Ser20, Asn21, Asn22, and Leu27. Among the three tetrapeptides, MANT demonstrated the least favorable binding energy of 81.36 (**Table 4.1**). Interactions with the IAPP pentamer consisted entirely of polar side-chain interactions facilitated via hydrogen bonding,

donating electrons from the N-terminal amide proton of Met to the hydroxylic oxygen of Ser20 of the C chain (**Figure 4.5F**). Additionally, MANT served as an electron acceptor from the electrophilic side chains of Ser20 and Asn22 of the C chain (**Figure 4.5F**). Both MANT and TNGQ interact directly with the side chain of Asn22, an interaction that is also observed with TNGQ and monomeric IAPP.[166] This is significant because Asn and Gln are highly susceptible to deamidation, a post-translational modification that occurs spontaneously in proteins and accelerates hIAPP fibrillation *in vitro*.[101,176,177] IAPP is abundant in Asn residues (six, accounting for 16% of its total amino acid content), three (Asn21, Asn22, and Asn35) of which are highly susceptible to deamidation and are instrumental in oligomer formation.[101,178] Thus, the role of MANT and TNGQ in increasing β-cell viability (**Figure 4.4A**) can be attributed to anti-fibrillation activity through the prevention of fibrillation-promoting deamidation of Asn21 and Asn22, and by blocking its role in Asn-Asn stacking interactions during IAPP oligomerization.[177] In addition, TNGQ formed more hydrophobic interactions with pentameric hIAPP than with MANT, especially at the region of residue Leu27-Ser28. Some flavonoids inhibit the aggregation of hIAPP by affecting the extended conformation of Ser28, which is positively correlated with the stability of hIAPP.[67] The formation of hydrophobic interactions may promote the stable binding of TNGQ to pentameric IAPP.

Table 4.1. Docking results for TNGQ, MANT, and YMSV binding to hIAPP pentamer (PDB: 6VW2).

Sequence	S	n	Interactions	
			Hydrogen bonds	Hydrophobic interactions
TNGQ	94.38	4	Ser*A20*, Asn*A22*, Asn*C22*	Ser*B20*, Ser*C20*, Ser*D20*, Asn*A21*, Asn*B21*, Asn*B22*, Asn*D22*, Leu*A27*, Leu*B27*, Leu*C27*, Leu*D27*, Ser*B28*, Ser*D28*
MANT	81.36	4	Ser*B20*, Ser*C20*, Ser*D20*, Asn*C22*	Ser*A20*, Asn*A21*, Asn*B21*, Asn*D21*, Asn*A22*, Asn*B22*, Asn*D22*, Leu*A27*, Leu*B27*, Leu*C27*
YMSV	91.83	3	Ser*A28*, Ser*B20*	Ser*A20*, Ser*C20,* Asn*B21*, Asn*C21*, Asn*C22*, Asn*B22*, Leu*A27*, Leu*B27*, Leu*C27*, Ser*A28*
Abbreviations: n, number of interacting chains; S, LibDock score.				

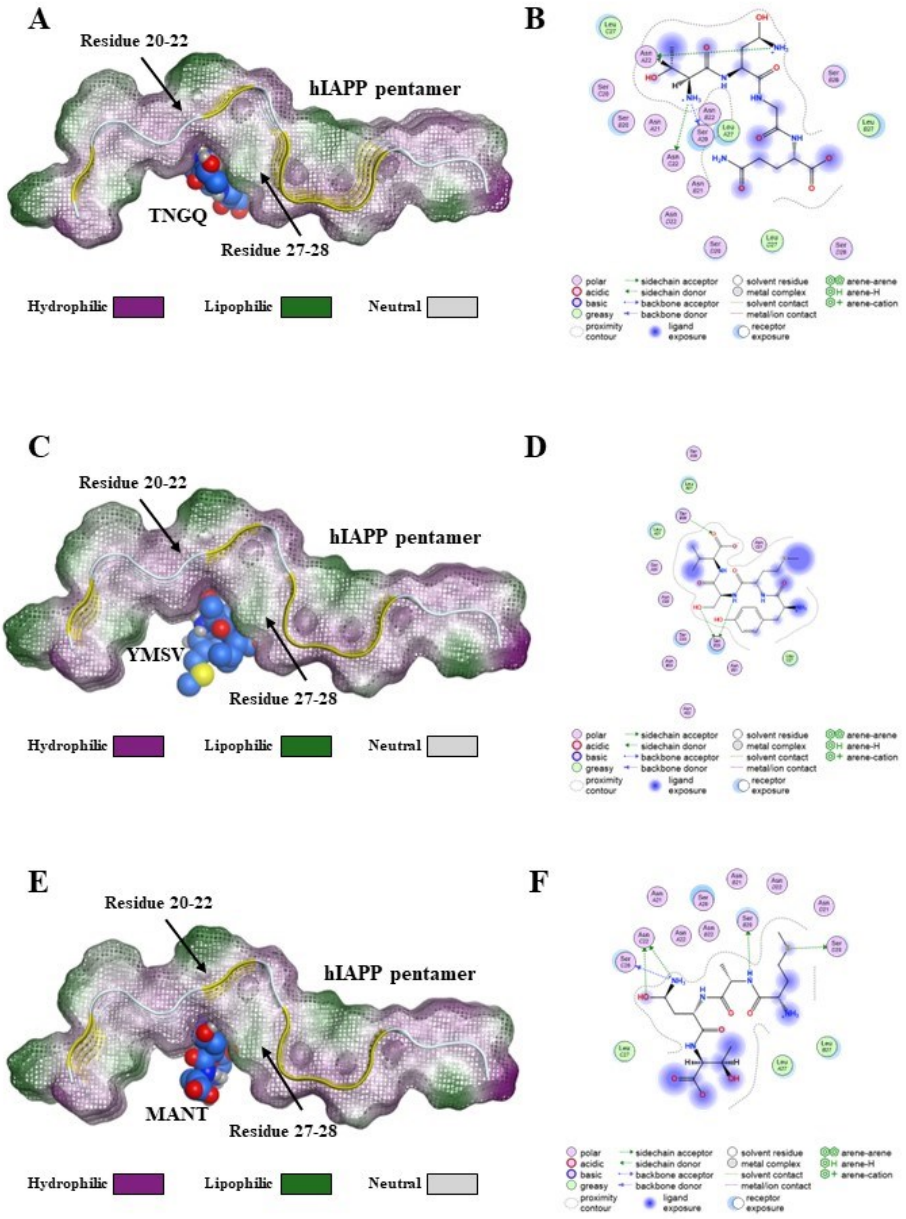

Figure 4.5. 3D and 2D interactions of **(A-B)** TNGQ, **(C-D)** YMSV, and **(E-F)** MANT with the hIAPP pentamer (PDB: 6VW2). Residues circled in pink participate in electrostatic interactions, indicated as polar residues, and residues circled in green participate in van der Waals interactions, indicated as "greasy" interactions. The green dotted lines indicate interactions facilitated by side chains, and the blue dotted lines indicate interactions facilitated by the backbone. The arrow at the end of the dotted lines indicates the direction of the proton acceptance or donation.

4.4. Conclusions

In this study, anti-fibrillation tetrapeptides, YMSV, MANT, and TNGQ, were evaluated to determine whether region-specific binding translates to increased cytoprotective effects against IAPP fibrillation. In line with a previous study, TNGQ remained the strongest of the three tetrapeptide inhibitors for reducing IAPP-induced calcein leakage across the membrane and minimizing fibrillar progression in GUVs. Interestingly, the anti-fibrillation activity of YMSV and MANT did not translate into significant cytoprotective effects in rat insulinoma RIN-m cells relative to cells treated with IAPP alone. Nonetheless, MANT had the strongest binding with pentameric IAPP, followed by YMSV and then TNGQ, all of which preferentially interacted with the amyloidogenic region of IAPP. It can be concluded that while binding interactions are necessary to elucidate the potential mechanisms of inhibition, it is not a holistic depiction of inhibitor potency. Notably, strong binding does not necessarily equate to anti-fibrillation activity, nor does higher peptide hydrophobicity, or the presence of aromatic amino acid residues, such as phenylalanine or other amino acids that participate in π-π interactions with IAPP. As demonstrated by TNGQ, fibrillation inhibitors do not need to bind to the hydrophobic residues of the amyloidogenic region of IAPP to affect anti-fibrillation activity. Rather, binding across the amyloidogenic region (incidentally, to highly hydrophilic residues, specifically Asn21 and Asn22) is important for preventing IAPP oligomer formation. While the three peptides demonstrated anti-fibrillation activity based on ThT fluorescence kinetics, only one peptide (TNGQ) translated into protective effects against IAPP-induced cytotoxicity. TNGQ was also the only tetrapeptide that exhibited cross-domain interactions, having binding interactions in the N-terminal membrane-binding domain and C-terminal self-association region of the IAPP monomer, and the amyloidogenic region of the IAPP pentameric model. This can be attributed to the effect of species-specific interactions in discouraging IAPP fibrillation and subsequent formation of toxic oligomeric species by binding to oligomer-promoting residues, such as Asn21 and Asn22, while preventing membrane rupture-inducing interactions by binding to the C-terminal region of IAPP monomers. Finally, the fibril disaggregatory effects of TNGQ can prevent mechanical-induced cellular membrane damage by reducing the length and diameter of the IAPP fibrils. Taken together, the multilevel inhibitory approach of TNGQ against IAPP fibrillation translates to the reduction of associated cytotoxicity, thus enhancing β-cell viability. Future research directions include understanding the mechanism of the cytoprotective effects of TNGQ on β-cells, for example, its

effects in managing IAPP fibrillation-induced reactive oxygen species production, membrane leakage, apoptotic pathways, autophagy response, and glucose-stimulated insulin secretion.

4.5. Acknowledgement

R.O.A. is a recipient of a Vanier Canada Graduate Scholarship. The authors would like to acknowledge Guan Wang at the Innovation Center of Nursing Research, Nursing Key Laboratory of Sichuan Province, State Key Laboratory of Biotherapy and Cancer Center, West China Hospital, Sichuan University, for the use of Discovery Studio 3.5. The authors acknowledge financial support from the Natural Sciences and Engineering Research Council of Canada (NSERC) [grant number RGPIN-2018-06839] and the University Research Chairs Program of the University of Ottawa, Canada.

Conflicts of interest

There are no conflicts to declare.

CHAPTER FIVE

POTENTIAL OF PEPTIDE-POLYPHENOL INTERACTIONS ON ENHANCING ISLET AMYLOID POLYPEPTIDE-INDUCED β-CELL DYSFUNCTION

Peptide-polyphenol interaction: Influence of anti-fibrillation inhibitors TNGQ-rutin combination on β-cell cytoprotective effects against IAPP-induced cell death, insulin secretion, and oxidative stress

Raliat O. Abioye, Oluwasemilogo H. Adetula, Julia Diem Hum, and Chibuike C. Udenigwe
Biochemical and Biophysical Research Communications, **2024**

DECLARATION FOR THESIS CHAPTER FIVE

Peptide-polyphenol interaction: Influence of anti-fibrillation inhibitors TNGQ-rutin combination on β-cell cytoprotective effects against IAPP-induced cell death, insulin secretion, and oxidative stress

This is to declare that there is no conflict of interest associated with this work and the contribution of the candidate is stated below:

Candidate's contribution	Conceptualization, methodology, validation, formal analysis, investigation, writing, review and editing, and visualization	80%

The following co-authors attest to the candidate's participation in a group publication as a component of their thesis and was active in the creation of this publication. The co-author's permission is as follows:

Name	Signature	Date
Oluwasemilogo H. Adetula		
Julia Diem Hum		
Chibuike C. Udenigwe		

5.0. Abstract

Type 2 diabetes development has been associated with islet amyloid polypeptide (IAPP) fibrillation. IAPP fibrils have various deleterious effects, such as oxidative stress and disruption of cellular membrane integrity, resulting in pancreatic β-cell toxicity. Rutin, a plant polyphenol, possesses promising cytoprotective effects as a fibrillation inhibitor. Similarly, bioactive peptides have been identified as potential inhibitors to IAPP fibrillation. In this study, the effect of peptide-polyphenol interactions between rutin and three peptides, TNGQ, MANT, and YMSV, on anti-fibrillation activity and cellular response was elucidated. Results indicated a 54.7-75.1% decrease in thioflavin T fluorescence, confirming anti-fibrillation activity. The mixture decreased the average particle diameters of IAPP more than the single inhibitors, suggesting a combined effect of peptide-rutin interactions in enhancing anti-fibrillation activity. IAPP fibrillation-induced rat insulinoma RIN-m cell death was restored in the presence of the peptide/rutin mixture, but the activity was lower relative to rutin alone, suggesting a non-additive effect of the mixture. Transmission electron microscopy showed a near-complete inhibition of IAPP fibrillation by TNGQ/rutin mixtures, which translated to a decreased production of membrane-bound IAPP oligomers in RIN-m cells based on immunofluorescence staining. Additionally, TNGQ/rutin mixtures significantly decreased reactive oxygen species production by 30%, higher than the effects of single inhibitors, but no effect was observed on glucose-stimulated insulin secretion. The results demonstrate the potential of multifunctional compounds as dual inhibitor systems in controlling IAPP fibrillation and provide insight into the implications of peptide-polyphenol interactions towards the rational development of novel anti-diabetic nutraceutical combinations.

Keyword: islet amyloid polypeptide; fibrillation; bioactive peptides; polyphenols; pancreatic β-cells; reactive oxygen species; insulin secretion; type 2 diabetes

5.1. Introduction

Protein misfolding and aggregation resulting in amyloid plaques formation have been implicated in the prognosis of several diseases, such Alzheimer's, prion, Parkinson's, and type 2 diabetes (T2D).[163,164] These diseases are largely multifactorial, wherein the fibrillation of the originally functional proteins or peptides form errant species that trigger a wide range of deleterious effects, such as impeded cellular signaling, loss of homeostasis, and metabolic dysregulation.[86,179] Several studies have reported the identification of compounds that prevent the

formation of protein fibrils, target the existing fibrils for degradation, or disaggregate fibrils into their functional species.[4,180–182] However, the multifactorial nature of these fibrillar pathogens is less explored, as the inhibitors are generally targeted on amyloidogenesis and seldom on other pathological manifestations of the formation of fibrillar species, such as reactive oxidative species production.

One of such examples is islet amyloid polypeptide (IAPP) or amylin, a hormonal peptide that functions endogenously in postprandial blood glucose regulation, gastric emptying, and satiety regulation.[4,6] In the β-cells of the pancreatic Islets of Langerhans, the 37-residue basic polypeptide is originally co-produced as a prohormone, along with insulin, then co-packaged and co-secreted by the endoplasmic reticulum and Golgi apparatus, respectively.[6,183] However, IAPP has an increased propensity to self-interact, resulting in the formation of fibrillar species that are toxic to β-cells, thus exacerbating T2D.[97,184] In fact, fibrillar IAPP species have been identified in the pancreas of over 95% of diabetic patients, highlighting their instrumental role in disease prognosis.[6,7,103] IAPP fibrillation-induced pancreatic β-cell toxicity is caused by various factors, all resulting in the reduction of β-cell mass, a major hallmark of T2D.[4,7,32] This process is exacerbated by the elevated secretion of insulin, and inadvertently IAPP, resulting in the increased circulation of IAPP and fibrillogenesis.[6] Specifically, the IAPP:insulin molar ratio of 1:100 secreted by β-cells for healthy individuals is increased to 1:20 in people with T2D, further exacerbating the potential of IAPP fibrillation-induced β-cell cytotoxicity.[184] Hence, targeting IAPP fibrillation in mitigating T2D disease progression is imperative. Several compounds, including peptides, polyphenols, terpenoids, carbohydrates, and some inorganic compounds, have been reported for their anti-fibrillation activities against IAPP. [4,46,97,142]

Anti-fibrillation compounds, although structurally diverse, have two main mechanisms of function: (1) direct binding of the inhibitor with monomeric IAPP, hence preventing subsequent self-association and formation of fibrils, and (2) binding and disaggregating preformed fibrils or fibrillar intermediates to revert to partially inhibited aggregates.[179] A third, less commonly considered mechanism consists of dual anti-fibrillation systems, comprising of two known fibrillation inhibitors of similar or different inhibition mechanisms. When used simultaneously or sequentially, the complete inhibition of fibrillation may occur, either directly where the combination completely inhibits the formation of aggregates, or indirectly where partially

inhibited aggregates are formed as intermediates.[179] Given the multiple mechanisms at play, the dual system provides strong potential for the development of unique anti-fibrillation combinations to enhance the inhibition of IAPP fibrillation compared to single inhibitor systems.

A plethora of research has gone into the use and functionality of peptide-polyphenol combinations as functional food components in improving biological functions.[185,186] However, some studies have reported a diminished or complete loss of bioactivity resulting from peptide-polyphenol interactions.[134,186] Alterations in bioactivity are due to direct binding, usually driven by noncovalent (H-bonding, electrostatic, π-π, etc.) interactions or, less commonly, covalent bonding between oxidized phenolics and lysine residues, forming peptide-phenolic cross-linkages.[134] Some peptides and polyphenols have been identified for their anti-fibrillation activity against IAPP.[61,91,166] For example, peptides YMSV, MANT, and TNGQ effectively inhibited IAPP fibrillation, with TNGQ also demonstrating strong fibril disaggregative activity [166]. Similarly, polyphenols rutin and quercetin have demonstrated strong anti-fibrillation activity across various amyloidogenic proteins and peptides, including IAPP, β-lactoglobulin, insulin, and β-amyloid, via a combination of monomeric binding and disaggregative effect to enhance anti-fibrillation activity.[92,96,187,188] Hence, in this study, known anti-fibrillation peptides, YMSV, MANT, and TNGQ, and polyphenol, rutin, were used as model compounds to investigate the effects of peptide-polyphenol interactions on anti-fibrillation activity and to understand the physiological implications of the bioactivity on pancreatic β-cell functionality.

5.2. Materials and methods

5.2.1. Materials

Tris(hydroxymethyl)aminomethane (Tris-base; ≥100.1%), sodium chloride (≥99%), sodium hydroxide (≥98%), dimethyl sulfoxide (DMSO), fetal bovine serum (FBS), penicillin-streptomycin, L-glutamine, 0.25% trypsin-EDTA, 37% formaldehyde, 4′,6′-diamindino-2-phenylindole, dihydrochloride (DAPI), and sodium bicarbonate (≥99%) were purchased from Thermo Fisher Scientific (Nepean, ON, Canada). 1,1,1,3,3,3-Hexafluoro-2-propanol (HFIP), rutin hydrate (≥94%), thioflavin T (ThT), sodium phosphate dibasic dihydrate (≥99%), potassium phosphate monobasic (≥99%), hydrogen chloride, 2′,7′-dichlorofluorescin diacetate (DCFH-DA), bovine serum albumin (≥98%), potassium chloride (≥99%), calcium chloride (≥97%), magnesium sulfate, anhydrous (≥97%), 4-(2-hydroxyethyl)piperazine-1-ethanesulfonic acid, N-(2-

hydroxyethyl)piperazine-N′-(2-ethanesulfonic acid) (HEPES, ≥99.5%), and D-(+)-glucose (≥99.5%) were purchased form MilliporeSigma (Oakville, ON, Canada). Human IAPP (amylin (1-37), human; ≥95%) modified with an amidated C-terminus and a Cys2-Cys7 disulfide bond was purchased from AnaSpec (Fremont, CA, USA). Peptides MANT (98.7%), YMSV (95.5%), and TNGQ (95.7%) were synthesized and supplied by GenScript (Piscataway, NJ, USA). UranyLess counterstain was purchased from Electron Microscopy Sciences (Hatfield, PA, USA). RIN-m rat insulinoma (CRL-2057) cells and RPMI-1640 medium (cat. No. 30-2001) were purchased from ATCC (Manassas, VA, USA). The CyQUANT™ MTT Cell Viability Assay Kit (cat. No. V13154) and wheat germ agglutinin Texas Red-X conjugated (cat. No. W21405) were purchased from Invitrogen (Waltham, MS, USA). Amyloid oligomers (A11) polyclonal antibody conjugated with FITC (cat. No. SPC-506D-FITC) was purchased from Cedarlane Labs (Burlington, ON, Canada). Ultra Sensitive Rat Insulin ELISA kit (cat. No. 90060) was purchased from Crystal Chem (Elk Grove Village, IL, USA).

5.2.2. Preparation of IAPP

To disaggregate preformed IAPP fibrils, 1 mg of IAPP was dissolved in 10 mL ice cold HFIP on ice for 30 min and then aliquoted at 0.1 mg/mL in 500 µL per Eppendorf tube. Thereafter, the tubes were sonicated on ice for 30 min, and then immediately centrifuged at 14,000 × g for 30 min at 4 °C. HFIP was dried in a fume hood for 16 h and the peptide films were stored at -80 °C until use. For each experiment not involving cells, peptide films were reconstituted in 500 µL of 1 M Tris buffer (pH 7.4) immediately prior to use.

5.2.3. Thioflavin T kinetics assay

Thioflavin T (ThT) dye was used to monitor IAPP fibrillation kinetics in the absence and presence of the anti-fibrillation compounds and combination. In 96-well black plates with clear bottoms, 5 µM IAPP in the absence or presence of 5 µM peptide (MANT, YMSV, or TNGQ), 5 µM rutin, or equimolar concentration (5 µM) of peptide/rutin mixture, and 10 µM ThT in 1 M Tris buffer (pH 7.4) was added to the respective wells. The plates were then sealed with Parafilm strips to minimize evaporation and incubated for 48 h at 37 °C. Endpoint fluorescence intensities were measured following the incubation period, using the Spark multimode microplate reader (Tecan, Stockholm, Sweden) at λ_{ex} 430 nm and λ_{em} 480 nm.

5.2.4. Dynamic light scattering analysis

Dynamic light scattering was used to measure the average particle size and polydispersity index of IAPP samples in the absence and presence of 5 μM peptides (MANT, YMSV, TNGQ), 5 μM rutin, or equimolar concentration of peptide-rutin combination. Each sample was incubated at 37 °C for 48 h and analyzed using the Nano-ZS Zetasizer (Malvern Instruments Ltd., Malvern, UK) with the Mark-Houwink parameters (*A* parameter of 0.428, *K* parameter of $7.67e^{-5}$ cm^2/s, backscattered angle of 173°, and refractive index of 1.330). All measurements were performed in disposable polystyrene cuvettes after an equilibration period of 10 s.

5.2.5. Transmission electron microscopy

Transmission electron microscopy (TEM) was performed to visualize the effect of the TNGQ-rutin combination on IAPP fibrillar morphology. Mixtures of 5 μM TNGQ, 5 μM rutin, a combination of 5 μM TNGQ, or 5 μM rutin and 5 μM IAPP in 1 M Tris buffer (pH 7.4) was incubated at 37 °C for 48 h. Subsequently, 10 μL of each mixture was placed on a 300-mesh Formvar-carbon-coated copper grid on Parafilm for 5 min, and the excess sample was blotted with Kimwipes. Each sample-loaded grid was counterstained with UranyLess for 1 min in the dark and the excess solution was removed. Thereafter, the stained grids were images using a JEM-1400Flash Electron Microscope (JEOL, Tokyo, Japan) at an accelerating voltage of 120 kV. All images were processed using the ImageJ software (NIH, Bethesda, MD).[117]

5.2.6. Cell culture and treatment

Rat insulinoma (RIN-m) cells were cultured in complete culture media consisting of sterile-filtered RPMI-1640 medium supplemented with 10% (v/v) FBS, 100 U/mL penicillin, 100 μg/mL streptomycin, and 2 mM L-glutamine. The cells were maintained at 37 °C in a humidified atmosphere containing 95% air and 5% CO_2. Once a ~80-95% confluency was reached, the cells were trypsinized using 0.25% trypsin-EDTA and either expanded or used for experiments. Cells were passaged on a weekly basis, refreshing media every 3-4 days, and passages 9-16 were used for all experiments at a cell density of 1×10^4 cells per well. Prior to treatments, cells were grown to ~70-80% confluency and then treated with 5 μM IAPP, with or without the addition of 5 μM peptide (MANT, YMSV, or TNGQ), rutin or their mixtures, and incubated at 37 °C with 5% CO_2

for an additional 24 h to allow for IAPP fibril formation, unless otherwise stated. All IAPP, sample, and ethanol solutions were prepared in complete culture media and sterile filtered prior to use.

5.2.7. Cell viability assay

The CyQUANT^{TM} MTT Cell Viability assay was used to evaluate the effectiveness of the anti-fibrillation peptides and rutin mixtures in mitigating IAPP fibrillation-induced cytotoxicity. Cells were cultured in transparent 96-well plates suitable for cell culture at 100 µL/well, then grown and treated as described previously. Post-treatment, the cells were harvested by replacing treatment medium with MTT reagent dissolved in complete culture medium and then incubated for 3 h at 37 °C with 5% CO_2. The resulting formazan crystals were dissolved with DMSO, and the color change was measured as absorbance at 569 nm wavelength using the Spark multimode microplate reader (Tecan, Stockholm, Sweden). Cell viability was expressed as a percentage of MTT reduction using the equation:

$$\%\ cell\ viability = \left(\frac{C-A}{B-A}\right) \times\ 100 \qquad 5.1$$

The absorbance of the treated cells, C, is compared with absorbance of the dead cell control (70% (v/v) ethanol), A, and the live cell control (complete culture media), B.

5.2.8. Immunofluorescence microscopy

Cells were grown in 6-well plates at a final volume of 2 mL/well and then grown until 75-80% confluency. Thereafter, cells were treated as previously described. Following a 24-h IAPP treatment in the absence and presence of TNGQ, rutin, or TNGQ/rutin mixtures, cells were harvested and washed twice with 1X PBS buffer (pH 7.4), and then fixed with 3.7% paraformaldehyde in PBS for 30 min at room temperature. Fixed cells were washed twice more with 1X PBS buffer (pH 7.4), and the cell membrane was stained with 5 µg/mL wheat germ agglutinin for 20 min at room temperature in the dark. The cells were washed once more with 1X PBS buffer (pH 7.4) and then permeabilized with 0.1% (v/v) Triton X-100 in PBS for 30 min at room temperature. Following the incubation period, the cells were washed twice with 1X PBS buffer (pH 7.4), blocked with 5% (w/v) BSA for 30 min at room temperature, and then washed with 0.1% (w/v) BSA in PBS (pH 7.4). Membrane-bound and internalized amylin oligomers were detected by incubating cells with FITC-conjugated oligomer-specific A110 antibody at a 1:375

dilution for 1.5 h at room temperature in the dark. Thereafter, cells were washed twice more with 0.1% (w/v) BSA in PBS (pH 7.4) and then incubated with 1:1000 DAPI for 5 min in the dark to stain nucleic acids. Cells were subsequently washed with 0.1% (w/v) BSA in PBS (pH 7.4) and then aspirated. Glass coverslips were added to each well and the cells were imaged using the Axio Imager 2 fluorescence microscope equipped with an Axiocam 506 camera (Carl Zeiss, Germany) using the FITC (λ_{ex} 495 nm λ_{em} 519 nm), TX-RED (λ_{ex} 592 nm λ_{em} 614 nm), and DAPI (λ_{ex} 353 nm λ_{em} 465 nm) channels. Images were processed using the Zen 2.3 pro software (Carl Zeiss, Germany).

5.2.9. Reactive oxidative species production assay

DCFH-DA was used to measure IAPP fibrillation-induced cellular reactive oxidative species (ROS) production in insulinoma cells in the absence or presence of TNGQ, rutin, or TNGQ/rutin mixtures. Cells were grown in black 96-well plates with clear bottoms at 100 µL/well until 75-80% confluency and then treated with IAPP with and without samples for 6 h to allow for ROS production. Next, 20 µM DCFH-DA in serum-free media (RPMI-1640) was added to each well and incubated for 30 min in the dark at 37 °C. Cells were then washed twice with 1X PBS buffer (pH 7.4) and suspended in PBS for detection. Thereafter, 2′,7′-dichlorofluorescein fluorescence intensity (λ_{ex} 485 nm λ_{em} 530 nm) was measured every 30 min for 3 h with the Spark multimode microplate reader, incubating at 37 °C with 5% CO_2 in between each measurement (Tecan, Stockholm, Sweden). The rate of ROS production was determined as slope of the linear regression of the fluorescence vs time plot.

5.2.10. Glucose-stimulated insulin secretion assay

To understand the cytoprotective effects of TNGQ, rutin, and TNGQ/rutin mixtures against IAPP fibrillation-induced effects on cellular functionality, the glucose sensitivity of RIN-m cells was assessed. Cells were grown in transparent 96-well plates at 100 µL/well and treated as described previously. Post-treatment, cells were washed with Krebs-Ringer bicarbonate HEPES (KRBH) buffer (115 mM NaCl, 4.7 mM KCl, 1.28 mM $CaCl_2$, 1.2 mM $MgSO_4$, 10 mM $NaHCO_3$, 20 mM HEPES, pH 7.4) supplemented with 1.1 mM glucose and 1 mg/mL BSA to remove all traces of complete culture medium, and then preincubated with in KRBH buffer supplemented with 1.1 mM glucose and 1 mg/mL BSA for 60 min at 37 °C at 5% CO_2. Following preincubation, cells were treated with 1.1 mM or 20 mM glucose in KRBH buffer and incubated for 60 min at 37

°C at 5% CO_2. The supernatants were collected from each well, and the glucose-stimulated insulin secretion was measured using the Ultra Sensitive Rat Insulin ELISA kit according to the manufacturer's protocol. Absorbance was measured at a wavelength of 450 nm using the Spark multimode microplate reader (Tecan, Stockholm, Sweden).

5.2.11. Statistical analysis

All results are expressed as the mean values of experimental replicates ± standard deviation. Statistical differences between the mean values were evaluated via one-way analysis of variance with GraphPad Prism version 10.2.3 for Windows (GraphPad Software, La Jolla, CA, USA) or SPSS Statistics version 29.0.2.0 (IBM, Armonk, NY, USA). Multiple comparisons between mean values were performed using the Šídák's test defined at α level = 0.05.

5.3. Results and discussion

5.3.1. Effect of peptide/rutin mixtures on IAPP fibrillation and fibrillar morphology

To observe the effect of peptide/rutin mixtures on anti-fibrillation activity, ThT fluorescence kinetics were performed. ThT is a nonfluorescent dye that, upon binding to the β-sheet-rich regions of IAPP fibrils, becomes fluorescent (**Figure 5.1A**). The extent of fibrillation inhibition by the peptides and rutin is then quantified by determining the percent fluorescent decrease relative to the uninhibited IAPP control. Endpoint ThT measurements indicated a significant decrease ($p < 0.05$) in IAPP fibrillation after 48 h for all inhibitor mixtures tested (**Figure 5.1B**). This translates to >50% decrease in ThT fluorescence intensity, indicating strong anti-fibrillation activity (**Figure 5.1C**). Rutin demonstrated the highest inhibition of 75.1 ± 12.5%, more than TNGQ of 54.7 ± 1.1% (**Figure 5.1C**), despite both possessing strong anti-fibrillation and disaggregative activity against IAPP as previously reported.[92,166] In combination, the anti-fibrillation activity of TNGQ/rutin mixtures tended to increase by 15.5% and decrease by 13.8% ($p > 0.05$) relative to TNGQ and rutin alone, respectively (**Figure 5.1C**). Similarly, the mixtures of YMSV or MANT with rutin did not show any obvious enhancement in anti-fibrillation activity (**Figure 5.1C**). The results suggest a non-additive effect of the inhibitor mixtures on anti-fibrillation activity.

The effect of anti-fibrillation activity on the average size of IAPP fibrils were also elucidated by DLS. As expected, a significant increase in particle diameter from 1256.7 ± 610.1

nm to 7153.7 ± 2769 nm was observed with IAPP after 48 h, confirming the presence of fibrillation (**Figure 5.1D**), comparable to a previous observation.[166] Addition of the peptide/rutin mixtures tended to increase ($p > 0.05$) the average particle diameter at the initial timepoint (**Figure 5.1D**), suggesting the formation of larger IAPP-peptide, IAPP-rutin, and IAPP-peptide-rutin complexes. Significant reductions in the average particle diameters were observed after 48 h for the peptide/rutin mixtures, with TNGQ/rutin mixturesshowing the highest decrease to 988.5 ± 189.2 nm, lower than the value previously observed for TNGQ or rutin alone.[92,166] This translates to an 86.2% decrease in particle diameter for the TNGQ/rutin mixture. Similarly, the MANT/rutin mixture significantly decreased the average particle diameter to 1317.2 ± 777.3 nm after 48 h (**Figure 5.1D**). On the other hand, the average particle diameter of the YMSV/rutin mixture did not change after 48 h (**Figure 5.1D**), suggesting that the YMSV/rutin mixture inhibited IAPP fibrillation via stabilization of the initial or intermediate fibrillar species. A high polydispersity index (> 0.7) of IAPP in the absence and presence of peptide-rutin combinations at 48 h is consistent with fibril formation and the presence of fibrillar intermediates of various sizes in the samples (**Figure 5.1E**). Furthermore, the shift from 295 nm to 531 nm and increase in peak intensity observed for IAPP after 48 h are characteristic of fibrillation (**Figure 5.1F**). Interestingly, a similar peak of larger size (615-825 nm) appeared at 0 h for all peptide/rutin mixtures, but it disappeared after 48 h with the formation of a new peak at 255 nm and 295 nm for YMSV and TNGQ, respectively. These peaks were also observed at the initial timepoint for IAPP control (**Figure 5.1F**). This suggests the reformation of early fibrillar intermediates, possibly by disaggregation of pre-formed fibrils, likely facilitated by rutin in the peptide/rutin mixtures. This indicates the retention of some previously reported anti-fibrillation and disaggregation activity of rutin within the peptide/rutin mixtures.[92] A larger shift in IAPP particle size distribution is observed for MANT/rutin mixture after 48 h, with an intense peak at 106 nm, which is smaller than the peak at 0 h (**Figure 5.1F**) suggesting that the strong anti-fibrillation may be due to disaggregative effects of the mixture.

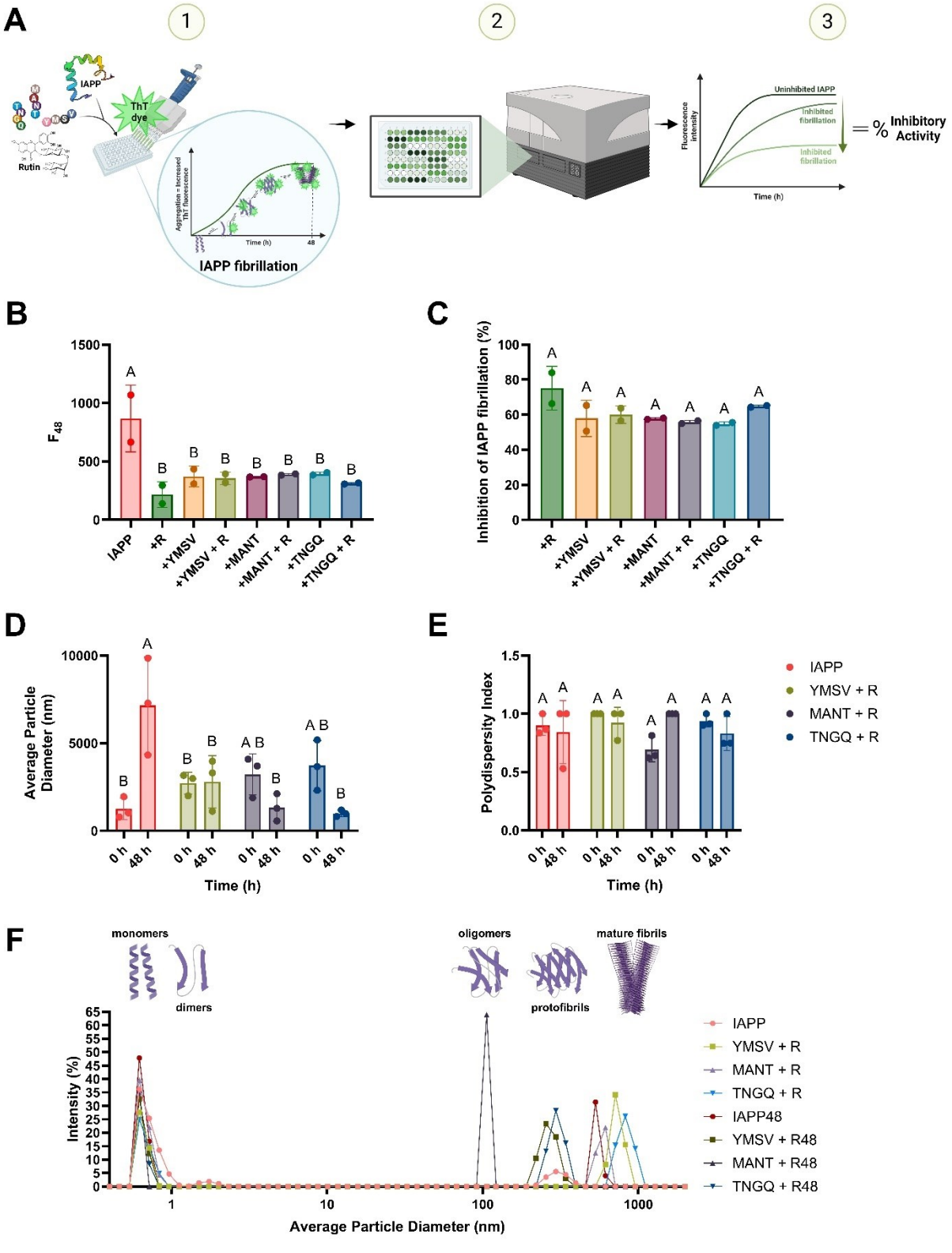
A
1
2
3
IAPP
ThT dye
Rutin
Aggregation = Increased ThT fluorescence
Time (h)
48
IAPP fibrillation
Uninhibited IAPP
Inhibited fibrillation
Inhibited fibrillation
Fluorescence intensity
Time (h)
= % Inhibitory Activity
B
F_{48}
1500
1000
500
0
IAPP
+R
+YMSV
+YMSV + R
+MANT
+MANT + R
+TNGQ
+TNGQ + R
C
Inhibition of IAPP fibrillation (%)
100
80
60
40
20
0
+R
+YMSV
+YMSV + R
+MANT
+MANT + R
+TNGQ
+TNGQ + R
D
Average Particle Diameter (nm)
10000
5000
0
0 h
48 h
Time (h)
E
Polydispersity Index
1.5
1.0
0.5
0.0
0 h
48 h
Time (h)
IAPP
YMSV + R
MANT + R
TNGQ + R
F
monomers
dimers
oligomers
protofibrils
mature fibrils
Intensity (%)
65
60
55
50
45
40
35
30
25
20
15
10
5
0
1
10
100
1000
Average Particle Diameter (nm)
IAPP
YMSV + R
MANT + R
TNGQ + R
IAPP48
YMSV + R48
MANT + R48
TNGQ + R48

Figure 5.1. (A) Preparation (1), detection (2), and quantification (3) of IAPP fibrillation using ThT fluorescent probe. **(B)** ThT fluorescence intensity and **(C)** percent inhibition of IAPP fibrillation in the absence and presence of single inhibitors (rutin, YMSV, MANT, and TNGQ) and inhibitor combinations (YMSV+rutin, MANT+rutin, and TNGQ+rutin). **(D)** Average particle diameter, **(E)** polydispersity index, and **(F)** size distribution of IAPP species upon the addition of peptide-rutin combinations (0 h) and after incubation (48 h). Bars with different letters indicate significantly different mean values ($p < 0.05$). R = rutin.

The effect of TNGQ/rutin mixtures on IAPP fibrillar morphology was assessed via TEM. As expected, dense fibrillar networks were observed in the control after 48 h, confirming IAPP fibrillation (**Figure 5.2A**). TNGQ and rutin independently inhibited IAPP fibrillation, resulting in the formation of truncated fibrils with TNGQ and the absence of fibrillar species with rutin (**Figure 5.2B-C**). Evidence of disaggregation of IAPP fibrils in the presence of TNGQ was also observed, indicated by the presence of amorphous species surrounding fibrillar IAPP (**Figure 5.2C**). TNGQ was previously reported to disaggregate preformed IAPP fibrils, likely due to TNGQ-IAPP monomer binding and shifting of the thermodynamic process of fibrillation towards the formation of monomeric and intermediate species.[166]. Similarly, the formation of amorphous aggregates in the presence of rutin was previously reported in IAPP and β-amyloid, resulting from strong anti-fibrillation activity.[92,96] In combination, complete inhibition of IAPP fibrillation is apparent with the lack of visible fibrillar species (**Figure 5.2D**). The proposed fibrillation patterns in the presence of the single and dual inhibitor systems follow the concept suggested by Ilm Chandel et al. that either a direct or indirect mechanism of fibrillar disaggregation occurs with the consecutive addition of inhibitors, where binding of inhibitors may occur (1) simultaneously, resulting in the direct formation of completely inhibited aggregates, or (2) consecutively, where the first inhibitor binding forms partially inhibited aggregates and the second inhibitor binding results in disaggregation into completely inhibited aggregates.[179]

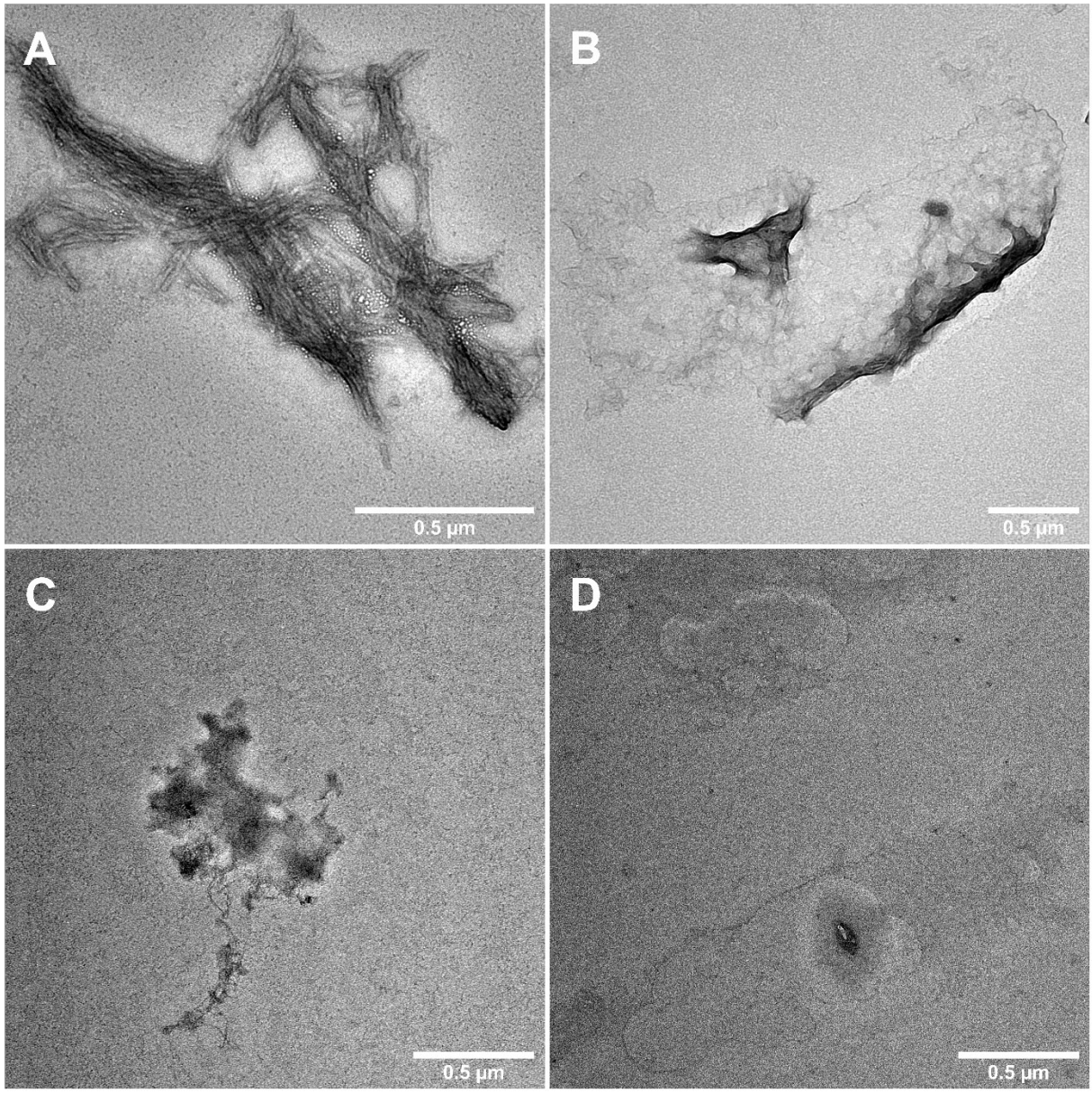

Figure 5.2. TEM images of **(A)** IAPP, **(B)** IAPP+TNGQ, **(C)** IAPP+rutin, and **(D)** IAPP+TNGQ+rutin after 48 h incubation. Scale bars represent 0.5 µm.

5.3.2. Effect of peptide/rutin interactions on IAPP fibrillation-induced cell death

To understand how the observed changes in the anti-fibrillation activity of peptide/rutin mixture affect IAPP fibrillation-induced cytotoxicity, pancreatic β-cell viability was assessed. As expected, IAPP fibrillation significantly reduced the cell viability of rat insulinoma (RIN-m) cells, with 5 µM IAPP decreasing viability to 2.6 ± 1.7%, demonstrating the extensive deleterious effects

of fibrillation-induced toxicity (**Figure 5.3**). Similar cytotoxic effects were observed with 25.6 μM hIAPP where treatment of RIN-m cells reduced β-cell viability by 80%.[25] Rutin significantly diminished the IAPP fibrillation-induced cytotoxicity by restoring cell viability to 55.2 ± 18.5%, thus showing the strongest cytoprotective effect of all samples (**Figure 5.3**). Rutin is a strong anti-fibrillation compound with equally potent cytoprotective effects against several amyloidogenic peptides, such as β-amyloid, where fibrillation inhibition resulted in ~20% increase in viability of SH-SY5Y cells at 100 nM rutin.[96] A significant increase in cell viability to 27.4 ± 4.5% and 46.0 ± 9.2% was also observed with YMSV-rutin and MANT-rutin combinations, respectively (**Figure 5.3**), compared to YMSV and MANT alone (5.0 ± 2.6% and 19.2 ± 15.7%, respectively). Despite the increased cell viability relative to the control and peptide-only conditions, the implication of peptide/rutin mixtures indicate non-additive effects as the cytoprotective activities of the combinations were lower than the sum of the effects of individual compounds. This indicates a loss of bioactivity upon combining each peptide with rutin. Conversely, while the TNGQ/rutin mixtures significantly increased cell viability to 37.0 ± 6.0%, relative to the control, there was a decrease in cytoprotective activity relative to TNGQ alone (47.5 ± 3.8%).

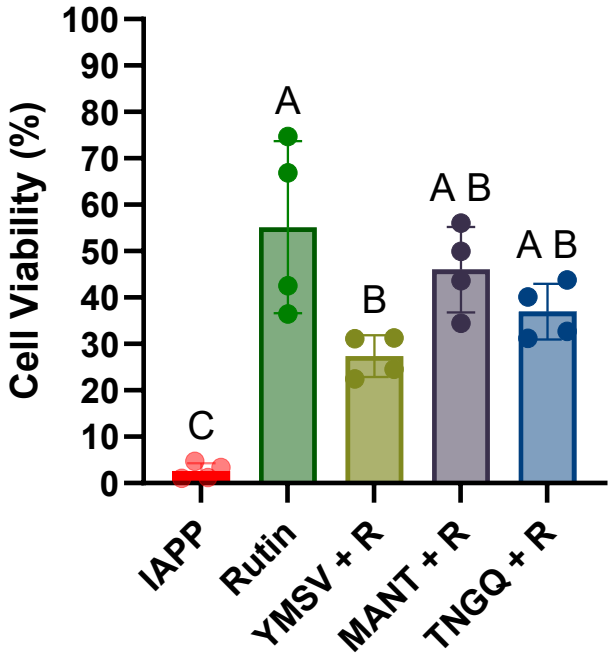

Figure 5.3. Cell viability of rat insulinoma (RIN-m) cells in the presence of 5 μM IAPP control and IAPP with rutin or peptide/rutin mixtures (YMSV+rutin, MANT+rutin, and TNGQ+rutin)

after 24 h. Bars with different letters indicate significantly different mean values ($p < 0.05$). R = rutin.

Given the non-additive effect of the peptide/rutin mixtures against IAPP fibrillation-induced cell death, the strongest individual inhibitors (TNGQ and rutin) were selected for further studies. This combination was used as a model to further understand how the resulting peptide/polyphenol mixture, and its effect on IAPP fibrillation, translate to the cellular functionality of pancreatic β-cells.

To understand how TNGQ/rutin mixtures affects hIAPP oligomer formation and cellular toxicity, immunofluorescence microscopy was used to localize the IAPP oligomers. Numerous hIAPP oligomeric deposits were observed surrounding the β-cells, with some appearing to be membrane-bound while others are located within the cells and around the nuclei (**Figure 5.4**). Similar intracellular oligomeric IAPP was previously reported with hIAPP-INS-1 cells and in the islets of 10-week-old hIAPP transgenic mice.[91,189] Oligomeric IAPP has long been identified as the main source of cytotoxicity, wherein the soluble fibrillar intermediates are embedded into the cell membranes, forming pores that disrupt membrane integrity and cause ionic imbalances, loss of signal transduction, and membrane rupture.[4,6,183] Furthermore, hIAPP concentrations ranging from 1-10 μM have markedly increased ability to reconstruct planar phospholipid bilayers into voltage-dependent channels with reduced selectivity, resulting in the formation of hIAPP pores that are permeable to Na^+, K^+, Ca^{2+}, and Cl^- ions.[184] The high prevalence of oligomeric IAPP species within this concentration range correlates with the intense decrease in cell viability (**Figure 5.3**). This confirms the deleterious role of the oligomeric intermediates in cellular functionality, likely driven by non-selective ion permeable pores. Similar localization of hIAPP in RIN-m cells was previously reported, with a strong prevalence of membrane-bound peptides and weaker distribution of intracellular IAPP, suggesting the early steps of internalization into the cells.[190] Internalization of IAPP is another mechanism of cytotoxicity. IAPP uptake occurs either directly via membrane-induced endocytosis or indirectly by interacting with the membrane-bound AMY receptor complexes, leading to non-endocytotic internalization. This can induce the formation of intracellular fibrils, which can interact with various organelles and cause cellular dysfunction. Alternatively, internalized IAPP can interact with the mitochondria, triggering ROS production and leading to cytotoxicity.[183] Individually, TNGQ and rutin significantly decreased the prevalence

of membrane-bound oligomeric IAPP, explaining their effects in restoring cell viability (**Figure 5.3** and **5.4**). In combination, extracellular oligomeric IAPP is minimal, confirming the strong anti-fibrillation activity (**Figure 5.1B**). However, it is worth noting the increased presence of intracellular oligomeric IAPP, which was minimal with single inhibitors (**Figure 5.4**). This could explain the reduced cytoprotective effect of TNGQ/rutin mixtures relative to rutin alone (**Figure 5.3**), highlighting the key role of intracellular IAPP oligomers on cell viability. Intracellularly, IAPP oligomerization has deleterious effects on mitochondrial function, resulting in increased ROS production, thus triggering apoptosis.[97,183]It is possible that direct peptide-polyphenol interactions reduced the accessibility and IAPP binding of the individual inhibitors, or resulted in complexes with reduced cellular uptake, thus hindering intracellular anti-fibrillation activity.[191]

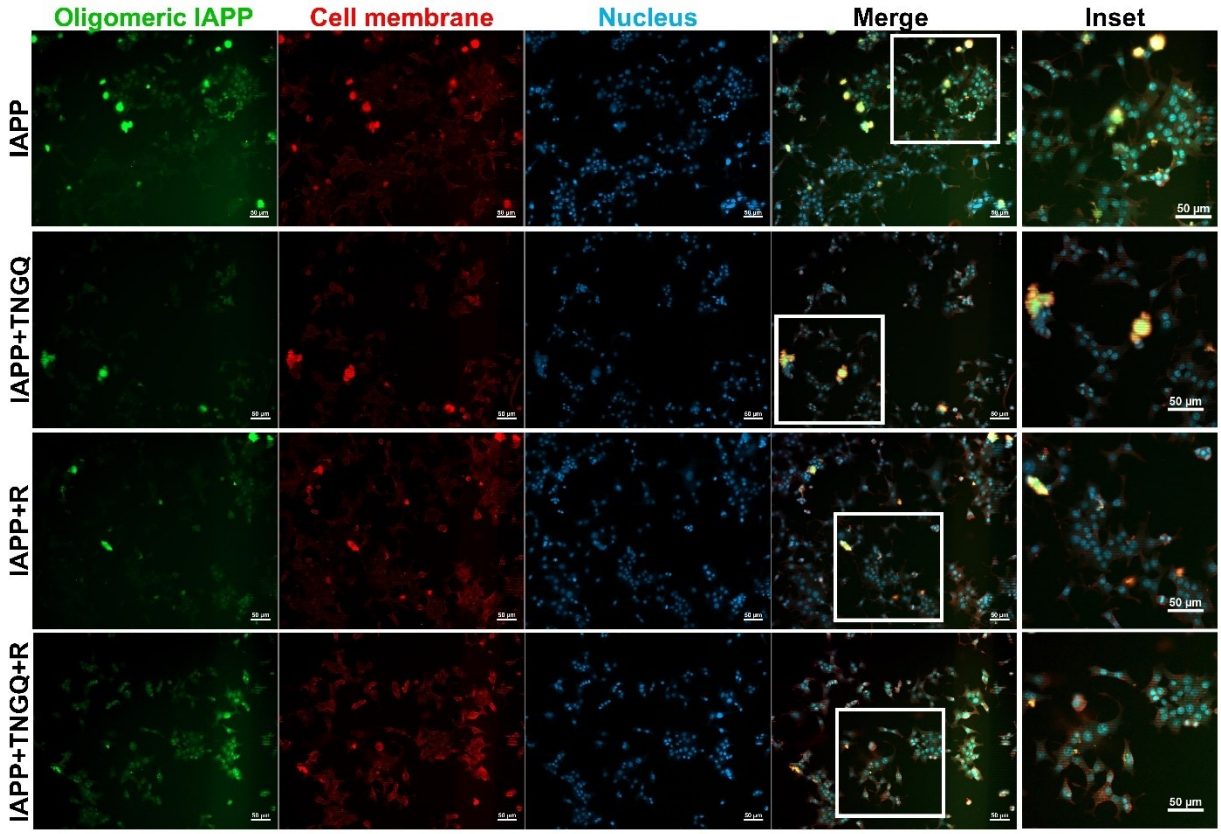

Figure 5.4. Fluorescence microscopy images of rat insulinoma (RIN-m) cells post-treatment with 5 µM IAPP in the absence or presence of 5 µM TNGQ, rutin, or a mixture of TNGQ/rutin for 24 h. Green, oligomeric and fibrillar IAPP; red, RIN-m cellular membrane; and blue, RIN-m nuclei. Scale bars represent 50 µm. White squares indicate the region expanded for inset.

5.3.3. TNGQ/rutin mixtures provide increased cellular functionality in the presence of IAPP fibrillation

MTT reduction assay is commonly used to evaluate cytotoxicity via mitochondrial function, but it reflects both reversible and irreversible cellular dysfunction that do not always result in cell death.[190] IAPP fibrillation induces a range of deleterious effects that may not be reflected in cell viability assays. Hence, ROS production and glucose-stimulated insulin secretion were also evaluated to assess the implications of anti-fibrillation activity of the compounds on cellular functionality.

IAPP fibrillation-induced β-cell toxicity occurs by multiple pathways, one of which is strongly associated with the overproduction of ROS in the mitochondria.[183,190] Thus, oxidative stress in IAPP-treated RIN-m cells was monitored using the ROS probe, DCFH-DA, to investigate whether the anti-fibrillation and cytoprotective activities of TNGQ, rutin, and TNGQ/rutin mixtures are related to a reduction in ROS levels. DCFH-DA is a nonfluorescent dye that readily diffuses through the cell membrane where it is hydrolyzed by esterases to form 2′,7′-dichlorofluorescin (DCFH) intracellularly. DCFH reacts with intracellular free radicals, including H_2O_2, $O_2^{\bullet-}$, and $^{\bullet}OH$, to form the green, fluorescent derivative, DCF, which is quantifiable as the amount of intracellular ROS.[192] Following exposure to IAPP in the absence or presence of the inhibitor samples for 6 h, to allow for the formation of oligomeric species, ROS levels in RIN-m cells were monitored over 3 h post-treatment. As shown in **Figure 5.5A**, oxidative stress was apparent in IAPP-treated cells, given the rapid increase in ROS production over 3 h. This indicates an impaired activation of intracellular antioxidant systems due to IAPP fibrillation. This result is crucial as IAPP fibrillation exerts pro-apoptotic effects through ROS production and mitochondrial dysfunction in T2D development.[183,190,193] Interactions between internalized IAPP and the mitochondrial membrane induces membrane depolarization, thus enhancing ROS production and mTOR-activated mitophagy, while also enhancing fibrillation of membrane-bound IAPP.[183] Continual fibrillation of internalized IAPP further induces oxidative stress and mitochondrial toxicity, explaining the increased ROS production (**Figure 5.5A-B**) and concomitant decrease in cell viability (**Figure 5.3**). The addition of the inhibitor combination reduced the rate of ROS production relative to IAPP control (**Figure 5.5A**). TNGQ tended to perform slightly better than rutin ($p > 0.05$), despite rutin being a stronger anti-fibrillation and antioxidant compound. Notably,

a significant decrease ($p < 0.05$) in ROS production relative to IAPP control was achieved only with the TNGQ/rutin mixture, which reduced oxidative stress by 30.5% (**Figure 5.5B**). The decrease in IAPP fibrillation-induced oxidative stress can be due to two mechanisms: (1) indirect effect via the anti-fibrillation mechanism whereby inhibition of IAPP fibrillation prevents fibrillation-induced oxidative stress, or (2) direct effect via radical scavenging mechanism whereby unbound rutin or TNGQ/rutin mixtures scavenge ROS produced as a result of IAPP-mitochondrial membrane interactions. Molecular docking with TNGQ and rutin separately showed their affinity for interaction with the membrane-binding and C-terminal domain of monomeric IAPP.[92,166] Both inhibitors share interactions with Asn3, Arg11, and Phe15 of the membrane-binding domain, suggesting that steric clashes are expected to impede their simultaneous interaction with IAPP. This could explain the non-additive effects of the peptide-polyphenol combination on anti-fibrillation and cytoprotective activities. This proposed mechanism means that the unbound rutin would act as a free radical scavenger, thus reducing oxidative stress in RIN-m cells. This provides a unique perspective to dual inhibition systems where both inhibitors may not necessarily need to directly bind to prevent deleterious effects. Rather, the unbound inhibitors many also maintain other bioactivity relevant to the disease being treated (i.e., an anti-fibrillation or disaggregative compound that is also antioxidative).

The implication of the anti-fibrillation activity of the compounds on β-cell sensitivity of glucose stimulation was also evaluated. hIAPP inhibits glucose-stimulated insulin secretion but its mechanism is not clearly understood.[184] In a non-disease state, increase in glucose concentration stimulates insulin release via increases in high voltage-gated calcium channel currents and elevated intracellular calcium concentrations (**Figure 5.5C**). However, the presence of extracellular IAPP fibrillation impedes glucose sensitivity through the desensitization of high voltage-gated calcium channels as a result of imbalances in intracellular calcium concentrations.[184] This is likely due to the formation of ion permeable membrane-bound oligomeric IAPP pores that allow for the uncontrolled flow of ions, thus diminishing the ability to accumulate intracellular calcium and desensitizing high-voltage-activated calcium channels (**Figure 5.5C**). Consequently, glucose sensitivity decreases in β-cells, thus reducing insulin exocytosis and blood glucose regulation.[184] To accurately mimic postprandial (hyperglycemic) conditions, in which IAPP would be most active, basal and high concentrations of glucose (1.1 and 20 mM, respectively) were used. IAPP is most actively produced and secreted under hyperglycemic conditions, where an increased demand

for insulin, to counteract high blood glucose levels, also results in elevated IAPP production, secretion, and function.[4,7,97] Thus, under basal conditions, insulin secretion is minimized, which is likened to the fasting state. A subsequent change to 20 mM glucose, mimicking postprandial hyperglycemia, was used to stimulate insulin secretion through the glucose-stimulated pathway, which is relevant for the pathological effects of hyperglycemia as seen in T2D. This depicts the acute response of β-cells to high glucose levels and enables the assessment of the effects of glucose levels on pancreatic β-cell function in the presence of IAPP fibrillation and associated complications. A glucose-dependent increase in insulin secretion was observed in treated RIN-m cells, although not significantly different ($p > 0.05$) under our experimental conditions (**Figure 5.5D**). Various pathways are involved in maintaining glucose homeostasis, including the release of hormone potentiators such as incretins which bind β-cell receptors to augment insulin secretion via peripheral mechanisms.[194] As such, various compensatory mechanisms can be activated in the event of IAPP fibrillation-induced complications in glucose sensing, explaining the observed lack of apparent impairments in glucose-stimulated insulin secretion.

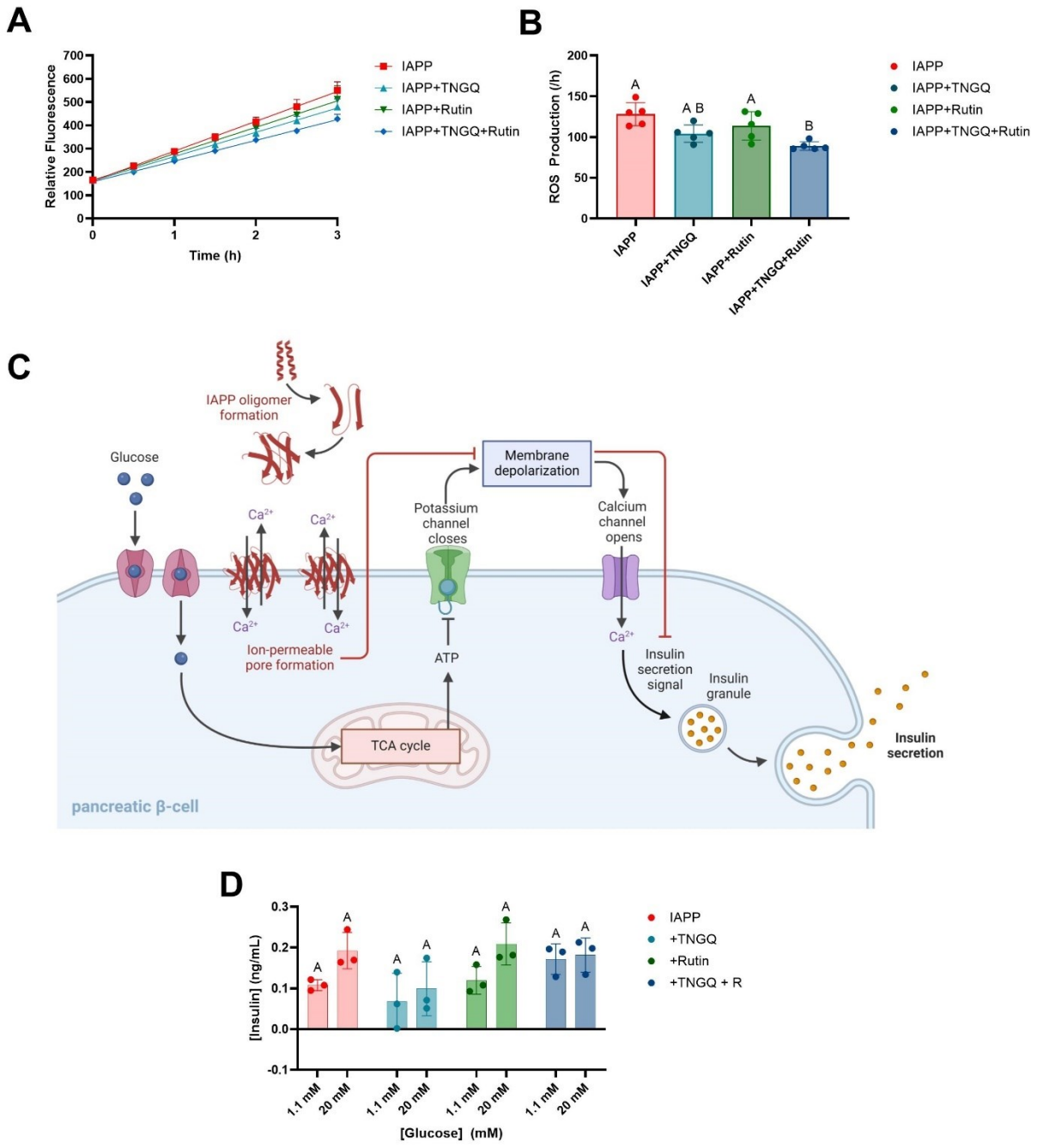

Figure 5.5. (A) Time-dependent oxidative response and **(B)** rate of ROS production in RIN-m cells following 6 h treatments with 5 μM IAPP in the absence and presence of TNGQ, rutin, and TNGQ/rutin mixtures. **(C)** Mechanism of glucose-stimulated insulin secretion in β-cells, and the effect of IAPP oligomerization on insulin secretion. **(D)** Glucose-stimulated insulin secretion in RIN-m cells in the presence of basal and high glucose concentrations, following 24 h treatments

with IAPP and the inhibitors. Bars with different letters indicate significantly different mean values ($p < 0.05$). R = rutin.

5.4. Conclusions

In this study, the effect of peptide/polyphenol mixtures, using anti-fibrillation peptides MANT, YMSV, and TNGQ and polyphenol, rutin, on IAPP fibrillation-induced β-cell dysfunction was studied. In summary, the anti-fibrillation activity was non-additive in all peptide/rutin mixtures, but the average particle size of IAPP decreased considerably compared to when single inhibitors were used. This indicates an apparent effect by the peptide/rutin mixtures on the development and distribution of mature IAPP fibrillar species. The peptide/rutin mixtures also reduced the IAPP fibrillation-induced β-cell death, but these effects were equally non-additive and tended to be lower than the cytoprotective effect of rutin alone, especially for the rutin/YMSV mixture. We propose that possible complexation between the aromatic residue of YMSV and the conjugated flavonol structure of rutin could facilitate π-π stacking, thus preventing IAPP binding and diminishing protective effects against IAPP fibrillation-induced cytotoxicity, and hence, were selected for studying their effectiveness on increasing β-cell functionality. The TNGQ/rutin mixtures inhibited completely the formation of IAPP fibrils and prevented the formation of membrane-bound oligomeric species in β-cells. This effect translated to significant reductions in IAPP fibrillation-induced cellular oxidative stress, an effect not observed in the presence of TNGQ or rutin alone. This study revealed important insights into the mechanisms of the dual inhibitor system. A large emphasis is placed on synergistic effects when considering classic dual inhibitor models, which would involve binding separate IAPP regions or the formation of new inhibitor complexes with superior activity than their individual counterparts. Alternatively, the dual inhibitor system at play in this study led to non-additive effects, which we propose to be the result of peptide/polyphenol mixtures that diminishing the anti-fibrillation activity of the single inhibitors or causing steric effects thus impeding cellular uptake and intracellular activity. Furthermore, binding of one inhibitor could prevent binding of the second inhibitor if they compete for shared interaction sites, which applies to rutin and TNGQ binding to IAPP. However, given the nature of IAPP fibrillation and presence of diverse fibrillar species at any given time, dual binding may not be necessary for maximal effect. This was supported by TEM and particle size results which showed that, despite the non-additive anti-fibrillation effects, the TNGQ/rutin mixtures

resulted in pronounced absence of IAPP fibrils beyond that of the individual inhibitors. Similarly, only the TNGQ/rutin mixtures significantly reduced IAPP fibrillation-induced oxidative stress in β-cells, likely because of direct inhibition of IAPP fibrillation or the radical scavenging antioxidant effect of the polyphenol. In conclusion, this study has revealed the prospects of dual inhibitor systems and provided perspectives on the inhibition mechanisms for anti-fibrillation activity. Considering the process of IAPP fibrillation significantly influences several downstream pathological pathways in T2D, considerations should be given to inhibitors or a combination of inhibitors that are multifunctional and provide additional bioactivities beyond anti-fibrillation. Given the fibrillar disaggregative potentials of some peptides and polyphenols, future studies are needed to elucidate these effects towards mitigating preformed IAPP fibril-induced cytotoxicity and their physiological implications on pancreatic β-cells and T2D *in vivo*.

5.5. Acknowledgements

R.O.A. is a recipient of the Vanier Canada Graduate Scholarship. The authors acknowledge the financial support from the Natural Sciences and Engineering Research Council of Canada (NSERC) [grant number RGPIN-2018-06839], and the University Research Chairs Program of the University of Ottawa, Canada.

Conflicts of interest

There are no conflicts to declare.

CHAPTER SIX

CONCLUSION

The main objective of this thesis was to investigate the role of food-derived compound structure on anti-fibrillation activity and effect on β-cell functionality and IAPP fibrillation-induced cytotoxicity. This research provides valuable insight into some peptide and polyphenol structural features that can enhance bioactivity, thus enabling rational design and systematic identification of strong anti-fibrillation compounds. The four research objectives that motivated this research are based on the eight key research questions listed in chapter one.

The first and second research questions, representing the first objective of this thesis, were addressed in chapter two. This chapter explored the structure and molar ratio of 12 phenolic compounds and four polyphenols, gallic acid, caffeic acid, rutin, and quercetin, were selected for biomolecular analysis to provide further mechanistic insights into structure-dependent anti-fibrillation activity. Rutin and quercetin exerted inhibitory effects likely by stabilizing monomeric IAPP and inhibiting the lag phase of fibrillation. Both compounds also exhibited disaggregatory effects on preformed IAPP fibrils. Structural analysis points to the importance of bulkiness and catechol moieties towards enhancing IAPP binding and subsequent anti-fibrillation activity. The presence of both structural features in rutin suggests why this flavonol glycoside was the most potent inhibitor of all the compounds tested. Despite this, quercetin, a major metabolite of rutin, maintained a comparable anti-fibrillation and fibrillar disaggregation activity, providing important insights on the role of biostability and metabolism. Molecular docking also highlighted the importance of hydrogen bonding and electrostatic interactions, in addition to π-π interactions, between IAPP and the compounds in anti-fibrillation activity. In summary, these findings demonstrate important structural features of phenolic compounds for inhibiting IAPP fibrillation or disaggregating existing fibrils.

The third research question was addressed in chapter three, along with research question four. This chapter aimed at elucidating the structural requirements of peptides for strong anti-fibrillation activity and understanding how IAPP-binding influenced fibrillation. From this study, three peptides, MANT, YMSV, and TNGQ were identified for their anti-fibrillation activity. Through biomolecular analysis, potential mechanisms of inhibition and the effect of structure and physicochemical properties of the peptides on activity were proposed. Despite the strong binding of MANT and YMSV to the amyloidogenic region of IAPP via hydrophobic and aromatic interactions, the weaker anti-fibrillation activity of both peptides demonstrated that strong inhibitor

binding to the amyloidogenic region is not imperative to inhibitor activity. On the other hand, TNGQ, the most active peptide inhibitor, preferentially bound the membrane-binding N-terminal and self-association C-terminal domains via hydrogen bonding and electrostatic interactions. Furthermore, TNGQ also demonstrated fibrillar disaggregation activities, a result of monomeric IAPP-TNGQ complexation shifting the monomer-fibril equilibrium towards the liberation of IAPP monomers from the growing end of formed fibrils. This provided new perspectives on the important physiochemical properties necessary for the increased anti-fibrillation mechanism and potency.

The fifth research question was addressed in chapter four and assessed the contribution of IAPP-binding patterns of the peptide inhibitors MANT, YMSV, and TNGQ to cytoprotective effects against IAPP fibrillation-induced membrane damage and cytotoxicity. Membrane damage was monitored using calcein encapsulated giant unilamellar vesicles (GUVs) as a model for β-cell membranes. Both YMSV and TNGQ significantly inhibited IAPP fibrillation-induced GUV leakage while MANT demonstrated moderative effects in the initial phases of fibrillation, but this activity diminished in the later phases of fibrillation. Of the three peptides, TNGQ was the only peptide that mitigated IAPP fibrillation-induced β-cell toxicity. On the other hand, YMSV and MANT did not increase β-cell viability in the presence of IAPP, further demonstrating that superior IAPP-binding does not always translate to an increased cytoprotective effects against IAPP fibrillation. TNGQ was the only peptide that interacted with the membrane-binding and self-association domains, thus highlighting the importance of these regions in fibrillation-induced β-cell damage.

The fifth, and final research chapter addressed the sixth, seventh, and eighth research questions, which focused on the study of dual inhibitor systems against IAPP fibrillation. Hence, the effects of peptide-polyphenol interactions were studied using the strongest anti-fibrillation polyphenol, rutin, and the three peptides, YMSV, MANT, and TNGQ. Anti-fibrillation activity was retained in the peptide-polyphenol combinations; however, the activity was non-additive. This translated to an increased β-cell viability in the presence of IAPP fibrillation. As the effect of peptide-polyphenol combinations were not as pronounced with YMSV and MANT, only TNGQ was selected to understand the effect of peptide-polyphenol interactions on anti-fibrillation activity. Transmission electron microscopy (TEM) revealed an increased inhibition of IAPP fibrils

by the combination, relative to TNGQ or rutin alone. The TNGQ/rutin mixtures also decreased the presence of membrane-bound oligomeric IAPP compared to the uninhibited or singly inhibited samples. This translated to a significant decrease in cellular oxidative stress only in the presence of the TNGQ/rutin mixtures, but not with TNGQ or rutin alone. Findings from this study provided novel perspectives about mechanisms of the dual inhibitor systems, and the role of peptide/polyphenol mixtures on anti-fibrillation activity. Specifically, new insights on the benefits of non-additive inhibitor systems, particularly for IAPP fibrillation inhibition, suggests that simultaneous binding may not be required for potent activity, especially considering that the nature of IAPP fibrillation encourages the existence of diverse fibrillar species at any given time. Like the manifestation of T2D disease itself, IAPP fibrillation triggers a multitude of deleterious effects; thus, multifunctional compounds that also target downstream effects should be considered for dual inhibition systems.

Taken together, all four thesis objectives, derived from the research questions in chapter one, were accomplished. The findings resulted in structure-function relationships for both polyphenols and peptide inhibitors. As a result, it was identified that π-π interactions were not the only driving forces behind fibrillation inhibition. Furthermore, novel insights on IAPP targeting sites were identified for enhanced anti-fibrillation activity, increased membrane protective effects, and reduced IAPP fibrillation-induced β-cell toxicity. Investigations on the role of potential peptide-polyphenol interactions on dual inhibition systems, for the first time, highlighted the importance of multifunctional compounds for future considerations. In conclusion, the four objectives accomplished the overall aim of this thesis to understand the role of food-derived compounds on anti-fibrillation activity and effect on β-cell functionality and IAPP fibrillation-induced toxicity.

Future directions

Findings and the insights gained from this thesis have expanded this research area to involve more considerations for future research.

Further research should include elucidation of the mechanism of the cytoprotective effects of TNGQ, rutin, and TNGQ/rutin mixtures and effects in managing IAPP fibrillation-induced apoptosis and recovering autophagy response, and β-cell functionality.

Considering the nature of T2D disease and the high prevalence of IAPP fibrils in most patients with T2D, in addition to anti-fibrillation activity, potential inhibitors should also disaggregate pre-existing fibrils. Given the fibrillar disaggregative potentials of the peptide, TNGQ, and polyphenols, rutin and quercetin, future studies are needed to elucidate these effects towards mitigating preformed IAPP fibril-induced cytotoxicity and their physiological implications on pancreatic β-cells and T2D *in vivo*. Future studies in understanding how disaggregation facilitates β-cell cytotoxicity and restores β-cell functionality should be considered.

Finaly, given the nature of the compounds studied in this thesis, biostability and bioavailability issues always present as a limitation for translational research. While it was determined that quercetin, the metabolite for the potent anti-fibrillation compound rutin, maintained comparable activity, more considerations towards delivery methods, and gastrointestinal biostability and bioactivity should be evaluated *in vivo*. Additionally, the peptides reported in this thesis were predicted to have low oral bioavailability. This factor should be evaluated further and addressed prior to *in vivo* studies to achieve significant IAPP fibrillation inhibitory effects in the pancreas. TNGQ is food-derived; thus, future research should include the development of sustainable processing methods, e.g., enzymatic hydrolysis or fermentation, to release the bioactive peptide from its parent proteins. Alternatively, delivery systems involving encapsulation and targeted release can be explored *in vivo*. This will help ensure that the anti-fibrillating compounds are accurately delivered to pancreatic β-cells, where they can exact their intended functions.

REFERENCES

(1) Marek, P. J.; Patsalo, V.; Green, D. F.; Raleigh, D. P. Ionic Strength Effects on Amyloid Formation by Amylin Are a Complicated Interplay Among Debye Screening, Ion Selectivity, and Hofmeister Effects. *Biochemistry* **2012**, *51*, 8478–8490. https://doi.org/https://doi.org/10.1021/bi300574r.

(2) Eisenberg, D. The Discovery of the α-Helix and β-Sheet, the Principal Structural Features of Proteins. *Proceedings of the National Academy of Sciences of the United States of America* **2003**, *100*, 11207–11210. https://doi.org/10.1073/pnas.2034522100.

(3) Iadanza, M. G.; Jackson, M. P.; Hewitt, E. W.; Ranson, N. A.; Radford, S. E. A New Era for Understanding Amyloid Structures and Disease. *Nature Reviews Molecular Cell Biology* **2018**, *19* (12), 755–773. https://doi.org/10.1038/s41580-018-0060-8.

(4) Abioye, R. O.; Udenigwe, C. C. Potential of Peptides and Phytochemicals in Attenuating Different Phases of Islet Amyloid Polypeptide Fibrillation for Type 2 Diabetes. *Food Science and Human Wellness* **2021**, *10*, 258–268. https://doi.org/10.1016/j.fshw.2021.02.017.

(5) Huang, C.; Haataja, L.; Gurlo, T.; Butler, A. E.; Wu, X.; Soeller, W. C.; Butler, P. C. Induction of Endoplasmic Reticulum Stress-Induced β-Cell Apoptosis and Accumulation of Polyubiquitinated Proteins by Human Islet Amyloid Polypeptide. *Endocrine and Metabolism* **2007**, *293* (6), 1656–1662. https://doi.org/10.1152/ajpendo.00318.2007.

(6) Westermark, P.; Andersson, A.; Westermark, G. T. Islet Amyloid Polypeptide, Islet Amyloid, and Diabetes Mellitus. *Physiological Reviews* **2011**, *91*, 795–826. https://doi.org/10.1152/physrev.00042.2009.

(7) Höppener, J. W. M.; Ahrén, B.; Lips, C. J. M. Islet Amyloid and Type 2 Diabetes Mellitus. *New England Journal of Medicine* **2000**, *343* (6), 411–419. https://doi.org/10.1056/nejm200008103430607.

(8) Mitra, A.; Sarkar, N. Sequence and Structure-Based Peptides as Potent Amyloid Inhibitors: A Review. *Archives of Biochemistry and Biophysics* **2020**, *695*, 108614. https://doi.org/10.1016/j.abb.2020.108614.

(9) Christensen, M.; Skeby, K. K.; Schiøtt, B. Identification of Key Interactions in the Inital Self-Assembly of Amylin in a Membrane Environment. *Biochemistry* **2017**, *56*, 4884–4894. https://doi.org/https://doi.org/10.1021/acs.biochem.7b00344.

(10) Qian, Z.; Zou, Y.; Zhang, Q.; Chen, P.; Ma, B.; Wei, G.; Nussinov, R. Atomistic-Level Study of the Interactions Between hIAPP Protofibrils and Membranes: Influence of pH and Lipid Composition. *BBA - Biomembranes* **2018**, *1860*, 1818–1825. https://doi.org/https://doi.org/10.1016/j.bbamem.2018.02.005.

(11) Hsu, Y.-H.; Chen, Y.-W.; Wu, M.-H.; Tu, L.-H. Protein Glycation by Glyoxal Promotes Amyloid Formation by Islet Amyloid Polypeptide. *Biophysical Journal* **2019**, *116*, 2304–2313. https://doi.org/10.1016/j.bpj.2019.05.013.

(12) Cao, P.; Abedini, A.; Raleigh, D. P. Aggregation of Islet Amyloid Polypeptide: From Physical Chemistry to Cell Biology. *Current Opinion in Structural Biology* **2013**, *23*, 82–89. https://doi.org/10.1016/j.sbi.2012.11.003.

(13) Wiltzius, J. J. W.; Sievers, S. A.; Sawaya, M. R.; Cascio, D.; Popov, D.; Riekel, C.; Eisenberg, D. Atomic Structure of the Cross-β Spine of Islet Amyloid Polypeptide (Amylin). *Protein Science* **2008**, *17* (9), 1467–1474. https://doi.org/10.1110/ps.036509.108.

(14) Chakraborty, S.; Mukherjee, B.; Basu, S. Pinpointing Proline Substitution to Be Responsible for the Loss of Amyloidogenesis in IAPP. *Chemical & Biology Drug Design* **2013**, *82*, 446–452. https://doi.org/10.1111/cbdd.12172.

(15) Bolarinwa, O.; Li, C.; Khadka, N.; Li, Q.; Wang, Y.; Pan, J.; Cai, J. γ-AApeptides-Based Small Molecule Ligands That Disaggregate Human Islet Amyloid Polypeptide. *Scientific Report* **2020**, *10* (95), 1–10. https://doi.org/10.1038/s41598-019-56500-0.

(16) Yang, J.; Sun, Y.; Xu, F.; Liu, W.; Mai, Y.; Hayashi, T.; Hattori, S.; Ushiki-Kaku, Y.; Onodera, S.; Tashiro, S. ichi; Ikejima, T. Silibinin Ameliorates Amylin-Induced Pancreatic β-Cell Apoptosis Partly via Upregulation of GLP-1R/PKA Pathway. *Molecular and Cellular Biochemistry* **2019**, *452* (1–2), 83–94. https://doi.org/10.1007/s11010-018-3414-9.

(17) Sivanesam, K.; Shu, I.; Huggins, K. N. L.; Tatarek-Nossol, M.; Kapurniotu, A.; Andersen, N. H.; Andersen, N. H. Peptide Inhibitors of the Amyloidogenesis of IAPP: Verification of the Hairpin-Binding Geometry Hypothesis. *FEBS Letters* **2016**, *590,* 2575-2583. https://doi.org/10.1002/1873-3468.12261.

(18) Olsson, M.; Herrington, M. K.; Reidelberger, R. D.; Permert, J.; Gebre-Medhin, S.; Arnelo, U. Food Intake and Meal Pattern in IAPP Knockout Mice with and without Infusion of Exogenous IAPP. *Scandinavian Journal of Gastroenterology* **2012**, *47* (2), 191–196. https://doi.org/10.3109/00365521.2011.638392.

(19) Bhowmick, D. C.; Jeremic, A. Functional Proteasome Complex Is Required for Turnover of Islet Amyloid Polypeptide in Pancreatic SS-Cells. *Journal of Biological Chemistry* **2018**, *293* (37), 14210–14223. https://doi.org/10.1074/jbc.ra118.002414.

(20) Press, M.; Jung, T.; König, J.; Grune, T.; Höhn, A. Protein Aggregates and Proteostasis in Aging: Amylin and ß-Cell Function. *Mechanisms of Ageing and Development* **2019**, *177*, 46–54. https://doi.org/10.1016/j.mad.2018.03.010.

(21) Ong, K. L.; Stafford, L. K.; McLaughlin, S. A.; Boyko, E. J.; Vollset, S. E.; Smith, A. E.; Dalton, B. E.; Duprey, J.; Cruz, J. A.; Hagins, H.; Lindstedt, P. A.; Aali, A.; Abate, Y. H.; Abate, M. D.; Abbasian, M.; Abbasi-Kangevari, Z.; Abbasi-Kangevari, M.; ElHafeez, S. A.; Abd-Rabu, R.; Abdulah, D. M.; Abdullah, A. Y. M.; Abedi, V.; Abidi, H.; Aboagye, R. G.; Abolhassani, H.; Abu-Gharbieh, E.; Abu-Zaid, A.; Adane, T. D.; Adane, D. E.; Addo, I. Y.;

Adegboye, O. A.; Adekanmbi, V.; Adepoju, A. V.; Adnani, Q. E. S.; Afolabi, R. F.; Agarwal, G.; Aghdam, Z. B.; Agudelo-Botero, M.; Arriagada, C. E. A.; Agyemang-Duah, W.; Ahinkorah, B. O.; Ahmad, D.; Ahmad, R.; Ahmad, S.; Ahmad, A.; Ahmadi, A.; Ahmadi, K.; Ahmed, A.; Ahmed, A.; Ahmed, L. A.; Ahmed, S. A.; Ajami, M.; Akinyemi, R. O.; Al Hamad, H.; Al Hasan, S. M.; AL-Ahdal, T. M. A.; Alalwan, T. A.; Al-Aly, Z.; AlBataineh, M. T.; Alcalde-Rabanal, J. E.; Alemi, S.; Ali, H.; Alinia, T.; Aljunid, S. M.; Almustanyir, S.; Al-Raddadi, R. M.; Alvis-Guzman, N.; Amare, F.; Ameyaw, E. K.; Amiri, S.; Amusa, G. A.; Andrei, C. L.; Anjana, R. M.; Ansar, A.; Ansari, G.; Ansari-Moghaddam, A.; Anyasodor, A. E.; Arabloo, J.; Aravkin, A. Y.; Areda, D.; Arifin, H.; Arkew, M.; Armocida, B.; Arnlov, J.; Artamonov, A. A.; Arulappan, J.; Aruleba, R. T.; Arumugam, A.; Aryan, Z.; Asemu, M. T.; Asghari-Jafarabadi, M.; Askari, E.; Asmelash, D.; Astell-Burt, T.; Athar, M.; Athari, S. S.; Atout, M. M. d. W.; Avila-Burgos, L.; Awaisu, A.; Azadnajafabad, S.; Darshan, B. B.; Babamohamadi, H.; Badar, M.; Badawi, A.; Badiye, A. D.; Baghcheghi, N.; Bagheri, N.; Bagherieh, S.; Bah, S.; Bahadory, S.; Bai, R.; Baig, A. A.; Baltatu, O. C.; Baradaran, H. R.; Barchitta, M.; Bardhan, M.; Barengo, N. C.; Barnighausen, T. W.; Barone, M. T. U.; Barone-Adesi, F.; Barrow, A.; Bashiri, H.; Basiru, A.; Basu, S.; Basu, S.; Batiha, A. M. M.; Batra, K.; Bayih, M. T.; Bayileyegn, N. S.; Behnoush, A. H.; Bekele, A. B.; Belete, M. A.; Belgaumi, U. I.; Belo, L.; Bennett, D. A.; Bensenor, I. M.; Berhe, K.; Berhie, A. Y.; Bhaskar, S.; Bhat, A. N.; Bhatti, J. S.; Bikbov, B.; Bilal, F.; Bintoro, B. S.; Bitaraf, S.; Bitra, V. R.; Bjegovic-Mikanovic, V.; Bodolica, V.; Boloor, A.; Brauer, M.; Brazo-Sayavera, J.; Brenner, H.; Butt, Z. A.; Calina, D.; Campos, L. A.; Campos-Nonato, I. R.; Cao, Y.; Cao, C.; Car, J.; Carvalho, M.; Castaneda-Orjuela, C. A.; Catala-Lopez, F.; Cerin, E.; Chadwick, J.; Chandrasekar, E. K.; Chanie, G. S.; Charan, J.; Chattu, V. K.; Chauhan, K.; Cheema, H. A.; Abebe, E. C.; Chen, S.; Cherbuin, N.; Chichagi, F.; Chidambaram, S. B.; Cho, W. C. S.; Choudhari, S. G.; Chowdhury, R.; Chowdhury, E. K.; Chu, D. T.; Chukwu, I. S.; Chung, S. C.; Coberly, K.; Columbus, A.; Contreras, D.; Cousin, E.; Criqui, M. H.; Cruz-Martins, N.; Cuschieri, S.; Dabo, B.; Dadras, O.; Dai, X.; Damasceno, A. A. M.; Dandona, R.; Dandona, L.; Das, S.; Dascalu, A. M.; Dash, N. R.; Dashti, M.; Davila-Cervantes, C. A.; De la Cruz-Gongora, V.; Debele, G. R.; Delpasand, K.; Demisse, F. W.; Demissie, G. D.; Deng, X.; Denova-Gutierrez, E.; Deo, S. V.; Dervišević, E.; Desai, H. D.; Desale, A. T.; Dessie, A. M.; Desta, F.; Dewan, S. M. R.; Dey, S.; Dhama, K.; Dhimal, M.; Diao, N.; Diaz, D.; Dinu, M.; Diress, M.; Djalalinia, S.; Doan, L. P.; Dongarwar, D.; dos Santos Figueiredo, F. W.; Duncan, B. B.; Dutta, S.; Dziedzic, A. M.; Edinur, H. A.; Ekholuenetale, M.; Ekundayo, T. C.; Elgendy, I. Y.; Elhadi, M.; El-Huneidi, W.; Elmeligy, O. A. A.; Elmonem, M. A.; Endeshaw, D.; Esayas, H. L.; Eshetu, H. B.; Etaee, F.; Fadhil, I.; Fagbamigbe, A. F.; Fahim, A.; Falahi, S.; Faris, M. A. I. E. M.; Farrokhpour, H.; Farzadfar, F.; Fatehizadeh, A.; Fazli, G.; Feng, X.; Ferede, T. Y.; Fischer, F.; Flood, D.; Forouhari, A.; Foroumadi, R.; Koudehi, M. F.; Gaidhane, A. M.; Gaihre, S.; Gaipov, A.; Galali, Y.; Ganesan, B.; Garcia-Gordillo, M. A.; Gautam, R. K.; Gebrehiwot, M.; Gebrekidan, K. G.; Gebremeskel, T. G.; Getacher, L.; Ghadirian, F.; Ghamari, S. H.; Nour, M. G.; Ghassemi, F.; Golechha, M.; Goleij, P.; Golinelli, D.; Gopalani, S. V.; Guadie, H. A.; Guan, S. Y.; Gudayu, T. W.; Guimaraes, R. A.; Guled, R. A.; Gupta, R.; Gupta, K.; Gupta, V. B.; Gupta, V. K.; Gyawali, B.; Haddadi, R.; Hadi, N. R.; Haile, T. G.; Hajibeygi, R.; Haj-Mirzaian, A.; Halwani, R.; Hamidi, S.; Hankey,

G. J.; Hannan, M. A.; Haque, S.; Harandi, H.; Harlianto, N. I.; Mahmudul Hasan, S. M.; Hasan, S. S.; Hasani, H.; Hassanipour, S.; Hassen, M. B.; Haubold, J.; Hayat, K.; Heidari, G.; Heidari, M.; Hessami, K.; Hiraike, Y.; Holla, R.; Hossain, S.; Hossain, M. S.; Hosseini, M. S.; Hosseinzadeh, M.; Hosseinzadeh, H.; Huang, J.; Huda, M. N.; Hussain, S.; Huynh, H. H.; Hwang, B. F.; Ibitoye, S. E.; Ikeda, N.; Ilic, I. M.; Ilic, M. D.; Inbaraj, L. R.; Iqbal, A.; Islam, S. M. S.; Islam, R. M.; Ismail, N. E.; Iso, H.; Isola, G.; Itumalla, R.; Iwagami, M.; Iwu, C. C. D.; Iyamu, I. O.; Iyasu, A. N.; Jacob, L.; Jafarzadeh, A.; Jahrami, H.; Jain, R.; Jaja, C.; Jamalpoor, Z.; Jamshidi, E.; Janakiraman, B.; Jayanna, K.; Jayapal, S. K.; Jayaram, S.; Jayawardena, R.; Jebai, R.; Jeong, W.; Jin, Y.; Jokar, M.; Jonas, J. B.; Joseph, N.; Joseph, A.; Joshua, C. E.; Joukar, F.; Jozwiak, J. J.; Kaambwa, B.; Kabir, A.; Kabthymer, R. H.; Kadashetti, V.; Kahe, F.; Kalhor, R.; Kandel, H.; Karanth, S. D.; Karaye, I. M.; Karkhah, S.; Katoto, P. D. M. C.; Kaur, N.; Kazemian, S.; Kebede, S. A.; Khader, Y. S.; Khajuria, H.; Khalaji, A.; Khan, M. A. B.; Khan, M.; Khan, A.; Khanal, S.; Khatatbeh, M. M.; Khater, A. M.; Khateri, S.; Khorashadizadeh, F.; Khubchandani, J.; Kibret, B. G.; Kim, M. S.; Kimokoti, R. W.; Kisa, A.; Kivimaki, M.; Kolahi, A. A.; Komaki, S.; Kompani, F.; Koohestani, H. R.; Korzh, O.; Kostev, K.; Kothari, N.; Koyanagi, A.; Krishan, K.; Krishnamoorthy, Y.; Defo, B. K.; Kuddus, M.; Kuddus, M. A.; Kumar, R.; Kumar, H.; Kundu, S.; Kurniasari, M. D.; Kuttikkattu, A.; Vecchia, C. La; Lallukka, T.; Larijani, B.; Larsson, A. O.; Latief, K.; Lawal, B. K.; Le, T. T. T.; Le, T. T. B.; Lee, S. W. H.; Lee, M.; Lee, W. C.; Lee, P. H.; Lee, S. W.; Lee, S. W.; Legesse, S. M.; Lenzi, J.; Li, Y.; Li, M. C.; Lim, S. S.; Lim, L. L.; Liu, X.; Liu, C.; Lo, C. H.; Lopes, G.; Lorkowski, S.; Lozano, R.; Lucchetti, G.; Maghazachi, A. A.; Mahasha, P. W.; Mahjoub, S.; Mahmoud, M. A.; Mahmoudi, R.; Mahmoudimanesh, M.; Mai, A. T.; Majeed, A.; Sanaye, P. M.; Makris, K. C.; Malhotra, K.; Malik, A. A.; Malik, I.; Mallhi, T. H.; Malta, D. C.; Mamun, A. A.; Mansouri, B.; Marateb, H. R.; Mardi, P.; Martini, S.; Martorell, M.; Marzo, R. R.; Masoudi, R.; Masoudi, S.; Mathews, E.; Maugeri, A.; Mazzaglia, G.; Mekonnen, T.; Meshkat, M.; Mestrovic, T.; Jonasson, J. M.; Miazgowski, T.; Michalek, I. M.; Minh, L. H. N.; Mini, G. K.; Miranda, J. J.; Mirfakhraie, R.; Mirrakhimov, E. M.; Mirza-Aghazadeh-Attari, M.; Misganaw, A.; Misgina, K. H.; Mishra, M.; Moazen, B.; Mohamed, N. S.; Mohammadi, E.; Mohammadi, M.; Mohammadian-Hafshejani, A.; Mohammadshahi, M.; Mohseni, A.; Mojiri-Forushani, H.; Mokdad, A. H.; Momtazmanesh, S.; Monasta, L.; Moniruzzaman, M.; Mons, U.; Montazeri, F.; Ghalibaf, A. A. M.; Moradi, Y.; Moradi, M.; Sarabi, M. M.; Morovatdar, N.; Morrison, S. D.; Morze, J.; Mossialos, E.; Mostafavi, E.; Mueller, U. O.; Mulita, F.; Mulita, A.; Murillo-Zamora, E.; Musa, K. I.; Mwita, J. C.; Nagaraju, S. P.; Naghavi, M.; Nainu, F.; Nair, T. S.; Najmuldeen, H. H. R.; Nangia, V.; Nargus, S.; Naser, A. Y.; Nassereldine, H.; Natto, Z. S.; Nauman, J.; Nayak, B. P.; Ndejjo, R.; Negash, H.; Negoi, R. I.; Nguyen, H. T. H.; Nguyen, D. H.; Nguyen, P. T.; Nguyen, V. T.; Nguyen, H. Q.; Niazi, R. K.; Nigatu, Y. T.; Ningrum, D. N. A.; Nizam, M. A.; Nnyanzi, L. A.; Noreen, M.; Noubiap, J. J.; Nzoputam, O. J.; Nzoputam, C. I.; Oancea, B.; Odogwu, N. M.; Odukoya, O. O.; Ojha, V. A.; Okati-Aliabad, H.; Okekunle, A. P.; Okonji, O. C.; Okwute, P. G.; Olufadewa, I. I.; Onwujekwe, O. E.; Ordak, M.; Ortiz, A.; Osuagwu, U. L.; Oulhaj, A.; Owolabi, M. O.; Padron-Monedero, A.; Padubidri, J. R.; Palladino, R.; Panagiotakos, D.; Panda-Jonas, S.; Pandey, A.; Pandey, A.; Pandi-Perumal, S. R.; Stoian, A. M. P.; Pardhan,

S.; Parekh, T.; Parekh, U.; Pasovic, M.; Patel, J.; Patel, J. R.; Paudel, U.; Pepito, V. C. F.; Pereira, M.; Perico, N.; Perna, S.; Petcu, I. R.; Petermann-Rocha, F. E.; Podder, V.; Postma, M. J.; Pourali, G.; Pourtaheri, N.; Prates, E. J. S.; Qadir, M. M. F.; Qattea, I.; Raee, P.; Rafique, I.; Rahimi, M.; Rahimifard, M.; Rahimi-Movaghar, V.; Rahman, M. O.; Rahman, M. A.; Rahman, M. H. U.; Rahman, M.; Rahman, M. M.; Rahmani, M.; Rahmani, S.; Rahmanian, V.; Rahmawaty, S.; Rahnavard, N.; Rajbhandari, B.; Ram, P.; Ramazanu, S.; Rana, J.; Rancic, N.; Ranjha, M. M. A. N.; Rao, C. R.; Rapaka, D.; Rasali, D. P.; Rashedi, S.; Rashedi, V.; Rashid, A. M.; Rashidi, M. M.; Ratan, Z. A.; Rawaf, S.; Rawal, L.; Redwan, E. M. M.; Remuzzi, G.; Rengasamy, K. R. R.; Renzaho, A. M. N.; Reyes, L. F.; Rezaei, N.; Rezaei, N.; Rezaeian, M.; Rezazadeh, H.; Riahi, S. M.; Rias, Y. A.; Riaz, M.; Ribeiro, D.; Rodrigues, M.; Rodriguez, J. A. B.; Roever, L.; Rohloff, P.; Roshandel, G.; Roustazadeh, A.; Rwegerera, G. M.; Saad, A. M. A.; Saber-Ayad, M. M.; Sabour, S.; Sabzmakan, L.; Saddik, B.; Sadeghi, E.; Saeed, U.; Moghaddam, S. S.; Safi, S.; Safi, S. Z.; Saghazadeh, A.; Sharif-Askari, N. S.; Sharif-Askari, F. S.; Sahebkar, A.; Sahoo, S. S.; Sahoo, H.; Saif-Ur-Rahman, K. M.; Sajid, M. R.; Salahi, S.; Salahi, S.; Saleh, M. A.; Salehi, M. A.; Salomon, J. A.; Sanabria, J.; Sanjeev, R. K.; Sanmarchi, F.; Santric-Milicevic, M. M.; Sarasmita, M. A.; Sargazi, S.; Sathian, B.; Sathish, T.; Sawhney, M.; Schlaich, M. P.; Schmidt, M. I.; Schuermans, A.; Seidu, A. A.; Kumar, N. S.; Sepanlou, S. G.; Sethi, Y.; Seylani, A.; Shabany, M.; Shafaghat, T.; Shafeghat, M.; Shafie, M.; Shah, N. S.; Shahid, S.; Shaikh, M. A.; Shanawaz, M.; Shannawaz, M.; Sharfaei, S.; Shashamo, B. B.; Shiri, R.; Shittu, A.; Shivakumar, K. M.; Shivalli, S.; Shobeiri, P.; Shokri, F.; Shuval, K.; Sibhat, M. M.; Silva, L. M. L. R.; Simpson, C. R.; Singh, J. A.; Singh, P.; Singh, S.; Siraj, M. S.; Skryabina, A. A.; Sohag, A. A. M.; Soleimani, H.; Solikhah, S.; Soltani-Zangbar, M. S.; Somayaji, R.; Sorensen, R. J. D.; Starodubova, A. V.; Sujata, S.; Suleman, M.; Sun, J.; Sundström, J.; Tabarés-Seisdedos, R.; Tabatabaei, S. M.; Tabatabaeizadeh, S. A.; Tabish, M.; Taheri, M.; Taheri, E.; Taki, E.; Tamuzi, J. J. L. L.; Tan, K. K.; Tat, N. Y.; Taye, B. T.; Temesgen, W. A.; Temsah, M. H.; Tesler, R.; Thangaraju, P.; Thankappan, K. R.; Thapa, R.; Tharwat, S.; Thomas, N.; Ticoalu, J. H. V.; Tiyuri, A.; Tonelli, M.; Tovani-Palone, M. R.; Trico, D.; Trihandini, I.; Tripathy, J. P.; Tromans, S. J.; Tsegay, G. M.; Tualeka, A. R.; Tufa, D. G.; Tyrovolas, S.; Ullah, S.; Upadhyay, E.; Vahabi, S. M.; Vaithinathan, A. G.; Valizadeh, R.; van Daalen, K. R.; Vart, P.; Varthya, S. B.; Vasankari, T. J.; Vaziri, S.; Verma, M. V.; Verras, G. I.; Vo, D. C.; Wagaye, B.; Waheed, Y.; Wang, Z.; Wang, Y.; Wang, C.; Wang, F.; Wassie, G. T.; Wei, M. Y. W.; Weldemariam, A. H.; Westerman, R.; Wickramasinghe, N. D.; Wu, Y. F.; Wulandari, R. D. W. I.; Xia, J.; Xiao, H.; Xu, S.; Xu, X.; Yada, D. Y.; Yang, L.; Yatsuya, H.; Yesiltepe, M.; Yi, S.; Yohannis, H. K.; Yonemoto, N.; You, Y.; Zaman, S. Bin; Zamora, N.; Zare, I.; Zarea, K.; Zarrintan, A.; Zastrozhin, M. S.; Zeru, N. G.; Zhang, Z. J.; Zhong, C.; Zhou, J.; Zielińska, M.; Zikarg, Y. T.; Zodpey, S.; Zoladl, M.; Zou, Z.; Zumla, A.; Zuniga, Y. M. H.; Magliano, D. J.; Murray, C. J. L.; Hay, S. I.; Vos, T. Global, Regional, and National Burden of Diabetes from 1990 to 2021, with Projections of Prevalence to 2050: A Systematic Analysis for the Global Burden of Disease Study 2021. *The Lancet* **2023**, *402* (10397), 203–234. https://doi.org/10.1016/s0140-6736(23)01301-6.

(22) Elsayed, N. A.; Aleppo, G.; Aroda, V. R.; Bannuru, R. R.; Brown, F. M.; Bruemmer, D.; Collins, B. S.; Hilliard, M. E.; Isaacs, D.; Johnson, E. L.; Kahan, S.; Khunti, K.; Kosiborod,

M.; Leon, J.; Lyons, S. K.; Murdock, L.; Perry, M. Lou; Prahalad, P.; Pratley, R. E.; Seley, J. J.; Stanton, R. C.; Gabbay, R. A. 2. Classification and Diagnosis of Diabetes: Standards of Care in Diabetes—2023. *Diabetes Care* **2023**, *46*, S19–S40. https://doi.org/10.2337/dc23-s002.

(23) Mietlicki-Baase, E. G. Amylin-Mediated Control of Glycemia, Energy Balance, and Cognition. *Physiology and Behavior* **2016**, *162,* 130–140. https://doi.org/10.1016/j.physbeh.2016.02.034.

(24) Nedumpully-Govindan, P.; Ding, F. Inhibition of IAPP Aggregation by Insulin Depends on the Insulin Oligomeric State Regulated by Zinc Ion Concentration. *Scientific Reports* **2015**, *5* (8240), 1–7. https://doi.org/https://doi.org/10.1038/srep08240.

(25) Palato, L. M.; Pilcher, S.; Oakes, A.; Lamba, A.; Torres, J.; Ledesma Monjaraz, L. I.; Munoz, C.; Njoo, E.; Rinauro, D. J.; Menefee, K. A.; Tun, A.; Jauregui, B. L.; Shapiro, S.; Nossiff, O. H.; Olivares, E.; Chang, K.; Nguyen, V.; Nogaj, L. A.; Moffet, D. A. Amyloidogenicity of Naturally Occurring Full-Length Animal IAPP Variants. *Journal of Peptide Science* **2019**, *25* (8), e3199. https://doi.org/10.1002/psc.3199.

(26) Chaari, A.; Ladjimi, M. Human Islet Amyloid Polypeptide (HIAPP) Aggregation in Type 2 Diabetes: Correlation Between Intrinsic Physicochemical Properties of HIAPP Aggregates and Their Cytotoxicity. *International Journal of Biological Macromolecules* **2019**, *136*, 57–65. https://doi.org/10.1016/j.ijbiomac.2019.06.050.

(27) Matveyenko, A. V; Gurlo, T.; Daval, M.; Butler, A. E.; Butler, P. C. Successful Versus Failed Adaptation to High-Fat Diet-Induced Insulin Resistance the Role of IAPP-Induced-Cell Endoplasmic Reticulum Stress. *Diabetes,* **2009** *58*, 906-916. https://doi.org/10.2337/db08-1464.

(28) Alves, N. A.; Dias, L. G.; Frigori, R. B. Synergistic Long-Range Effects of Mutations Underlie Aggregation Propensities of Amylin Analogues. *Journal of Molecular Modeling* **2019**, *25* (9), 1–11. https://doi.org/10.1007/s00894-019-4137-x.

(29) Kumar, S.; Walter, J. Phosphorylation of Amyloid Beta (Aß) Peptides - A Trigger for Formation of Toxic Aggregates in Alzheimer's Disease. *Aging* **2011**, *3* (8), 1–10. https://doi.org/10.18632/aging.100362.

(30) Serrano, A. L.; Lomont, J. P.; Tu, L.-H.; Raleigh, D. P.; Zanni, M. T. A Free Energy Barrier Caused by the Refolding of an Oligomeric Intermediate Controls the Lag Time of Amyloid Formation by hIAPP. *Journal of the American Chemical Society* **2017**, *139*, 16748–16758. https://doi.org/10.1021/jacs.7b08830.

(31) Sarkar, D.; Maity, N. C.; Shome, G.; Varnava, K. G.; Sarojini, V.; Vivekanandan, S.; Sahoo, N.; Kumar, S.; Mandal, A. K.; Biswas, R.; Bhunia, A. Mechanistic Insight into Functionally Different Human Islet Polypeptide (hIAPP) Amyloid: The Intrinsic Role of the C-Terminal Structural Motifs. *Physical Chemistry Chemical Physics* **2022**, *24* (36), 22250–22262. https://doi.org/10.1039/D2CP01650H.

(32) Brender, J. R.; Salamekh, S.; Ramamoorthy, A. Membrane Disruption and Early Events in the Aggregation of the Diabetes Related Peptide IAPP from a Molecular Perspective. *Accounts of Chemical Research* **2012**, *45* (3), 454–462. https://doi.org/10.1021/ar200189b.

(33) Porat, Y.; Abramowitz, A.; Gazit, E. Inhibition of Amyloid Fibril Formation by Polyphenols: Structural Similarity and Aromatic Interactions as a Common Inhibition Mechanism. *Chemical Biology & Drug Design* **2006**, *67*, 27–37. https://doi.org/10.1111/j.1747-0285.2005.00318.x.

(34) Tu, L. H.; Raleigh, D. P. The Role of Aromatic Interactions in Amyloid Formation by Islet Amyloid Polypeptide. *Biochemistry* **2013**, *52* (2), 333. https://doi.org/10.1021/bi3014278.

(35) Kapurniotu, A.; Bernhagen, J.; Greenfield, N.; Al-Abed, Y.; Teichberg, S.; Frank, R. W.; Voelter, W.; Bucala, R. Contribution of Advanced Glycosylation to the Amyloidogenicity of Iselt Amyloid Polypeptide. *European Journal of Biochemistry* **1998**, *251*, 208–216. https://doi.org/10.1046/j.1432-1327.1998.2510208.x.

(36) Abedini, A.; Derk, J.; Schmidt, A. M. The Receptor for Advanced Glycation Endproducts Is a Mediator of Toxicity by IAPP and Other Proteotoxic Aggregates: Establishing and Exploiting Common Ground for Novel Amyloidosis Therapies. *Protein Science* **2018**, *27* (7), 1166–1180. https://doi.org/10.1002/pro.3425.

(37) Dunkelberger, E. B.; Buchanan, L. E.; Marek, P.; Cao, P.; Raleigh, D. P.; Zanni, M. T. Deamidation Accelerates Amyloid Formatin and Alters Amylin Fiber Structure. *Journal of the American Chemical Society* **2012**, *134*, 12658–12667. https://doi.org/10.1021/ja3039486.

(38) Nguyen, P. T.; Zottig, X.; Sebastiao, M.; Bourgault, S. Role of Site-Specific Asparagine Deamidation in Islet Amyloid Polypeptide Amyloidogenesis: Key Contributions of Residues 14 and 21. *Biochemistry* **2017**, *56* (29), 3808–3817. https://doi.org/10.1021/acs.biochem.7b00209.

(39) Hoffmann, A. R. F.; Saravanan, M. S.; Lequin, O.; Killian, J. A.; Khemtemourian, L. A Single Mutation on the Human Amyloid Polypeptide Modulates Fibril Growth and Affects the Mechanism of Amyloid-Induced Membrane Damage. *BBA - Biomembranes* **2018**, *1860*, 1783–1792. https://doi.org/10.1016/j.bbamem.2018.02.018.

(40) Peretz, Y.; Malishev, R.; Kolusheva, S.; Jelinek, R. Nanoparticles Modulate Membrane Interactions of Human Islet Amyloid Polypeptide (hIAPP). *BBA - Biomembranes* **2018**, *1860*, 1810–1817. https://doi.org/10.1016/j.bbamem.2018.03.029.

(41) Arosio, P.; Vendruscolo, M.; Dobson, C. M.; Knowles, T. P. J. Chemical Kinetics for Drug Discovery to Combat Protein Aggregation Diseases. *Cell Press* **2014**, *35* (3), 127–135. https://doi.org/10.1016/j.tips.2013.12.005.

(42) Engel, M. F. M.; Khemtémourian, L.; Kleijer, C. C.; Meeldijk, H. J. D.; Jacobs, J.; Verkleij, A. J.; Kruijff, B. de; Killian, J. A.; Höppener, J. W. M. Membrane Damage by Human Islet

Amyloid Polypeptide Through Fibril Growth at the Membrane. *PNAS* **2008**, *105* (16), 6033–6038. https://doi.org/10.1073/pnas.0708354105.

(43) Dong, X.; Qiao, Q.; Qian, Z.; Wei, G. Recent Computational Studies of Membrane Interaction and Disruption of Human Islet Amyloid Polypeptide: Monomers, Oligomers and Protofibrils. *Biochimica et Biophysica Acta – Biomembranes* **2018**, *1860*, 1826–1839. https://doi.org/10.1016/j.bbamem.2018.03.006.

(44) Thormann, E. On Understanding of the Hofmeister Effect: How Addition of Salt Alters the Stability of Temperature Responsive Polymers in Aqueous Solutions. *RSC Advances* **2012**, *2*, 8297–8305. https://doi.org/10.1039/c2ra20164j.

(45) Zhang, Y.; Cremer, P. S. Interactions Between Macromolecules and Ions: The Hofmeister Series. *Current Opinions in Chemical Biology* **2006**, *10*, 658–663. https://doi.org/10.1016/j.cbpa.2006.09.020.

(46) Ilitchev, A. I.; Giammona, M. J.; Schwarze, J. N.; Buratto, S. K.; Bowers, M. T. Zinc-Induced Conformational Transitions in Human Islet Amyloid Polypeptide and Their Role in the Inhibition of Amyloidosis. *Journal of Physical Chemistry* **2018**, *122*, 9852–9859. https://doi.org/10.1021/acs.jpcb.8b06206.

(47) Salamekh, S.; Brender, J. R.; Hyung, S. J.; Nanga, R. P. R.; Vivekanandan, S.; Ruotolo, B. T.; Ramamoorthy, A. A Two-Site Mechanism for the Inhibition of IAPP Amyloidogenesis by Zinc. *Journal of Molecular Biology* **2011**, *410* (2), 294–306. https://doi.org/10.1016/j.jmb.2011.05.015.

(48) Lee, S. J. C.; Choi, T. S.; Lee, J. W.; Lee, H. J.; Mun, D.-G.; Akashi, S.; Lee, S.-W.; Lim, M. H.; Kim, H. I. Structure and Assembly Mechanisms of Toxic Human Islet Amyloid Polypeptide Oligomers Associated with Copper. *Chemical Science* **2016**, *7*, 5398–5406. https://doi.org/10.1039/c6sc00153j.

(49) Algrably, M.; Czaban, I.; Jaremko, Ł.; Jaremko, M. Interaction of Amylin Species with Transition Metals and Membranes. *Journal of Inorganic Biochemistry* **2019**, *191*, 69–76. https://doi.org/10.1016/j.jinorgbio.2018.11.004.

(50) Zhu, D.; Gong, G.; Wang, W.; Du, W. Disaggregation of Human Islet Amyloid Polypeptide Fibril Formation by Ruthenium Polypyridyl Complexes. *Journal of Inorganic Biochemistry* **2017**, *170*, 109–116. https://doi.org/10.1016/j.jinorgbio.2017.02.008.

(51) Su, X.; Wang, K.; Liu, N.; Chen, J.; Li, Y.; Duan, M. All-Atom Structure Ensembles of Islet Amyloid Polypeptides Determined by Enhanced Sampling and Experiment Data Restraints. *Proteins* **2019**, *87*, 541–550. https://doi.org/10.1002/prot.25677.

(52) Ratha, B. N.; Kar, R. K.; Kalita, S.; Kalita, S.; Raha, S.; Singha, A.; Garai, K.; Mandal, B.; Bhunia, A. Sequence Specificity of Amylin-Insulin Interaction: A Fragment-Based Insulin Fibrillation Inhibition Study. *BBA - Proteins and Proteomics* **2019**, *1867*, 405–415. https://doi.org/10.1016/j.bbapap.2019.01.007.

(53) Porat, Y.; Stepensky, A.; Ding, F.-X.; Naider, F.; Gazit, E. Completely Different Amyloidogenic Potential of Nearly Identical Peptide Fragments. *Biopolymers* **2003**, *69*, 161–164. https://doi.org/10.1002/bip.10386.

(54) Westermark, P.; Engström, U.; Johnson, K. H.; Westermark, G. T.; Betsholtz, C. Islet Amyloid Polypeptide: Pinpointing Amino Acid Residues Linked to Amyloid Fibril Formation. *PNAS* **1990**, *87*, 5036–5040. https://doi.org/10.1073/pnas.87.13.5036.

(55) Marshall, K. E.; Morris, K. L.; Charlton, D.; O'Reilly, N.; Lewis, L.; Walden, H.; Serpell, L. C. Hydrophobic, Aromatic, and Electrostatic Interactions Play a Central Role in Amyloid Fibril Formation and Stability. *Biochemistry* **2011**, *50*, 2061–2071. https://doi.org/10.1021/bi101936c.

(56) Profit, A. A.; Felsen, V.; Chinwong, J.; Mojica, E.-R. E.; Desamero, R. Z. B. Evidence of π-Stacking Interactions in the Self-Assembly of hIAPP22-29. *Proteins* **2013**, *81*, 690–703. https://doi.org/10.1002/prot.24229.

(57) Malmos, K. G.; Blancas-Mejia, L. M.; Weber, B.; Buchner, J.; Ramirez-Alvarado, M.; Naiki, H.; Otzen, D. ThT 101: A Primer on the Use of Thioflavin T to Investigate Amyloid Formation. *Amyloid* **2017**, *24* (1), 1–16. https://doi.org/10.1080/13506129.2017.1304905.

(58) Dubey, R.; Kulkarni, S. H.; Dantu, S. C.; Panigrahi, R.; Sardesai, D. M.; Malik, N.; Acharya, J. D.; Chugh, J.; Sharma, S.; Kumar, A. Myricetin Protects Pancreatic β-Cells from Human Islet Amyloid Polypeptide (hIAPP) Induced Cytotoxicity and Restores Islet Function. *Biological Chemistry* **2021**, *402* (2), 179–194. https://doi.org/10.1515/hsz-2020-0176.

(59) Höppener, J. W.; Jacobs, H. M.; Wierup, N.; Sotthewes, G.; Sprong, M.; de Vos, P.; Berger, R.; Sundler, F.; Ahrén, B. Human Islet Amyloid Polypeptide Transgenic Mice: In Vivo and Ex Vivo Models for the Role of hIAPP in Type 2 Diabetes Mellitus. *Journal of Diabetes Research* **2008**, *2008*, 697035. https://doi.org/10.1155/2008/697035.

(60) Huggins, K. N. L.; Bisaglia, M.; Bubacco, L.; Tatarek-Nossol, M.; Kapurniotu, A.; Andersen, N. H. Designed Hairpin Peptides Interfere with Amyloidogenesis Pathways: Fibril Formation and Cytotoxicity Inhibition, Interception of the Preamyloid State. *Biochemistry* **2011**, *50* (38), 8202–8212. https://doi.org/10.1021/bi200760h.

(61) Shi, Y.; Lv, W.; Jiao, A.; Zhang, C.; Zhang, J. A Novel Pentapeptide Inhibitor Reduces Amyloid Deposit Formation by Direct Interaction with hIAPP. *International Journal of Endocrinology* **2019**, *2019*. https://doi.org/10.1155/2019/9062032.

(62) Xuan, Q.; He, J.; Chai, R.; Wang, C.; Wang, Y.; Wang, P. Monomer-Targeting Affinity Peptide Inhibitors of Amyloid with No Self-Fibrillatin and Low Cytotoxicity. *Chemical Communications* **2020**, *56*, 1633–1636. https://doi.org/10.1039/c9cc08671d.

(63) Manathunga, L.; Zhyvoloup, A.; Baghai, A.; Raleigh, D. P. Differential Effects of Aromatic Residues on Amyloid Formation and Cytotoxicity of Human IAPP. *Biochemistry* **2022**, *61* (21), 2334–2343. https://doi.org/10.1021/acs.biochem.2c00267.

(64) He, M.; Hao, J.; Feng, C.; Yang, Y.; Shao, Z.; Wang, L.; Mao, W. Anti-Diabetic Activity of a Sulfated Galactoarabinan with Unique Structural Characteristics from *Cladophora oligoclada* (Chlorophyta). *Carbohydrate Polymers* **2022**, *278*, 118933. https://doi.org/10.1016/j.carbpol.2021.118933.

(65) Meng, F.; Abedini, A.; Plesner, A.; Verchere, C. B.; Raleigh, D. P. The Flavanol (-)-Epigallocatechin 3-Gallate Inhibits Amyloid Formation by Islet Amyloid Polypeptide, DIsaggregates Amyloid Fibrils and Protects Cultured Cells Against IAPP Induced Toxicity. *Biochemistry* **2010**, *49* (37), 8127–8133. https://doi.org/10.1021/bi100939a.

(66) Franko, A.; Rodriguez Camargo, D. C.; Böddrich, A.; Garg, D.; Rodriguez Camargo, A.; Rathkolb, B.; Janik, D.; Aichler, M.; Feuchtinger, A.; Neff, F.; Fuchs, H.; Wanker, E. E.; Reif, B.; Häring, H.-U.; Peter, A.; Hrabě de Angelis, M. Epigallocatechin Gallate (EGCG) Reduces the Intensity of Pancreatic Amyloid Fibrils in Human Islet Amyloid Polypeptide (hIAPP) Transgenic Mice. *Scientific Reports* **2018**, *8* (1116), 1–12. https://doi.org/10.1038/s41598-017-18807-8.

(67) Wang, Y.; Lv, Y.; Jin, L.; Liang, G. Revealing the Mechanism of EGCG, Genistein, Rutin, Quercetin, and Silibinin Against hIAPP Aggregation via Computational Simulations. *Interdisciplinary Sciences* **2020**, *12* (1), 59–68. https://doi.org/10.1007/s12539-019-00352-9.

(68) Ren, B.; Liu, Y.; Zhang, Y.; Cai, Y.; Gong, X.; Chang, Y.; Xu, L.; Zheng, J. Genistein: A Dual Inhibitor of Both Amyloid ß and Human Islet Amylin Peptides. *ACS Chemical Neuroscience* **2018**, *9*, 1215–1224. https://doi.org/10.1021/acschemneuro.8b00039.

(69) Sun, J.; Murata, T.; Shigemori, · Hideyuki. Inhibitory Activities of Phenylpropanoids from Lycopus Lucidus on Amyloid Aggregation Related to Alzheimer's Disease and Type 2 Diabetes. *Journal of Natural Medicine* **2020**, *74*, 579–583. https://doi.org/10.1007/s11418-020-01398-6.

(70) Sun, J.; Jiang, G.; Shigemori, H. Inhibitory Activity on Amyloid Aggregation of Rosmarinic Acid and Its Substructures From Isodon Japonicus. *Natural Product Communications* **2019**, *14* (5), 1–5. https://doi.org/10.1177/1934578X19843039.

(71) Jiang, G.; Takase, M.; Aihara, Y.; Shigemori, H. Inhibitory Activities of Kukoamines A and B from Lycii Cortex on Amyloid Aggregation Related to Alzheimer's Disease and Type 2 Diabetes. *Journal of Natural Medicine* **2020**, *74* (1), 247–251. https://doi.org/10.1007/s11418-019-01337-0.

(72) Hmidene, A. Ben; Hanaki, M.; Murakami, K.; Irie, K.; Isoda, H.; Shigemori, H. Inhibitory Activities of Antioxidant Flavonoids from Tamarix Gallica on Amyloid Aggregation Related to Alzheimer's and Type 2 Diabetes Diseases. *Biological and Pharmaceutical Bulletin* **2017**, *40* (2), 238–241. https://doi.org/10.1248/bpb.b16-00801.

(73) Ren, B.; Liu, Y.; Zhang, Y.; Zhang, M.; Sun, Y.; Liang, G.; Xu, J.; Zheng, J. Tanshinones Inhibit hIAPP Aggregation, Disaggregate Preformed HIAPP Fibrils, and Protect Cultured

Cells. *Journal of Materials Chemistry B* **2017**, *6* (1), 56–67. https://doi.org/10.1039/c7tb02538f.

(74) García-Viñuales, S.; Ilie, I. M.; Santoro, A. M.; Romanucci, V.; Zarrelli, A.; Di Fabio, G.; Caflisch, A.; Milardi, D. Silybins Inhibit Human IAPP Amyloid Growth and Toxicity through Stereospecific Interactions. *Biochimica et Biophysica Acta (BBA) - Proteins and Proteomics* **2022**, *1870* (5), 140772. https://doi.org/10.1016/j.bbapap.2022.140772.

(75) Xu, J.; Wang, Y.; Zheng, T.; Huo, Y.; Du, W. Biflavones Inhibit the Fibrillation and Cytotoxicity of the Human Islet Amyloid Polypeptide. *Journal of Materials Chemistry B* **2022**, *10* (24), 4650–4661. https://doi.org/10.1039/d2tb00230b.

(76) Zheng, T.; Wang, Y.; Zhao, C.; Xu, J.; Huang, X.; Du, W. Triterpenoids Impede the Fibrillation and Cytotoxicity of Human Islet Amyloid Polypeptide. *International Journal of Biological Macromolecules* **2022**, *199*, 189–200. https://doi.org/10.1016/j.ijbiomac.2021.12.127.

(77) Wang, Y.; Hu, T.; Wei, J.; Yin, X.; Gao, Z.; Li, H. Inhibitory Activities of Flavonoids from Scutellaria Baicalensis Georgi on Amyloid Aggregation Related to Type 2 Diabetes and the Possible Structural Requirements for Polyphenol in Inhibiting the Nucleation Phase of hIAPP Aggregation. *International Journal of Biological Macromolecules* **2022**, *215*, 531–540. https://doi.org/10.1016/j.ijbiomac.2022.06.107.

(78) Sampei, T.; Wu, Y.; Shigemori, H. Amyloid Polypeptide Disaggregation Activity of Passion Fruit Seed-Derived Polyphenol Compounds. *Natural Product Communications* **2022**, *17* (9). https://doi.org/10.1177/1934578x221092710.

(79) Velander, P.; Wu, L.; Hildreth, S. B.; Vogelaar, N. J.; Mukhopadhyay, B.; Helm, R. F.; Zhang, S.; Xu, B. Catechol-Containing Compounds Are a Broad Class of Protein Aggregation Inhibitors: Redox State Is a Key Determinant of the Inhibitory Activities. *Pharmacological Research* **2022**, *184*, 106409. https://doi.org/10.1016/j.phrs.2022.106409.

(80) Nomoto, D.; Tsunoda, T.; Shigemori, H. Effects of Clovamide and Its Related Compounds on the Aggregations of Amyloid Polypeptides. *Journal of Natural Medicine* **2021**, *75* (2), 299–307. https://doi.org/10.1007/s11418-020-01467-w.

(81) Tanaka, T.; Betkekar, V. V.; Ohmori, K.; Suzuki, K.; Shigemori, H. Evaluation of Amyloid Polypeptide Aggregation Inhibition and Disaggregation Activity of A-Type Procyanidins. *Pharmaceuticals* **2021**, *14* (11), 1118. https://doi.org/10.3390/ph14111118.

(82) Floris, S.; Fais, A.; Medda, R.; Pintus, F.; Piras, A.; Kumar, A.; Kuś, P. M.; Westermark, G. T.; Era, B. Washingtonia Filifera Seed Extracts Inhibit the Islet Amyloid Polypeptide Fibrils Formations and α-Amylase and α-Glucosidase Activity. *Journal of Enzyme Inhibition Medicinal Chemistry* **2021**, *36* (1), 517–524. https://doi.org/10.1080/14756366.2021.1874945.

(83) Li, R.; Liang, T.; Xu, L.; Li, Y.; Zhang, S.; Duan, X. Protective Effect of Cinnamon Polyphenols against STZ-Diabetic Mice Fed High-Sugar, High-Fat Diet and Its Underlying

Mechanism. *Food and Chemical Toxicology* **2013**, *51* (1), 419–425. https://doi.org/10.1016/j.fct.2012.10.024.

(84) Auberval, N.; Dal, S.; Bietiger, W.; Seyfritz, E.; Peluso, J.; Muller, C.; Zhao, M.; Marchioni, E.; Pinget, M.; Jeandidier, N.; Maillard, E.; Schini-Kerth, V.; Sigrist, S. Oxidative Stress Type Influences the Properties of Antioxidants Containing Polyphenols in RINm5F Beta Cells. *Evidence-Based Complementary and Alternative Medicine* **2015** *2015,* 859048. https://doi.org/10.1155/2015/859048.

(85) Dragan, S.; Andrica, F.; Serban, M.-C.; Timar, R. Polyphenols-Rich Natural Products for Treatment of Diabetes. *Current Medicinal Chemistry* **2015**, *22* (1), 14–22.

(86) Zraika, S.; Hull, R. L.; Udayasankar, J.; Aston-Mourney, K.; Subramanian, S. L.; Kisilevsky, R.; Szarek, W. A.; Kahn, S. E. Oxidative Stress Is Induced by Islet Amyloid Formation and Time-Dependently Mediates Amyloid-Induced Beta Cell Apoptosis. *Diabetologia* **2009**, *52* (4), 626–635. https://doi.org/10.1007/s00125-008-1255-x.

(87) Yan, J.; Zhao, J.; Yang, R.; Zhao, W. Bioactive Peptides with Antidiabetic Properties: A Review. *International Journal of Food Science and Technology* **2019**, *54* (6), 1909–1919. https://doi.org/10.1111/ijfs.14090.

(88) Munhoz, A. C. M.; Frode, T. S. Isolated Compounds from Natural Products with Potential Antidiabetic Activity - A Systematic Review. *Current Diabetes Reviews* **2017**, *14* (1), 36–106. https://doi.org/10.2174/1573399813666170505120621.

(89) Ishii, S.; Chino, H.; Ode, K. L.; Kurikawa, Y.; Ueda, H. R.; Matsuura, A.; Mizushima, N.; Itakura, E. CCPG1 Recognizes Endoplasmic Reticulum Luminal Proteins for Selective ER-Phagy. *Molecular Biology of the Cell* **2023**, *34* (4), ar29. https://doi.org/10.1091/mbc.e22-09-0432.

(90) Pallauf, K.; Rimbach, G. Autophagy, Polyphenols and Healthy Ageing. *Ageing Research Reviews* **2013**, *12* (1), 237–252. https://doi.org/10.1016/j.arr.2012.03.008.

(91) Lin, J.; Jiao, A.; Lv, W.; Zhang, C.; Shi, Y.; Yang, Z.; Sun, N.; Li, X.; Zhang, J. Pentapeptide Protects INS-1 Cells From hIAPP-Mediated Apoptosis by Enhancing Autophagy Through MTOR Pathway. *Frontiers in Pharmacology* **2019**, *10* (896). https://doi.org/10.3389/fphar.2019.00896.

(92) Abioye, R. O.; Okagu, O. D.; Udenigwe, C. C. Inhibition of Islet Amyloid Polypeptide Fibrillation by Structurally Diverse Phenolic Compounds and Fibril Disaggregation Potential of Rutin and Quercetin. *Journal of Agricultural Food Chemistry* **2022**, *70* (1), 392–402. https://doi.org/10.1021/acs.jafc.1c06918.

(93) Gazit, E. A Possible Role for Pi-Stacking in the Self-Assembly of Amyloid Fibrils. *FASEB Journal* **2002**, *16* (1), 77–83. https://doi.org/10.1096/fj.01-0442hyp.

(94) Gazit, E. Mechanisms of Amyloid Fibril Self-Assembly and Inhibition. *FEBS Journal* **2005**, *272* (23), 5971–5978. https://doi.org/10.1111/J.1742-4658.2005.05022.x.

(95) Gilead, S.; Gazit, E. The Role of the 14-20 Domain of the Islet Amyloid Polypeptide in Amyloid Formation. *Journal of Diabetes Research* **2008**, *2008*, 256954. https://doi.org/10.1155/2008/256954.

(96) Jiménez-Aliaga, K.; Bermejo-Bescós, P.; Benedí, J.; Martín-Aragón, S. Quercetin and Rutin Exhibit Antiamyloidogenic and Fibril-Disaggregating Effects in Vitro and Potent Antioxidant Activity in APPswe Cells. *Life Sciences* **2011**, *89* (25–26), 939–945. https://doi.org/10.1016/j.lfs.2011.09.023.

(97) Abioye, R. O.; Udenigwe, C. C. Structural Basis and Functional Significance of Food-Derived Inhibitors of Islet Amyloid Polypeptide Fibrillation toward Antidiabetic Effects. *Current Opinions in Food Science* **2024**, *56*, 101146. https://doi.org/10.1016/j.cofs.2024.101146.

(98) Tenidis, K.; Waldner, M.; Bernhagen, J.; Fischle, W.; Bergmann, M.; Weber, M.; Merkle, M. L.; Voelter, W.; Brunner, H.; Kapurniotu, A. Identification of a Penta- and Hexapeptide of Islet Amyloid Polypeptide (IAPP) with Amyloidogenic and Cytotoxic Properties. *Journal of Molecular Biology* **2000**, *295* (4), 1055–1071. https://doi.org/10.1006/jmbi.1999.3422.

(99) Zhang, S.; Liu, J.; Saafi, 'Etuate L.; Cooper, G. J. S. Induction of Apoptosis by Human Amylin in RINm5F Islet Beta-Cells Is Associated with Enhanced Expression of P53 and P21WAF1/CIP1. *FEBS Letter* **1999**, *455* (3), 315–320. https://doi.org/10.1016/s0014-5793(99)00894-7.

(100) Kapurniotu, A. Amyloidogenicity and Cytotoxicity of Islet Amyloid Polypeptide. *Peptide Science* **2001**, *60* (9), 438–459. https://doi.org/10.1002/1097-0282(2001)60:6<438::aid-bip10182>3.0.co;2-a.

(101) Milardi, D.; Gazit, E.; Radford, S. E.; Xu, Y.; Gallardo, R. U.; Caflisch, A.; Westermark, G. T.; Westermark, P.; Rosa, C. La; Ramamoorthy, A. Proteostasis of Islet Amyloid Polypeptide: A Molecular Perspective of Risk Factors and Protective Strategies for Type II Diabetes. *Chemical Reviews* **2021**, *121* (3), 1845. https://doi.org/10.1021/acs.chemrev.0c00981.

(102) Kahn, S. E.; D'Alessio, D. A.; Schwartz, M. W.; Fujimoto, W. Y.; Ensinck, J. W.; Gerald J. Taborsky, Jr.; Daniel J. Porte, Jr. Evidence of Cosecretion of Islet Amyloid Polypeptide and Insulin by Beta-Cells. *Diabetes* **1990**, *39* (5), 634–639. https://doi.org/10.2337/diab.39.5.634.

(103) Zhang, S.; Liu, H.; Chuang, C. L.; Li, X.; Au, M.; Zhang, L.; Phillips, A. R. J.; Scott, D. W.; Cooper, G. J. S. The Pathogenic Mechanism of Diabetes Varies with the Degree of Overexpression and Oligomerization of Human Amylin in the Pancreatic Islet β Cells. *FASEB Journal* **2014**, *28* (12), 5083–5096. https://doi.org/10.1096/fj.14-251744.

(104) Costes, S. Targeting Protein Misfolding to Protect Pancreatic Beta-Cells in Type 2 Diabetes. *Current Opinion in Pharmacology* **2018**, *43*, 104–110. https://doi.org/10.1016/j.coph.2018.08.016.

(105) Janciauskiene, S.; Ahrén, B. Fibrillar Islet Amyloid Polypeptide Differentially Affects Oxidative Mechanisms and Lipoprotein Uptake in Correlation with Cytotoxicity in Two Insulin-Producing Cell Lines. *Biochemical and Biophysical Research Communations* **2000**, *267* (2), 619–625. https://doi.org/10.1006/bbrc.1999.1989.

(106) Babych, M.; Nguyen, P. T.; Côté-Cyr, M.; Kihal, N.; Quittot, N.; Golizeh, M.; Sleno, L.; Bourgault, S. Site-Specific Alkylation of the Islet Amyloid Polypeptide Accelerates Self-Assembly and Potentiates Perturbation of Lipid Membranes. *Biochemistry* **2021**, *60* (29), 2285–2299. https://doi.org/10.1021/acs.biochem.1c00308.

(107) Saghir, A. El; Farrugia, G.; Vassallo, N. The Human Islet Amyloid Polypeptide in Protein Misfolding Disorders: Mechanisms of Aggregation and Interaction with Biomembranes. *Chemistry and Physics of Lipids* **2021**, *234*, 105010. https://doi.org/10.1016/j.chemphyslip.2020.105010.

(108) Scollo, F.; Tempra, C.; Lolicato, F.; Sciacca, M. F. M.; Raudino, A.; Milardi, D.; La Rosa, C. Phospholipids Critical Micellar Concentrations Trigger Different Mechanisms of Intrinsically Disordered Proteins Interaction with Model Membranes. *Journal of Physical Chemistry Letters* **2018**, *9* (17), 5125–5129. https://doi.org/10.1021/acs.jpclett.8b02241.

(109) Sciacca, M. F.; Lolicato, F.; Tempra, C.; Scollo, F.; Sahoo, B. R.; Watson, M. D.; García-Viñuales, S.; Milardi, D.; Raudino, A.; Lee, J. C.; Ramamoorthy, A.; La Rosa, C. Lipid-Chaperone Hypothesis: A Common Molecular Mechanism of Membrane Disruption by Intrinsically Disordered Proteins. *ACS Chemical Neuroscience* **2020**, *11* (24), 4336–4350. https://doi.org/10.1021/acschemneuro.0c00588.

(110) Sequeira, I. R.; Poppitt, S. D. Unfolding Novel Mechanisms of Polyphenol Flavonoids for Better Glycaemic Control: Targeting Pancreatic Islet Amyloid Polypeptide (IAPP). *Nutrients* **2017**, *9* (7), 788. https://doi.org/10.3390/nu9070788.

(111) Araújo, A. R.; Reis, R. L.; Pires, R. A. Natural Polyphenols as Modulators of the Fibrillization of Islet Amyloid Polypeptide. In *Advances in Experimental Medicine and Biology*; Springer, Singapore, 2020; Vol. 1250, pp 159–176. https://doi.org/10.1007/978-981-15-3262-7_11.

(112) Ghorbani, A. Mechanisms of Antidiabetic Effects of Flavonoid Rutin. *Biomedicine & Pharmacotherapy* **2017**, *96*, 305–312. https://doi.org/10.1016/j.biopha.2017.10.001.

(113) Abdel-Moneim, A.; Yousef, A. I.; El-Twab, S. M. A.; Reheim, E. S. A.; Ashour, M. B. Gallic Acid and p -Coumaric Acid Attenuate Type 2 Diabetes-Induced Neurodegeneration in Rats. *Metabolic Brain Disease 2017 32:4* **2017**, *32* (4), 1279–1286. https://doi.org/10.1007/s11011-017-0039-8.

(114) Latha, R. C. R.; Daisy, P. Insulin-Secretagogue, Antihyperlipidemic and Other Protective Effects of Gallic Acid Isolated from Terminalia Bellerica Roxb. in Streptozotocin-Induced Diabetic Rats. *Chemico-Biological Interactions* **2011**, *189* (1–2), 112–118. https://doi.org/10.1016/j.cbi.2010.11.005.

(115) Adisakwattana, S. Cinnamic Acid and Its Derivatives: Mechanisms for Prevention and Management of Diabetes and Its Complications. *Nutrients* **2017**, *9* (2), 163. https://doi.org/10.3390/nu9020163.

(116) Micsonai, A.; Wien, F.; Bulyáki, É.; Kun, J.; Moussong, É.; Lee, Y. H.; Goto, Y.; Réfrégiers, M.; Kardos, J. BeStSel: A Web Server for Accurate Protein Secondary Structure Prediction and Fold Recognition from the Circular Dichroism Spectra. *Nucleic Acids Research* **2018**, *46*, W315. https://doi.org/10.1093/nar/gky497.

(117) Schindelin, J.; Arganda-Carreras, I.; Frise, E.; Kaynig, V.; Longair, M.; Pietzsch, T.; Preibisch, S.; Rueden, C.; Saalfeld, S.; Schmid, B.; Tinevez, J.-Y.; White, D. J.; Hartenstein, V.; Eliceiri, K.; Tomancak, P.; Cardona, A. Fiji: An Open-Source Platform for Biological-Image Analysis. *Nature Methods* **2012**, *9* (7), 676–682. https://doi.org/10.1038/nmeth.2019.

(118) Pettersen, E. F.; Goddard, T. D.; Huang, C. C.; Couch, G. S.; Greenblatt, D. M.; Meng, E. C.; Ferrin, T. E. UCSF Chimera—A Visualization System for Exploratory Research and Analysis. *Journal of Computational Chemistry* **2004**, *25* (13), 1605–1612. https://doi.org/10.1002/jcc.20084.

(119) Trott, O.; Olson, A. J. AutoDock Vina: Improving the Speed and Accuracy of Docking with a New Scoring Function, Efficient Optimization, and Multithreading. *Journal of Computational Chemistry* **2010**, *31* (2), 455–461. https://doi.org/10.1002/jcc.21334.

(120) Keller, A.; Fritzsche, M.; Yu, Y. P.; Liu, Q.; Li, Y. M.; Dong, M.; Besenbacher, F. Influence of Hydrophobicity on the Surface-Catalyzed Assembly of the Islet Amyloid Polypeptide. *ACS Nanotechnology* **2011**, *5* (4), 2770–2778. https://doi.org/10.1021/nn1031998.

(121) Marek, P.; Abedini, A.; Song, B. Ben; Kanungo, M.; Johnson, M. E.; Gupta, R.; Zaman, W.; Wong, S. S.; Raleigh, D. P. Aromatic Interactions Are Not Required for Amyloid Fibril Formation by Islet Amyloid Polypeptide but Do Influence the Rate of Fibril Formation and Fibril Morphology. *Biochemistry* **2007**, *46* (11), 3255–3261. https://doi.org/10.1021/bi0621967.

(122) Park, G.; Xue, C.; Wang, H.; Guo, Z. Distinguishing the Effect on the Rate and Yield of Aβ42 Aggregation by Green Tea Polyphenol EGCG. *ACS Omega* **2020**, *5*, 21497-21505. https://doi.org/10.1021/acsomega.0c02063.

(123) Sun, Q.; Wedick, N. M.; Tworoger, S. S.; Pan, A.; Townsend, M. K.; Cassidy, A.; Franke, A. A.; Rimm, E. B.; Hu, F. B.; van Dam, R. M. Urinary Excretion of Select Dietary Polyphenol Metabolites Is Associated with a Lower Risk of Type 2 Diabetes in Proximate but Not Remote Follow-Up in a Prospective Investigation in 2 Cohorts of US Women. *The Journal of Nutrition* **2015**, *145* (6), 1280–1288. https://doi.org/10.3945/jn.114.208736.

(124) Mirhashemi, S. M.; Aarabi, M.-H. To Evaluate Likely Antiamyloidogenic Property of Ferulic Acid and Baicalein against Human Islet Amyloid Polypeptide Aggregation, in Vitro Study. *African Journal of Pharmacy and Pharmacology* **2012**, *6* (9), 671–676. https://doi.org/10.5897/ajpp12.033.

(125) Zhang, J.; Chen, Y.; Li, D.; Cao, Y.; Wang, Z.; Li, G. Colorimetric Determination of Islet Amyloid Polypeptide Fibrils and Their Inhibitors Using Resveratrol Functionalized Gold Nanoparticles. *Microchimica Acta 2015 183:2* **2015**, *183* (2), 659–665. https://doi.org/10.1007/s00604-015-1687-1.

(126) Cheng, B.; Liu, X.; Gong, H.; Huang, L.; Chen, H.; Zhang, X.; Li, C.; Yang, M.; Ma, B.; Jiao, L.; Zheng, L.; Huang, K. Coffee Components Inhibit Amyloid Formation of Human Islet Amyloid Polypeptide in Vitro: Possible Link between Coffee Consumption and Diabetes Mellitus. *Journal of Agriculture and Food Chemistry* **2011**, *59* (24), 13147–13155. https://doi.org/10.1021/jf201702h.

(127) Bastianetto, S.; Yao, Z.-X.; Papadopoulos, V.; Quirion, R. Neuroprotective Effects of Green and Black Teas and Their Catechin Gallate Esters against β-Amyloid-Induced Toxicity. *European Journal of Neuroscience* **2006**, *23* (1), 55–64. https://doi.org/10.1111/j.1460-9568.2005.04532.x.

(128) Aitken, J. F.; Loomes, K. M.; Riba-Garcia, I.; Unwin, R. D.; Prijic, G.; Phillips, A. S.; Phillips, A. R. J.; Wu, D.; Poppitt, S. D.; Ding, K.; Barran, P. E.; Dowsey, A. W.; Cooper, G. J. S. Rutin Suppresses Human-Amylin/HIAPP Misfolding and Oligomer Formation in-Vitro, and Ameliorates Diabetes and Its Impacts in Human-Amylin/hIAPP Transgenic Mice. *Biochemical and Biophysical Research Communications* **2017**, *482* (4), 625–631. https://doi.org/10.1016/j.bbrc.2016.11.083.

(129) Di Giovanni, S.; Eleuteri, S.; Paleologou, K. E.; Yin, G.; Zweckstetter, M.; Carrupt, P.-A.; Lashuel, H. A. Entacapone and Tolcapone, Two Catechol O-Methyltransferase Inhibitors, Block Fibril Formation of-Synuclein and-Amyloid and Protect against Amyloid-Induced Toxicity. *Journal of Biological Chemistry* **2010**, *285* (20), 14941–14954. https://doi.org/10.1074/jbc.M109.080390.

(130) Cohen, S. I. A.; Cukalevski, R.; Michaels, T. C. T.; Šarić, A.; Törnquist, M.; Vendruscolo, M.; Dobson, C. M.; Buell, A. K.; Knowles, T. P. J.; Linse, S. Distinct Thermodynamic Signatures of Oligomer Generation in the Aggregation of the Amyloid-β Peptide. *Nature Chemistry 2018 10:5* **2018**, *10* (5), 523–531. https://doi.org/10.1038/s41557-018-0023-x.

(131) Okagu, O. D.; Wang, B.; Acquah, C.; Udenigwe, C. C. Protein-Based Nanodelivery Systems for Food Applications. *Encyclopedia of Food Chemistry* **2019**, 719–726. https://doi.org/10.1016/b978-0-08-100596-5.21864-7.

(132) Hua, S. Lipid-Based Nano-Delivery Systems for Skin Delivery of Drugs and Bioactives. *Frontiers in Pharmacology* **2015**, *6*, 219. https://doi.org/10.3389/fphar.2015.00219.

(133) Wang, H.; Wang, C.; Zou, Y.; Hu, J.; Li, Y.; Cheng, Y. Natural Polyphenols in Drug Delivery Systems: Current Status and Future Challenges. *Giant* **2020**, *3*, 100022. https://doi.org/10.1016/J.GIANT.2020.100022.

(134) Udenigwe, C. C.; Abioye, R. O.; Okagu, I. U.; Obeme-Nmom, J. I. Bioaccessibility of Bioactive Peptides: Recent Advances and Perspectives. *Current Opinions in Food Science* **2021**, *39*, 182–189. https://doi.org/10.1016/j.cofs.2021.03.005.

(135) Swallah, M. S.; Fu, H.; Sun, H.; Affoh, R.; Yu, H. The Impact of Polyphenol on General Nutrient Metabolism in the Monogastric Gastrointestinal Tract. *Journal of Food Quality* **2020**, *2020*. https://doi.org/10.1155/2020/5952834.

(136) Fu, Y.; Liu, W.; Soladoye, O. P. Towards Innovative Food Processing of Flavonoid Compounds: Insights into Stability and Bioactivity. *LWT* **2021**, *150*, 111968. https://doi.org/10.1016/j.lwt.2021.111968.

(137) Wang, J. B.; Wang, Y. M.; Zeng, C. M. Quercetin Inhibits Amyloid Fibrillation of Bovine Insulin and Destabilizes Preformed Fibrils. *Biochemical and Biophysical Research Communication* **2011**, *415* (4), 675–679. https://doi.org/10.1016/j.bbrc.2011.10.135.

(138) Kahn, S. E.; Andrikopoulos, S.; Verchere, C. B. Islet Amyloid. *Diabetes* **1999**, *48* (2), 241–242. https://doi.org/10.2337/diabetes.48.2.241.

(139) Asthana, S.; Mallick, B.; Alexandrescu, A. T.; Jha, S. IAPP in Type II Diabetes: Basic Research on Structure, Molecular Interactions, and Disease Mechanisms Suggests Potential Intervention Strategies. *Biochimica et Biophysica Acta (BBA) - Biomembranes* **2018**, *1860* (9), 1765–1782. https://doi.org/10.1016/j.bbamem.2018.02.020.

(140) Lorenzo, A.; Yankner, B. A. Beta-Amyloid Neurotoxicity Requires Fibril Formation and Is Inhibited by Congo Red. *Proceedings of the National Academy of Sciences* **1994**, *91* (25), 12243–12247. https://doi.org/10.1073/pnas.91.25.12243.

(141) Lorenzo, A.; Razzaboni, B.; Weir, G. C.; Yankner, B. A. Pancreatic Islet Cell Toxicity of Amylin Associated with Type-2 Diabetes Mellitus. *Nature* **1994**, *368* (6473), 756–760. https://doi.org/10.1038/368756a0.

(142) Pithadia, A.; Brender, J. R.; Fierke, C. A.; Ramamoorthy, A. Inhibition of IAPP Aggregation and Toxicity by Natural Products. *Journal of Diabetes Research* **2016**, *2016*, 2046327.

(143) Tak, Y.; Kaur, M.; Amarowicz, R.; Bhatia, S.; Gautam, C. Pulse Derived Bioactive Peptides as Novel Nutraceuticals: A Review. *International Journal of Peptide Research and Therapeutics* **2021**, *27* (3), 2057–2068. https://doi.org/10.1007/s10989-021-10234-8.

(144) Daroit, D. J.; Brandelli, A. In Vivo Bioactivities of Food Protein-Derived Peptides – a Current Review. *Current Opinions in Food Science* **2021**, *39*, 120–129. https://doi.org/10.1016/j.cofs.2021.01.002.

(145) Miles, A. J.; Wallace, B. A. CDtoolX, a Downloadable Software Package for Processing and Analyses of Circular Dichroism Spectroscopic Data. *Protein Science* **2018**, *27* (9), 1717–1722. https://doi.org/10.1002/pro.3474.

(146) Zhou, P.; Jin, B.; Li, H.; Huang, S. Y. HPEPDOCK: A Web Server for Blind Peptide–Protein Docking Based on a Hierarchical Algorithm. *Nucleic Acids Research* **2018**, *46* (W1), W443–W450. https://doi.org/10.1093/nar/gky357.

(147) Daina, A.; Michielin, O.; Zoete, V. SwissADME: A Free Web Tool to Evaluate Pharmacokinetics, Drug-Likeness and Medicinal Chemistry Friendliness of Small Molecules. *Scientific Reports* **2017**, *7* (1), 1–13. https://doi.org/10.1038/srep42717.

(148) Gupta, S.; Kapoor, P.; Chaudhary, K.; Gautam, A.; Kumar, R.; Consortium, O. S. D. D.; Raghava, G. P. S. In Silico Approach for Predicting Toxicity of Peptides and Proteins. *PLoS One* **2013**, *8* (9), e73957. https://doi.org/10.1371/journal.pone.0073957.

(149) Huang, S. Y.; Zou, X. An Iterative Knowledge-Based Scoring Function for Protein–Protein Recognition. *Proteins: Structure, Function, and Bioinformatics* **2008**, *72* (2), 557–579. https://doi.org/10.1002/prot.21949.

(150) Van De Waterbeemd, H. In Silico Models to Predict Oral Absorption. *Comprehensive Medicinal Chemistry II* **2007**, *5*, 669–697. https://doi.org/10.1016/b0-08-045044-x/00145-0.

(151) Peter Ertl; Bernhard Rohde, and; Selzer, P. Fast Calculation of Molecular Polar Surface Area as a Sum of Fragment-Based Contributions and Its Application to the Prediction of Drug Transport Properties. *Journal of Medicinal Chemistry* **2000**, *43* (20), 3714–3717. https://doi.org/10.1021/jm000942e.

(152) Veber, D. F.; Johnson, S. R.; Cheng, H.-Y.; Smith, B. R.; Ward, K. W.; Kopple, K. D. Molecular Properties That Influence the Oral Bioavailability of Drug Candidates. *Journal of Medicinal Chemistry* **2002**, *45* (12), 2615–2623. https://doi.org/10.1021/jm020017n.

(153) Delaney, J. S. ESOL: Estimating Aqueous Solubility Directly from Molecular Structure. *Journal of Chemical Information and Computer Sciences* **2004**, *44* (3), 1000–1005. https://doi.org/10.1021/ci034243x.

(154) Martin, Y. C. A Bioavailability Score. *Journal of Medicinal Chemistry* **2005**, *48* (9), 3164–3170. https://doi.org/10.1021/jm0492002.

(155) Ratha, B. N.; Ghosh, A.; Brender, J. R.; Gayen, N.; Ilyas, H.; Neeraja, C.; Das, K. P.; Mandal, A. K.; Bhunia, A. Inhibition of Insulin Amyloid Fibrillation by a Novel Amphipathic Heptapeptide. *Journal of Biological Chemistry* **2016**, *291* (45), 23545–23556. https://doi.org/10.1074/jbc.m116.742460.

(156) Paslawski, W.; Andreasen, M.; Nielsen, S.; Lorenzen, N.; Thomsen, K.; Kaspersen, J.; Pedersen, J.; Otzen, D. High Stability and Cooperative Unfolding of α-Synuclein Oligomers. *Biochemistry* **2014**, *53* (39), 6252–6263. https://doi.org/10.1021/bi5007833.

(157) Nagel-Steger, L.; Owen, M. C.; Strodel, B. An Account of Amyloid Oligomers: Facts and Figures Obtained from Experiments and Simulations. *ChemBioChem* **2016**, *17* (8), 657–676. https://doi.org/10.1002/cbic.201500623.

(158) Kapurniotu, A.; Schmauder, A.; Tenidis, K. Structure-Based Design and Study of Non-Amyloidogenic, Double N-Methylated IAPP Amyloid Core Sequences as Inhibitors of IAPP Amyloid Formation and Cytotoxicity. *Journal of Molecular Biology* **2002**, *315* (3), 339–350. https://doi.org/10.1006/jmbi.2001.5244.

(159) Scrocchi, L. A.; Chen, Y.; Waschuk, S.; Wang, F.; Cheung, S.; Darabie, A. A.; McLaurin, J. A.; Fraser, P. E. Design of Peptide-Based Inhibitors of Human Islet Amyloid Polypeptide Fibrillogenesis. *Journal of Molecular Biology* **2002**, *318* (3), 697–706. https://doi.org/10.1016/s0022-2836(02)00164-x.

(160) Sivanesam, K.; Andersen, N. H. Inhibition of Human Amylin Amyloidogenesis by Human Amylin-Fragment Peptides: Exploring the Effects of Serine Residues and Oligomerization upon Inhibitory Potency. *Biochemistry* **2017**, *56* (40), 5373–5379. https://doi.org/10.1021/acs.biochem.7b00739.

(161) Wang, L.; Lei, L.; Li, Y.; Wang, L.; Li, F. A hIAPP-Derived All-d-Amino-Acid Inhibits HIAPP Fibrillation Efficiently at Membrane Surface by Targeting α-Helical Oligomeric Intermediates. *FEBS Letters* **2014**, *588* (6), 884–891. https://doi.org/10.1016/j.febslet.2014.02.020.

(162) Cao, Q.; Boyer, D. R.; Sawaya, M. R.; Ge, P.; Eisenberg, D. S. Cryo-EM Structure and Inhibitor Design of Human IAPP (Amylin) Fibrils. *Nature Structural & Molecular Biology* **2020**, *27* (7), 653–659. https://doi.org/10.1038/s41594-020-0435-3.

(163) Tao, Y. X.; Conn, P. M. Pharmacoperones as Novel Therapeutics for Diverse Protein Conformational Diseases. *Physiological Reviews* **2018**, *98* (2), 697–725. https://doi.org/10.1152/physrev.00029.2016.

(164) Johnson, S. M.; Wiseman, R. L.; Sekijima, Y.; Green, N. S.; Adamski-Werner, S. L.; Kelly, J. W. Native State Kinetic Stabilization as a Strategy to Ameliorate Protein Misfolding Diseases: A Focus on the Transthyretin Amyloidoses. *Accounts of Chemical Research* **2005**, *38* (12), 911–921. https://doi.org/10.1021/ar020073i.

(165) Abioye, R. O.; Okagu, I. U.; Udenigwe, C. C. Targeting Glucose Transport Proteins for Diabetes Management: Regulatory Roles of Food-Derived Compounds. *Journal of Agriculture and Food Chemistry* **2022**, *70* (17), 5284–5290. https://doi.org/10.1021/acs.jafc.2c00817.

(166) Abioye, R. O.; Okagu, O. D.; Udenigwe, C. C. Disaggregation of Islet Amyloid Polypeptide Fibrils as a Potential Anti-Fibrillation Mechanism of Tetrapeptide TNGQ. *International Journal of Molecular Sciences* **2022**, *23* (4), 1972. https://doi.org/10.3390/ijms23041972.

(167) Okagu, O. D.; Abioye, R. O.; Udenigwe, C. C. Curcumin–Induced Stabilization of Protein–Based Nano-Delivery Vehicles Reduces Disruption of Zwitterionic Giant Unilamellar Vesicles. *Molecules* **2022**, *27* (6), 1941. https://doi.org/10.3390/molecules27061941/s1.

(168) Mantil, E.; Buznytska, I.; Daly, G.; Ianoul, A.; Avis, T. J. Role of Lipid Composition in the Interaction and Activity of the Antimicrobial Compound Fengycin with Complex

Membrane Models. *Journal of Membrane Biology* **2019**, *252* (6), 627–638. https://doi.org/10.1007/s00232-019-00100-6.

(169) Cabaleiro-Lago, C.; Lynch, I.; Dawson, K. A.; Linse, S. Inhibition of IAPP and IAPP(20-29) Fibrillation by Polymeric Nanoparticles. *Langmuir* **2010**, *26* (5), 3453–3461. https://doi.org/10.1021/la902980d.

(170) Wu, M. H.; Chan, A. C.; Tu, L. H. Role of Lysine Residue of Islet Amyloid Polypeptide in Fibril Formation, Membrane Binding, and Inhibitor Binding. *Biochimie* **2020**, *177*, 153–163. https://doi.org/10.1016/j.biochi.2020.08.012.

(171) Elenbaas, B. O. W.; Khemtemourian, L.; Killian, J. A.; Sinnige, T. Membrane-Catalyzed Aggregation of Islet Amyloid Polypeptide Is Dominated by Secondary Nucleation. *Biochemistry* **2022**, *61* (14), 1465–1472. https://doi.org/10.1021/acs.biochem.2c00184.

(172) Radovan, D.; Opitz, N.; Winter, R. Fluorescence Microscopy Studies on Islet Amyloid Polypeptide Fibrillation at Heterogeneous and Cellular Membrane Interfaces and Its Inhibition by Resveratrol. *FEBS Letters* **2009**, *583* (9), 1439–1445. https://doi.org/10.1016/j.febslet.2009.03.059.

(173) Gao, M.; Winter, R. The Effects of Lipid Membranes, Crowding and Osmolytes on the Aggregation, and Fibrillation Propensity of Human IAPP. *Journal of Diabetes Research* **2015**, *2015* (849017), 1–21. https://doi.org/10.1155/2015/849017.

(174) Wirth, F.; Heitz, F. D.; Seeger, C.; Combaluzier, I.; Breu, K.; Denroche, H. C.; Thevenet, J.; Osto, M.; Arosio, P.; Kerr-Conte, J.; Verchere, C. B.; Pattou, F.; Lutz, T. A.; Donath, M. Y.; Hock, C.; Nitsch, R. M.; Grimm, J. A Human Antibody against Pathologic IAPP Aggregates Protects Beta Cells in Type 2 Diabetes Models. *Nature Communications* **2023**, *14* (1), 1–15. https://doi.org/10.1038/s41467-023-41986-0.

(175) Scrocchi, L. A.; Ha, K.; Chen, Y.; Wu, L.; Wang, F.; Fraser, P. E. Identification of Minimal Peptide Sequences in the (8–20) Domain of Human Islet Amyloid Polypeptide Involved in Fibrillogenesis. *Journal of Structural Biology* **2003**, *141* (3), 218–227. https://doi.org/10.1016/s1047-8477(02)00630-5.

(176) Kato, K.; Nakayoshi, T.; Kurimoto, E.; Oda, A. Mechanisms of Deamidation of Asparagine Residues and Effects of Main-Chain Conformation on Activation Energy. *International Journal of Molecular Sciences* **2020**, *21* (19), 7035. https://doi.org/10.3390/ijms21197035.

(177) Akter, R.; Cao, P.; Noor, H.; Ridgway, Z.; Tu, L. H.; Wang, H.; Wong, A. G.; Zhang, X.; Abedini, A.; Schmidt, A. M.; Raleigh, D. P. Islet Amyloid Polypeptide: Structure, Function, and Pathophysiology. *Journal of Diabetes Research* **2016**, *2016* (2798269), 1–18. https://doi.org/10.1155/2016/2798269.

(178) Akter, R.; Zou, J.; Raleigh, D. P. Differential Effects of Serine Side Chain Interactions in Amyloid Formation by Islet Amyloid Polypeptide. *Protein Science* **2020**, *29* (2), 555–563. https://doi.org/10.1002/pro.3782.

(179) Chandel, T. I.; Zaman, M.; Khan, M. V.; Ali, M.; Rabbani, G.; Ishtikhar, M.; Khan, R. H. A Mechanistic Insight into Protein-Ligand Interaction, Folding, Misfolding, Aggregation and Inhibition of Protein Aggregates: An Overview. *International Journal of Biological Macromolecules* **2018**, *106*, 1115–1129. https://doi.org/10.1016/j.ijbiomac.2017.07.185.

(180) Freyssin, A.; Page, G.; Fauconneau, B.; Rioux Bilan, A. Natural Polyphenols Effects on Protein Aggregates in Alzheimer's and Parkinson's Prion-like Diseases. *Neural Regeneration Research* **2018**, *13* (6), 955–961. https://doi.org/10.4103/1673-5374.233432.

(181) Stalder, P.; Serdiuk, T.; Ghosh, D.; Fleischmann, Y.; Malinovska, L.; Davranche, A.; Haenseler, W.; Boudou, C.; Tsika, E.; Ouared, A.; Stöhr, J.; Melki, R.; Riek, R.; Souza, N. de; Picotti, P. An Approach to Characterize Mechanisms of Action of Anti-Amyloidogenic Compounds in Vitro and in Situ. *bioRxiv* **2023**, 2023.12.18.572111. https://doi.org/10.1101/2023.12.18.572111.

(182) Bu, X. Le; Rao, P. P. N.; Wang, Y. J. Anti-Amyloid Aggregation Activity of Natural Compounds: Implications for Alzheimer's Drug Discovery. *Molecular Neurobiology* **2016**, *53* (6), 3565–3575. https://doi.org/10.1007/s12035-015-9301-4.

(183) Guillemain, G.; Lacapere, J. J.; Khemtemourian, L. Targeting HIAPP Fibrillation: A New Paradigm to Prevent β-Cell Death? *Biochimica et Biophysica Acta (BBA) - Biomembranes* **2022**, *1864* (10), 184002. https://doi.org/10.1016/j.bbamem.2022.184002.

(184) Fernández, M. S. Human IAPP Amyloidogenic Properties and Pancreatic β-Cell Death. *Cell Calcium* **2014**, *56* (5), 416–427. https://doi.org/10.1016/j.ceca.2014.08.011.

(185) Li, Y.; He, D.; Li, B.; Lund, M. N.; Xing, Y.; Wang, Y.; Li, F.; Cao, X.; Liu, Y.; Chen, X.; Yu, J.; Zhu, J.; Zhang, M.; Wang, Q.; Zhang, Y.; Li, B.; Wang, J.; Xing, X.; Li, L. Engineering Polyphenols with Biological Functions via Polyphenol-Protein Interactions as Additives for Functional Foods. *Trends in Food Sciences and Technology* **2021**, *110*, 470–482. https://doi.org/10.1016/j.tifs.2021.02.009.

(186) Lin, D.; Sun, L. C.; Huo, W. Sen; Zhang, L. J.; Chen, Y. L.; Miao, S.; Cao, M. J. Improved Functionality and Safety of Peptides by the Formation of Peptide-Polyphenol Complexes. *Trends in Food Science and Technology* **2023**, *141*, 104193. https://doi.org/10.1016/J.tifs.2023.104193.

(187) Al-Shabib, N. A.; Khan, J. M.; Malik, A.; Sen, P.; Alsenaidy, M. A.; Husain, F. M.; Alsenaidy, A. M.; Khan, R. H.; Choudhry, H.; Zamzami, M. A.; Khan, M. I.; Shahzad, S. A. A Quercetin-Based Flavanoid (Rutin) Reverses Amyloid Fibrillation in β-Lactoglobulin at pH 2.0 and 358 K. *Spectrochimica Acta Part A: Molecular and Biomolecular Spectroscopy* **2019**, *214*, 40–48. https://doi.org/10.1016/j.saa.2019.02.004.

(188) Mahendra, V. P.; Yogendra Prasad, K.; Ganesan, P.; Kumar, R. Mechanism of Rutin Mediated Inhibition of Insulin Amyloid Formation and Protection of Neuro-2a Cells from Fibril-Induced Apoptosis. *Molecular Biology Reports* **2020**, *47* (4), 2811–2820. https://doi.org/10.1007/S11033-020-05393-8.

(189) Lin, C. Y.; Gurlo, T.; Kayed, R.; Butler, A. E.; Haataja, L.; Glabe, C. G.; Butler, P. C. Toxic Human Islet Amyloid Polypeptide (h-IAPP) Oligomers Are Intracellular, and Vaccination to Induce Anti-Toxic Oligomer Antibodies Does Not Prevent h-IAPP–Induced β-Cell Apoptosis in h-IAPP Transgenic Mice. *Diabetes* **2007**, *56* (5), 1324–1332. https://doi.org/10.2337/db06-1579.

(190) Tomasello, M. F.; Sinopoli, A.; Attanasio, F.; Giuffrida, M. L.; Campagna, T.; Milardi, D.; Pappalardo, G. Molecular and Cytotoxic Properties of HIAPP17–29 and RIAPP17–29 Fragments: A Comparative Study with the Respective Full-Length Parent Polypeptides. *Eur Journal of Medicinal Chemistry* **2014**, *81*, 442–455. https://doi.org/10.1016/J.ejmech.2014.05.038.

(191) Pérez-Gregorio, R.; Soares, S.; Mateus, N.; de Freitas, V. Bioactive Peptides and Dietary Polyphenols: Two Sides of the Same Coin. *Molecules* **2020**, *25* (15), 3443. https://doi.org/10.3390/molecules25153443.

(192) LeBel, C. P.; Ischiropoulos, H.; Bondy, S. C. Evaluation of the Probe 2',7'-Dichlorofluorescin as an Indicator of Reactive Oxygen Species Formation and Oxidative Stress. *Chemical Research in Toxicology* **1992**, *5* (2), 227–231. https://doi.org/10.1021/tx00026a012.

(193) Konarkowska, B.; Aitken, J. F.; Kistler, J.; Zhang, S.; Cooper, G. J. S. Thiol Reducing Compounds Prevent Human Amylin-Evoked Cytotoxicity. *FEBS Journal* **2005**, *272* (19), 4949–4959. https://doi.org/10.1111/j.1742-4658.2005.04903.x.

(194) Deepa Maheshvare, M.; Raha, S.; König, M.; Pal, D. A Pathway Model of Glucose-Stimulated Insulin Secretion in the Pancreatic β-Cell. *Frontiers in Endocrinology (Lausanne)* **2023**, *14*, 1185656. https://doi.org/10.3389/fendo.2023.1185656.

APPENDICES

Appendix A: Copyright and Consent Notes

Appendix A1

Consent by co-authors

Names	Signature	Date
Chibuike C. Udenigwe		
Ogadimma D. Okagu		
Martha S. Yiridoe		
Chenyang Wang		
Tyler J. Avis		
Tamer A. E. Ahmed		
Riadh Hammami		
Oluwasemilogo H. Adetula		
Julia Diem Hum		

Appendix A2

Copyright from Elsevier – Food Science and Human Wellness

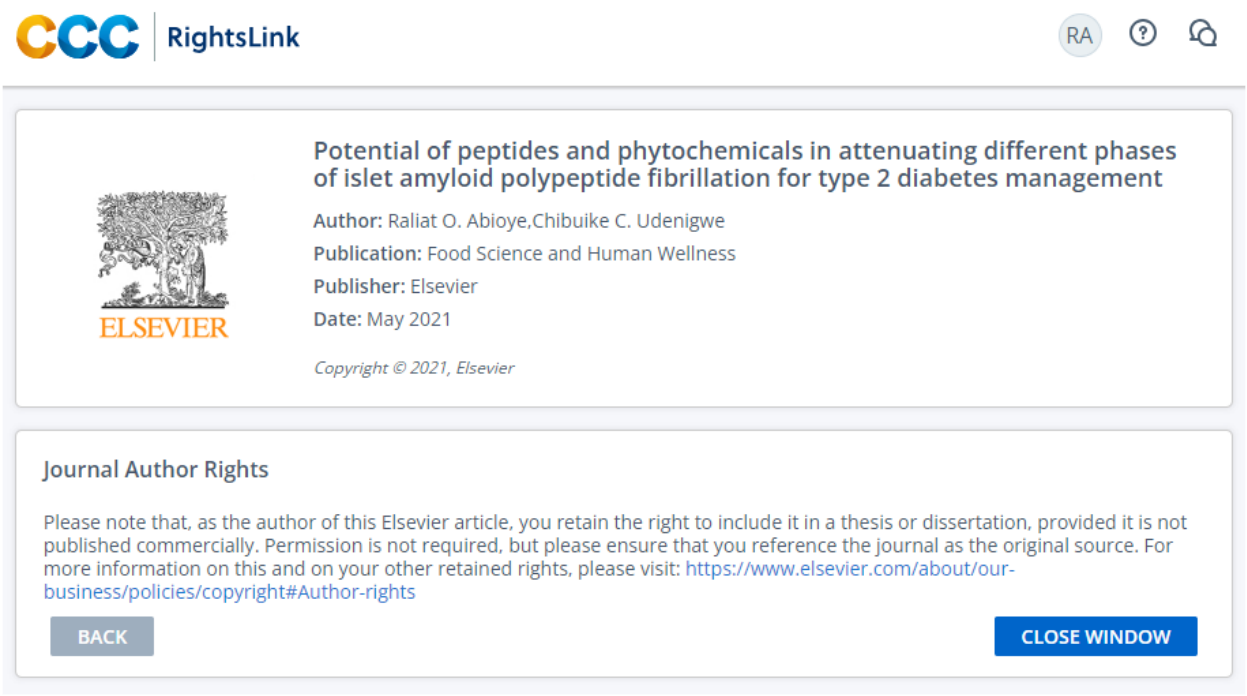

Appendix A3

Copyright from Elsevier – Current Opinion in Food Science

Appendix A4

Copyright from ACS – Biochemistry (Figure Adaptation)

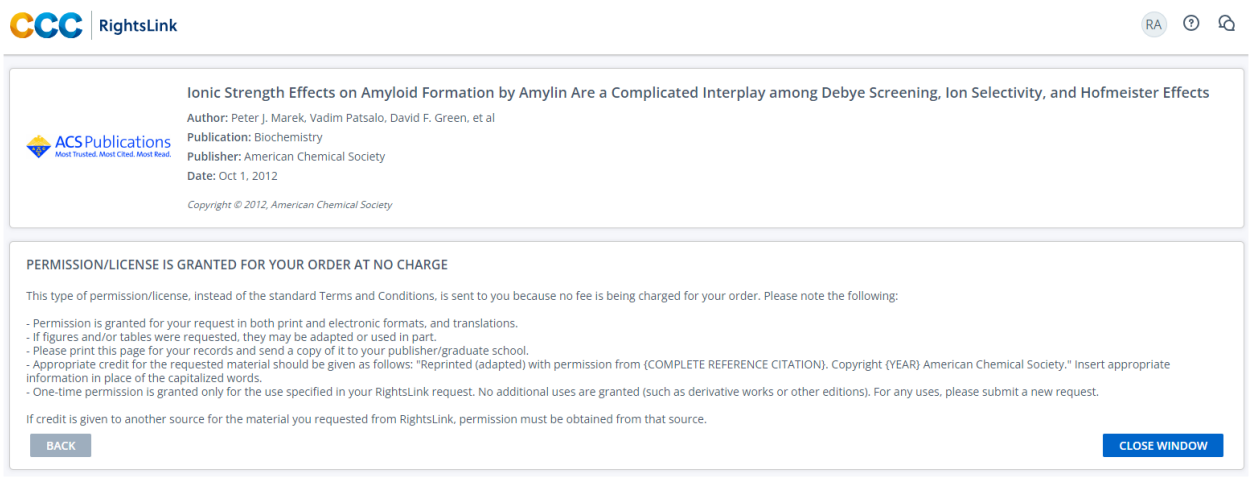

Appendix A5

Copyright from ACS – Journal of Agricultural and Food Chemistry

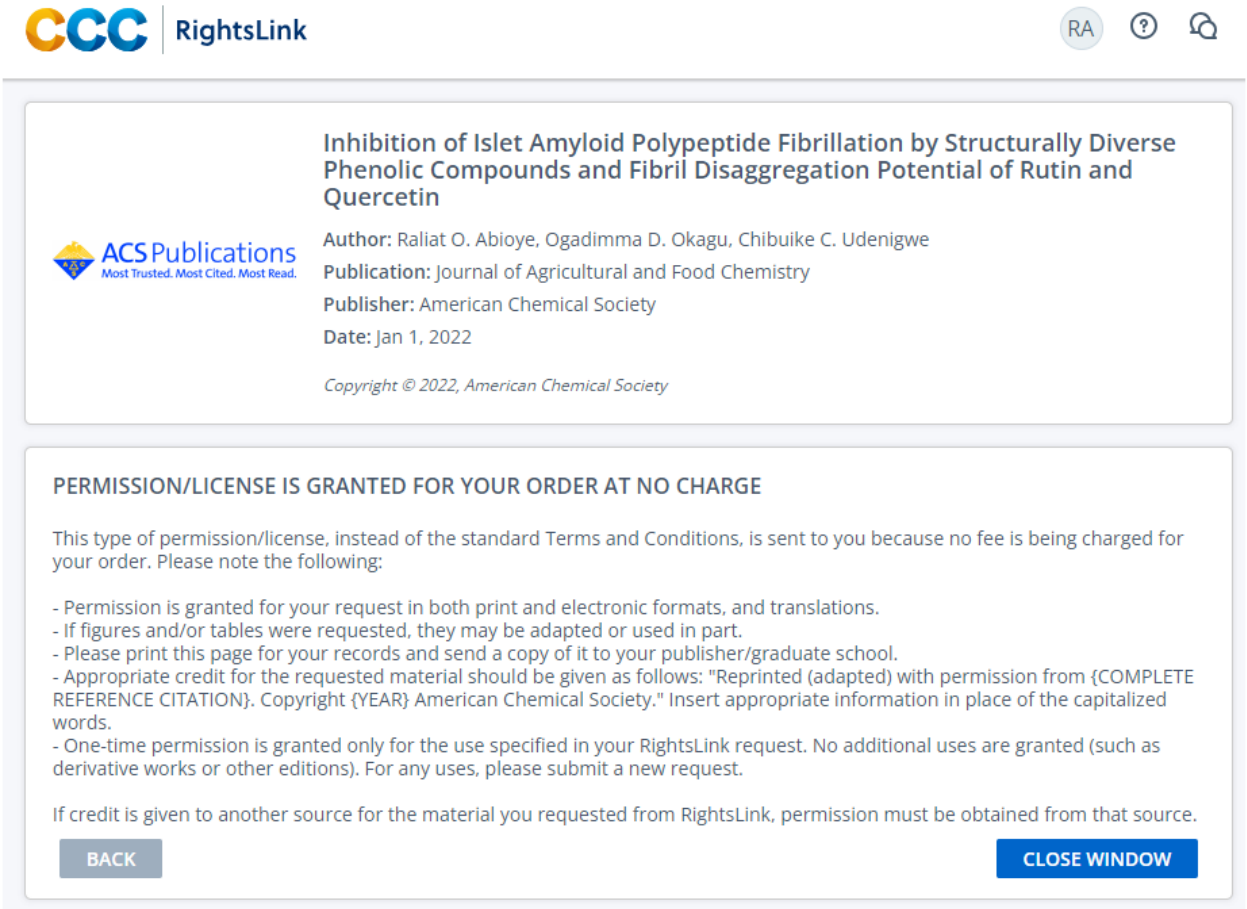

CCC RightsLink

RA

ACS Publications
Most Trusted. Most Cited. Most Read.

Inhibition of Islet Amyloid Polypeptide Fibrillation by Structurally Diverse Phenolic Compounds and Fibril Disaggregation Potential of Rutin and Quercetin

Author: Raliat O. Abioye, Ogadimma D. Okagu, Chibuike C. Udenigwe
Publication: Journal of Agricultural and Food Chemistry
Publisher: American Chemical Society
Date: Jan 1, 2022

Copyright © 2022, American Chemical Society

PERMISSION/LICENSE IS GRANTED FOR YOUR ORDER AT NO CHARGE

This type of permission/license, instead of the standard Terms and Conditions, is sent to you because no fee is being charged for your order. Please note the following:

- Permission is granted for your request in both print and electronic formats, and translations.
- If figures and/or tables were requested, they may be adapted or used in part.
- Please print this page for your records and send a copy of it to your publisher/graduate school.
- Appropriate credit for the requested material should be given as follows: "Reprinted (adapted) with permission from {COMPLETE REFERENCE CITATION}. Copyright {YEAR} American Chemical Society." Insert appropriate information in place of the capitalized words.
- One-time permission is granted only for the use specified in your RightsLink request. No additional uses are granted (such as derivative works or other editions). For any uses, please submit a new request.

If credit is given to another source for the material you requested from RightsLink, permission must be obtained from that source.

BACK CLOSE WINDOW

Appendix A6

MDPI open access permission for International Journal of Molecular Science

MDPI Open Access Information and Policy

All articles published by MDPI are made immediately available worldwide under an open access license. This means:

- everyone has free and unlimited access to the full-text of *all* articles published in MDPI journals;
- everyone is free to re-use the published material if proper accreditation/citation of the original publication is given;
- open access publication is supported by the authors' institutes or research funding agencies by payment of a comparatively low Article Processing Charge (APC) for accepted articles.

Permissions

No special permission is required to reuse all or part of article published by MDPI, including figures and tables. For articles published under an open access Creative Common CC BY license, any part of the article may be reused without permission provided that the original article is clearly cited. Reuse of an article does not imply endorsement by the authors or MDPI.

External Open Access Resources

Those who are new to the concept of open access might find the following websites or the *Open Access Explained!* video informative:

- Wikipedia article on Open Access
- Open Access Network

Meaning of Open Access

In accordance with major definitions of open access in scientific literature (namely the Budapest, Berlin, and Bethesda declarations), MDPI defines *open access* by the following conditions:

- peer-reviewed literature is freely available without subscription or price barriers,
- literature is immediately released in open access format (no embargo period), and
- published material can be re-used without obtaining permission as long as a correct citation to the original publication is given.

Open Access Explained!

Until 2008, most articles published by MDPI contained the note: "© *year* by MDPI (http://www.mdpi.org). Reproduction is permitted for noncommercial purposes". During 2008, MDPI journals started to publish articles under the Creative Commons Attribution License and are now using the latest version of the CC BY license, which grants authors the most extensive rights. All articles published by MDPI before and during 2008 should now be considered as having been released under the post-2008 Creative Commons Attribution License.

This means that all articles published in MDPI journals, including data, graphics, and supplements, can be linked from external sources, scanned by search engines, re-used by text mining applications or websites, blogs, *etc.* free of charge under the sole condition of proper accreditation of the source and original publisher. MDPI believes that open access publishing fosters the exchange of research results amongst scientists from different disciplines, thus facilitating interdisciplinary research. Open access publishing also provides access to research results to researchers worldwide, including those from developing countries, and to an interested general public. Although MDPI publishes all of its journals under the open access model, we believe that open access is an enriching part of the scholarly communication process that can and should co-exist with other forms of communication and publication, such as society-based publishing and conferencing activities.

Important Note: some articles (especially *Reviews*) may contain figures, tables or text taken from other publications, for which MDPI does not hold the copyright or the right to re-license the published material. Please note that you should inquire with the original copyright holder (usually the original publisher or authors), whether or not this material can be re-used.

Every conceivable effort has been made to provide credit to the rightful proprietors of any copied materials. Any copyright holder who has been excluded or erroneously acknowledged should please contact me.

Thank you.